ACTA UNIVERSITATIS CAROLINAE

AUC **GEOGRAPHICA**

60
1/2025

CHARLES UNIVERSITY • KAROLINUM PRESS

The 1 January 2024 Noto Peninsula co-seismic landslides hazards: Preliminary results

Christopher Gomez[1,2,*]

[1] Kobe University, Faculty of Oceanology, Laboratory of Sediment Hazards and Disaster Risk, Japan
[2] Universitas Gadjah Mada, Department of Geography, PSBA Laboratory, Yogyakarta, Indonesia
[*] Corresponding author: christophergomez@bear.kobe-u.ac.jp

ABSTRACT

On the first day of 2024, a strong Mw.7.6 earthquake followed by a tsunami shook the Noto Peninsula (Japan) located on the coast facing the Sea of Japan. It resulted in numerous casualties, infrastructures and dwelling destroyed. The earthquake also triggered an estimated 5,000 coastal and mountain co-seismic mass-movements, from which 930 were identified by aerial photographs and digitized from the emergency aerial photographs (2/1/2024). The goal has been to provide a preliminary assessment of their distribution and characteristics. The medium surface of the landslides was found to be 1,749 m^2, with numerous small < 50 m^2 landslides and at least one large deep-seated landslide (0.8 km × 1 km). The mountain landslides were concentrated around two clusters, which were not close to the epicentre, but around 7 km and 10 km from the epicentre. From a disaster-risk perspective, the 1/1/2024 Noto Peninsula earthquake is typical of a 'coastal earthquake' where the coastal landslides, even sparse collapsed on the main artery of the peninsula, the ring road, isolating communities and hampering the disaster relief process.

KEYWORDS

co-seismic landslides; Japan; Noto earthquake; geomorphology

Received: 3 June 2024
Accepted: 23 July 2024
Published online: 22 August 2024

Gomez, C. (2024): The 1 January 2024 Noto Peninsula co-seismic landslides hazards: Preliminary results. AUC Geographica 60(1), 3–10
https://doi.org/10.14712/23361980.2024.11

1. Introduction

On 1 January 2024, while local inhabitants had gathered for the New Year celebration and the "Oshogatsu yasumi", a Mw. 7.6 earthquake (N37.5, E137.2) shook the Noto Peninsula (Fig. 1) and sent seismic waves that were felt in the majority of the main island of Honshu.

Near the epicentre, the intensity reached the maximum level (JMA 2024): 7 on the Japanese Earthquake Intensity Scale (Alcantara-Ayala et al. 2022). It resulted in a first estimated 100 casualties as per 6 January, and 168 on the 8 January in the Noto Peninsula alone, with these numbers likely to rise even further.

1 January was not a "freak" single event. The Noto peninsula has been seismically active during the measurable historical period, with raised shorelines, the 1720–1950 shoreline being up to < 40 cm a.s.l., the 1430–1665 shoreline around 60 cm a.s.l., and the 1025 to 1235 shoreline between 80 cm and 100 cm a.s.l. (Shishikura et al. 2009). The 2024 event is not the first destructive event of the 21st century in the peninsula. The 25 March 2007 earthquake and tsunami caused one casualty, injured 338 and impacted around 33,700 dwellings (Sakai et al. 2008). Triggered by a known submarine fault (Katagawa et al. 2005), it resulted in a first estimated Mw 6.6 (Sakai et al. 2008) to 6.7 (Kato et al. 2008) < 20 cm wave tsunamigenic event (Tanioka 2008), with horizontal and vertical displacements both < 20 mm overall (Hashimoto et al. 2008) and with local uplift of 50 cm (Shishikura et al. 2009). This event had been the largest event in 100 years for the peninsula (Nakajima 2022). This "single" event ended after a set of aftershocks, but in 2018 a long-lived swarms or clusters of earthquakes was identified, with a high density of events (Nakajima 2022). In May 2018, a swarm of four years began. It generated > 20,000 Mw > 5.0 earthquakes (Amezawa et al. 2023). Such event has been attributed to the migration of the hypocentres and the fluid supply combined with the permeability of the environment (Amezawa et al. 2023), making the Noto peninsula an earthquake-prone area.

Unfortunately, as it is often the case in hilly and mountainous areas, earthquakes are often associated with co-seismic landslides (e.g. in Greece, Italy, Japan, New-Zealand, Chile, Nepal, etc. (Towhata et al. 2022). Their size and number are usually scaled with the magnitude of the earthquake (Malamud et al. 2024) and the distance to the epicentre (Keefer 2000). Furthermore, earthquake-triggered landslides can be further enhanced by antecedent or concurrent precipitation as it reduces the shear strength of material, as it was notably observed during the 2018 Iburi Earthquake in Hokkaido for instance (Gomez and Hotta 2021). Comparatively however, co-seismic landslides in the Noto Peninsula have historically been small and scarce: in 2007, despite of a Mw 6.6–6.7 earthquake occurring after rainfalls (50 mm over three days), only 61 landslides were recorded for the whole Noto peninsula for past events (Goto 2007), compared to the ~7,000 landslides recorded in Hokkaido for the Iburi-earthquake (Murakami et al. 2022). Contrasting with the co-seismic landslides in the Iburi area, the

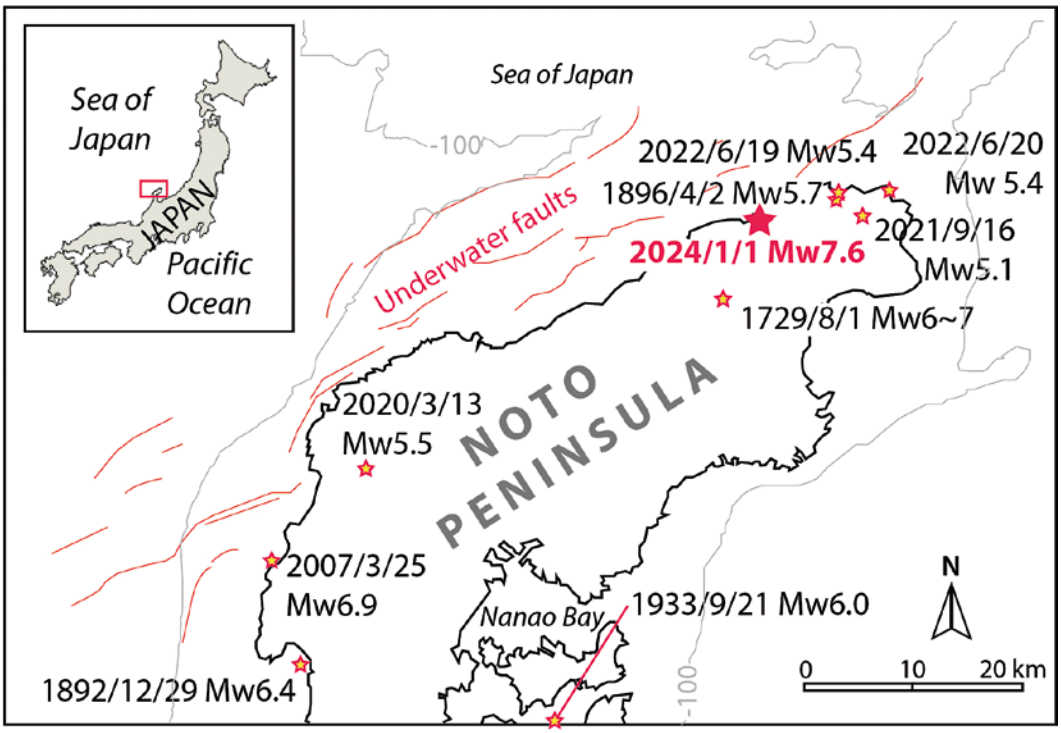

Fig. 1 The 2024 earthquakes and the major recorded historical earthquakes.

landslides travelled shorter distances, characteristics that can be attributed to the local conditions (Okada et al. 2008).

Because each earthquake and its geographical setting produces different types and distribution of co-seismic landslides, documenting each set of events brings us closer to understanding the unfolding of such hazards. Consequently, the present contribution investigates the geometry and the spatial distribution of co-seismic landslides that occurred because of the Mw. 7.6 earthquake of January 2024.

2. Methods

The present research has been occurring while the earthquake sequence was ongoing (with the latest strong motion earthquake recorded on the 3 June 2024 around 6:30 in the morning). As reconstruction has not begun yet, the author took the decision to base this preliminary work based on remote sensing data solely.

2.1 Ethical disaster investigation

As the disaster is unfolding and field-work should not trump the suffering of local populations, the present contribution is solely based on remote-sensing data, in order not to accentuate the burden on local communities. This methodological approach is motivated and in line with the "manifesto" (Power, Prestige & Forgotten Values: A Disaster Studies Manifesto 2024).

2.2 Data source and processing

On 2 January 2024, the Japanese government took a set of aerial photographs of the Noto Peninsula for emergency management purposes. From this dataset, 235 cloud-free photographs were selected. The set of photographs was then stitched together using structure from motion (Agisoft, Metashape-Pro software) and geodetic points of the peninsula (www.gsi.go.jp). As structure from motion reconstructs the elevation as well as it collates the photographs, the generated topography was also used to rectify the images and generate an orthophotograph.

2.3 Information Extraction and calculation

The orthophotograph was then imported in the QGIS Geographical Information System environment to hand-digitize the clearly identifiable landslides. From the digitized polygons, the landslides length and width were calculated using an oriented bounding box, and the direction of the oriented vector was determined by extracting the altitude of the edges of the bounding box. The results from GIS were then exported to the Python environment, where the data was handled as a panda dataframe to conduct the descriptive statistics used in the present contribution (the table data is available upon request), that explains the type of landslides that occurred.

2.4 Secondary data

This contribution also relies on secondary data. The geological map of the Noto peninsula (Yoshikawa et al. 2020) as well as the earthquake information that was collected from the Japanese Meteorological Agency (2024).

3. Results

3.1 The majority of the landslides is < 100 m long

The 1 January 2024 earthquakes triggered at least (digitized landslides) 930 co-seismic landslides. Their mean length reached 132 m for a median length of 94 m. Despite a number of small-size events (a quarter is shorter than 54 m) the maximum length exceeded a kilometre (Tab. 1). The mean area of landslides is 5,353 m^2 and the largest one 373,962 m^2.

From this set of landslides, a majority is < 200 m long (Fig. 2). The smaller landslides have a ratio of length/width > 2.0 while the larger landslides are less elongated (Fig. 2). The mean length of the landslides with a ratio length over width > 2.0 have lengths that are on average < 184 m. Despite valley confined landslides, the length/width ratio does not exceed 3.24, coinciding with the visual recognition of numerous shallow translational landslides that travelled short distances.

3.2 Landslides concentrated between 7 and 10 km away from the epicentre

The spatial distribution of the co-seismic landslides of the 1 January 2024 shows two hotspots (summarized in Fig. 6). They are concentrated in two areas of Tertiary terrain: (1) between the Iizuka formation (Siliceous siltstone) and the Awagura formation (volcanic

Tab. 1 Statistical characteristics of the digitized 930 landslides (as per 2/1/2024).

	Area [m^2]	Width [m]	Length [m]	Perimeter [m]
mean	5,353	66	132	395
std	15,543	63	127	365
min	23	4	8	31
25%	742	29	54	174
50%	1,749	45	94	287
75%	4,788	81	154	471
max	373,962	868	1,078	3,701

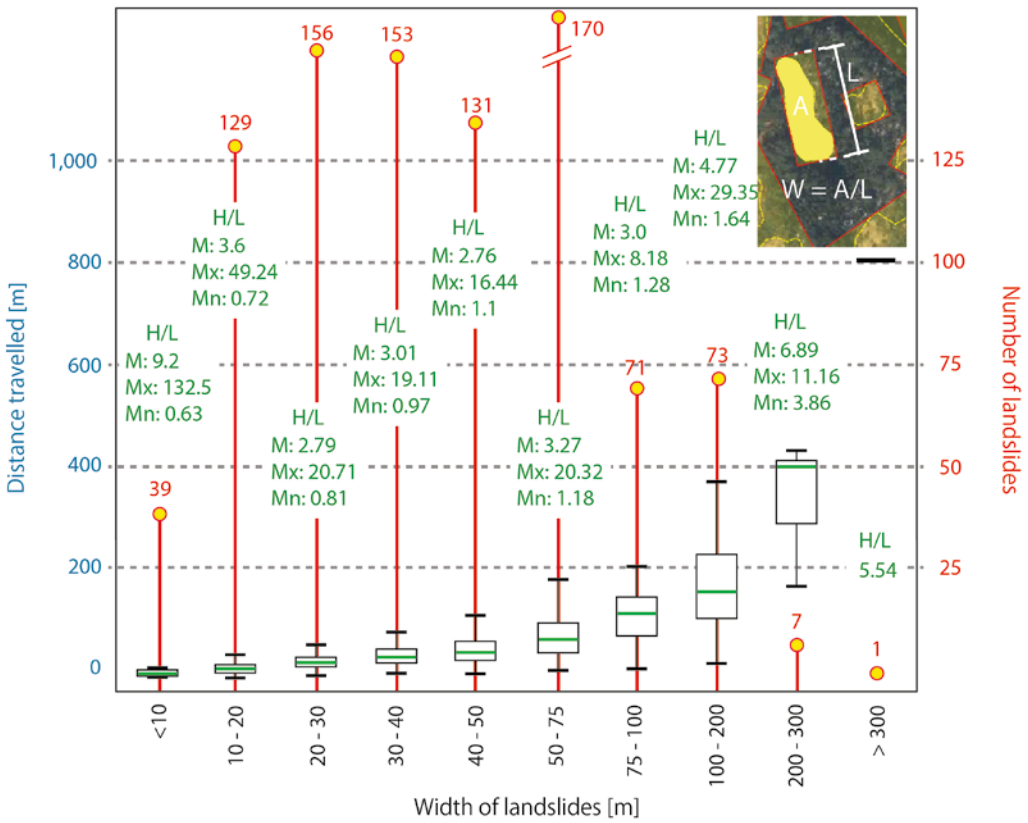

Fig. 2 Landslides length by classed width (the red plots and number in black is the number of landslides per class; the blue number on the left of the bar plot is the mean length per class, and the green horizontal number is the ratio of mean length over mean width).

rock intercalated with siltstone) and (2) in the Horyuzan formation (mixture of Dacite volcanic rocks with siltstone and conglomerate). The two concentrations of landslides are both at a ~10 km distance from the epicentre (Fig. 3). The coastal landslides are sparser and of smaller magnitude than the one in the West, as they occurred mostly in the Awagura and the Iizuka formations (Fig. 3).

In the Awagura hot-spot of landslides, the largest event (Fig. 4) occurred and it is more than a kilometre wide and about 800 m wide (estimated from aerial photographs to be Length: 1078 and Width: 868 m).

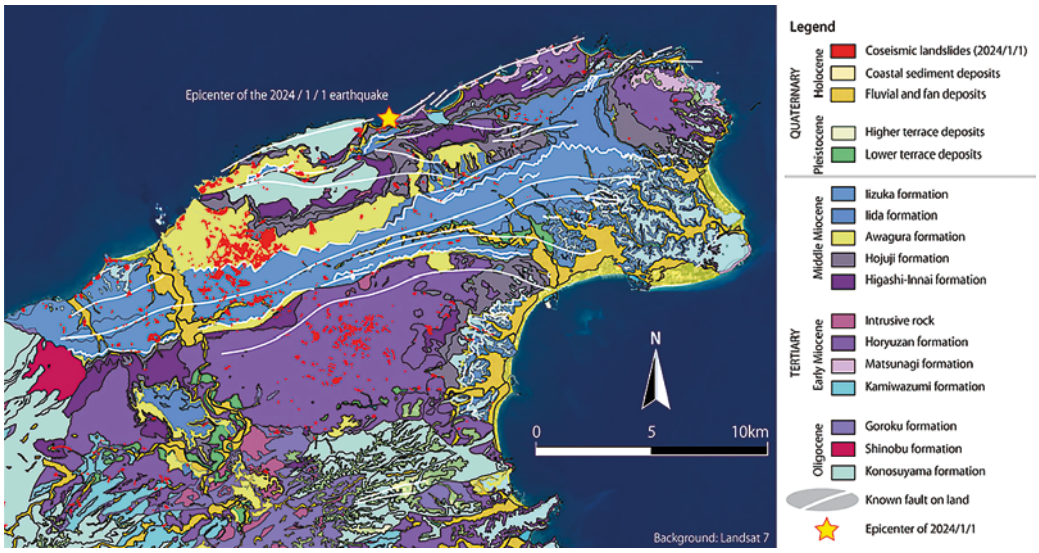

Fig. 3 Spatial distribution of the 1 January 2024 landslides across the geological structure of the Noto Peninsula (Map drawn from the Geological map of Japan (Yoshikawa et al. 2020) and the digitized 2024 landslides (GSJ 2024); please note that the coloring was adapted for improved readability).

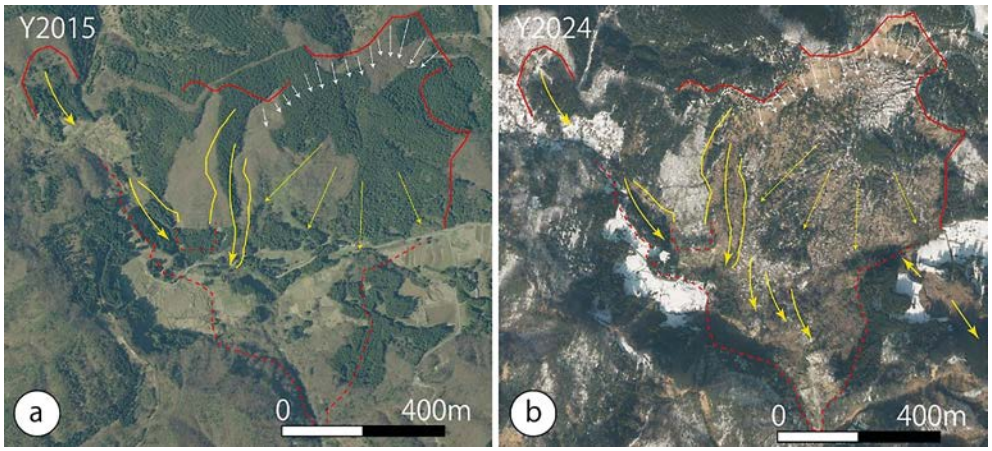

Fig. 4 The largest deep seated landslide, located in the Awagura formation. The red lineaments are the visible crown of the landslides, while the yellow arrow shows direction of spread. The dotted red line represents the toe of the landslides, and white arrows are the locations where the sliding plane is now visible.

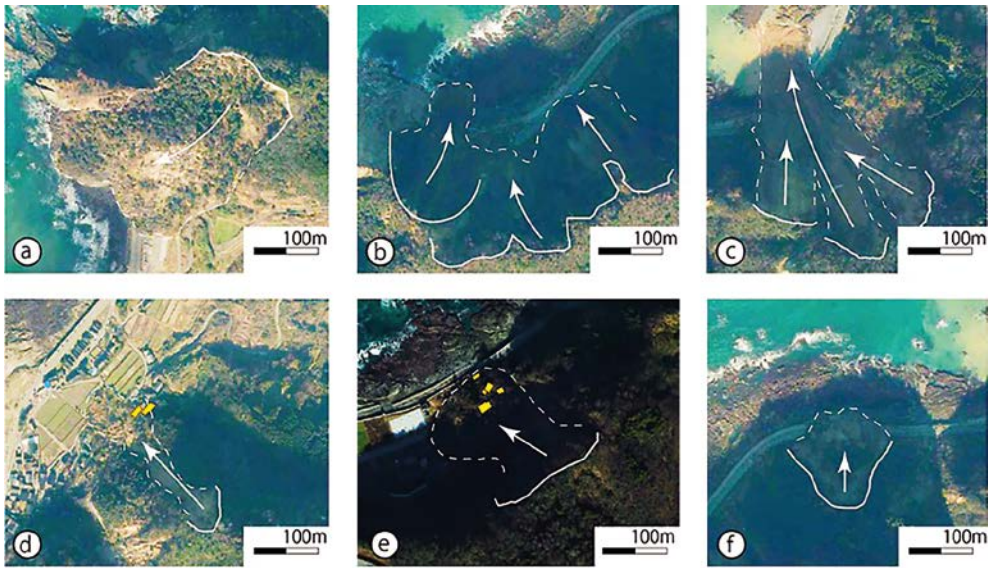

Fig 5. Coastal landslides cutting the "ring-road" of the island to the West of the Epicentre. The Yellow boxing marks dwellings that have been buried by the landslides.

The entire slope travelled over the agriculture terraces at its toe (Fig. 4). The event contrasts with the majority of the smaller-scale co-seismic landslides that often occurred as valley-constrained earth-flows (Tab. 1).

The coastal landslides that cut the road reach 300 and 400 m in length from the crown to the toe of the landslide. Translational landslide on complex or curved failure plane (Fig. 5a,f) have been observed as well as shallow landslides on sliding planes parallel to the surface (Fig. 5b–e). The material remained relatively cohesive at places (Fig. 5d–f) while some other slides created deposits that reveal a granular-flow or rock avalanches. These different slides exist within a single rock formation and similar topographies, with different types of events juxtaposed to one another (Fig. 5b: the event on the left is a rock avalanche, while the two other events on the right have a deposit that are more compacts.

Only 1.7% (i.e. 16 events) of the total number of landslides cut the coastal road, covering lengths between 17 m and 566 m length, for an average length of road cut of 179 m for each event. The size of the coastal landslides however is larger than the average, because in the mountainous areas numerous smaller landslides also took place.

4. Discussion

The co-seismic landslides triggered by the 2024/01/01 earthquake are concentrated at two locations, centred on 7 km and 10 km distances from the epicentre (Fig. 6).

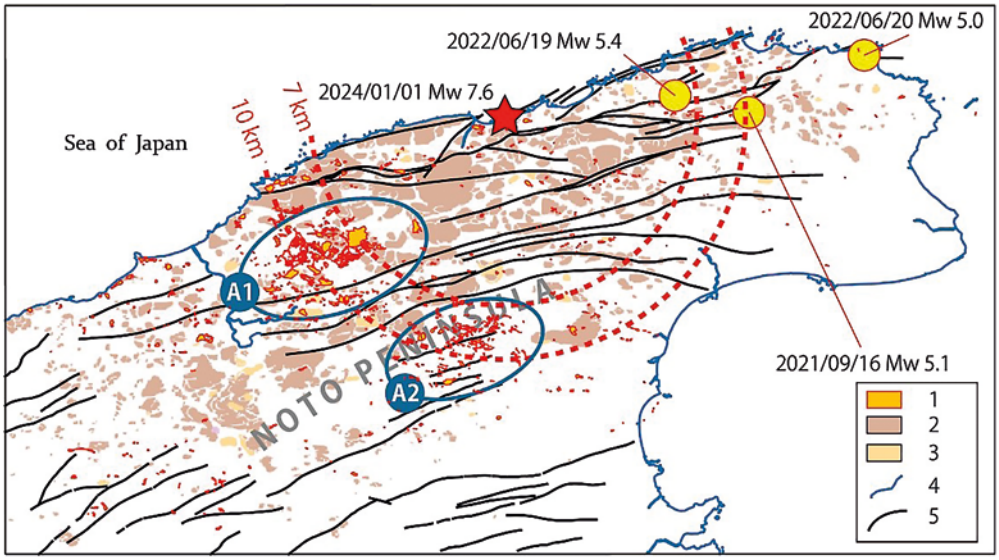

Fig. 6 Synthesis map: The January 2024 co-seismic landslides are not controlled by past- and active landslides.
(1: Landslides digitized for the present study; 2: Existing active landslides; 3: Potential active landslides; 4: Coastline of the Noto Peninsula; 5: Known faults on land. The red star shows the 2024 earthquake epicentre, and the yellow circle the previous ones in 2022.
Zones A1 and A2 are the areas where landslides are zones of landslides concentration.

The cluster A1 occurred mostly in the Awagura formation, while A2 is in the Horyuzan formation. Despite a large number of mapped landslides and potential landslides, the 2024 co-seismic landslides mostly occurred in new areas. Except for the largest landslide and its surrounding (Fig. 4 and in A1, Fig. 6) the co-seismic landslides occurred in previously unaffected (or unmapped) areas. The present set of co-seismic landslides present at least two oddities, when compared to other events in the scientific literature. Keefer (2000) describes a spatial density of landslides that is correlated with the distance to the epicentre as it is often the case, but for the Noto Peninsula co-seismic landslides, they are centred in two areas that are around 7 km and 10 km from the epicentre. By comparison with the 2018 Hokkaido co-seismic landslides that were concentrated in the Iburi mountains, the results show that they are concentrated in two main geological formations, which may show either the role of the formation in amplifying the seismic waves, either the role of the topography and the geomorphological specificities. Another hypothesis that may be stressed here, like for the Iburi earthquake is the position and orientation of the main faults and how they communicate the seismic energy to the surface.

The landslides are also showing a mixture of shapes. The 2018 Iburi earthquake generated landslides all close to the relation LD = 2.2492 $W^{1.0296}$, where LD is the length of the deposit and W is the width of the deposit (Murakami et al. 2022), but for the co-seismic landslides of the Noto Peninsula, such relation could not be observed, even after dividing them in classes (Fig. 2). Compared to the co-seismic landslides of the coastal earthquake of Kaikoura (Mw 7.8), the runouts are also smaller: in Kaikoura the longest was 2.7 km (Massey et al. 2018).

In the aftermath of the 2011 Earthquake that shook Canterbury and the coastal town of Christchurch in New Zealand, professor Deirdre Hart coined the term "coastal disaster" during one of her oral intervention. The idea acknowledges the particular characteristics of settlement and the role of the coastal geomorphology and sedimentology (estuarine sediments, loose Quaternary sediments, etc.) combined with coastal settlements (sea-side roads, blue-edge real estate) on the making of a coastal multihazards and eventually a disaster (Hart et al. 2018). Arguably, the 1 January 2024 earthquake that shook the Noto Peninsula is one these events as well, and the co-seismic landslides concur with this idea. As in Christchurch, only a few failures on the lifeline that could not be built with redundancies in coastal areas, resulted in a slower response and a difficult recovery, once cut by co-seismic landslides. In the mountain area of the Noto Peninsula, the rupture of the access roads has had a similar effect. A comparable issue also arose in 2016, in the aftermath of the Kaikoura earthquake in New Zealand, where coastal co-seismic landslides cut the main coastal road as well as the train track (Massey et al. 2018), although the Kaikoura earthquake triggered more than 10,000 landslides (about 10 folds compared to the Noto Peninsula). Consequently, the 1/1/2024 Noto Peninsula co-seismic landslide distribution of co-seismic landslides is at odd with traditional models and seemed to have occurred in areas where previous landslides have not occurred. The difficulty to understand the geometry and distribution of co-seismic landslides is also a reminder that a large amount of data concerning soils and geology

were notably created for resource mapping, but not to understand hazards, and there is certainly a need to develop new method to refine the mapping of soils and geology in the same way that point cloud has done for topography or radar for rainfalls.

5. Conclusion

The 2024/1/1 earthquake that struck the Noto peninsula is the latest event in a series of recent and historical earthquakes that were directly recorded or that can be evidenced from the large number of secondary landslides, which cover the peninsula. The co-seismic landslides concentrated in two areas, away from the epicentre, which makes the event atypical compared to others found in the scientific literature. The event also emphasized the channel to sustainable development in seismically active peninsula and islands, where the coastal road is a lifeline trapped in between potential tsunami damages on one side and the landslides on the other side.

Acknowledgements

The author is in dept to the company KokusaiKogyo, which provided verification data for this work as well as the Japanese government, which made the aerial photographs used in the present contribution available at a very early stage for recovery and the supporting scientific and engineering efforts. The author would also like to thank two anonymous reviewers for their careful reading and contribution that led to an improved manuscript.

References

Alcantara-Ayala, I., Gomez, C., Chmutina, K., van Niekerk, D., Raju, E., Marchezini, V., Rom Cadag J., Gaillard, J. C. (2022): Disaster Risk, Routlege, https://doi.org/10.4324/9781315469614-3.

Amezawa, Y., Hiramatsu, Y., Miyakawa, A., Imanishi, L., Otsubo, M. (2023): Long-Living Earthquake Swarm and Intermittent Seismicity in the Northeastern Tip of the Noto Peninsula, Japan. Geophysical Research Letters 50(8), e2022GL102670, https://doi.org/10.1029/2022GL102670.

Gomez, C., Hotta, N. (2021): Deposits' Morphology of the 2018 Hokkaido Iburi-Tobu Earthquake, Mass Movements from LiDAR & Aerial Photographs. Remote Sensing 13(17), 3421, https://doi.org/10.3390/rs13173421.

Goto, S. (2007): On slope disasters by the Noto Hanto Earthquake in 2007. Prompt reports of geodisasters by the Noto Hanto Earthquake in 2007. The University of Tokyo, 20–26 (in Japanese).

GSJ – Geological Survey of Japan (2024): Online map of landslides of Japan. Available online: https://gbank.gsj.jp/owscontents/howto.html accessed on 9. 1. 2024 (in Japanese).

Hart, D. E., Giovinazzi, S., Byun, D.-S., Davis, C., Ko, S. Y., Gomez, C., Hawke, K., Todd, D. (2018): Enhancing resilience by altering our approach to earthquake and flooding assessment: multi-hazards. Proceedings of the 16th European Conference on Earthquake Engineering, Thessaloniki, Greece, 1–13.

Hashimoto, M., Takahashi, H., Doke, R., Kasahara, M., Takeuchi, A., Onoue, K., Hoso, Y., Fukushima, Y., Nakamura, K., Ohya, F., Honda, R., Ichiyanagi, M., Yamaguchi, T., Maeda, T., Hiramatsu, Y. (2008): Postseismic displacements following the 2007 Noto peninsula earthquake detected by dense GPS observation. Earth, Planets and Space 60, 139–144, https://doi.org/10.1186/BF03352775.

JMA – Japanese Meteorological Agency (2024): Earthquake information 2024/01/01 16, 24. Available online: https://www.data.jma.go.jp/multi/quake/quake_detail.html?eventID=20240101162429&lang=jp accessed on 9.1.2024 (in Japanese).

Katagawa, H., Hamada, M., Yoshida, S., Kadosawa, H., Mitsuhashi, A., Kono, I., Kinugasa, Y. 2005. Geological Development of the West Sea Area of the Noto Peninsula District in the Neogene Tertiary to Quaternary, Central Japan. Journal of Geography 114(5), 791–810, https://doi.org/10.5026/jgeography.114.5_791.

Kato, A., Sakai, S., Iidaka, T., Iwasaki, T., Kurashimo, E., Igarashi, T., Hirata, N., Kanazawa, T., and the Group for the aftershock observations of the 2007 Noto Hanto Earthquake (2008): Three-dimensional velocity structure in the source region of the Noto Hanto Earthquake in 2007 imaged by a dense seismic observation. Earth, Planets and Space 60, 105–110, https://doi.org/10.1186/BF03352769.

Keefer, D. K. (2000): Statistical analysis of an earthquake-induced landslide distribution: the 1989 Loma Prieta, California Event. Engineering Geology 58(3–4), 231–249, https://doi.org/10.1016/S0013-7952(00)00037-5.

Malamud, B. D., Turcotte, D. L., Guzzetti, F., Reichenbach, P. (2004): Landslides, earthquakes and erosion, Earth and Planetary Science Letters 229(1–2), 45–59, https://doi.org/10.1016/j.epsl.2004.10.018.

Massey, C., Townsend, D., Rathje, E., Allstadt, K. E., Lukovic, B., Kaneko, Y., Bradley, B., Wartman, J., Jibson, R. W., Petley, D. N., Horspool, N., Hamling, I., Carey, J., Cox, S., Davidson, J., Dellow, S., Godt, J. W., Holden, C., Jones, J., Kaiser, A., Little, M., Lyndsell, B., McColl, S., Morgenstern, R., Rengers, F. K., Rhoades, D., Rosser, B., Strong, D., Singeisen, C., Villeneuve, M. (2018): Landslides Triggered by the 14 November 2016 M_w 7.8 Kaikōura Earthquake, New Zealand. Bulletin of the Seismological Society of America 108 (3B), 1630–1648, https://doi.org/10.1785/0120170305.

Murakami, Y., Mizugaki, S., Fujinami, T. (2022): Quantification of sediment and fallen trees generated by landslides in the 2018 Hokkaido Eastern Iburi Earthquake. Journal of the Japan Society of Erosion Control Engineering 74(6), 3–10.

Nakajima, J. (2022): Crustual structure beneath earthquake swarm in the Noto peninsula, Japan. Earth, Planets and Space 74, 160, https://doi.org/10.1186/s40623-022-01719-x.

Okada, Y., Ochiai, H., Kurokawa, U., Ogawa, Y., Asano, S. (2008): A channelized long run-out debris slide triggered by the Noto Hanto Earthquake in 2007, Japan.

Landslides 5, 235–239, https://doi.org/10.1007/s10346-007-0090-3.
Radix. Power, Prestige & Forgotten Values: A Disaster Studies Manifesto. Manifesto/Accord – RADIX: Radical Interpretations of Disasters (radixonline.org) (accessed on 17. 7. 2024).
Sakai, S., Iidaka, T., Iwasaki, T., Kurashimo, E., Igarashi, T., Hirata, N., Kanazawa, T. and the group for the joint aftershock observation of the 2007 Noto Hanto Earthquake. 2008. Highly resolved distribution of aftershocks of the 2007 Noto Hanto Earthquake by a dense seismic observation. Earth, Planets and Space 60, 83–88, https://doi.org/10.1186/BF03352765.
Shishikura, M., Echigo, T., Namegaya, Y. (2009): Evidence for coseismic and aseismic uplift in the last 1000 years in the focal area of a shallow thrust earthquake on the Noto Peninsula, west-central Japan. Geophysical Research Letters 36(2), L02307, 1–5.
Tanioka, Y. (2008): Analysis of the tsunami generated by the 2007 Noto Hanto earthquake. Earth, Planets and Space 60, 123–125, https://doi.org/10.1186/BF03352772.
Towhata, I., Wang, G., Xu, Q., Massey, C. (2022): Coseismic Landslides, Phenomena, Long-Term Effects and Mitigation, https://doi.org/10.1007/978-981-19-6597-5.
Yoshikawa, T., Kano, K., Yanagisawa, Y., Komazawa, M., Joshima, M., Kikawa, E. (2020): Sumisaki, Noto-Iida, and Horyuzan Geological Map, Geological Survey of Japan, AIST.

Regionalization and analysis of rally event visitors: A case study of Czech Rally Championship events

Jakub Kura[1,2,*]

[1] Masaryk University, Department of Geography, Czechia
[2] University of Eastern Finland, Department of Geographical and Historical Studies, Finland
[*] Corresponding author: 396491@mail.muni.cz

ABSTRACT
This paper focuses on small-scale events of sport tourism, which potentially play an important role in the tourism industry of host regions by attracting a significant number of visitors. It examines seven rallying events in Czechia, seeking to determine whether these events share common characteristics or possess unique features that distinguish one from another. Utilizing online surveys, the results indicate similar patterns of different events in terms of accommodation and dining options, with only minor differences influenced by specific factors, such as event duration or importance. Notable distinctions among different events include differences in their geographical background and the average spending of visitors, with the Barum Czech Rally Zlín standing out from the other events.

KEYWORDS
small-scale events; rallying; Czechia; regionalization; sport tourism; motosport tourism

Received: 26 August 2023
Accepted: 11 September 2024
Published online: 11 October 2024

Kura, J. (2024): Regionalization and analysis of rally event visitors: A case study of Czech Rally Championship events.
AUC Geographica 60(1), 11–23
https://doi.org/10.14712/23361980.2024.13

1. Introduction

Tourism as a field provides a wide range of attractivities for visitors, and both regional and national level tourism agencies regularly publish reports with the numbers of visitors to the most visited places within a given spatial unit. Czechia is no exception – CzechTourism (2022) annually publishes a list of top 50 attractions. The number of visitors to these sites ranges from 1.7 million to 180,000 visitors a year. Furthermore, this list of attractions is divided according to various characteristics, such as region and attraction type. However, one kind of tourism attractivities is completely missing – sport tourism events. These tourism attractors could also attract large numbers of visitors, the biggest of which could have potential to be placed among the top 50 attractions. This type of tourism event attracts numbers of visitors and includes examples such as editions of the biathlon world cup in Nové Město na Moravě, where each edition is estimated to have more than 100,000 visitors in attendance (iDnes 2016; HN 2013) or Czech Grand Prix in MotoGP It used to take place at Masaryk circuit in Brno and attracted approximately 200,000–250,000 visitors (iSport 2019; BIKERACING 2008). A similar number of visitors gathers annually in Zlín region for the Barum Czech Rally Zlín (hereinafter abbreviated as BCRZ), which is nowadays presumably today's biggest small-scale event in Czechia's event tourism as the event is visited by around 250,000 visitors (Motor Max 2022). This number of attendees has been surpassed by only a few events in recent years, for instance, IIHF World Championships in 2015 and in 2004 which, respectively, attracted more than 700,000 and 500,000 visitors (IIHFWORLDS2015 2015; MSHOKEJ2004 2004). These, however, are classified as mega-events by Higham (1999).

We can conclude that sporting events have the potential to be among Czechia's top tourism attractivities and thus play an important role in the country's tourism sector. Furthermore, if we cross out mega-events, we could conclude that motoring events are among the most visited sport tourism events in Czechia. Therefore, it is quite surprising that sport events are a scarcely researched topic and only a handful of studies can be found – the majority are scholarly and focus either on motorsport or biathlon. For example, Hrušák (2013) and Píža (2013) studied BCRZ, and Kyselý (2016) compared selected sporting events, such as the Brno GP and biathlon world cup in Nové Město na Moravě. Biathlon itself was a focus of Kalousková (2016), Kutal (2014) and Klapač (2014). Most of these works, with exception of Kyselý (2016), focus on a single event and analyze it without comparison to others.

The paper therefore aims to focus on seven selected rally events held annually in Czechia with the goal of finding mutual differences and common aspects and, therefore, discovering whether rally events have unique characteristics distinguishing one event from the other or not.

2. Literature review

Visiting sporting events can be classified as participating in tourism because everyone except the locals travels to participate in sport tourism. And is doing so in accordance with UN Tourism (1995) definition of tourism: "Tourism comprises the activities of persons traveling to and staying in places outside their usual environment for not more than one consecutive year for leisure, business, and other purposes." For other authors, sport tourism is defined as a specific kind of tourism on the crossroads of sport and tourism (Galvasová 2008; Palatková and Zichová 2011; Pigeassou 2004). Deery, Jago, and Fredline (2004) add that there is constant debate as to what kind of sport can still be counted as sport tourism, whether all sport should be included or just participation in competitive sports (Neirotti, 2003). In this paper, sport tourism is defined as travel for the purpose of attending or participating in competitive sporting events.

Similarly, there are according to Hinch and Higham (2011) differences in participation – whether its active or passive. Although these categories overlap as many fall into both, Ratkowski and Ratkowska (2018) nonetheless define these two groups as "athletes" and "spectators," The majority of whom are the latter (Gibson 1998).

After defining sport tourism and its participants, another debate arises as scholars argue about the roots of sport tourism. Hinch and Higham (2011) posit that people have traveled for centuries for sport, and this habit can be dated back to Ancient Greece and its Olympic Games. The long history of sport tourism is also mentioned by Ritchie and Adair (2004), Weed and Bull (2009), and Huggins (2013). Another approach views sport tourism as a modern phenomenon, emerging with the advent of greater free time and disposable income for travel. However, scholars generally agree that sport tourism is a relatively new research field that has gained prominence in recent decades (Gibson 2017). Since then, sport has begun to be treated as a central research focus and not just a byproduct of other tourism research (Mollah, Cuskelly and Hill 2021; Ritchie and Adair 2002; Hinch and Higham 2001). The research here is focused on modern era (Huggins 2013), and since the 1980s, the majority has dealt with mega-events such as the Olympic Games of World Cups (Weed 2009).

Sport tourism, as a part of event tourism, has similar traits to other types, such as event or festival tourism, because it could work as a tool for promoting region or creating a destination image (Harcup 2000; Dychkovskyy and Ivanov 2020; Pioš, Skoczylas and BrzeziñSka-Wójcik 2014). Like other forms of event tourism, sport tourism is frequently analyzed in terms

of its economic impact, particularly the financial benefits it brings to the host region. This includes economic contributions from both the event and public sector support (Brown et al. 2015; Dwyer, Jago and Forsyth 2016; Chung, Hou and Kuo 2011). Contrariwise, there are also aspects that differentiate sport tourism from other forms. The main difference is target audience and hence target visitors, as each kind of event has a (slightly) different target audience. This results in differences in length of stay, loyalty to the event, or participant preferences when choosing accommodation or dining (Pioš, Skoczylas and BrzeziñSka-Wójcik 2014; Ferrucci et al. 2021; Gomez-Casero et al. 2020; Cudny, Jolliffe and Guz 2022).

Focusing on motorsport, most scholars study the biggest events, such as Formula 1 or World Rally Championship (WRC). Nonetheless, these events are still small-scale events according to Higham (1999) as they do not fulfill the characteristics of mega-events. Although the initial expenditures required for a new destination to host such an event are quite high, as it usually requires building new facilities to required standards of the series, after this initial expenditure, the benefits of small-scale events start to apply. The venues are constructed for long-term use, unlike certain one-time mega-events like the Olympic Games. Circuit racing (such as Formula 1) has high expenditures for maintaining venues and facilities, but as was previously mentioned, these facilities are intended for use across multiple editions of the event. In recent years, the initial expenditures have also often been funded by the public sector with the aim of promoting the country or region and increasing tourism (Ramasamy and Yeung 2020; Henderson et al. 2010; Ramasamy, Wu and Yeung 2020; Galliera 2006; Larasati, Mahadewi and Surata 2023; Nugroho and Pradini 2022). Circuit racing is hence the most popular in academia research.

In rallying, a similar trend found in circuits starts to emerge as most scholars focus on the biggest events from the WRC (Hassan and McCulloch 2007, 2008; Hassan and O'Connor 2009; Naess 2014). These scholars usually study the geographical background of the events and the visitors' sociology, such as what motivates fans to visit the event. The economic aspects of organizing these events are also popular, with attention paid to estimating visitor spending at the events or the benefits supporting these events brings to the public sector. Finally, scholars deal with the role rally events play in regional tourism.

Only a handful scholars focus on smaller events. Hassan and O'Connor (2007), for example, conducted research on the French national event Rally Le Torquet in addition to the WRC events. Barajas, Coates, and Sanchez-Fernandez (2016) and their study of the Spanish championship event Rally Ourense is another example. In Czechia, there is research of the BCRZ (Hrušák 2013; Píža 2013; Kura 2017), which is part of the European Rally Championship and therefore an event with importance between the WRC and national events. Aside from the two mentioned exceptions, research omits national-level events despite the economic impact and important role they play in regional tourism, according to Wilson (2006).

2.1 Importance of event size

When dividing (sporting) events by size, the starting point is the classification of Gratton, Dobson, and Shibli (2000), who categorized six major British sporting events based on economic indicators and participant numbers, establishing four event types, labeled A through D Wilson (2006) introduced a fifth category, Type E, representing minor national-level events characterized by limited economic impact and minimal media attention. This typology was fine-tuned by Duglio and Beltramo (2017) and is presented in Fig. 1.

The literature review makes clear that there is a limited body of research regarding sport tourism

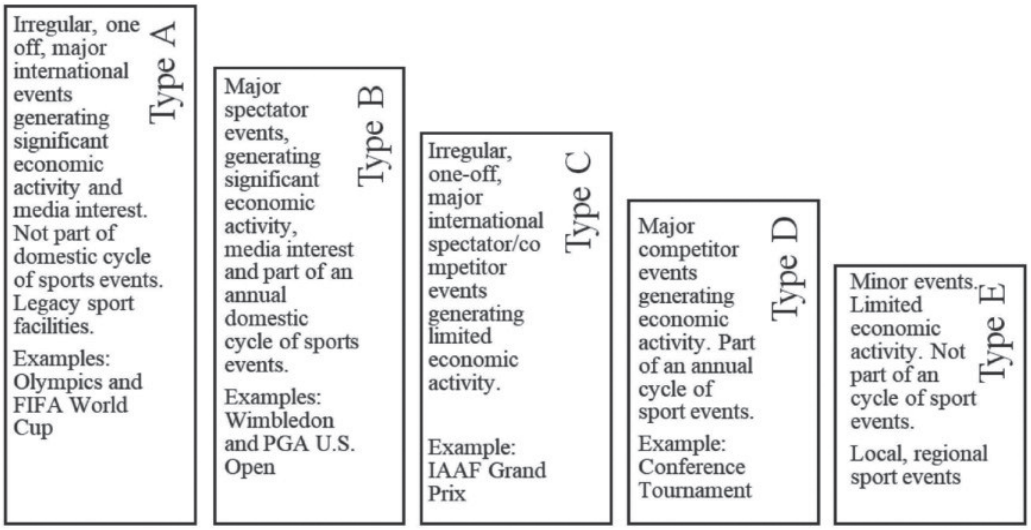

Fig. 1 Typology of events. Source: Rowley and Smith (2022)

and motoring events in general. Focusing on rallying, the literature is even more scarce. Only a handful of texts are aimed at smaller rally events like national championships. These events however could play a substantial role for the hosting region and be beneficial for it, as is shown in Fig. 1.

Therefore, this research is seeking a novel approach, the aim of which is to deepen understanding of rally events in Czechia. The primary research question aims to assess whether there are any significant differences among rallying events annually held in Czechia – a topic that has not been previously explored in academic literature. Previously, research has predominantly focused on individual events. This research contributes a novel perspective by examining multiple rallying events simultaneously. It addresses a gap in the literature by comparing the characteristics and differences of these events within the specific context of Czechia, which has not been explored previously.

To date, as previous paragraphs showed, scholarly attention has largely been directed towards comparing events mainly within WRC. However, smaller events on a regional scale have been overlooked in research endeavors. Therefore, this study fills a significant gap in the literature by conducting research at a broader level and within the specific context of Czechia, thus representing a notable advancement in the field.

3. Methodology

3.1 Events in the case study

The paper focuses on selected annual rally events with the aim of identifying their geographical background and discovering whether there are significant differences in the habits and customs of each event's visitors. As the research employs a comparative analysis, seven rally events were selected (Tab. 2 provides an overview) – some of these events were at the time also part of foreign national and international championships.

Barum Czech Rally Zlín (BCRZ) stands out as the largest event, spanning three days and annually drawing over 100 participating crews – in 2019, there were 127 crews, with 34% coming from foreign countries. In contrast, the other events listed in the MČR championship typically attract fewer than 100 participants, with Rally Bohemia having the lowest number of 68 participants. Moreover, these events tend to have a smaller proportion of foreign competitors compared to BCRZ. Rally Pačejov lasted only one day, yet it attracted the highest number of participants among all studied events, with 146 crews participating.

Regarding visitor numbers, data is often unavailable as event organizers rarely publish such figures. However, it is known that BCRZ typically draws over 200,000 visitors, with approximately one-tenth of them coming from abroad (Rally Zlín 2016). Information about visitor numbers for other events is usually found only in press releases or news articles. Generally, these events have a smaller audience compared to BCRZ. For instance, in previous years, Rally Bohemia attracted around 100,000 visitors (iDnes.cz 2013), while Rallye Český Krumlov typically sees attendance from several tens of thousands of visitors (Kudyznudy .cz 2024).

3.2 Material and Methods

Research was conducted via an online questionnaire survey utilizing a combination of closed and open-ended questions. Distribution of the questionnaire to respondents was online via the websites and social media pages of each event and via webpages focusing on rallying. Online research was selected due to the expansive nature of the research area, with events occurring throughout various times and regions of Czechia. As noted by Eysenbach and Wyatt (2002), this approach to research proves advantageous when dealing with widely dispersed research groups. Furthermore, the efficacy of online research in

Tab. 1 Brief introduction of studied events.

Event name	Center	Event period	Championship[1]
Valašská rally	Valašské Meziříčí	29. 3. – 31. 3. 2019	MČR, CRT, SK
Rally Šumava	Klatovy	26. 4. – 27. 4. 2019	MČR
Rallye Český Krumlov	Český Krumlov	17. 5. – 18. 5. 2019	MČR, CRT
Rally Hustopeče	Hustopeče	14. 6. – 15. 6. 2019	MČR, CEZ, SK
Rally Bohemia	Mladá Boleslav	12. 7. – 14. 7. 2019	MČR
Rally Pačejov	Horažďovice	26. 7. – 27. 7. 2019	RSS
BCRZ	Zlín	16. 8. – 18. 8. 2019	MČR, ERC

1 Each rally is listed in various championships with different importance. Rally Pačejov was part of the second-tier Czech championship, called RSS. Some events were part of the third-level European rally championships, the CRT or the CEZ. Rally Hustopeče and Valašská were part of the Slovak Rally Championship, and BCRZ was part of the European Rally Championship.

such scenarios has been underscored by the findings of Hickman et al. (2019) and Milković et al. (2023).

Scholars also mention that using online surveying is beneficial for targeting desired research group and controlling the sample while including fewer mistakes, blank items, and item refusals (Nayak and Narayan 2019). On the flip side, it's crucial to acknowledge the limitations inherent in this type of research, particularly the limited ability for researchers to influence the research audience. Menon et al. (2020) highlighted that online surveying relying on voluntary participation faces limitations due to unknown target populations and potentially biased samples. This sentiment was echoed by Azzam and Jacobson (2013) and Akbulut (2015), who emphasized the importance for researchers to exercise caution when interpreting data collected through online questionnaires, as response biases may skew the results.

To ensure the quality of the data collected through online surveying and to address the potential limitations mentioned earlier, questionnaires from BCRZ were compared with the results of the authors' previous research conducted at Barum Czech Rally Zlín (Kura 2017), where data were gathered both online and in-person. In that study, the data from offline surveying did not show any significant difference from those gathered online. Therefore, in line with Yu et al. (2022) or Gosling et al. (2004), it can be argued that the benefits of online surveying outweigh possible limitations. Moreover, in the context of rally research, such limitations did not seem to influence the results.

The questioning was conducted mainly in the week following each given event; thus, respondents had all the information needed to complete the questionnaire in their recent memory, ensuring minimal risk of a memory fade bias. To ensure that the data gathered would have enough representativeness, a demographic distribution of respondents was compared to other rally events in Czechia (Píža 2013; Hrušák 2013; Kura 2017) and internationally (Hassan and O'Connor 2009; Hassan and McCulloch 2007, 2008; Barajas, Coates and Sanchez-Fernandes 2016) without any significant difference. To ensure the representativeness of the sample at least two hundred questionnaires were gathered from each rally event, approximately 1% of the unique visitors from each rallying event.

In Tab. 2 are provided short demographic characteristics of the respondents. Several patterns emerge in the structure of the respondents: the data shows that rallying is still a male-dominant sport and, for all the events, the majority of visitors are male, which is in accordance with other rally events studied (Píža 2013; Hassan and McCulloch 2007; Hassan and O'Connor 2009). Visitors to rally events studied show no difference to previous scholars in age structure either, with the dominant group being of productive age between 20 and 35 years. The research mentioned above did not deal with the education of the respondents; therefore, only Czech events were compared. The data showed that an ISCED 2011 level 3 of education (upper secondary education) prevails, a similar structure of education to the Czech population – the most recent census showed that 63% of Czech inhabitants had finished ISED 2011 Level 3 of education (CSU 2023).

Tab. 2 Structure of respondents.

Category	Valašská rally	Rally Šumava	Rallye Český Krumlov	Rally Hustopeče	Rally Bohemia	Rally Pačejov	BCRZ
Gender							
Male	91.1%	87.8%	82.2%	88.7%	86.7%	89.9%	88.2%
Female	8.9%	12.2%	17.8%	11.3%	13.3%	10.1%	11.8%
Age							
Younger than 16	0.0%	0.0%	0.0%	0.0%	0.0%	0.0%	2.5%
16–25	23.8%	20.3%	18.4%	19.1%	19.3%	14.7%	27.7%
26–35	36.3%	32.9%	38.5%	37.4%	30.9%	35.6%	28.8%
36–45	23.3%	23.8%	22.6%	16.6%	23.2%	18.7%	23.2%
46–55	10.7%	11.5%	12.3%	16.5%	12.7%	15.5%	12.8%
56 and older	5.9%	11.5%	8.2%	10.4%	13.9%	15.5%	5.0%
Education (ISCED 2011)							
Level 2/ lower secondary education	4.1%	6.1%	4.1%	4.3%	7.4%	8.6%	7.1%
Level 3/ upper secondary education	77.4%	75.6%	80.2%	73.1%	79.3%	71.9%	69.4%
Higher	18.5%	18.3%	15.7%	22.6%	13.3%	19.5%	23.5%

Source: our questionnaire survey

The questionnaire itself was constituted of five parts, with each focusing on a distinctive topic area. The initial part of the questionnaire focused on transportation methods and the place of origin of the visitors. The subsequent part sought to comprehend the habits and customs of the spectators during their time in the event's hosting region, with particular emphasis on their choice of accommodation, food consumption, and other activities tied to the rally combined with an estimation of their spending for these services. It also asked whether the rally was the sole reason for their visit to the hosting region.

The two following parts of the questionnaire were focused on aspects not connected with this paper, such as reasons to visit the region besides the rally. The concluding section of the survey collected demographic details, such as respondent age, gender, and educational background. In total, 2,300 questionnaires were gathered for the research, with 887 respondents gathered from events other than the BCRZ, the latter was at the center of other research being conducted by the author, and therefore subject to more profound questioning with a bigger research sample.

Various statistical analyses were utilized to analyze the data according to the nature of each question on the questionnaire. For the numerical variables, such as distance traveled to the event center or length of stay at the event, the data were first checked by Shapiro-Wilk test as to whether they were distributed normally. As the data for numerical variables in all questions showed abnormal distribution, a Kruskal-Wallis test was used to determine whether there were statistically significant differences between the events. To learn the differences between the exact events, a Mann-Whitney U test (with Bonferoni correction) was additionally applied. Additionally, a Chi-square test was used to find out the independence of the data where it was suitable.

4. Results

As respondents specified their place of residence, it was possible to measure the distance traveled to the event center. These distances are averaged as a person traveling, for example, to Mladá Boleslav from the south of Prague would cover a few kilometers more than a person traveling from the north of Prague. The general summary about travel to the events is showed in the table 3 below.

The distances traveled to each event were first examined using a basic statistical analysis to determine the median and average values. As is shown in the Fig. 2 map, distance decay plays a role as most visitors arrive at the events from neighboring municipalities. Three groups of events could be differentiated according to average travel distance. The highest average distance was BCRZ, which is the most international event and has a significant share of visitors from abroad. The second group of events consists of the Valašská rally, Rally Hustopeče, and Rallye Český Krumlov, with an average traveled distance hovering around 100 km. The last three events have the smallest reach as these are not part of any international championship. Using the Kruskal-Wallis test indicated statistically significant differences among the events ($H (6, n = 1109) = 17.457$, $p = 0.00774$). These differences were observed only among some of the events according to post-hoc pair-wise Mann-Whitney U test (with Bonferroni correction for multiple testing). Differences were found between Rally Hustopeče and following events: Rallye Šumava ($p = 0.012$), Rally Bohemia ($p = 0.0045$) and Rally Pačejov ($p = 0.012$). In conclusion, while differences were observed in the average distance traveled to each event, only Rally Hustopeče displayed statistically significant differences when compared to the other events.

As more than half of the visitors were not local (locals were defined as respondents living in the LAU1 where the city with the rally center is located) respondents were asked what their primary reason was for arriving at the event region. A Chi-Square test ($\chi^2 (6, N = 802) = 14.77$, $p = .022$) revealed a statistically significant association between visitors' arrival in the region and their participation in the rally. This suggests that the rally events are a key driver of local tourism, attracting visitors who would not have otherwise traveled to the region. In other words, the rally events were an important player in local tourism as they attracted a number of visitors who otherwise would not have come without the rally. To further explore the significant differences in motivations for attending motorsport events, a post-hoc analysis using adjusted residuals was performed. Two events emerged with notable deviations from expected frequencies. The Valašská Rally showed a significantly higher number of respondents indicating the rally as their sole reason for visiting the region (Adjusted Residual = +1.59), while fewer respondents than expected cited additional reasons for their attendance (Adjusted Residual = −1.87). On the other hand, Rallye

Tab. 3 Distance traveled to the center (see Tab. 1) of each event.

	Valašská rally	Rally Šumava	Rallye Český Krumlov	Rally Hustopeče	Rally Bohemia	Rally Pačejov	BCRZ
Median	60	48.5	50	97	50	52	153
Average	95.80	85.68	102.35	127.59	80.15	81.57	207.57

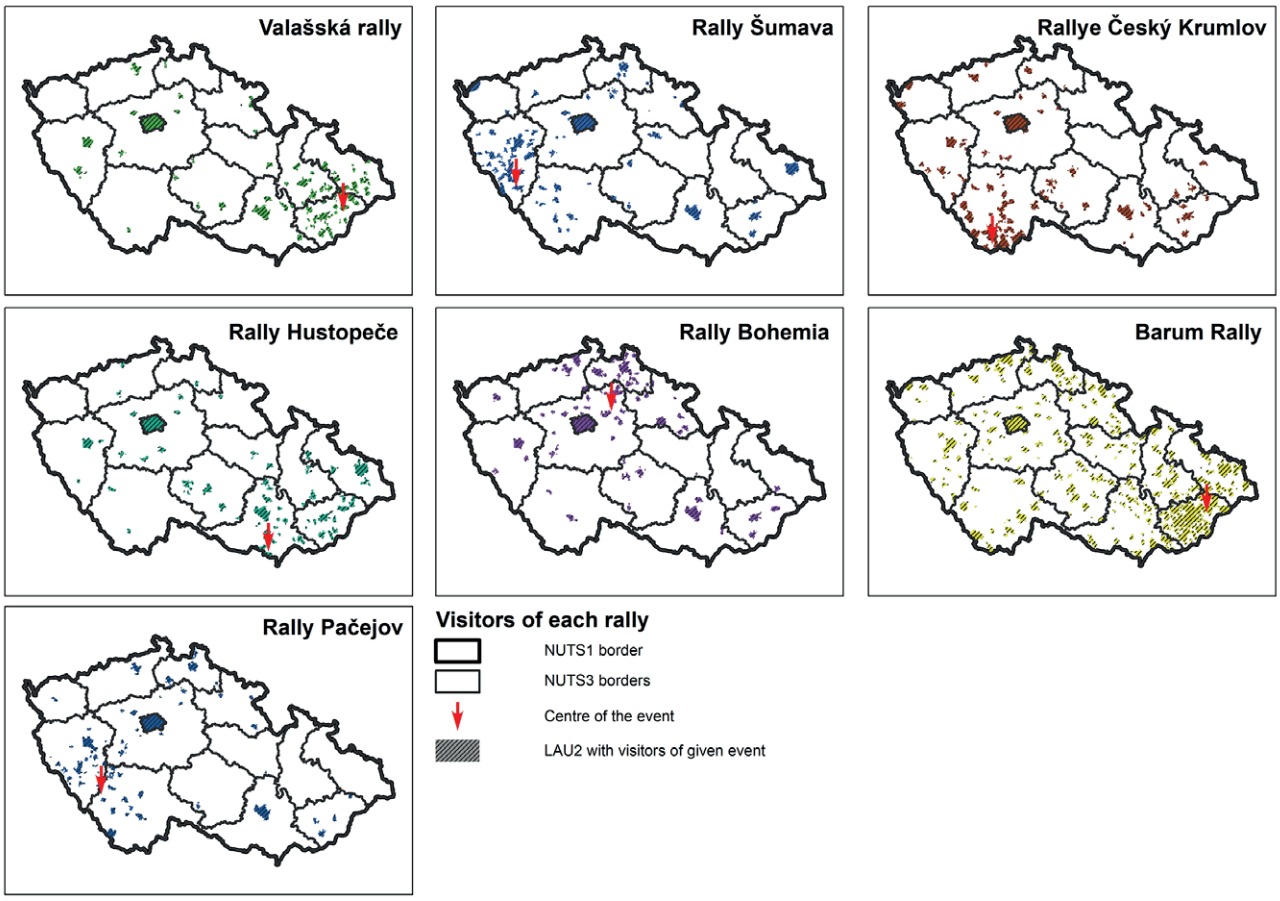

Fig. 2 Geographical distribution of event visitors.

Šumava had fewer respondents than expected attending solely for the rally (Adjusted Residual = −1.21) and more attendees for other reasons (Adjusted Residual = +1.43).

Fig. 3 provides insight into the length of stay. The key factor influencing the length of stay was the duration of the event itself (shown in Tab. 1). The majority of events span two days, with only BCRZ lasting three days, while Rally Pačejov is a single-day event. To analyze potential differences among the events, focus was put on whether there are variations in the duration of attendees' stay beyond the event's scheduled duration. The results of the chi-square test of independence for the categorized stay data indicated a significant association between event type and the decision to extend the stay (χ^2 (6, N = 802) = 193.43, p < .00001).

At Rally Hustopeče, nearly 90% of attendees extended their stay beyond the event's scheduled duration, making it the event with the highest

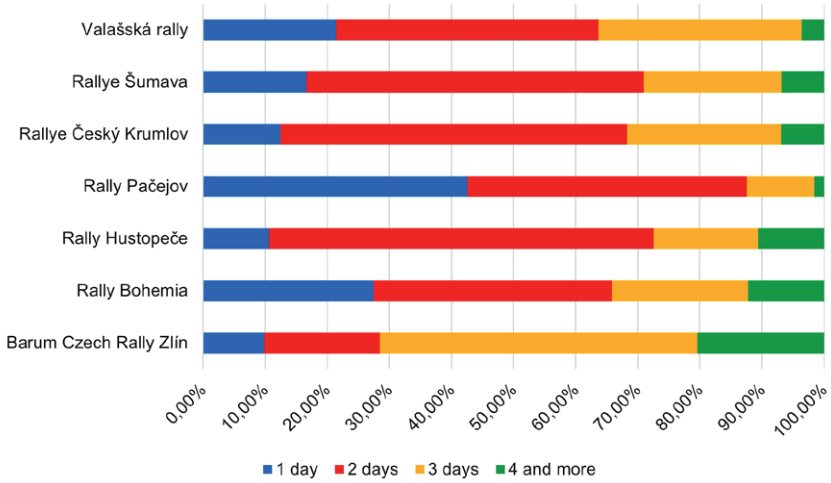

Fig. 3 Length of stay among visitors per event.

likelihood of prolonged visits among all those studied. In contrast, at Rally Pačejov, only 12% of respondents extended their stay beyond the event day. For the remaining events, approximately one-third of attendees prolonged their stay.

Regarding the shortening of stay, this trend is most notable at Rally Bohemia and BCRZ, where around one-quarter of visitors opted for a shorter duration than the event's scheduled length.

4.1 Habits and customs during the rally visit

Two basic categories of habits and customs, obtaining (a) accommodation and (b) dining, during the events were observed. Focusing on accommodation options, the first notable finding was that the most frequent option is returning home. Accommodation was also affected by the duration of the event. Two-thirds of the visitors to Rally Pačejov spent the night at home as the event was only a single day. For the rest of the events, at least 40% of the visitors returned home every night. From a geographical perspective, there is clearly a visible difference in distance between the event center and the place of residence. Visitors spending only a day at the event venue are willing to travel approximately 55 km, whereas those spending two or more days at the event and still returning home travel nightly on average only 35 km.

A chi-square test of independence was conducted to evaluate the relationship between event types and attendees' accommodation preferences. The test revealed statistically significant differences among the events (χ^2 (48, N = 802) = 343.65, p < .00001) and post-Hoc Analysis with Adjusted Residuals showed which events. Invelt Rally Pačejov showed a significant tendency for attendees to participate only during the day and not stay overnight (Adjusted Residual = 5.06). Several events showed unique patterns in accommodation types that significantly differed from expected values under the hypothesis of independence (χ^2 (48, N = 802) = 343.65, p < .00001). The type of accommodation which significantly differed was sleeping in cars or in tents for the BCRZ (Adjusted Residual = 2.39). At Rally Hustopeče more attendees than expected stayed in hotels (Adjusted Residual = 2.45).

As regards obtaining food and drinks, the questionnaire respondents were able to combine given options and, therefore, in order to summarize, each occurrence of each individual option was counted to get a distribution of popularity for each option.

An overview of the usage of each dining option is provided in Fig. 4. In general, the most popular option was using the food stalls at the event location. A Chi-Square test was used to learn whether there is a significant association between the event and the dining options preferred by the respondents. The results indicated no statistically significant association between the type of event and the chosen dining options (χ^2 (18, N = 802) = 20.14, p = .325) and suggested that the share of each dining option is consistent across events. It could be therefore assumed that the visitors to all the studied events have similar habits and the differences among them are statistically insignificant.

4.2 Economic aspects of rally events

Small-scale events can have a smaller but stable economic impact on the hosting region and scholars utilized the economic impact of events as a differing factor for dividing events into types. Due to the lack of the data about exact number of visitors, this research was only able to estimate the average spending per person per day.

In the questionnaires, the respondents wrote down their average daily spending on (1) accommodation, (2) food and drinks, and (3) other expenses such as fuel, entry fees, car rental, and various other possible expenses related to their stay at the event. For each of these three categories, the respondents were given spending intervals, and they filled in the expenditures

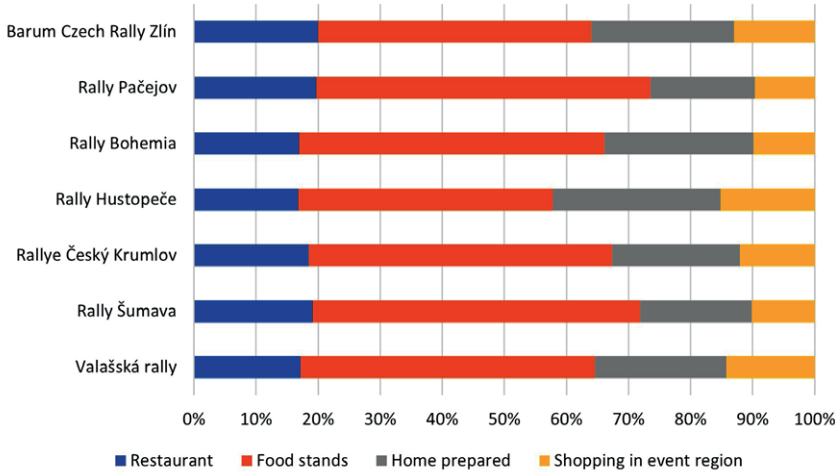

Fig. 4 Share of food and drink obtaining options among visitors at each event.

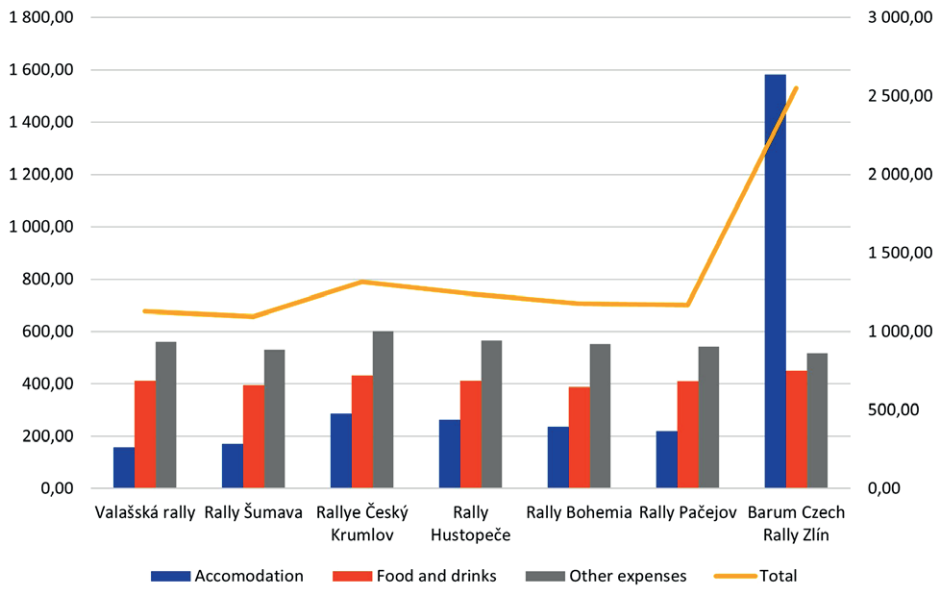

Fig. 5 Structure of spending in CZK among visitors of each event.

incurred most often for each kind. As Fig. 5 shows, overall, one event differs from the rest: BCRZ.

Switching our focus to the other events, the average daily spending per person is 1,200 CZK and all events differ from this mean value by a maximum of 120 CZK. The highest spending among the remaining events was by visitors of Rallye Český Krumlov, which, as was shown in Table 2, has the largest average geographical background among the remaining events.

For all the studied events, there is a high portion of those who return home for the night (40% or more depending on the event, as was discussed in the previous section); therefore, those who spent nothing on accommodation and other goods were excluded. Despite this, the same pattern emerges: BCRZ is by far the event with the highest spending and Rally Hustopeče follows. The difference between the events when BCRZ is not included is nearly the same, with differences of approximately 10%.

5. Discussion

The paper focuses on selected events from the Czech Rally Championship with the aim of finding out the geographical and tourism habits of their visitors. Each event was studied via a questionnaire that was conducted online during and after each event. This type of research was chosen with consideration for both the benefits and limitations of online questioning. Given the wide range of potential respondents, online surveying offered a cost-effective means of reaching this audience, as demonstrated by studies such as those by Hickman et al. (2019) and Milković et al. (2023). However, potential biases resulting from the semi-unknown audience and the method of questionnaire distribution, as highlighted by Azzam and Jacobson (2013) and Akbulut (2015), were carefully considered. A sample of results was compared to previous research conducted by the author (Kura 2017), where part of the questionnaires was collected in-person. Since no significant differences were found between the samples, it can be inferred that these limitations of the research were effectively mitigated.

The first analysis of geographical background and travel distance suggests that the events can be categorized into three distinct groups based on their reach and visitor distribution (Fig. 2). In this stage of the research, BCRZ stood out. However, further statistical analysis using the Mann-Whitney U test (with Bonferroni correction) indicated that Rally Hustopeče was the only event that significantly differed from the others. This is probably caused by the location of the event and its listing in both the Czech and Slovak rally championships, which resulted in different arrival patterns among its visitors and thus larger distances traveled. Another reason could also the fact, that the results suggested that Rally Hustopeče has the highest portion of visitors who exhibited likelihood to prolong their stay in the region beside the rally.

Focusing back on the purely geographical background of the events, besides BCRZ, the remaining events show a relatively uniform pattern, with the majority of visitors coming to these rally events from the hosting region or those that border it. For all the studied events, there was no difference from other scholars dealing with rallying (Hassan and McCulloch 2007; Hassan and O'Connor 2009) in the fact that the event itself is the main reason the visitors come to the hosting region. This result was also found out by scholars focusing on Barum Czech Rally Zlín (Píža 2013; Hrušák 2013) when focusing on the structure of visitors of the BCRZ. These findings underscore the significant role that rallying events play in driving tourism in the host regions, particularly by attracting visitors who might not otherwise travel to these

areas (Egresi and Kara 2014; Nicholson and Pearce 2001). Thus, it could be concluded that rally events bring a significant number of visitors to the hosting region who would otherwise not come. This observation is further strengthened by the statistically significant association found between visitors' arrival to the region and their attendance at the rally. The results suggest that a significant portion of visitors would not have come to the region in the absence of the rally, highlighting the direct contribution of these events to local tourism. This underscores the direct impact of the rallying events on tourism in the region, supporting the importance and relevance of the study's focus on these events.

The focus of the research on the length of stay at the event centered on whether respondents chose to extend or shorten their stay in the region beyond the duration of the event. The chi-square test of independence for the categorized stay data revealed a significant association between event type and the decision to extend the stay.

Rally Hustopeče again demonstrated the highest likelihood of attendees extending their stay, possibly due to factors such as its cross-border appeal and dual inclusion in both the Czech and Slovak rally championships. Conversely, Rally Pačejov exhibited a lower likelihood of stay extension. This could possibly be attributed to the fact that in the year of the research, the event lasted only one day. Therefore, respondents may have attended solely for that day and did not seek accommodation, returning home after the event concluded.

As regards accommodation and dining options, there are mostly similarities among the events, with just a few differences. As a relatively high proportion of the visitors to all the studied events are based in the hosting region, the most frequent option for spending the night is to return home. However, there are differences between those who spend one day at the event and those who spend more days as the latter on average travel half the distance to the event center in comparison to those who come for just one day. Besides this accommodation option, the most popular choice is to spend the night in hotels, with only a few differences among the events emerging. For BCRZ and Rally Pačejov, there is a statistically significant number of those who visit the event for only one day, whereas Rallye Český Krumlov and Rally Hustopeče have a significantly different option of tenting near the special stages. All the events share the same patterns of visitor habits with respect to dining options, with the majority preferring food stands at the event venue followed by the consummation of food prepared at home and then restaurants.

Last but not least, the paper estimated visitors spending during the events and found that the highest average spending is made by visitors to BCRZ as it is the event with the greatest share of hotel usage, which is clearly visible in the average daily spending on accommodation. It is this specific spending category that explains why the BCRZ is so different from other events as the remaining expenditures are quite similar to the rest of the studied events. Like previous research focusing on this event (Hrušák 2013; Píža 2013; Kura 2017) has shown, this event has also a broader geographical background of visitors and a higher share of the foreign visitors who tend to spend more. There were no statistically significant differences in spending among the remaining events, with Rallye Český Krumlov having highest spending if the rest as it an event with broader geographical background.

6. Conclusion

This paper contributes to the existing body of knowledge and supports the further understanding of the role of small-scale events. By focusing on seven rally events held annually in Czechia, the paper aims to broaden the understanding of these kinds of events as most scholars in tourism research focus on mega-events and study them as individual and unique events without comparisons (Ramasamy and Yeung 2020; Henderson et al. 2010; Larasati, Mahadewi and Surata 2023; Nugroho and Pradini, 2022).

There are, of course, several studies comparing rallying events, but these focus on comparing events of world importance (Hassan and McCulloch 2007, 008; Hassan and O'Connor, 200) and just a handful of research is focused on national-level events (Barajas, Coates and Sanchez-Fernandez 2016). These should be perceived as typical small-scale events, somewhere between Gratton, Dobson, and Shibli's (2000) Type D classification and the Type E events added by Wilson (2006).

The results showed that among the studied events, there are no great differences between them, and the significant differences were solely in small aspects of the visitors' behavior.

The results of the study are constrained by the focus on the visitors of these events, and thus the findings apply to these attendees. Moreover, there could be limits caused by the questionnaire, which focused on the measurable aspects of the visitors' behavior. It did not focus on deeper motivations and explanations for visitor behavior during the event visits. This could be understood as a limitation of online research, which was focused on getting a broad sample of respondents so as to identify the general characteristics of the event visitors.

Future research should focus on possible changes in the visitors to the events according to changes in the championship status of the event or on the long-term analysis of visitors who attend these events to provide more durable and more profound insights into the evolving pattern of visitor behavior and their spending patterns.

Acknowledgements

The paper was written within the project "MUNI/A/1469/2023 Geographical Research on Social and Natural Processes in Times of Change" (specific research), which will be implemented in 2023 by the Institute of Geography, Faculty of Science, Masaryk University.

References

Akbulut, Y. (2015): Predictors of inconsistent responding in web surveys. Internet Research 25(1), 131–147, https://doi.org/10.1108/intr-01-2014-0017.

Azzam, T., Jacobson, M. R. (2013): Finding a comparison group. American Journal of Evaluation 34(3), 372–384, https://doi.org/10.1177/1098214013490223.

Barajas, A., Coates, D., Sanchez-Fernandez, P. (2015): Beyond retrospective assessment sport event economic impact studies as a management tool for informing event organization. European Research on Management and Business Economics 22(3), 124–130, https://doi.org/10.1016/j.iedee.2015.05.001.

Bikeracing (2008): Návštěvnost Cardion ab Grand Prix zlomila další record. Available online: https://www.bikeracing.cz/moto-racing/road-racing/motogp/navstevnost-cardion-ab-grand-prix-zlomila-dalsi-rekord-a1466/ (accessed on 31. 7. 2023).

Brown, S., Getz, D., Pettersson, R., Wallstam, M. (2015): Event evaluation: Definitions, concepts and a state of the art review. International Journal of Event and Festival Management 6(2), 135-157, https://doi.org/10.1108/IJEFM-03-2015-0014.

CSU (2023): Sčítání 2021: Vzdělání. Available online: https://www.scitani.cz/vzdelani (accessed on 1. 8. 2023).

Cudny, W., Jolliffe, L., Guz, A. (2022): Heritage event as tourist attraction: The case of Dymarki Swietokrzyskie, Poland. GeoJournal 87, 2975–2992, https://doi.org/10.1007/s10708-021-10407-4.

CzechTourism (2022): Turisté mají v České republice nejraději zoologické zahrady, technické památky, koupání a Pražský hrad. Available online: https://www.czechtourism.cz/cs-CZ/a379e3ab-cae1-419c-9094-6a8f4f244128/article/turiste-maji-v-ceske-republice-nejradeji-zoologick (accessed on 31. 7. 2023).

Deery, M., Jago, L., Fredline, L. (2004): Sport tourism or event tourism: are they one and the same? Journal of Sport & Tourism 9(3), 235–245, https://doi.org/10.1080/1477508042000320250.

Duglio, S., Beltramo, R. (2017): Estimating the Economic Impacts of a Small-Scale Sport Tourism Event: The Case of the Italo-Swiss Mountain Trail CollonTrek. Sustanability 9(3), 343–359, https://doi.org/10.3390/su9030343.

Dwyer, L., Jago, L., Forsyth, P. (2016): Economic evaluation of special events: Reconciling economic impact and cost–benefit analysis. Scandinavian Journal of Hospitality and Tourism, 16(2), 115–129, https://doi.org/10.1080/15022250.2015.1116404.

Dychkovskyy, S., Ivanov, S. (2020): Festival tourism as part of international tourism and a factor in the development of cultural tourism. Information & Media 89, 73–82, https://doi.org/10.15388/Im.2020.89.41.

Egresi, I., Kara, F. (2014): Motives of Tourists Attending Small-scale Evens: The Case of Three Local Festivals and Events in Istanbul, Turkey. GeoJournal of Tourism 14(2), 93–110.

Eysenbach, G., Wyatt, J. (2002): Using the internet for surveys and health research. Journal of Medical Internet Research 4(2): e13, https://doi.org/10.2196/jmir.4.2.e13.

Ferrucci, L., Rodriguez, M. C., Sarti, S., Splendiani, S. (2021): Segmenting cultural event visitors using the latent class approach: the case of "Sensational Umbria" photo exhibition by Steve McCurry. Il Capitale Culturale. Studies on the Value of Cultural Heritage (24), 261–292.

Gosling, S. D., Vazire, S., Srivastava, S., John, O. P. (2004): Should we trust web-based studies? A comparative analysis of six preconceptions about internet questionnaires. American psychologist 59(2), 93–104, https://doi.org/10.1037/0003-066X.59.2.93.

Hickman, E., Kharouf, H., Sekhon, H. (2019): An omnichannel approach to retailing: demystifying and identifying the factors influencing an omnichannel experience. The International Review of Retail, Distribution and Consumer Research 30(3), 266–288, https://doi.org/10.1080/09593969.2019.1694562.

Galliera, E. (2006): The Creation of an Event in Order to Promote Tourism: The Moto GP in Misano.

Galvasová, I., Binek, J., Holeček, J., Chabičovská, K., Szczyrba, Z. (2008): Průmysl cestovního ruchu. Ministerstvo pro místní rozvoj ČR, Praha.

Gibson, H. J. (1998): Active sport tourism: who participates? Leisure Studies 17(2), 155–170, https://doi.org/10.1080/026143698375213.

Gibson, H. (2017): Sport tourism and theory and other developments: Some reflections. Journal of Sport & Tourism 21(2), 153–158, https://doi.org/10.1080/14775085.2017.1319514.

Gomez-Casero, G., Jara Alba, C. A., López-Guzman, T., Pérez Gálvez, J. C. (2020): Theatre festival as a tourist attraction: A case study of Almagro International Classical Theatre Festival, Spain. International Journal of Culture, Tourism and Hospitality Research 14(4), 599–617, https://doi.org/10.1108/IJCTHR-04-2019-0061.

Gratton, C., Dobson, N., Shibli, S. (2000): The economic importance of major sports events: a case-study of six events. Managing Leisure 5(1), 17–28, https://doi.org/10.1080/136067100375713.

Harcup, T. (2000): Re-imaging a post-industrial city: The Leeds St Valentine's Fair as a civic spectacle. City 4(2), 215–231, https://doi.org/10.1080/13604810050147839.

Hassan, D., McCulloch, D. (2007): An Economic Impact Study of Round 15 of the World Rally Championship 2007: Rally Ireland. Rally Ireland.

Hassan, D., McCulloch, D. (2008): A report examining the socio-economic impact of the World Rally Championship 2007. University of Ulster, Ulster.

Hassan, D., O'Connor, S. (2009): The socio-economic impact of the FIA World Rally Championship 2007. Sport in Society 12(6), 709–724, https://doi.org/10.1080/17430430902944134.

Henderson, J. C., Foo, K., Lim, H., Yip, S. (2010): Sports events and tourism: The Singapore formula one grand prix. International Journal of Event and Festival Management 1(1), 60–73, https://doi.org/10.1108/17852951011029306.

Higham, J. (1999): Commentary – Sport as an Avenue of Tourism Development: An Analysis of the Positive and Negative Impacts of Sport Tourism. Current Issues in Tourism 2(1), 82–90, https://doi.org/10.1080/13683509908667845.

Hinch, T. D., Higham, J. E. (2001): Sport tourism: A framework for research. International Journal of Tourism Research 3(1), 45–58, https://doi.org/10.1002/1522-1970(200101/02)3:1<45::AID-JTR243>3.0.CO;2-A.

Hinch, T., Higham, J. (2011): Sport tourism development. Channel View Publications, Clevedon.

HN (2013): Šampionát biatlonistů v Novém Městě na Moravě čeká 150 tisíc návštěvníků. Available online: https://hn.cz/ostatni-sporty/c1-59177790-sampionat-biatlonistu-v-novem-meste-na-morave-ceka-150-tisic-navstevniku (accessed on 31. 7. 2023).

Hrušák, J. (2013): Význam BCRZ pro cestovní ruch Zlínského kraje [Master thesis]. Univerzita Palackého v Olomouci (in Czech).

Huggins, M. (2013): Sport, tourism and history: current historiography and future prospects. Journal of Tourism History 5(2), 107–130, https://doi.org/10.1080/1755182X.2013.828782.

Chung, M. L., Hou, Y. H., Kuo, C. T. (2011): The study of tourism economic benefits and consumer behavior on the religion culture festival activities and its innovation marketing strategies management from the Dajia Jenn Lann Temple, Beigang Chao Tian Temple, and Lugang Tin Hau Temple as examples. IEEE International Summer Conference of Asia Pacific Business Innovation and Technology Management, Dalian, China, 183–187, https://doi.org/10.1109/APBITM.2011.5996319.

iDnes.cz (2013): Rallye Bohemia uvidí až sto tisíc lidí, odhaduje šéf závodu. Available online: https://www.idnes.cz/sport/motorsport/rallye-bohemia-rozhovor-se-sefem-zavodu.A130710_1949613_motorsport_bem (accessed on 13. 4. 2024).

iDnes (2016): POHLED: Češi v Novém Městě vyhráli. Už předtím, než přijela Koukalová. Available online: https://www.idnes.cz/sport/biatlon/biatlon-nove-mesto-na-morave.A161218_212452_biatlon_par (accessed on 31. 7. 2023).

IIHFWORLDS2015 (2015): Attendance record broken. Available online: http://www.iihfworlds2015.com/en/news/attendance-record-broken (accessed on 20.6.2023).

iSport (2019): Moto GP v Brně nalákalo přes 186 tisíc diváků, návštěvnost potěšila primátorku. Available online: https://isport.blesk.cz/clanek/ostatni-motorismus-moto-gp/366894/moto-gp-v-brne-nalakalo-pres-186-tisic-divaku-navstevnost-potesila-primatorku.html (accessed on 31. 7. 2023).

Kalousková, M (2016): Přínosy event marketingu pro destinaci [Master thesis]. Vysoká škola hotelová v Praze (in Czech).

Klapač, K. (2014): Přínosy Mistrovství světa v biatlonu v Novém Městě na Moravě [Master thesis]. Masarykova Univerzita (in Czech).

Kura, J. (2017): S vůní benzínu – návštěvnost motoristických akcí [Master thesis]. Masarykova Univerzita (in Czech).

Kudyznudy.cz (2024): Rallye Český Krumlov 2024. Available online: https://www.kudyznudy.cz/akce/rallye-cesky-krumlov-4 (accessed on 13. 4. 2024).

Kutal, P. (2014): Marketingová komunikace sportovní akce [Master thesis]. Technická univerzita v Liberci (in Czech).

Kyselý, J. (2016): Geografická analýza vybraných sportovních akcí v ČR a jejich možné dopady na rozvoj regionu [Bachelor thesis]. Masarykova Univerzita (in Czech).

Larasati, M. R. P., Mahadewi, N. A. M. E., Surata, I. N. (2023): The Role of Sports Events as an Alternative Tourism in Lombok: A Case Study of the Implementation of the MOTO GP Mandalika. Jurnal Bisnis dan Manajemen 3(3), 373–393.

Menon, V., Zothangliana, R., Andrade, C. (2020): Depression during the pandemic in turkey. International Journal of Social Psychiatry 67(7), 957–957, https://doi.org/10.1177/0020764020965991.

Jelić Milković, S., Lončarić, R., Kralik, I., Kristić, J., Crnčan, A., Djurkin Kušec, I. Canavari, M. (2023): Consumers' preference for the consumption of the fresh black slavonian pig's meat. Foods 12(6): 1255, https://doi.org/10.3390/foods12061255.

Mollah, M. R. A., Cuskelly, G., Hill, B. (2021): Sport tourism collaboration: A systematic quantitative literature review. Journal of Sport & Tourism 25(1), 3–25, https://doi.org/10.1080/14775085.2021.1877563.

Motor Max (2022): Barum Czech Rally Zlín přinese do rozpočtu státu stovky miliónů. Available online: https://motor-max.cz/2022/07/04/barum-czech-rally-zlin-prinese-do-rozpoctu-statu-stovky-milionu/ (accessed on 30. 5. 2023).

MSHOKEJ2004 (2004): The attendance record was broken. Available online: http://www.mshokej2004.cz/www/index.php?action=main_article&id=1088&subject=2& (accessed on 15. 6. 2023).

Naess, H. E. (2014): A Sociology of the World Rally Championship. 1. London: Palgrave Macmillan.

Nayak, M. S. D. P., Narayan, K. A. (2019): Strengths and weaknesses of online surveys. technology. IOSR Journal of Humanities and Social Sciences 24(5), 31–38, https://doi.org/10.9790/0837-2405053138.

Neirotti, L. (2003): An Introduction to Sport and Adventure Tourism in S. Hudson (ed.) Sport and Adventure Tourism, The Haworth Hospitality Press: New York, pp. 1–26.

Nicholson, R. E., Pearce, D. G. (2001): Why do people attend events: A comparative analysis of visitor motivations at four South Island events. Journal of Travel Research 39(4), 449–460, https://doi.org/10.1177/004728750103900412.

Nugroho, A. M., Pradini, G. (2022): The Effect of Successful City Branding and MotoGP Tourism Events on Tourists' Decision to Revisit Mandalika. Budapest International Research and Critics Institute-Journal (BIRCI-Journal) 5(3), 22672–22683, https://doi.org/10.33258/birci.v5i3.6280.

Palatková M., Zichová, J. (2011): Ekonomika turismu: turismus České republiky: vymezení a fungování trhu turismu, přístupy k hodnocení významu a vlivu turismu,

charakteristika turismu České republiky. Grada publishing, Praha.
Pigeassou, C. (2004): Contribution to the definition of sport tourism. Journal of Sport & Tourism 9(3), 287–289, https://doi.org/10.1080/1477508042000320205.
Píža, P. (2013): Přínosy BCRZ pro Zlínský kraj v oblasti cestovního ruchu [Master thesis]. Masarykova univerzita, Brno (in Czech).
Pioš, K., Skoczylas, K., BrzeziñSka-Wójcik, T. (2014): The Current Condition and Possibilities of Development of Festival Tourism in the Lublin Region. Polish Journal of Sport and Tourism 21(2), 119–126, https://doi.org/10.2478/pjst-2014-0012.
Rally Zlín (2016): Ekonomické přínosy BCRZ 2016. Rally Zlín, Zlín (in Czech).
Ramasamy, B., Wu, H. W., Yeung, M. (2020): Hosting Annual International Sporting Events and Tourism: Formula 1, Golf or Tennis (CEIBS Working Paper, No. 013/2020/ECO), https://doi.org/10.1177/13548166211029053.
Ramasamy, B., Yeung, M. C. (2020): Does Formula-1 Grand Prix Attract Tourists? Tourism Analysis 25(4), 473–479, https://doi.org/10.3727/108354220X16020580167829.
Ratkowski, W., Ratkowska, J. (2018): Sports events as a determinant of sport tourism. Baltic Journal of Health 10(1), 86–94, https://doi.org/10.29359/BJHPA.10.1.09.
Ritchie, B., Adair, D. (2002): The growing recognition of sport tourism. Current Issues in Tourism 5(1), 1–6, https://doi.org/10.1080/13683500208667903.
Ritchie, B. W., Adair, D. (2004): Sport tourism: An introduction and overview. Sport Tourism: Interrelationships, Impacts and Issues 15(6), 1–29, https://doi.org/10.21832/9781873150672-003.
Rowley, A., Smith, J. (2022): An investigation of the economic impact of small-scale sports events: The case of a medium-sized city in the Western United States. Acta Universitatis Carolinae Kinanthropologica 58(1), 19–37, https://doi.org/10.14712/23366052.2022.2.
UN Tourism (1995): Concepts, Definitions, and Classifications for Tourism Statistics. Technical Manual No. 1. World Tourism Organisation, Madrid.
Weed, M. (2009): Progress in sports tourism research? A meta-review and exploration of futures. Tourism Management 30(5), 615–628, https://doi.org/10.1016/j.tourman.2009.02.002.
Weed, M., Bull, Ch. (2009): Sports Tourism: Participants, Policy and Providers (Oxford: Butterworth and Heinemann, Routledge.
Wilson R. (2006): The economic impact of local sport events: significant, limited or otherwise? A case study of four swimming events. Managing Leisure 11(1), 57–70, https://doi.org/10.1080/13606710500445718.
Yu, B., Yue-Hong, H., Yin, S., Zhang, X. (2022): The community residents' nimby attitude on the construction of community ageing care service centres: a cross-sectional study. BMC Health Services Research 22(1), 93, https://doi.org/10.1186/s12913-022-07478-5.

From economic turbulence to demographic change: Tracing the pathways of the second demographic transition in post-socialist contexts

Stefan Johnson*

Charles University, Faculty of Science, Department of Demography and Geodemography, Czechia
* Corresponding author: stefan.johnson@natur.cuni.cz

ABSTRACT
Building on the rich tapestry of demographic and economic research, this paper extends the analysis of the Second Demographic Transition (SDT) within the milieu of Czechia, Slovakia, Poland, Romania, and Austria, shedding light on the nuanced interplay between economic variables and demographic indices such as the Total Fertility Rate and the Sobotka's Second Demographic Transition Behavioral Index (SDT1). Drawing from an extensive dataset spanning over two decades, the study applies Pearson's correlation analysis, Holt's Exponential Smoothing, and stepwise regression to unravel the complexities of demographic behaviors in the face of economic prosperity and inequality, as measured by GDP, Gini coefficient, and the Human Development Index. The findings reaffirm the pivotal role of economic factors in shaping demographic trends and highlight the divergent paths Czechia, Slovakia, Poland, and Romania have embarked upon compared to Austria, a representation of Western Europe's demographic evolution. This comparative analysis underscores the significance of wealth distribution in influencing demographic outcomes, offering a comprehensive understanding of the second demographic progression in the context of economic transitions. The research contributes to the broader discourse on demographic changes, providing insightful implications for policy and future studies in the dynamic landscape of Central and Eastern Europe and beyond.

KEYWORDS
second demographic transition; economic transition; post-socialist; demography; total fertility rate

Received: 4 June 2024
Accepted: 2 September 2024
Published online: 18 October 2024

Johnson, S. (2024): From economic turbulence to demographic change: Tracing the pathways of the second demographic transition in post-socialist contexts. AUC Geographica 60(1), 24–45
https://doi.org/10.14712/23361980.2024.15

1. Introduction

The Second Demographic Transition (SDT) is characterized in a demographic context by evolving familial configurations, delayed initial marriages and first childbirths, sub-replacement fertility rates, increased extramarital births, cohabitation, and escalated divorce rates. Since Lesthage and van de Kaa's seminal introduction of the SDT concept in 1987, a substantial body of research has emerged, concentrating on the extent of SDT adoption across various nations (Zaidi and Morgan 2017). Initially conceptualized within a Western context, excluding the factors associated with mortality, scholars examining post-socialist countries (PSCs) have raised critical inquiries regarding the applicability of SDT frameworks to these regions, which displayed divergent developmental trajectories. It is important to note that the Second Demographic Transition theory is not universally accepted, as initially mentioned by Cliquet (1991), who believed value changes are essential, but economic factors should be addressed. Coleman posited that the theory was part of a more extensive explanation but not the transition on its own (2004).

This divergence between PSCs and Western European countries' transitions prompted significant scholarly investigation. A central line of inquiry pertained to how populations responded to sociocultural and economic transformations in the context of SDT-related phenomena, such as shifts in familial structures and fertility patterns. In the Western European context, the advent of the SDT coincided with economic affluence, a change in family values, and increased female participation in the workforce and higher education. In contrast, the post-socialist transition was marked not by economic prosperity but by economic upheaval. Post-1990, populations like those of Czechia, Poland, Romania, and Slovakia experienced reduced employment rates and increased unemployment and uncertainty, which had not been experienced previously – socialist countries previously had a near-zero unemployment rate. Notably, female unemployment rates in Romania and Czechia were lower than in Austria, a regionally comparative economy with a differing economic system. This observation led to the hypothesis that there are dual economic pathways to the SDT: one through economic prosperity and the other via economic crisis, yielding comparable demographic outcomes and familial behavior.

Sobotka (2008) developed two indices to gauge the progression of the SDT: the behavioral SDT index (SDT1) and the values-based SDT index (SDT2). SDT1 was introduced to define the degree to which select countries comparatively changed based on teen fertility rate, age of women at first marriage, the mean age of the woman at primo childbirth, the percentage of extramarital births, and the proportion of cohabitation. The SDT1 index revealed pronounced distinctions between Western and Northern European countries and PSCs, exhibiting significantly lower scores (Sobotka 2008). This study seeks to examine temporal shifts in the SDT1 index and to ascertain the economic and socioeconomic factors influencing these variations, focusing on the Total Fertility Rate (TFR) in Czechia, Austria, Poland, Romania, and Slovakia.

The research methodology encompasses three primary predictive techniques to examine the dependent variables (TFR and SDT1), aiming to identify the most accurate model and explore potential inter-variable relationships. Initially, Pearson's correlation coefficient will detect possible associations among the variables – TDR, TFR, and SDT1 Index, GDP per capita PPP (GDP), Gini coefficient of income inequality (GINI), and Human Development Index (HDI). These insights will provide a preliminary, non-causal understanding of the possible association between variables. Subsequently, two time-series methodologies will be applied to evaluate the STD1 and TFR variables' predictability and assess the suitability of regression models: Holt's Exponential Smoothing with Trend Adjustment and Simple Linear Regression. The accuracy will be measured by mean absolute deviation (MAD). Finally, the stepwise regression model will determine the most predictive independent variables for SDT1 and TFR.

Prior studies have demonstrated a correlation between TFR and SDT1, suggesting a parallel fluctuation between these measures. Additionally, correlations have been established between TFR and macroeconomic indicators such as GDP, GINI, and HDI. Given the World Bank's classification of PSCs as lower-middle and upper-middle income nations and their relatively lower SDT1 scores compared to Western counterparts, this study will explore the influence of GDP and GINI on SDT progression in post-socialist European countries and Austria as a control population (Lesthaeghe 2020), thereby shedding light on potential drivers of demographic transitions in this region. These populations were chosen particularly due to their closeness in fertility and familial structure (Rychtarikova and Monnier 1992). Austria was chosen as a control population in the study due to the geographical and historical similarities, but differing political and economic history, in combination with the East-West division despite geographical location.

This research provides a nuanced understanding of the Second Demographic Transition (SDT) within the post-socialist countries (PSCs) context, focusing on the interplay between socioeconomic factors and demographic changes in Czechia, Poland, Romania, and Slovakia. The study's multifaceted approach, encompassing the behavioral-based index, aims to elucidate the temporal dynamics and predictive factors of the SDT1 index and Total Fertility Rate (TFR). Incorporating various methodological tools, including

Pearson's correlation coefficient, time-series analyses, and multiple regression, will offer a comprehensive understanding of the relationships and potential causative factors influencing these demographic phenomena. The study's findings are anticipated to contribute to the broader discourse on demographic transitions, particularly in the context of economic and social transformations experienced by post-socialist populations.

2. Literature review

The Second Demographic Transition (SDT) phenomenon is predominantly characterized by shifts in societal attitudes and practices related to marriage, cohabitation, childbearing, and divorce. This shift was especially pronounced in Western European populations, where an increasing social acceptance of premarital cohabitation emerged. Advances in contraceptive technologies facilitated more effective family planning, leading to delayed childbirth and a consequent reduction in period total fertility rates. While Western Europe began witnessing these demographic shifts as early as the 1960s, as delineated by van de Kaa (1987), recent scholarship, such as that by Zaidi and Morgan (2017), has pointed to the ethnocentric limitations of this theory, emphasizing its grounding in Western and postmodern values. In this regard, postmodernism is used in the context expressed by van de Kaa (2002), where the population has exceptional economic security, high standards of living, and access to fair and reliable democratic processes.

Contrasting this Western experience, post-socialist countries (PSCs) underwent a more delayed demographic evolution. Rychtarikova (1999) proposed that the post-1990 demographic shift in PSCs was more reflective of crisis behavior than a response to the economic affluence and postmodernist influences experienced in Western Europe. Sobotka (2008) furthered this position by suggesting that the SDT can follow two distinct paths: one emerging from economic prosperity and the other from economic adversity. However, this theory and the associated data, spanning 1990 to 2004, have yet to be revisited, despite mentions more recently by Lesthaeghe and Permanyer (2014) and Lesthaeghe (2020). Sobotka (2008) noted that the conventional development path in the SDT aligns with economic well-being and higher education. In contrast, the alternative path, consistent with Rychtarikova's (1999) crisis behavior concept, might be more applicable to PSCs. The present research seeks to determine whether PSCs are still following the same trajectory as previously or if their paths have converged with those on the conventional path.

Lesthaeghe (2020) observed varying phases and extents of cohabitation across European countries. For instance, Austria and other German-speaking nations experienced an early surge in cohabitation between 1970 and 1979. In contrast, Romania and Poland experienced such trends in the 1990s, and even then, the extent was more muted compared to Western Europe. Lesthaeghe's (2020) analysis, utilizing data from the Generations and Gender Survey (GGS), also highlighted the interplay between educational attainment and cohabitation patterns. In Poland, for example, the period from 1990 to 1999 saw no significant correlation between education levels and cohabitation, but this changed in the subsequent years, particularly among higher-educated individuals. Romania displayed similar patterns, with notable distinctions in cohabitation based on educational attainment emerging in later years. Cohabitation differs from region to region in Czechia, where half of cohabitation, or "de facto marriage" as it is sometimes referred to, is the population aged 25–39 (Cesky Statisticky Urad 2014).

The economic struggles of Romania, as discussed by Ban-Ner and Montias (1991) and Ban (2012), centered around debt, capital-intensive industrial strategies, and the faltering socialist state, leading to profound socio-demographic impacts, including a sharp decline in fertility post-decentralization. As detailed by Ouanes and Madhav Thakur (1997) and Kolodko (2009), Poland's situation mirrored Romania's, with the economic crisis reaching its lowest points in 1993. The economic instability, exacerbated by debt servicing challenges and currency issues, severely impacted Poland's economic stability. Czechia, in contrast, experienced a more democratic transition away from socialism, driven by personal choice, as described by Lijphart (1992). This peaceful transition in Czechoslovakia provided the macroeconomic elements of success, and when Slovakia and Czechia split, this macroeconomic foundation was inherited by Slovakia. Unfortunately, however, when Slovakia attempted to float its currency, the economy took a heavy hit and caused a stagnation in economic growth (Koyame-Marsh 2011).

2.1 Fertility transitions

Fertility rates are a pivotal marker in the study of demographic transitions. As noted by Sobotka (2008), the transition period from socialism in European countries was characterized by a palpable sense of crisis, a sentiment that resonated in Czechia as much as it did in post-Ceaușescu Romania (Ben-Ner and Montias 1991; Kocourková et al. 2022). The research by Kocourková, Slabá, and Šťastná (2022) delves into the socioeconomic impacts on fertility trends, revealing a notable decline in fertility rates starting from 1990, which persisted below pre-democratization levels. This tells a more critical fertility story than simply fewer women having children. Bongaarts and Feeney (1998) made a case that period

fertility rates did not accurately describe the ongoing fertility trends in a population, and life course is essential to consider – meaning that postponement was more common during economic crises. This trend was mirrored during the 2008 financial crisis, further underscoring the influence of economic stability on timing associated with Total Fertility Rates (TFR), thus supporting the crisis response theory posited by Rychtarikova (1999) and Sobotka (2008). Kocourková, Slabá, and Šťastná's (2022) cohort-based approach to analyzing fertility shifts addresses previous criticisms regarding the reliance on period fertility as a metric, as pointed out by Lesthaeghe and Permanyer (2014).

In Czechia, similar to their Western European counterparts, women experienced increased opportunities for travel, university education, and self-actualization. Parallel trends were observed in Romania, where Ianoş and Heller (2004) noted that shifting to a market economy led to significant demographic changes through mass temporary and permanent emigration. However, this shift did not equate to childlessness; instead, a postponement in fertility was observed, as highlighted in Sobotka's (2015) Czechia cohort analysis. The cross-sectional perspective in Fig. 1 observes the upward shift in the mean age of mothers at childbirth. In Austria, since 2011, the birth rates among women under 20 have surpassed those over 40 (Sobotka 2015; Beaujouan 2018). Moreover, Vienna, which traditionally exhibited lower fertility rates relative to the rest of the country, has seen its rates converge with the national average (Sobotka 2015), meaning that the country's rural and less dense regions are experiencing low total fertility rates similar to those in the capital city.

Poland, too, witnessed a decrease in total fertility rates following the shift from socialism (Kotowska et al. 2008). In response, Poland adopted pro-natalist policies, including increasingly restrictive abortion laws. However, these measures have not significantly influenced fertility rates, likely due to the prevalence of effective contraception (Cook et al. 2023). Kotowska et al. (2008) identified several socioeconomic factors impacting fertility, particularly material and economic disparities and limitations in social welfare for families desiring children. Poland's rapid transition mirrors that of other PSCs, yet it stands out for its continued decline in TFR since 1990, unlike Czechia, Romania, and the Slovak Republic, as observed in Fig. 2 – attributed to better contraceptives and personal choice (Cook et al. 2023).

This data illustrates the mean age of mothers at all live births in each period. As can be observed in this time series graph, there has been a consistent increase in age across all countries. Slovakia and Czechia are unique population groups that appear to have a stagnated pattern of transition.

Fig. 2 illustrates the change in period total fertility rates across Czechia, Austria, Poland, Romania, and Slovakia. Austria, as the most post-modernist countries in the study, had the lowest change in fertility behaviour; whereas, Poland had the most significant change. Czechia, Romania, and Slovakia have all experienced increased total fertility rates, indicating that it may be a case of postponement of childbirth rather than decreased desire for children.

The Total Fertility Rate (TFR) is a pivotal indicator within the framework of the Second Demographic Transition (SDT), underscoring the significance of personal choice and fertility dynamics in modern demographic studies (Lesthaeghe 2020). Sobotka (2008) proposed that economies may undertake one of two principal trajectories toward the SDT, highlighting the intricate challenges that post-socialist economies encounter when transitioning to market economies. This narrative is consistently reflected across the landscapes of Czechia (Kocourková et al. 2022; Sobotka 2015), Poland (Kotowska et al. 2008; Cook et al. 2023), Romania (Ban 2012; Ianoş and Heller 2004), and Slovakia (Sobotka 2008; Rychtarikova 1999), where similar fertility trends have been documented despite varying degrees of transition levels and economic well-being.

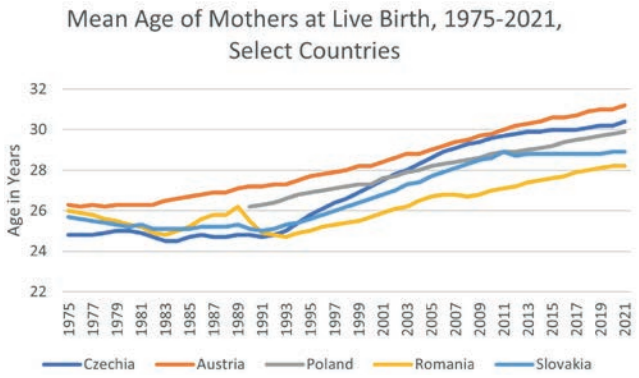

Fig. 1 Mean Age of Mothers at Live Childbirth, 1975–2021.

Data Source: Eurostat (2023). Mean age of Mothers at first birth data was taken from Eurostat – Poland's data was limited to 1991 onward.

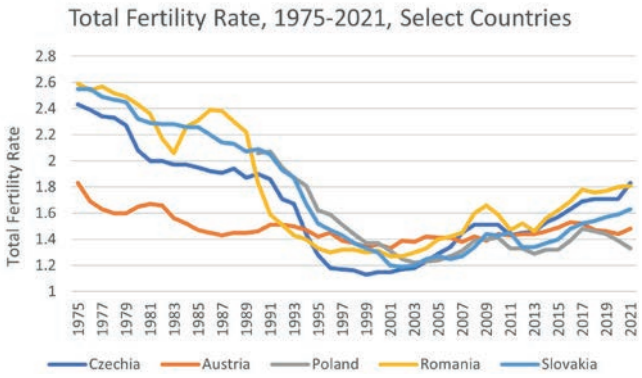

Fig. 2 Total Fertility Rates, 1975–2021, Select Countries.

Data Source: Eurostat (2023).

2.2 Nuptiality and divorce trends and transitions

A primary factor associated with the second demographic transition is the structural changes in unions and family structure in postmodernist countries. Trost (1978) examined the emergence of cohabitation in Nordic countries; between 1950 and 1964, 58–68% of Icelandic couples cohabitated in "marriage-like conditions". The "lifestyle" was suggested to be one for the adventurous at the time, with some characterizing women who entered cohabitation as lacking interests and values typically associated with marriage (Bernard 1982, p. 159; Blanc 1984). In Czechia, between 1985 and 1990, it is estimated that 31–37% of couples cohabitated before their first marriage (Možný and Rabušic 1992); typically, with plans to marry. This concept differs from the shift from the *golden age of marriage to the dawn of cohabitation*, as it implies a remaining relative importance of marriage (Sobotka et al. 2003). The European Values Survey (EVS) recorded that more respondents agreed that *marriage is outdated* in Czechia and Slovakia. Fig. 3 illustrates the percentage of extramarital births in select countries. Rabušic and Manea (2019) discuss the changing perception of single motherhood and cohabitation in 1991 and 2017 in both Czechia and Slovakia.

In Slovakia, like Czechia, there has been a rise in cohabitation and non-traditional relationship forms, leading to a higher rate of extramarital childbirth compared to Romania and Poland (Potančoková et al. 2008). Czechia has the highest rate of extramarital births among the countries studied, followed closely by Austria and Slovakia. Conversely, Poland and Romania are among the European countries with the lowest rates of extramarital births (Rotariu 2010). In Poland and Romania, as of 2021, the mean ages for married and unmarried mothers at first live birth are 28.8 and 25.9, and 28.2 and 24.5, respectively. In Austria and Czechia, these ages are higher, with Austria having mean ages of 30.6 for married and 28.7 for unmarried mothers, and Czechia demonstrating similar patterns.

Fig. 3 indicates that growing share of extramarital births in each of the select countries. Poland and Romania continue to have a growing Percentage; Czechia and Slovakia appear to be stagnated. Austria appears to be on the decline. What is most notable about this data is the percentage of extramarital childbirths in Czechia compared to Austria, which was overtaken after 2010.

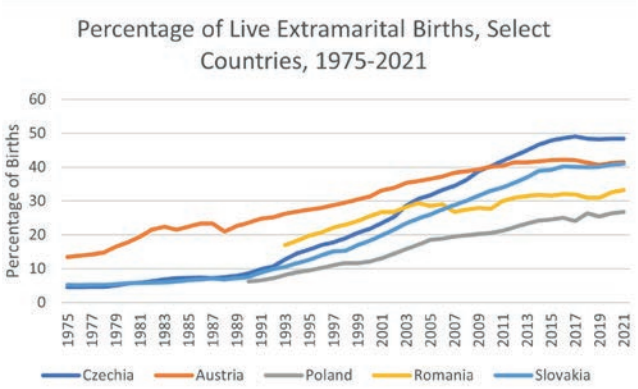

Fig. 3 Percentage of Total Extramarital Live Births in Select Countries, 1975–2021.

Data Source: Eurostat (2024).

In contrast to Czechia, Romania exhibits a markedly lower prevalence of cohabitation among couples. As of 2002, merely 6.5% of Romanian couples cohabited, a stark difference from other European countries (Wiik et al. 2012). The country experienced a decline in Crude Marriage Rates (CMR) from 1970 to 1989, which conversely saw an increase in female

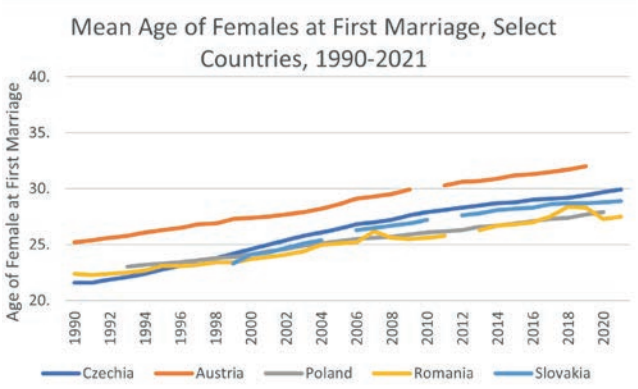

Fig. 4 Mean Age of Females at First Marriage, Select Countries, 1990–2021.

Data Source: Eurostat (2023).

Tab. 1 Percent of Consensual Unions by Country 2011 Census.

Country	Total Unions	Total Consensual Unions	Percent of Unions as Consensual Unions [%]
Austria	1,614,273	321,689	16.6
Czechia	1,856,715	237,933	11.4
Poland	8,206,239	313,114	3.7
Romania	4,666,020	340,019	6.8
Slovakia	761,811	70,337	8.5
Total	17,105,058	1,283,092	7.0

Data Source: Eurostat (2024).

educational attainment and employment in every post-socialist country except Romania (Cornia and Panicci 1996).

This figure describes the increased mean age of primo-nuptiality in Czechia, Austria, Romania, Poland, and Slovakia. In each of these countries, there is a clear positive trend. There was a sudden increase in age for Romania, which quickly readjusted during the COVID-19 pandemic years. Austria maintains the oldest mean age of primo-nuptiality, > 32 years old. Romania, with the lowest, has a mean age of < 27.6.

Despite this decline in marriage rates in Poland and an upward shift in the average age of first marriage – from 22.5 years in 1993 to 27.9 years in 2020 – Poland still maintains the second-youngest average age at primo-marriage among the studied countries, as depicted in Fig. 4. Notably, all countries in this study have seen an increase in the mean age of first marriage for females. In a unique deviation, Romania experienced a brief anomalous period between 2017 and 2019, where the average age of first marriage peaked before reverting to levels close to those observed before 2017, followed by a more predictable and consistent pattern.

Oláh and Frątczak (2003) observed that in Poland and Romania, the increased opportunities for women in employment and education did not significantly alter with the crude marriage rate, a contrast to the trends seen in Western nations and even in Czechia and Slovakia. Traditional gender roles, particularly regarding household responsibilities, have remained essentially unchanged in Poland, potentially influencing marital and childbirth dynamics.

2.3 Human Development Index, GDP, Gini, and Second Demographic Transition

The choice of Gross Domestic Product (GDP) over Gross National Income (GNI) as the primary economic indicator in this study is underpinned by several key considerations. Firstly, GDP offers a more concentrated measure of economic activity at the national level, which is particularly pertinent for this analysis as it excludes the potentially distorting effects of remittances. This focus ensures a more precise depiction of actual economic activities within the studied countries. Moreover, GDP's prevalent use among policymakers underscores its vital role in elucidating the relationship between economic output and various socioeconomic and socio-demographic variables. This widespread adoption enhances the validity and comparability of our findings, aligning them with established policy frameworks. GDP's significance is further highlighted by van de Kaa (2002), who identified it as a structural component and an explanatory factor in the Second Demographic Transition (SDT). Bloom et al. (2001) also suggested that GDP is influenced by the Total Fertility Rate (TFR), positioning it as a dependent variable in their analysis. Finally, it discusses the key policy variables that, combined with reduced fertility and increases in the working-age population, have contributed to economic growth in some areas of the developing world.

As a measure of income equality, the Gini coefficient ranges from 0 (perfect equality) to 1 (perfect inequality). Mierau and Turnovsky (2014) discovered a correlation between rising TFR and increased income inequality. Although it was proposed that wealth distribution becomes more unequal with increasing life expectancy, Kopczuk and Saez (2004) demonstrated that wealth has been concentrated in the top decile for over five decades, proposing that wealth inequality may be more static than dynamic in relation to demographic changes. This suggests wealth inequality could be independent, not necessarily dependent on demographic transitions.

Lesthaeghe and Permanyer (2014) provided insights into the impact of the Human Development Index (HDI) on TFR across various European regions. They identified two primary clusters: Cluster A, comprising mainly Nordic and Anglo populations, and Cluster B, including 25 countries such as Czechia, Slovakia, Romania, Poland, and Austria, characterized by low to moderate TFR. Notably, the relationship between TFR and HDI in both clusters was weak, indicating that these variables might not sufficiently explain the variance in TFR.

This study treats GDP, HDI, and the GINI as independent variables. While GDP has been previously identified as independent in relation to the SDT (Sobotka 2008), its influence on SDT1 is mediated by social norms. The GINI relationship with TFR suggests a link between increasing inequality and rising fertility rates (Mierau and Turnovsky 2014). These indicators provide a robust foundation for examining economic and socioeconomic predictors in relation to crucial demographic measures like TFR and the SDT1 Behavioural Index. By evaluating the SDT Index against GDP, this paper aims to ascertain whether there is a consistent trajectory in line with Sobotka's (2008) propositions.

3. Methodology

This paper aims to identify whether these countries remain on the same "path" in demographic transition or if the paths have changed in any way. The initial SDT indices (SDT1 and SDT2) were developed using data from 1990 and 2004. These data were from a period before the accession of Romania to the EU and the year Czechia entered the European Union (2004). The SDT1 index is calculated by observing the Mean Age of Mothers at First Birth (MAFB), the Sum of Age-Specific Fertility Rates Below age 20 per 1,000 (TEENFERT), the Percentage of Non-Marital Live Births (NONMAR),

Tab. 2 SDT1 Behavioural Index Indicators.

Factor	Factor Abbreviation	SDT score = 0	SDT Score = 5	SDT Score = 10
Mean Age of Mother at First Birth	MAFB	< 24	27	> 30
Age Specific Fertility Rate Below Age 20 (per 1,000)	TEENFERT	> 180	90	0
Percentage of Non-Marital Live Births	NONMAR	0	30	> 60
Total First Marriage Rate	TFMR	> 0.80	0.60	< 0.40
Mean Age at First Marriage	MAFM	< 23	27	> 31
Total Divorce Rate	TDR	< 0.15	0.35	> 0.55

Source: Sobotka (2008).

Total First Marriage Rates (TFMR), Mean Age at First Marriage (MAFM), and Total Divorce Rate (TDR). The model thresholds were set out by Sobotka (2008) and illustrated in Tab. 2.

The rates are each scored based on the scoring criteria, aggregated, and averaged, leading to the SDT1 index score, where 0 is not considered to be transitioning, and 10 is regarded as an advanced second demographic transition. Sobotka added 0.5 to each of the indexed scores for countries where unmarried cohabitation counts for more than 10 percent of the total unions in the country. For this research, the most recent data available at the time of this research is from the 2011 census, as the data from the 2021 census is not yet robust enough within the same context. The breakout and percent of each of the countries' unions is illustrated in Tab. 1.

Based on the 2011 census, Austria and Czechia are the only countries that receive the 0.5 increase. These indices are a basis for each country's perceived transition level based on the leading indicators associated with the second demographic transition. This research, along with revisiting the SDT1 indices for 2004-2021, will entail econometric methods of analysis, including Holt's Exponential Smoothing model and simple linear regression, used to depict changes in both level and trend elements of TFR and STD1 index indicators. Stepwise regression will be implemented to define the predictability of the data. For a baseline data analysis, Pearson's r correlative testing will identify preliminary associations between demographic variables and economic data, including GDP, GINI, and HDI. This framework will provide insight into several key concepts.

This study will re-examine the transition level experienced by former socialist countries while also examining the factor associations to Sobotka's SDT1 Index. These data will also provide insight into these select countries' trends in associative and time-series approaches. These combined approaches will provide evidence of whether these data are predictable and associated with one another. In the following section, the sources and calculation methods for data will be expanded upon. Appendix 1 describes the data types, sources, and the mode of calculation for the indicators used in the study.

3.1 Exploring relationships using Pearson's r

Pearson's r will be initially used to develop a baseline understanding of the relationships between the variables. This basis will provide insight into the level of potential relationships between each variable and use these data to determine the most critical variables to test in a regression test. The results for the Pearson correlations will also provide insight into the potential way select values interact while also understanding how multiple dependent variables may fluctuate similarly.

3.2 Time series analyses

This analysis will examine the variables' predictability of TFR and STD1 and which of the two models is best for predicting the variables. The two methods will be time series simple linear regression and Holt's Exponential Smoothing with trend. Holt's does not include a seasonality component, which allows the model to predict without the assumption of cyclicality. Regression is a commonly accepted approach, so the equations have yet to be included in this research; however, Holt's equations are included in the following section.

3.3 Holt's Exponential Smoothing

Holt's Exponential Smoothing (Holt's) is a linear model that addresses data that increases in a trended pattern. The method of analysis has been used in the past due to its relative ease, cross-disciplinary usage, and the general accuracy of the model (Maia and de Carvalho 2011). The results will be compared against the results of the simple linear regression analyses using Mean Absolute Deviation (MAD). Holt's is expressed in two functions: a level component (L) – the baseline values of the series in a simple forecast, and the trend component (T) – a representation of the increased trend in the model. To conduct this analysis, observed values (Y) from the previous period(s) have to be known. A smoothing constant for the L is used in the level equation(α), and a smoothing constant for the T variable is placed in the trending component equation (β). The predicted future value ($\hat{Y}$) is then calculated.

Equations (1), (2), and (3) illustrate the principle components.

Equation 1 Holt's Exponential Smoothing

$$L_t = \alpha Y_{t-1} + (1-\alpha)(L_{t-1} + T_{t-1}) \quad (1)$$

$$T_t = \beta(L_t - L_{t-1})) + (1 - \beta)T_{t-1} \quad (2)$$

$$\hat{y}_t = L_t + T_t \quad (3)$$

This output will provide an understanding of the data's predictability based on the trends of the known data points. The model parameters (α and β) will be adjusted to best fit the data series.

For the first period, a naïve approach to forecasting will be used – the forecast (L) for 2007 will be the actual (A) value from 2006. In this example, the smoothing constant α = 0.2 and the trending constant β = 0.495. These constants are dynamic and adjusted to the best fit. The Czech data is: Y_{2006}^{TFR} = 1.34: T_{2006}^{TFR} = *0.066*, L_{2006}^{TFR} = 1.302. Equations (4), (5), and (6) illustrate the process.

$$L_{2007}^{TFR^{CZ}} = (0.2)(A_{2006}^{TFR}) + (1 - 0.2)(L_{2006}^{TFR} + T_{2006}^{TFR})$$

$$L_{2007}^{TFR^{CZ}} = 1.36 \quad (4)$$

$$T_{2007}^{TFR^{CZ}} = 0.495(L_{2007}^{TFR} - L_{2006}^{TFR}) + (1 - 0.495)T_{2006}^{TFR}$$

$$T_{2007}^{TFR^{CZ}} = 0.068 \quad (5)$$

$$\hat{Y}_{2007}^{TFR^{CZ}} = L_{2007}^{TFR} + T_{2007}^{TFR}$$

$$\hat{Y}_{2007}^{TFR^{CZ}} = 1.43 \quad (6)$$

Using Holt's Exponential Smoothing with a trend, the level plus trend for 2007 ($\hat{Y}_{2007}^{TFR^{CZ}}$ is 1.43; the actual for 2007 was 1.45; therefore, there is an absolute deviation of 0.02. This method of forecasting is used in each of the countries' dependent variables: TFR and the SDT1 behavioural index.

3.4 Comparing models using MAD

Holt's and Time Series Regression are employed to project the dependent variables in a time series. One is linear in nature and only has a smoothing predictor (regression); conversely, Holt's considers trends in data and can exaggerate changes over time. The two methods will be compared for accuracy against the known data points using mean absolute deviation, where the lowest deviation represents a more accurate forecast than with a higher number. Each country will be compared for each of the dependent variables.

$$MAD = \frac{1}{n}\sum_n |x_i - \hat{x}_i| \quad (7)$$

In this equation, the forecasted value (x_i) is subtracted from the observed value ($\hat{x}_i$) of the period (i). Then, all the absolute differences between the and the are divided by the n of periods. This represents the mean absolute deviation (MAD). This is one of the statistical methods used to compare forecasting methods to determine a more accurate method. If linear regression is the ideal mode, it contributes to a case to a stepwise regression model.

3.5 Stepwise regression

Stepwise regression progressively adds independent variables to a multivariate regression model while eliminating independent variables that have little or no impact on the dependent variables. Equations (8), (9), and (10) represent the multiple regression formula steps, with SDT1 or TFR as the dependent variable. This would be an example of the 5 steps of the function, provided that all x-variables impact the predictability of y-variables. The initial point in the model is the y-intercept.

Equation 3: Multiple Regression, Stepwise

$$\hat{Y} = \beta_0 + \beta_1 \times x_1 + \beta_2 \times x_2 + \cdots + \beta_5 \times x_5 \quad (8)$$

$$SDT1 = \beta_0 + \beta_1 \times GDP + \beta_2 \times GINI + \beta_3 \times HDI \quad (9)$$

$$TFR = \beta_0 + \beta_1 \times GDP + \beta_2 \times GINI + \beta_3 \times SDT1 + \beta_4 \times HDI \quad (10)$$

Each independent variable is tested and combined to find the best fit for the analysis. Cluster analysis for examined cases (countries) will be conducted based on explanatory variables of the best-fitting models, implementing Ward's clustering. This clustering will provide insight into the closeness in relationship between the five populations.

3.6 Data: Demographic indicators

The six indicators of the SDT1 index and the observed dependent and independent indicators were calculated using several data sets within the Eurostat database. Appendix 1 lists the indicators, data sets, descriptions, and calculation methods. Eurostat's indicators have been used when available, including mean age at first marriage (MAFM) and Total Divorce Rate (TDR). Several indicators were calculated for the SDT1 index, comprising Teen Fertility Rate (Fertility < 20 years) (TEENFERT), Total First Marriage Rate (TFMR), and Percent of Non-Marital Births (NONMAR).

3.7 Data: Economic and socioeconomic indicators

The data used in this study to accurately identify predictability relies on accurate and meaningful economic data. The variables used in this study are GDP, GINI, and the HDI. Each of these variables plays a role in understanding the structural differences in

Tab. 3 Historical World Bank Income Categories, Select Countries 2004–2020.

	World Bank Income Classification				
Country	2004	2008	2012	2016	2020
Austria	High	High	High	High	High
Czechia	Upper-Middle	High	High	High	High
Poland	Upper-Middle	Upper-Middle	High	High	High
Romania	Lower-Middle	Upper-Middle	Upper-Middle	Upper-Middle	Upper-Middle1
Slovakia	Upper-Middle	High	High	High	High

Romania was categorized as a high-income country in 2019 and 2021; 2020 was anomalous in this trend.
Data Source: World Bank Historical Income Levels.

economies. For instance, a country may have a strong GDP per Capita PPP (hereafter GDP) but weak purchasing power, thereby reducing the actual power of the currency in the market. Gini is an indicator of wealth distribution – providing insight into the income quantiles spread of wealth. The perfect distribution of wealth with GINI is 0, whereas the concentration of wealth to one person or entity is "perfect inequality".

Each independent variable will be progressively added to the models to identify the predictability of each variable. Interestingly, the HDI has yet to be used in studies within this context, though analyses have been conducted to observe the relationship between TFR, HDI, and GINI. GDP has been used in several studies, but these indicators have yet to be used in tandem with the SDT1 Behavioural Index. These indicators will build a case to identify the second demographic transition path based on the SDT1 index in relation to GINI, GDP, and HDI – all factors associated with the dual paths of SDT proposed by Sobotka.

To further understand the World Bank income classification, Tab. 3 illustrates the income classification of each studied country. In 2016, the World Bank classification based on GDP per capita shifted downwards, meaning the GDP thresholds were lowered because of the *World Bank Atlas Method* conducted in July of each year (Fantom and Serajuddin 2016). This may be due to the slowed growth compared to previous years relative to the rest of the world. By 2020, the income classifications appeared to return to previous levels, but this reduced threshold may be a reason for Romania's classification as "high income" in 2019 and not 2020.

4. Results

The initial findings associated with calculating the SDT1 indices reflect that countries continued to transition, albeit some more than others. Czechia, Slovakia, and Romania follow similar patterns, albeit at varying levels. During the COVID-19 pandemic in 2021, all countries experienced a decline in the SDT1 index (Fig. 5). The most impactful indicators of these shifts are associated with TDR and TFMR. Total marriage rates and total divorce rates declined in all countries. In 2020, Romania had the most intensive spike, which resulted from TFMR and TDR, similarly experienced by Slovakia. Poland's spike in 2020 was primarily associated with TFMR, while all other index scores maintained the same pattern. Czechia's spike only slightly dropped, and it was similar due to the drop in TFMR (Fig. 5).

Slovakia's TEENFERT rate is the explanatory factor associated with the immediate drops in 2017 and 2019 when the teen fertility rate was more significant than 180 live births from females below 20 years per 1,000. Slovakia has traditionally had the highest TEENFERT levels in these five countries and became more emphasized in 2017 through 2021. These indices will be used to understand further the association between the economic variables and the demographic behavior expressed in these countries. Fig. 5 illustrates the transition in the SDT1 index between 2004 and 2021.

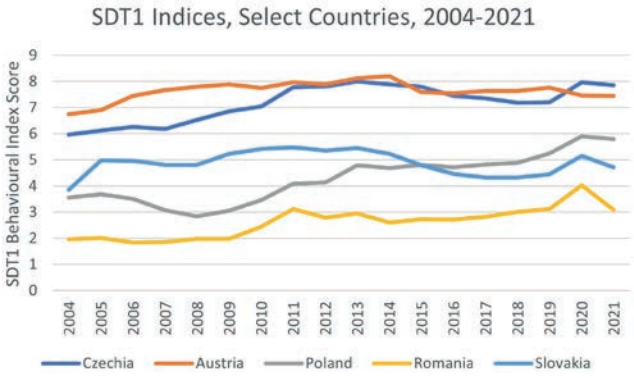

Fig. 5 SDT1 Indices, Select Countries 2004–2021.
Data source: Author's own calculations.

Using Sobotka's SDT1 "Behavioral Index" framework, each of the five countries' indices were calculated considering the six indicators. Observable is the instance in 2020 when Austria and Czechia switched roles as the leader. All countries appeared to have improved; however, it also appears that COVID-19 impacted the index.

4.1 Pearson's r correlation

Pearson's r was chosen as an initial method of testing, which is ideal for testing linear relationships with complete available data. The following section will describe and introduce the results of the correlative tests for the factors SDT1, HDI, GDP, GINI, TFR, and TDR. The purpose is to develop a basis for testing between variables in the subsequent regression stage of the study. In this phase, any correlation that results as a moderate or greater level (≥0.4 and ≤−0.4) will be subsequently selected for the regression analysis, either independently or as part of a multivariate model.

Sobotka's dual path theory posits that there are two streams that countries may take that impact the SDT1 index, representing the level of transition. As Western countries became more prosperous, the drive to SDT maturity became more pronounced; in contrast, Central and Eastern European countries tended to have an inverse relationship – lower GDPs and economic uncertainty created a sense of crisis, which has been proposed as one of the reasons for change. GDP, GINI, and HDI have been found to affect TFR and SDT1, amongst other variables, directly or indirectly. The null hypothesis is that SDT1 and TFR should have a strong negative correlation, where TFR should become lower as SDT1 increases (Sobotka 2008). Fig. 6 illustrates the relationship between the two variables across the five countries between 2004 and 2021.

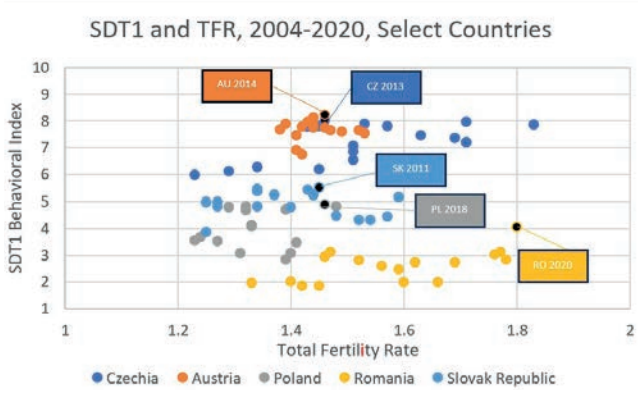

Fig. 6 SDT1 Index and Total Fertility Rate, Select Countries 2004–2020.

Data Source: TFR: Eurostat (2024); SDT1: Author's Own Calculations.

This scatter plot illustrates the correlation between the SDT1 Behavioral Index and the Total Fertility Rate of each of the five select countries. The boxes and arrows indicate the highest SDT1 indices. Notably, the highest SDT1 indices seem to all be when 1.46 > TFR > 1.45, while Romania is the outlier, with a TFR of 1.8 at the highest SDT1.

The most substantial relationship between the SDT1 index and TFR is moderate and found only in Romania and Czechia. The strongest non-negative correlation was observed in Czechia (0.601), while the lowest correlation was in the Slovak Republic (−0.114), and Austria demonstrated nearly no correlation (0.100). The two variables are unrelated despite the moderate correlations associated with SDT1 and TFR. Thus, the results did not support the hypothesis of a negative correlation between TFR and STD1. The mean r coefficient amongst the five countries was 0.304, with a MAD of 0.264. Despite a below-moderate correlation coefficient, Romania and Czechia should be further investigated using a more robust model, such as multivariate regression. Complete descriptive data results can be viewed in Tab. 4, and a complete audit of the Pearson r results is in Appendix 2.

Tab. 4 Descriptive Data, Pearson's r Coefficients 2004–2021, Select Countries.

	Min	Max	Mean	MAD	Range
SDT1-HDI	0.131	0.874	0.611	0.204	0.743
SDT1-GDP	0.036	0.856	0.566	0.252	0.820
SDT1-GINI	−0.621	0.687	−0.030	0.390	1.308
SDT1-TDR	−0.297	0.902	0.300	0.414	1.199
SDT1-TFR	−0.114	0.633	0.309	0.253	0.747
HDI-GDP	0.844	0.978	0.936	0.037	0.135
HDI-TDR	−0.849	0.639	−0.296	0.539	1.489
HDI-TFR	0.668	0.914	0.803	0.063	0.246
GDP-GINI	−0.867	0.338	−0.336	0.448	1.205
GDP-TDR	−0.879	0.588	−0.374	0.539	1.467
GDP-TFR	0.731	0.962	0.844	0.082	0.231
GINI-TDR	−0.348	0.754	0.168	0.347	1.103
GINI-TFR	−0.813	0.195	−0.398	0.411	1.008
TFR-TDR	−0.887	−0.044	−0.503	0.367	0.844

The most significant coefficients are between GDP and TFR, with a minimum and maximum value of 0.731 and 0.962, respectively, and a mean absolute deviation of only 0.082 – the second lowest MAD of the correlative study. There may be a connection between GDP and TFR; the result discovered here implies that all the countries' TFRs increased with GDP simultaneously. Compounding these results with the outputs between SDT1 and GDP, it becomes clearer how GDP may be associated with the demographic transition.

There appears to be a distinct relationship between the Human Development Index (HDI) and TFR, further validating the findings of Myrskylä, Kohler, and Billari (2009). With a min-max of 0.668 and 0.914 and a low MAD of 0.063, this output is the most significant of the correlative tests, as seen in Fig. 7. Because of the strength of the relationship, HDI will be used as an initial independent value in the stepwise framework. Similar steps will be taken with the TDR independent variable, as HDI has a strong relationship with GDP and SDT1, but GDP and SDT1 do not have as significant a relationship. In the search for predictor values, GDP will be used as a compounding variable.

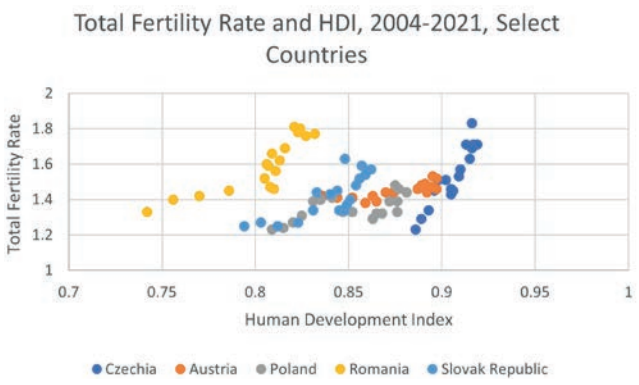

Fig. 7 Total Fertility Rate and HDI 2004–2021, Select Countries.
Data Source: TFR: Eurostat (2024); HDI: World Bank (2023).

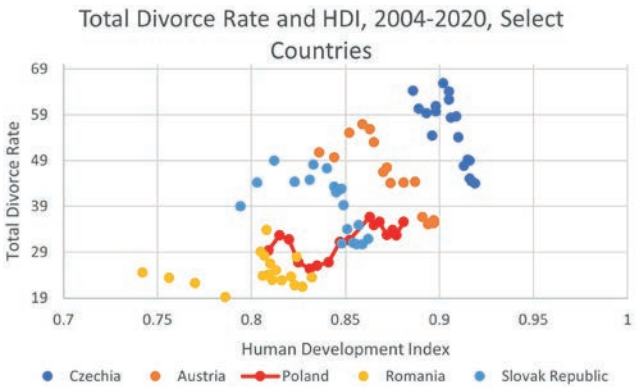

Fig. 8 Total Divorce Rate and HDI 2004–2020, Select Countries.
Data Source: TDR: Eurostat (2024); World Bank (2023).

The correlation between HDI and TFR is quite strong and has a linear path; that is, it follows a chronological pattern in the development of both indicators. As the Human Development Index increased, so did the TFR. Though the outliers of the patterns are not counter to the normal developments, the correlation between Austria and Poland is less pronounced. The patterns of the other three PSCs remain very closely aligned in pattern despite differences in levels of human development.

Considering the relationship between HDI-TFR and TFR-GDP, it is essential to note that GDP and HDI have strong relationships: 0.937 (Czechia), 0.963 (Austria), 0.978 (Poland), 0.844 (Romania), and 0.844 (Slovak Republic). According to Hamadeh, Rompaey, Metreau, Eapen's (2022) data, Romania was classified as a Lower Middle-Income country in 2004, and Poland, Slovakia, and Czechia were classified as middle-income countries. In only two years, from 2004 to 2006, Czechia progressed to a high-income country, and Romania was classified as an upper-middle-income country. A year later, the Slovak Republic caught up to Czechia; however, it was not until 2009 that Poland was classified as a high-income country. Romania finally caught up to the rest of Europe in 2019 and was classified as a high-income country; however, this may have partly been due to a lowered threshold from 2016 to 2019, causing a temporary relegation to upper-middle income in 2020. This contextualizes the value associated with GINI, GDP, and other indicators.

Fig. 8 demonstrates an inverse relationship between TDR and HDI in Czechia, Austria, and the Slovak Republic. Interestingly, Poland exhibited a moderate positive correlation, while Romania had minor results, illustrated in the figure as a line. In a previous study by Vlasov et al. (2023), the relationship between TDR and HDI was negligible – like the experience in Romania. When identifying the depth of these results, it becomes apparent that the total fertility and divorce rates have a relationship with HDI and, subsequently, a strong relationship with both GDP and SDT.

This figure illustrates the association between divortiality and the Human Development Index. The negative correlations between the variables in Czechia, Slovakia, and Austria can be observed, while there appears to be an inverse relationship between the variables in Poland and Romania. There does not appear to be a common threshold across the countries; however, there do appear to be similar trends. Simpson's Paradox appears in this example.

The initial findings from this step of the research uncovered several interesting insights. The results included the moderate relationship between SDT1 and TFR and the surprisingly strong relationship between GDP and HDI with TFR, and SDT1 (Appendix 2). Three countries had moderately strong negative correlations between GINI and TFR, and interestingly, the TFR and TDR in Czechia with the GINI demonstrated the same but inverse coefficient GINI/TDR = 0.754; GINI/TFR = −0.754). Fig. 9 demonstrates an interesting take on the Simpsons Paradox – in each of the five populations, there is an inverse relationship between TDR and GINI; however, when all data is combined, there is a positive correlation between TDR and GINI.

4.2 Holt's Exponential Smoothing and linear regression testing

Before progressing with associative testing techniques, Holt's Exponential Smoothing forecasting technique was run to determine the level of predictability of variables TFR and STD1 in a time series model. results are interesting, especially compared to a linear regression time-series model. Holt's indicated a higher MAD (Mean Absolute Deviation) than the single-factor time-series regression model (Tab. 7). This means that on their own, without any predictor values, variables of TFR and STD1 had a slightly lower level of predictability using the α and β (Holts) than the alternative method of linear regression time-series model (LR).

Tab. 6 Holt's Exponential Smoothing Constants, Variables.

	α	β
SDT1	0.05	0
TFR	0.2	0.495

Note: α = level component, β = trending component.

Tab. 7 illustrates the better prediction of the linear regression model against the exponential smoothing model, with the actual values of the TFR in Czechia as an example. The figure below illustrates that the MAD of the TFR forecast for Czechia is much lower, with regression (2.63), than Holt's (4.72).

The trending component of exponential smoothing exaggerated the peak and drops as observed in Fig. 9. Under every condition, simple linear regression is better than Holt's for these data. Holt's method tends to be over-aggressive because of the trending from the beta (β) constant. In this case, Holt's method is not ideal for forecasting Romania's TFR because of the sudden shifts in trend; however, it adequately forecasted the TFR for Austria. Under these circumstances, the forecasting for both Linear Regression and Holt's is nearly identical for Austria – meaning that either would be reasonably accurate. Neither of these methods perfectly predicts SDT1 or TFR; however, in general, linear regression was a better fit aggregated over the years. As observed in Fig. 10, the predictability for SDT1 remained quite similar using both models.

Fig. 9 illustrates the difference in the predictability of the two single-variable forecasting methods – Holt's Exponential Smoothing and Simple Linear Regression. These have both been used in Czechia and Austria using the TFR data. Due to Austria's relatively low variance compared to Czechia's, both methods work well; however, the greater variance in Czechia's data caused Holt's method to deviate more than Linear Regression.

In Fig. 10, SDT1 for Romania and Austria are predicted using Holt's Exponential Smoothing and Simple Linear Regression. Austria's observed data tends to have a low variance, which makes the predictability with both methods quite accurate. Romanian's data had slightly less aggregate variance and, therefore, less deviation than Austrian data. Under both circumstances, simple linear regression is a better predictor model, though Holt's adequately predicts SDT1 for Austria and Romania.

Despite being generally poor fit for predicting the TFR, Holt's forecasts the changes in the SDT1 Behavioural Index reasonably well. This may be due to the closeness to trend projection for the changes in Austrian levels from 2005–2015, where linear regression had continued to over-predict, Holt's tended to maintain a closer relationship with the observed data. This is not unlike the data found when predicting Romania's SDT1 index. These findings may be due to the relatively level behavioral index – Holt's β was 0, meaning that the leveling function was the only predictor. The linear regression and Holt's models are good fits for predicting the SDT1 index, although the linear regression model remains slightly better.

These two models are accurate by individual measures; however, the linear regression model tends

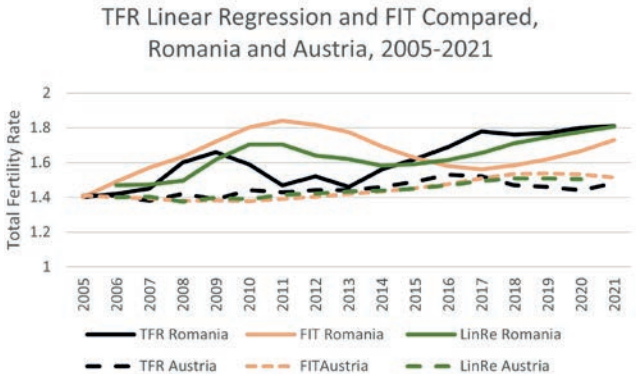

Fig. 9 Linear Regression and Holt's Exponential Smoothing Compared, TFR, Romania and Austria.

Data Source: Author's Own Calculations.

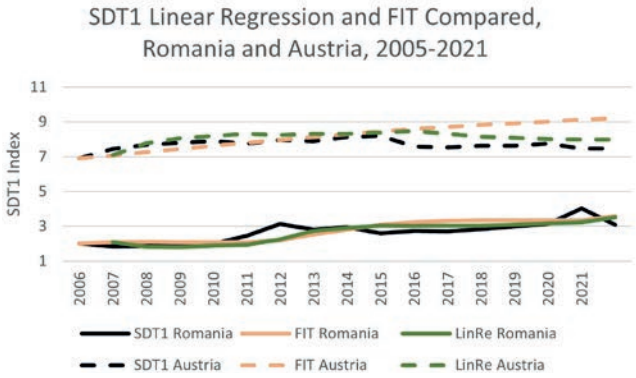

Fig. 10 Linear Regression and Holt's Exponential Smoothing Compared, SDT1, Romania and Austria.

Data Source: Author's Own Calculations, Excel.

Tab. 7 MAD, Linear Regression and Exponential Smoothing with Trend.

	CZ		AU		PL		RO		SK	
	Holts	LR	Holts	LR	Holts	LR	Holts	LR	Holts	LR
SDT1	0.31	**0.31**	0.35	**0.18**	0.29	**0.27**	0.26	**0.21**	0.71	**0.32**
TFR	4.72	**2.63**	2.52	**2.41**	4.28	**1.95**	3.19	**1.85**	5.22	**2.57**

Data Sources: Author's Own Calculations, Excel.

to predict SDT1 and TFR better. There appears to be a pattern of predictability; however, as dependent variables on their own, there is an opportunity to explore the predictability of these patterns by observing independent variables' changes and their associations to the dependent variables. By implementing an associative technique using the stepwise regression model, it is anticipated that there will be more accurate predictors of change.

4.3 Stepwise regression

Stepwise regression assessed the predictive capacity of independent variables such as GDP, GINI, and HDI on SDT1, and GDP, GINI, HDI, and SDT1 on TFR. Utilizing a 95% probability-in-confidence level, the model was adjusted to remove variables with a Probability of f (removal level) set at > 0.1, indicating variables were excluded if they fell below 90% probability. The analysis revealed significant, albeit varying, strengths among the independent variables across different countries, demonstrating an overall significant connection and establishing these models as robust predictors for TFR and SDT1. The predictive capacity for SDT1 was weaker than TFR, presenting a range from moderate to strong associations based on a combination of the adjusted R^2, Standard Beta Coefficient, and significance level. The standard beta coefficient was chosen as a metric due to the standardized output in relation to the varying size of the data for each of the variable outputs.

4.3.1 Stepwise linear regression, Y = TFR

The comparative analysis of predictive models for TFR outcomes across the study populations revealed distinct variations, highlighting the nuanced relationship between demographic trends and economic indicators (Tab. 8). GDP was identified as a vital predictor across the dataset, with the notable exception of Poland, indicating divergent socioeconomic or policy influences on fertility within this context. In Czechia, the SDT1 index had a negligible influence on TFR predictability. Its statistical insignificance ($p < 0.05$) and exclusion from the model suggest a limited or non-existent connection in this specific analysis. Similarly, the SDT1 index did not emerge as a significant factor in model predictability in Poland, contrasting with its discernible impact on the models for Austria and Romania. As encapsulated by GINI, wealth distribution dynamics demonstrated a varying degree of predictive strength in Poland and notably enhanced the model's predictive accuracy for Czechia. This underscores the importance of considering economic disparities alongside GDP in understanding the socioeconomic determinants of fertility rates, emphasizing the complex interdependencies between economic conditions and demographic behaviors.

Stepwise regression analysis, a methodical approach designed to identify the most statistically significant independent variables affecting dependent variables, often identifies variables with p-values as low as 0.000. This outcome indicates a significant relationship, underscoring the method's utility in discerning key predictors from potential variables. However, it is essential to acknowledge the limitations inherent to stepwise regression, including potential overfitting, biased estimates, and the model's sensitivity to the order of variable inclusion. These factors can affect the reliability and interpretability of the results, particularly in datasets prone to multicollinearity or when many variables are considered.

In the analysis of Austria's fertility trends, the HDI demonstrated a relationship of moderate strength, suggesting that HDI alone did not emerge as a dominant predictive factor. This observation points to the nuanced role of HDI in modeling fertility rates, highlighting the complexity of socioeconomic influences on demographic patterns. While HDI is a composite measure encompassing life expectancy, education, and income, pivotal in understanding socioeconomic development and its demographic implications, its predictive capacity may depend on interaction with other socioeconomic and cultural variables. This nuanced interpretation suggests that, particularly in economically advanced contexts like Austria, the relationship between HDI and fertility trends

Tab. 8 Select Stepwise Regression Outputs, TFR.

Country	Model	Adjusted R2	Stand. Coef. Beta	Significance	F
Czechia	(1) GDP	.920	0.962	0.000	184.537
	(2) GINI	.940	−0.260	0.027	126.598
Austria	(1) HDI	.570	0.773	0.000	22.216
	(2) SDT1	.685	−0.411	0.000	18.389
	(3) GDP	.756	−0.948	0.000	17.504
Poland	(1) GINI	.618	−0.801	0.000	26.333
Romania	(1) GDP	.812	0.908	0.000	70.046
	(2) SDT1	.851	−0.385	0.000	46.725
Slovakia	(1) GDP	.739	0.869	0.000	43.363

Source: Author's Own Calculations, SPSS.

necessitates a comprehensive analytical approach, considering a broader array of factors beyond HDI to accurately capture the dynamics at play.

Within the context of the four PSCs examined, a consistent linkage was observed between GDP growth and variations in TFR. This relationship not only underscores the impact of economic expansion on demographic patterns but also highlights the critical role of wealth distribution within these countries, as evidenced by the GINI coefficient. Such findings clarify the intricate dynamics between economic development, income inequality, and fertility trends, suggesting that economic prosperity and its equitable distribution across the population are pivotal determinants of fertility rates in these settings. This analysis highlights the complex matrix of economic and socio-demographic factors that orchestrate fertility behaviors, signifying a comprehensive framework for understanding how economic policies and societal wealth distribution mechanisms influence demographic outcomes.

Fig. 11's dendrogram illustrates the likeness of three countries, Poland, Slovakia, and Czechia, using Ward's Clustering. SK and RO are the most similar and PL and CZ are the second most closely related. The closeness of PL and CZ may be related to the inclusion of GINI – the only two populations in this study with this variable included.

Delving deeper into the comparative analysis of nations based on the dataset, employing Ward's hierarchical clustering utilizing two distinct groupings by the second distancing level. The elements and codes can be found in Appendix 3. This method reveals a pronounced affinity between Romania and Slovakia and a notable closeness between Poland and Czechia, suggesting a significant degree of similarity in their demographic and economic profiles. Austria becomes associated with this cluster at a secondary level, marked by a semipartial R2 of 0.2240 (R2 = 0.437) when juxtaposed with Poland and Czechia (R2 = 0.661), and itself, highlighting the relative divergence in their characteristics. Furthermore, Austria's positioning is markedly distant from the Slovakia-Romania nexus, with a semipartial R2 of 0.1267, suggesting a dissimilarity that could be attributed primarily to the differential roles of the HDI in Austria and the SDT1 index in both Romania and Austria. This variance underscores the nuanced underpinnings of demographic and economic indicators in shaping the relational dynamics between these nations, suggesting that HDI and SDT1 are pivotal factors in understanding the broader socioeconomic landscape across these countries.

A key finding from this data is the relationship of economic factors on the transitions in fertility in the top three countries and the SDT1 index and HDI in the bottom two. These results indicate that the SDT1 behavioural index can be used as a predicting indicator for Romania and Slovakia but does not help predict Czechia, Austria, and Poland; instead, economic well-being is a stronger predictor. What is most exciting about this clustering is the indication that economic prosperity and distribution of wealth are vital explanatory variables that had previously been negatively related. The implications of these results will be further expanded upon in Discussions.

4.3.2 Stepwise linear regression, Y = SDT1

Predicting the SDT1 behavior index trend was not as prominent as with TFR; however, key takeaways exist. Firstly, Slovakia had the least significant model (Tab. 9). No independent variables fit the model with a probability-in (PIN) level of < 0.05; therefore, it was necessary to increase the PIN to < 0.1 – meaning that there was a lower probability that the variables impacted the dependent variables. This data was related to the significance of GINI in all models except for Romania. The limited use of HDI in the stepwise approach for AU, PL, and RO was surprising, as in previous literature, it was found that HDI had an impact on demographic change. GINI predicts SDT1, but HDI – including life expectancy, GNI, and educational attainment – only impacted to a shallow degree

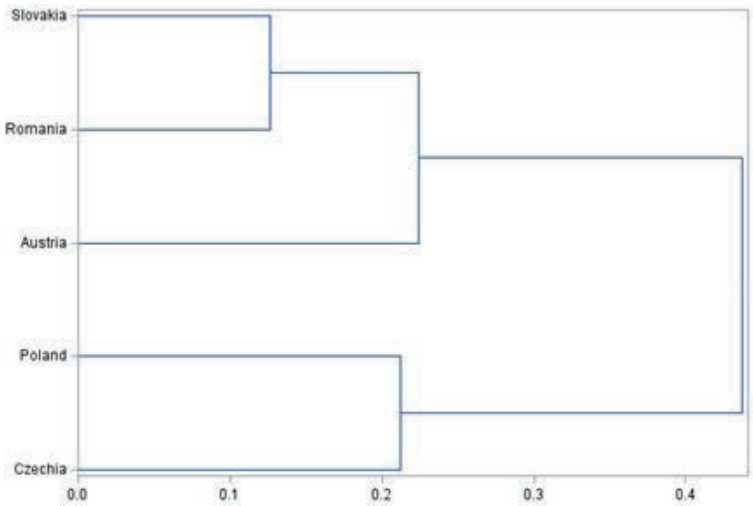

Fig. 11 Dendrogram, Adjusted R2, Ward's Clustering, TFR
Source: Author's Own Analysis, SAS.

Tab. 9 Select Stepwise Regression Outputs, SDT1.

Country	Model	Adjusted R2	Stand. Coef. Beta	Significance	F
Czechia	(1) HDI	0.582	0.763	0.000	20.923
	(2) GINI	0.797	0.936	0.000	27.462
Austria	(1) GINI	0.444	0.692	0.002	13.801
Poland	(1) GDP	0.806	0.905	0.000	67.505
	(2) GINI	0.876	0.422	0.000	57.641
Romania	(1) GDP	0.668	0.830	0.000	33.199
Slovakia*	(1) GINI**	0.229	0.204	0.061	4.164
	(2) HDI**	0.436	0.206	0.024	5.019

* No variables met the threshold of significance < 0.05
** Probability-in threshold was altered to < 0.1
Source: Author's Own Calculations, SPSS.

Model 1 in Czechia (R2 = 0.582) and Model 2 in Slovakia (R2 = 0.436).

Czechia and Poland have negative correlations between SDT1 and GINI (–0.413 and –0.621, respectively; (Appendix 2) – meaning that as wealth distribution becomes more equal, SDT1 behaviors continue progressing with the expectations of the Second Demographic Transition. This contrasts with Austria, where there is a surprising positive correlation between GINI and SDT1 – the more unequally wealth is distributed, the higher the SDT1 rates rise. It is at a moderate Pearson r coefficient (0.687;), and GINI explains about 47.9% of the variances in SDT1. This is a primary indicator of the two paths of the SDT; however, wealth distribution appears to be a differentiating factor rather than economic prosperity.

Unexpectedly, HDI was not a significant predictor of SDT1 change in Romania or Poland despite generally strong Pearson r correlations (0.706 and 0.874, respectively). When isolating the variables HDI and SDT1 and running regression analyses, there is evidence to explore the impact of the SDT1 index on the HDI, as the R2 of those isolated variables in linear regression is 0.764, and a significance level of < 0.001 and an F score of 45.31. This indicates that SDT1 is an independent rather than a dependent variable, as initially posited.

The dendrogram of Ward's hierarchal clustering below, Fig. 12, illustrates that Slovakia and Czechia have the highest level of closeness in terms of clustering, with Romania and Austria matching about five points later. CZ and SK are similar in that they are both dissimilar to the rest. The R2 for Slovakia-Czechia is 0.891 – close in similarity and important in the model; however, it only explains 10.9% of the model variance (semipartial R2 = 0.1087). In the Second level, where the nexus of Romania and Austria (R2 = 0.719, Semipartial R2 = 0.1720) meet Poland (Cluster 4), the R2 is 0.472. This may have more to do with the inclusion of GINI into the models for each country than any other variable.

This dendrogram illustrates the likeness and predictability of Czechia, Austria, Poland, Romania, and Slovakia by variables and significance. This graph shows the likeness of Austria and Romania, and Slovakia and Czechia. Poland had similar probability-in variables; however, it also exhibited the highest adjusted R2 of all populations examined.

This research examined the intricate dynamics between demographic shifts, epitomized by the SDT1

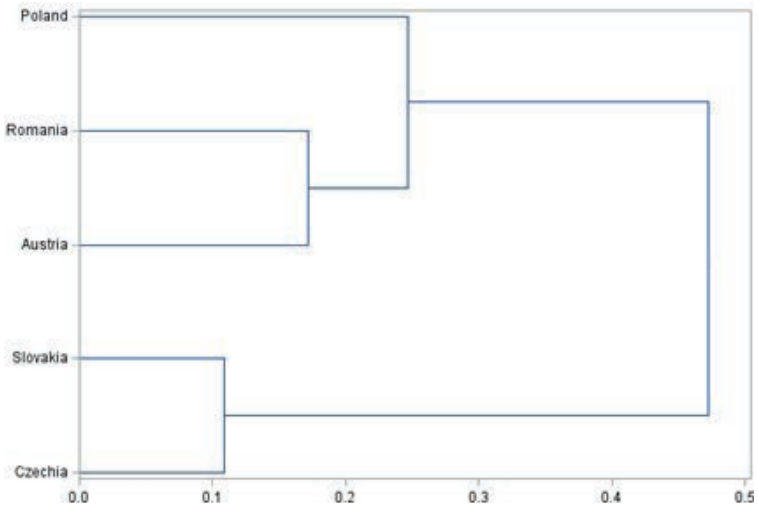

Fig. 12 Dendrogram, Adjusted R2, Ward's Clustering, SDT1.
Source: Author's Own Analysis, SAS.

indices, and economic indicators amidst the backdrop of the COVID-19 pandemic. The study has explained some complex interrelations that impact these phenomena by employing various analytical models, including Pearson's r correlation coefficients, Holt's Exponential Smoothing, linear time regression, and stepwise multiple regression analyses. The analysis results have unveiled a significant, though diverse, influence of economic metrics such as GDP, GINI, and HDI on demographic patterns, particularly regarding total fertility rates (TFR) and the SDT1 index, which includes several demographic indicators. These findings demonstrate a moderate to strong linkage between these economic measures and demographic outcomes, highlighting the critical influence of economic growth, income distribution, and human developmental achievements upon population and demographic transitions. Intriguingly, Czechia, Slovakia, and Romania exhibited congruent trends in demographic shifts, albeit with varying intensities, underscored by the direct impact of economic variables on these transitions.

Furthermore, the study has uncovered an unexpected resilience and predictive capacity of demographic trends in response to economic alterations, as evidenced by the accuracy of Holt's Exponential Smoothing compared with linear regression models. This indicates that demographic variables react predictably to economic fluctuations and follow patterns that can be forecasted with considerable precision. The research also pinpointed certain limitations, such as the minimal influence of the SDT1 behavioural index in forecasting fertility under these population contexts. This highlights the multifaceted nature of demographic changes, which elude variance explanation by economic indices alone. The correlation strength and significance disparity across various nations accentuate the role of unique national attributes, including cultural norms, societal structures, and policy frameworks, in shaping demographic conduct.

Through stepwise regression analysis, the investigation further refined population change conception, earmarking GDP and GINI as recurrent predictors across numerous models and explaining the intricate role of the SDT1 index in forecasting demographic shifts. This substantiates the notion that the demographic transformations observed in the countries under review are profoundly entangled with economic status, wealth allocation, and levels of development. An intriguing result of these analyses is the impact of GDP and GINI and the remaining differences in SDT1's influence on TFR. Of the study, the highest and lowest GDP nations (Austria and Romania, respectively) produced results in the stepwise regression model where SDT1 was a predictor of TFR. Both of these countries, Austria and Romania, also have the highest GINI coefficient, indicating the most significant wealth inequality.

5. Discussion and implications

This research explored the complex interplay between the Second Demographic Transition Index (SDT1) and an array of economic variables, shedding light on the intricacies of demographic evolution in the modern landscape. Our analysis has uncovered a nuanced, though deep, connection between the SDT1 index – a barometer for behavioral shifts in demographic indicators, including the age of marriage, cohabitation, childbearing, and teen fertility. These connections bring to the forefront the significant influence of economic conditions, as captured through the Gross Domestic Product per capita PPP (GDP) and the Gini coefficient, on the patterns of demographic behavior that span diverse socioeconomic backdrops.

Delving deeper, the study supports how the SDT1 index acts as a pivotal lens through which the evolution of societal behaviors can be assessed, reflecting broader changes in behavior toward family life and reproductive decisions. The intricate relationship between this index and demographic outcomes highlights the sensitivity of fertility and marital stability to the undercurrents of economic prosperity and income distribution. It is evident that economic variables such as GDP and the Gini coefficient are not mere background factors but are intimately linked with the foundation of demographic changes, influencing decisions at the most personal and societal levels.

The economic landscape, characterized by the GDP, provides a backdrop against which the drama of demographic transitions unfolds, suggesting that an economy's vibrancy can significantly sway demographic trends. Concurrently, as a measure of income inequality, the Gini coefficient offers insights into the disparities within this economic backdrop, further influencing demographic behaviors. This duality of economic prosperity and distribution paints a complex picture of how economic realities shape demographic shifts, from fertility patterns to marital formations and dissolutions.

The findings from this study extend beyond mere statistical correlations, weaving a narrative that captures the dynamic interplay between economic conditions and demographic transitions. They underscore the critical need for a holistic understanding of demographic changes, encompassing the economic drivers and the societal responses to these changes. This investigation, therefore, contributes to the academic discourse on the socioeconomic underpinnings of demographic rates and highlights the importance of integrating economic insights with demographic research to fully grasp the multifaceted nature of societal evolution in the contemporary era.

5.1 The dual paths re-examined

Sobotka (2008) posited that the second demographic transition is driven not by a single common reason

but by a conventional path, which signified economic prosperity and a post-socialist path through economic crisis. This research initially recreated the SDT1 index to identify the changes observed from year to year since 2004. In this timeframe, it is clear that every country is trending toward more intense behaviors associated with the second demographic transition. The most notable jumps in SDT1 were in Poland (2.35), Romania (2.07), and Czechia (1.99), while Austria appeared to remain nearly stagnant. Initially, Austria was one of the countries on the primary path of transition, while post-socialist countries experienced the alternative pathway. This data leads to signs that these two paths are converging. This is most evident in Czechia and Poland, where economic prosperity and behavioral transitions have occurred.

Though this paper focuses on four select PSCs and Austria, which provides some insight into variable transitions, there is an opportunity to expand this research to cover more geographies, populations, and gender-specific dynamics, including using the gender equality index and the Global Gender Gap Report. The phenomena associated with changing economic and political structures and subsequent effects related to population and fertility change maintain significant value in policy and research. This critical longitudinal study should be tracked over several decades, as these patterns may influence policies as much as policies seem to influence the paths.

6. Conclusion

Population dynamics are ever-changing, and the phenomena that influence these distinctive changes are broad. The PSCs examined in this paper have shown signs of considerable movement towards the second demographic transition with respect to traditionally postmodernist countries. In terms of influence upon the second demographic transition, levels of income inequality tend to be the most significant predictor of change. Of the PSCs, only Romania showed evidence of SDT behavior's impact on fertility changes. This indicates that behavioral changes associated with the second demographic transition are more likely impacted by GINI and GDP than human development. This is also true for changes in fertility patterns, which are most predictable based on GDP and GINI.

Regarding factors predicting TFR, Poland and Slovakia are most alike, whereas Austria is the least similar to any other country. This is in contrast to the predictability of SDT1, where Slovakia is the least like the rest of the countries. Several factors may cause this to be the case, but the explanatory factors that are most insightful with respect to the overall changes in GDP, where in 2019, Slovakia became the weakest economy of the population groups and had the lowest GINI coefficient, meaning the most significant income equality. The most significant shifts were with Czechia, which recorded the highest SDT1 index of the 5 populations. Besides the highest total fertility rate, Czechia is uniquely positioned among PSCs and all the countries in the study. Czechia has transitioned exceptionally well since 1989 compared to other PSCs and is on par with the rest of the post-modernist European countries.

Overall, the SDT1 behavioural index provides some insight into the changing fertility rate phenomena across Europe; however, the index appears to be a dependent variable and holds very limited predictability for fertility. Conversely, fertility rates appear to have no meaningful impact on the SDT1 behavioural index. Future research should include a more robust set of countries and perhaps a regional SDT1 behavioral index for several countries to determine the most and least transitioned regions within each country. This may provide insight into how different population densities contextualize the root issue. It is imperative to recognize that the SDT1 is a valuable index that may act as a barometer for changing conditions but is not necessarily a predictor of fertility changes.

Acknowledgements

Many warm thanks to Professor Rychtarikova of Charles University, Prague, for all of the support and guidance through this process – it has been a pleasure. I also want to thank my Doctoral supervisor, Professor Sykora, who has been pivotal in my development as a demography researcher.

References

Ban, C. (2012): Sovereign Debt, Austerity, and Regime Change: The Case of Nicolae Ceausescu's Romania. East European Politics and Societies 26(4), 743–776, https://doi.org/10.1177/0888325412465513.

Beaujouan, É. (2018): Late Fertility Intentions and Fertility in Austria. Vienna: Austrian Academy of Sciences (ÖAW), Vienna Institute of Demography (VID), https://doi.org/10.1553/0x003ccd3c.

Ben-Ner, A., Montias, J. M. (1991): The Introduction of Markets in a Hypercentralized Economy: The Case of Romania. Journal of Economic Perspectives 5(4), 163–170, https://doi.org/10.1257/jep.5.4.163.

Bernard, J. (1982): Future of Marriages. New Haven: Yale University Press.

Blanc, A. K. (1984): Nonmarital Cohabitation and Fertility in the United States and Western Europe. Population Research and Policy Review 3, 181–193, https://doi.org/10.1007/BF00154336.

Bloom, D. E., Canning, D., Sevilla, J. (2001): Economic Growth and the Demographic Transition. Working Paper 8685, https://doi.org/10.3386/w8685.

Bongaarts, J., Feeney, G. (1998): On the Quantum and Tempo of Fertility. Population and Development Review 24(2), 271–291, https://doi.org/10.2307/2807974.

Cesky Statisticky Urad (2014): Nesezdaná soužití: hlavně ve velkých městech (Cohabitation: Mainly in Big Cities): Prague: CZSO.
Cliquet, R. L. (1991): The second demographic transition: fact or fiction? Council of Europe 29.
Coleman, D. (2004): Why we don't have to believe without doubting in the "Second Demographic Transition" – some agnostic comments. Vienna Yearbook of Population Research, 11–24, https://doi.org/10.1553/populationyearbook2004s11.
Cook, L. J., Iarskaia-Smirnova, E. R., Kozlov, V. A. (2023): Trying to Reverse Demographic Decline: Pro-Natalist and Family Policies in Russia, Poland and Hungary. Social Policy and Society 22(2), 355–375, https://doi.org/10.1017/S1474746422000628.
Cornia, G. A., Panicci, R. (1996): The Transition's Population Crisis: An Econometric Investigration of Nuptiality, Fertiluty, and Mortality in Severely Distressed Economies. MOCT-MOST 6, 95–129, https://doi.org/10.1007/BF02430940.
Eurostat. (2023): Fertility Indicators. Available online: https://ec.europa.eu/eurostat/databrowser/view/demo_find__custom_10017309/default/table?lang=en (accessed on 5.3.2024).
Eurostat. (2024): Families by type, size and NUTS 3 region. Available online: https://ec.europa.eu/eurostat/databrowser/view/cens_11fts_r3/default/table?lang=en&category=cens.cens_11r.cens_11rdf (accessed on 3.4.2024).
EuroStat (2024): Fertility indicators. Available online: https://ec.europa.eu/eurostat/databrowser/view/demo_find/default/table?lang=en&category=demo.demo_fer (accessed on 10.4.2024).
Eurostat (2024): Live births by mother's age and legal marital status. Available online: https://ec.europa.eu/eurostat/databrowser/view/demo_fagec__custom_10027240/default/table?lang=en (accessed on 10.4.2024).
Fantom, N., Serajuddin, U. (2016): The World Bank's Classification of Countries by Income. Policy Research Working Paper. Available online: https://documents1.worldbank.org/curated/en/408581467988942234/pdf/WPS7528.pdf (accessed on 20.4.2024).
Frejka, T. (1980): Fertility Trends and Policies: Czechoslovakia in the 1970s. Population and Development Review 6(1), 65-93, https://doi.org/10.2307/1972655.
Gini, C. (1912): Variabilità e mutabilità: contributo allo studio delle distribuzioni e delle relazioni statistiche. Tipografia.
Hamadeh, N., Rompaey, C. V., Metreau, E., Eapen, S. G. (2022): New World Bank country classifications by income level: 2022–2023. Washington DC.: World Bank. Available online: https://blogs.worldbank.org/en/opendata/new-world-bank-country-classifications-income-level-2022-2023.
Hernandez, E. L. (2018): Is the Second Demographic Transition Going Global? And Why? In PAA 2018 Annual Meeting. PAA.
Ianoș, I., Heller, W. (2004): Spatial Patterns of Economy and Migration in Post-Socialist Romania. Europa Regional, 4–12. https://nbn-resolving.org/urn:nbn:de:0168-ssoar-48099-6.
Kocourková, J., Slabá, J., Šťastná, A. (2022): The role of cohorts in the understanding of the changes in fertility in Czechia since 1990. AUC Geographica 57(1), 61–74, https://doi.org/10.14712/23361980.2022.6.
Kolodko, G. W. (2009): A two-thirds of success. Poland's post-communist transformation 1989–2009. Communist and Post-Communist Studies 42(3), 325–251, https://doi.org/10.1016/j.postcomstud.2009.07.005.
Kopczuk, W., Saez, E. (2004): Top wealth shares in the United States, 1916–2000: Evidence from estate tax returns. National Tax Journal 57(2.2), 445–487, https://doi.org/10.17310/ntj.2004.2S.05.
Kotowska, I., Jóźwiak, J., Matysiak, A., Baranowska, A. (2008): Poland: Fertility decline as a response to profound societal and labour market changes? Demographic Research 19, 795–854, https://doi.org/10.4054/DemRes.2008.19.22.
Koyame-Marsh, R. O. (2011): The Complexities of Economic Transition: Lessons from the Czech Republic and Slovakia. International Journal of Business and Social Science 2(19), 71–85.
Lesthaeghe, R. (2020): The second demographic transition, 1986–2020: sub-replacement fertility and rising cohabitation – a global update. Journal of Population Sciences 76, 10, https://doi.org/10.1186/s41118-020-00077-4.
Lesthaeghe, R., Permanyer, I. (2014): European sub-replacement fertility: Trapped or recovering. Population studies center research report, 14–822. Available online:https://citeseerx.ist.psu.edu/document?repid=rep1&type=pdf&doi=a370d7e8887d15516f442de4fe48dcb8c4d3ae61 (accessed on 20.3.2024).
Lijphart, A. (1992): Democratization and constitutional choices in Czecho-Slovakia, Hungary and Poland 1989–91. Journal of Theoretical Politics 4(2), 207–223, https://doi.org/10.1177/0951692892004002005.
Maia, A. L., de Carvalho, F. D. (2011): Holt's exponential smoothing and neural network models for forecasting interval-valued time series. International Journal of Forecasting 27(3), 740–759, https://doi.org/10.1016/j.ijforecast.2010.02.012.
Mierau, J. O., Turnovsky, S. J. (2014): Demography, growth, and inequality. Economic Theory 55, 29–68, https://doi.org/10.1007/s00199-013-0749-z.
Myrskylä, M., Kohler, H. P., Billari, F. C. (2009): Advances in development reverse fertility declines. Nature 460, 741–743, https://doi.org/10.1038/nature08230.
Možný, I., Rabušic, L. (1992): Unmarried Cohabitation in Czechoslovakia. Czechoslovak Sociological Review 28, 107–117. Available online: https://www.jstor.org/stable/41133198 (accessed on 30.3.2024).
Oláh, L. S., Frątczak, E. (2003): Gendering family formation. First marriage and first birth in Hungary and Poland. In Population of Central and Eastern Europe. Challenges and Opportunities, 219–250, Warsaw.
Ouanes, A., Madhav Thakur, S. (1997): CHAPTER 1 Poland's Transition to the Market: An Overview. In Macroeconomic Accounting and Analysis in Transition Economies, 1-11. Washington DC: International Monetary Fund, https://doi.org/10.5089/9781557756282.071.
Potančoková, M., Vaňo, B., Pilinská, V., Jurčová, D. (2008): Slovakia: Fertility between tradition and modernity. Demographic Research 19, 973–1018, https://doi.org/10.4054/DemRes.2008.19.25.

Rabušic, L., Manea, B. C. (2019): Marriage, Childbearing and Single Motherhood: Trends in Attitudes and Behaviour in Czechia and Slovakia from 1991 to 2017. Sociální studia 16(2), 25–50, https://doi.org/10.5817/SOC2019-2-25.

Rotariu, T. (2010): Nonmarital Births in Romania versus Other European Countries-A Few Considerations. Studia Universitatis Babes-Bolyai-Sociologia 55(2), 37–60.

Rychtarikova, J. (1999): Is Eastern Europe Experiencing a Second Demographic Transition? AUC Geographica 34(1), 19–44.

Rychtarikova, J., Monnier, A. (1992): The Division of Europe into East and West. Population: An English Selection 4, 129–159. Available online: https://www.jstor.org/stable/2949121 (accessed on 10.4.2024).

Sobotka, T. (2008): The diverse faces of the Second Demographic Transition in Europe. Demographic research 19, 172–223, https://doi.org/10.4054/DemRes.2008.19.8.

Sobotka, T. (2015): Low fertility in Austria and the Czech Republic: Gradual policy adjustments. Vienna Institute of Demography Working Papers 2. Available online: https://hdl.handle.net/10419/110987 (accessed on 15.4.2024)

Sobotka, T., Zeman, K., Kantorová, V. (2003): Demographic shifts in the Czech Republic after 1989: A second demographic transition view. European Journal of Population/Revue européenne de démographie 19, 249–277, https://doi.org/10.1023/A:1024913321935.

Trost, J. (1978): A Renewed Social Institution: Non-marital Cohabitation. Acta Sociologica 21(4), 303-316, https://doi.org/10.1177/000169937802100402.

van de Kaa, D. (1987): Europe's second demographic transition. Population Bulletin 42(1), 1-59.

van de Kaa, D. J. (2002): The Idea of a Second Demographic Transition in Industrialized Countries. Sixth Welfare Policy Seminar of the National Institute of Population and Social Security 1-34. Tokyo. Available online https://www.ipss.go.jp/webj-ad/Webjournal.files/population/2003_4/kaa.pdf (accessed on 10.4.2024).

Vlasov, M., Polbitsyn, S. N., Olumekor, M., Haddad, H. (2023): Exploring the Role of Socio-Cultural Factors on the Development of Human Capital in Multi-Ethnic Regions. Sustainability 15(21): 15438, https://doi.org/10.3390/su152115438.

Wiik, K. A., Keizer, R., Lappegard, T. (2012): Relationship Quality in Europe. Journal of Marriage and Family, 389–398. Available online https://hdl.handle.net/10419/192615 (accessed on 15.4.2024).

World Bank Group. (2024): World Bank Country and Lending Groups. Available online: https://datahelpdesk.worldbank.org/knowledgebase/articles/906519-world-bank-country-and-lending-groups (accessed on 15.4.2024).

Zaidi, B., Morgan, S. P. (2017): The Second Demographic Transition Theory: A Review and Appraisal. Annual Review of Sociology 43, 473–492, https://doi.org/10.1146/annurev-soc-060116-053442.

Appendix 1 Data, Sources, and Methodology.

Name	Code	Dataset	Description of Dataset	Calculation Method
Median Age at First Childbirth	MAFB	Eurostat, Fertility Indicators (demo_find)	Dataset has several indicators, one of which is MAFB	No calculation Required
Age Specific Rate Below Age 20/1000	TEENFERT	Eurostat, Live Births by Mothers Age (demo_fordagec) Eurostat, Population on 1 January by age and sex (demo_pjan)	Total live births by age – < 14 to > 20. B_{x_t} Total Population by Age and Sex P_{x_t}	Live births in a year divided by the average of the next year's 1 January population, summed to represent the total fertility for under-20 years old. $\sum_{t}^{r,<20} \frac{B_{x_t}}{(P_{x_t}+P_{x_{t+1}})/2}$
Total First Marriage Rate (n_{x^r})	TFMR	Eurostat, Population on 1 January by Age, Sex, and Legal Marital Status (demo_pjanmarsta) Eurostat, First-Time Marrying Persons by Age and Sex (demo_nsinagec)	Total population on the first day of the year by age and sex. Marital Status did not impact this calculation. P_{x_t} Primo-Nuptiality by age and sex, up to 59 years $PN^1_{x_t}$	Primo-Nuptiality rates per age is the number of first marriages. This is calculated by summing each of the age-specific primo-nuptiality rates, as illustrated: $\sum_{t}^{r} \frac{PN^1_{x_t}}{(P_{x_t}+P_{x_{t+1}})/2}$
Percent of Non-Marital live Births	NONMAR	Eurostat, Live Births by Mothers Age and Legal Marital Status (demo_fagec)	Two points of data were derived from this data set. First were non-marital live births: $B^{nm}_{x_t}$ The second was the total live births: $B^{P}_{x_t}$	The Percentage of non-marital live births has been calculated as: $\frac{B^{nm}_{x_t}}{B^{P}_{x_t}}$ The output represents the percentage of extra-marital live births each year.
Mean Age at First Marriage	MAFM	Eurostat, Marriage Indicators (demo_nind)	Data includes 8 indicators. The indicator used for this study was "Mean Age at First Marriage – Females"	No calculation Required
Total Divorce Rate	TDR	Eurostat, Divorce Indicators (demo_ndivind)	Data includes 3 indicators. The indicator used for this study was "Divorces per 100 marriages"	No calculation is required.
Total Fertility Rate	TFR	Eurostat, Live Births by Mothers Age (demo_fordagec) Eurostat, Population on 1 January by age and sex (demo_pjan)	Total live births by age group > 14 to < 20. B_{x_t} Total Population by Age and Sex P_{x_t}	$\sum_{t}^{r} \frac{B_{x_t}}{(P_{x_t}+P_{x_{t+1}})/2}$
GINI Index	GINI	World Bank GINI Coefficients (SI.POV.GINI)	GINI Index indicates the disparity in income from upper and lower earners based on income deciles.	No calculation – indexed on the World Bank
Gross Domestic Product per Capita, Purchasing Power Parity	GDP	World Bank Gross Domestic Product per Capita PPP (Current USD) (NY.GDP.PCAP.PP.CD)	World Bank Calculation of the gross domestic product per person at purchasing power parity and standard.	No calculation- indexed on World Bank
Human Development Index	HDI	UNDP Human Development Report HDI (HDR23-24_Stistical_Annex_HDI_Table)	United Nations HDI is calculated based on education, health, and GNI – updated annually	No calculation, Indexed by UNDP

Appendix 2 Pearson's r Coefficients, All Countries.

	Czechia	Austria	Poland	Romania	Slovakia
SDT1-HDI	0.763	0.579	0.874	0.706	0.131
SDT1-GDP	0.644	0.467	0.856	0.830	0.036
SDT1-GINI	−0.413	0.687	−0.621	0.159	0.037
SDT1-TDR	−0.297	−0.137	0.902	0.437	0.597
SDT1-TFR	0.601	0.100	0.323	0.633	−0.114
HDI-GDP	0.937	0.963	0.978	0.844	0.956
HDI-GINI	−0.828	0.419	−0.845	0.528	−0.328
HDI-TDR	−0.775	−0.849	0.639	0.115	−0.612
HDI-TFR	0.914	0.792	0.668	0.850	0.792
GDP-GINI	−0.717	0.338	−0.867	0.110	−0.542
GDP-TDR	−0.873	−0.879	0.588	0.013	−0.718
GDP-TFR	0.962	0.753	0.731	0.908	0.869
GINI-TDR	0.754	−0.104	−0.348	0.089	0.449
GINI-TFR	−0.754	0.036	−0.813	0.195	−0.655
TFR-TDR	−0.834	−0.887	−0.044	−0.044	−0.704

Source: Author's Own Calculations, SPSS.

Appendix 3 Clustering Input, TFR.

	GDP	GINI	HDI	SDT1
Austria	0.756	0	0.570	0.685
Czechia	0.920	0.940	0	0
Poland	0	0.618	0	0
Romania	0.812	0	0	0.851
Slovakia	0.739	0	0	0

Appendix 4 Clustering Input, SDT1.

	GDP	GINI	HDI
Austria	0	0.797	0.582
Czechia	0	0.444	0
Poland	0.806	0.876	0
Romania	0.668	0	0
Slovakia	0	0.229	0.436

Appendix 5 Ward's Hierarchical Clustering Outputs, TFR.

Cluster History, TFR					
# Clusters	Clusters Joined		Freq	Semipartial R^2	R^2
4	Romania	Slovakia	2	0.1267	.873
3	Czechia	Poland	2	0.2123	.661
2	Austria	CL4	3	0.2240	.437
1	CL3	CL2	5	0.4370	.000

Appendix 6 Ward's Hierarchical Clustering Outputs, SDT1.

Cluster History, SDT1					
# Cluster	Clusters Joined		Freq	Semipartial R2	R2
4	Czechia	Slovakia	2	0.1086	.891
3	Austria	Romania	2	0.1720	.719
2	CL3	Poland	3	0.2472	.472
1	CL4	CL2	5	0.4722	.000

Identification of optimal Sentinel-1 SAR polarimetric parameters for forest monitoring in Czechia

Daniel Paluba[1], Bertrand Le Saux[2], Francesco Sarti[3], Přemysl Štych[1,*]

[1] Charles University, Faculty of Science, Department of Applied Geoinformatics and Cartography, EO4Landscape Research Team, Czechia
[2] European Space Agency (ESA/ESRIN), Φ-lab – Climate Action, Sustainability and Science Department (EOP-S), Earth Observation Programmes Directorate, Italy
[3] European Space Agency (ESA/ESRIN), Earth Observation Programmes Directorate, Italy
* Corresponding author: stych@natur.cuni.cz

ABSTRACT

Time series analysis of synthetic aperture radar data (SAR) offers a systematic, dynamic and comprehensive way to monitor forests. The main emphasis of this study is on the identification of the most suitable and best performing Sentinel-1 SAR polarimetric parameters for forest monitoring. This is accomplished through: 1) a pairwise correlation analysis of SAR polarimetric parameters, multispectral optical vegetation indices and ancillary data, 2) a univariate binary time series classification for differentiation between forest types and 3) a visual exploration of time series. For this purpose, 600 validated broad-leaved and 600 coniferous forest areas in Czechia were used. Nine different SAR polarimetric parameters were examined, including VH and VV polarizations, VV/VH and VH/VV polarization ratios, the Radar Vegetation Index, Radar Forest Degradation Index, polarimetric radar vegetation index and the original and modified versions of the dual polarimetric SAR vegetation index. The pairwise correlation analysis revealed that most of the derived SAR polarimetric parameters were functions of each other with nearly identical behavior ($r > |0.96|$). The strongest correlation of $r \sim 0.50$ between SAR and optical features was found for broad-leaved forest for VV/VH and VH/VV. The highest overall accuracy in the time series classification of forest types was achieved by VH (76%), while for VV, VV/VH and VH/VV it was higher than 60%. Furthermore, the time series analysis of these parameters showed seasonal behaviors of the SAR features in both forest types. These results demonstrated the high relevance of using VH, VV, VV/VH and VH/VV time series in forest monitoring compared to other SAR polarimetric parameters. This study also introduces a novel pipeline to generate multi-modal time series datasets in Google Earth Engine (MMTS-GEE), used to generate data for the analysis. MMTS-GEE combines spatially and temporally aligned SAR and multispectral data, extended with topographic and weather data, and a land cover class label. Its high versatility enables its use in time series analyses, intercomparisons and in machine learning applications for tabular time series data. The GEE code for the proposed tool and analysis is freely available to the research community.

KEYWORDS

time series; Google Earth Engine; SAR; time series classification; forest; Sentinel-2; Czechia

Received: 6 May 2024
Accepted: 24 October 2024
Published online: 4 December 2024

Paluba, D., Le Saux, B., Sarti, F., Štych, P. (2024): Identification of optimal Sentinel-1 SAR polarimetric parameters for forest monitoring in Czechia. AUC Geographica 60(1), 46–60
https://doi.org/10.14712/10.142/23361980.2024.18

1. Introduction

Time series analysis of remote sensing (RS) data offers a dynamic and comprehensive way to monitor the Earth's surface and atmosphere in a systematic way. One of the most dynamically changing land cover types is vegetation, especially forests, being influenced by several anthropogenic and natural factors (Senf and Seidl 2021; Ma et al. 2023; Forzieri et al. 2022). Forest change is an important ecological process leading to reestablishment of forest biomass and structure (Bartels et al. 2016); therefore, incorporating time series in their monitoring is essential. Currently, the two most commonly used open-access RS data types are optical multispectral data (e.g., from Landsat or Sentinel-2 missions) and synthetic aperture radar (SAR) data (e.g., from the Sentinel-1 mission).

Optical vegetation indices, such as the Normalized Difference Vegetation Index (NDVI), Enhanced Vegetation Index (EVI), or biophysical and structural parameters, such as the Leaf Area Index (LAI) and Fraction of Absorbed Photosynthetically Active Radiation (FAPAR) are one of the most-known and most-used parameters for vegetation and forest monitoring in the optical domain (Zeng et al. 2022). NDVI is the most popular VI due to its simplicity, long history, and the fact that it can be created from the data of almost every RS sensor (Huang et al. 2021). EVI has improved sensitivity in high biomass regions compared to NDVI and it reduces the influence of the ground and atmosphere signal on the canopy response (Huete et al. 2002). LAI and FAPAR were identified as terrestrial Essential Climate Variables (ECV) by the Global Climate Observing System (WMO et al. 2011). These VIs are also generated on the global scale for operational use, e.g. NDVI and EVI from the MODIS or from NASA Visible Infrared Imaging Radiometer Suite (VIIRS) (at 250–1000 m and 16 days of spatial and temporal resolution, respectively) (Didan 2021b; 2021a; Didan and Barreto 2018), LAI and FPAR from MODIS and VIIRS (500 m and 4–8 days) (Myneni, Knyazikhin, and Park 2021; Myneni and Knyazikhin 2018), NDVI, LAI and FAPAR from the Copernicus Global Land Service (CGLS) (300 m and 10 days) (Fuster et al. 2020) or the Pan-European Sentinel-2 LAI, FAPAR and NDVI products (10 m and 1 day) (Smets et al. 2023).

Vegetation indices based on optical data are heavily dependent on sunlight, making them less effective in areas with frequent cloud cover. For this reason, SAR polarimetric parameters have also been developed for vegetation monitoring in recent years. They are based on a combination of backscatter coefficient from SAR polarizations, e.g. co-polarization ratios (PR) of VH/VV or VV/VH, Radar Vegetation Index (RVI), Radar Forest Degradation Index (RFDI), polarimetric radar vegetation index (PRVI), dual polarimetric SAR vegetation index (DPSVI) (Frison et al. 2018; Chang, Shoshany, and Oh 2018; Alvarez-Mozos et al. 2021; Hird et al. 2017; Kim and van Zyl 2000; Periasamy 2018; dos Santos, Da Silva, and do Amaral 2021) or incorporate also the phase information, such as the Dual-pol radar vegetation index (DpRVI) or the Compact-pol RVI (CpRVI) (Mandal et al. 2020a; 2020b). Compared to optical indices, which are altered primarily by physiological, biophysical, and biochemical changes in vegetation throughout the year, SAR signals can be strongly influenced not only by structural changes during the year but also by environmental factors such as precipitation and temperature (Olesk et al. 2015; Benninga, van der Velde, and Su 2019; Rüetschi, Small, and Waser 2019; Paluba et al. 2023). Environmental effects can alter the moisture content and, consequently, the dielectric properties of objects, which typically change throughout the year.

For the purpose of finding the most suitable combination of optical and SAR data for environmental monitoring, relationship/correlation between them has been evaluated. Moderate to high correlations were found between NDVI and SAR polarizations (VH and VV), polarimetric indices (Radar Vegetation Index – RVI, VH/VV, VV/VH and other) for crop monitoring, (e.g., in Alvarez-Mozos et al. 2021; Filgueiras et al. 2019; Holtgrave et al. 2020; Jiao, McNairn, and Dingle Robertson 2021) and interferometric coherence (Bai et al. 2020). However, these analyses were performed on an image-by-image basis and no time series data were included. Frison et al. (2018) were focused on the aspect of time series and a strong correlation between NDVI and the co-polarimetric ratio VH/VV for forest time series was found.

Effective computing platforms and algorithms are needed to assess, pre-process and test a wide range of data types, especially in time series analysis and machine learning approaches, such as classification or regression tasks. Current cloud-based platforms, such as Google Earth Engine (GEE), allow access to a wide range of datasets, as well as processing power in the cloud, without the need to download data locally or own high computational resources (Gorelick et al. 2017). The wide use of GEE is documented by recognized publication databases, such as the Web of Science (webofscience.com), where a total of 3,937 published contributions including the "Google Earth Engine" keyword in the abstract, title or keywords was found, while 1,032 were published last year, in 2023 (accessed on 16.7.2024). GEE has a prominent role in current forest monitoring efforts. The Global Forest Watch (Global Forest Watch 2014), using the power of GEE, collects global and regionally oriented forest datasets to provide deforestation (Reiche et al. 2021) or fire alerts (Tyukavina et al. 2022), map forest loss and gain (Hansen et al. 2013), primary forest distribution (Turubanova et al. 2018), forest greenhouse gas emissions (Harris et al. 2021) or identify the drivers of forest loss (Curtis et al. 2018) to mention a few.

Nowadays, there are about 400 RS datasets for deep learning applications, including Satellite Time

Series Datasets (Dufourg et al. 2024), as reported in Schmitt et al. (2023). These datasets contain data from various sensors and RS platforms, even their combinations, focusing on different topics, covering various geographical locations and time steps. Most of these datasets are mono-temporal, covering selected patches globally, but only for a single time step. Their publication dates vary, affecting the up-to-dateness of data, and their sizes range from a few megabytes to tens of terabytes. Although DL models trained on large geographic scales can work on local levels, their use in time series analysis for a defined area of interest would be challenging due to local specifics, time scale or equipped sensors.

For this purpose, in this work, a GEE pipeline to create multi-modal time series datasets (MMTS-GEE), specifically temporally and spatially paired labeled time series of S1, S2 and ancillary data (DEM and weather data), is developed. MMTS-GEE enables generation of paired time series for any time period (based on data availability) and over any geographic region as well as preprocessing data including cloud masking, speckle filtering and feature extraction. Selected and validated forest areas in Czechia were used to extract time series of selected SAR and optical indices/parameters, as well as ancillary data. The main goal and scientific contribution of this study is to identify the most suitable and best performing SAR polarimetric parameters for forest monitoring. It was accomplished through performing a pairwise correlation analysis of SAR, optical and ancillary data, time series classification in forest type differentiation and visual inspection of time series. The GEE code for the MMTS-GEE tool repository has been made available on GitHub to support open science.

1.1 Data

The main data sources for this study are Copernicus Sentinel-1 SAR data (S1) and Sentinel-2 multispectral data (S2) operated by the European Space Agency (ESA). The S1 C-band (with 5.405 GHz central frequency) SAR data in Ground-range detected (GRD) were accessed from GEE with a pixel size of 10 m and a spatial resolution of about 20 × 22 m. Therefore, a spatial resolution of 20 m was used in all data processing in GEE and in further analyses. S1 data acquired before 2022 were used to explore the full potential of both Sentinel-1A and B satellites, which provided a 6-day temporal resolution until the end of 2021 when an anomaly occurred with the Sentinel-1B satellite (Pinheiro et al. 2022). The S2 mission with its two sun-synchronously orbiting satellites provides images of the Earth's surface in the optical domain every 5 days with a spatial resolution of 10, 20 and 60 m, depending on wavelength.

To enhance multi-modality and address the relationship between SAR backscatter and topographic and climatic features, the Copernicus DEM digital elevation model (C-DEM) and weather data from the ERA-5 Land mission were also assessed. The C-DEM is a digital surface model representing the surface of the Earth, including buildings, infrastructure and vegetation for the time frame between 2011 and 2015 (European Space Agency and Airbus 2022). It is based on TanDEM-X satellite products provided by the German Aerospace Center (DLR) and Airbus Defence and Space. In this work, the C-DEM GLO-30 product was used, which represents a global DEM with a spatial resolution of 30 m. C-DEM was used to provide information on elevation, calculating slope, and local incidence angle (LIA). LIA, the angle between the look (incidence) vector of the SAR signal and the vector normal to the surface, was calculated for each S1 image separately based on the methodology of Paluba et al. (2021).

The ERA5-land is a reanalysis dataset from the original ERA5 dataset with an hourly temporal resolution and with an enhanced resolution of 0.1 arc degrees with a native resolution of 9 km (Copernicus Climate Change Service 2019, p. 5). The dataset includes 50 variables in an hourly step from 1981, from which two variables were used: "temperature_2m", an average temperature of air 2 meters above the surface; and "total_precipitation", accumulated liquid and frozen water, including rain and snow, that falls to the Earth's surface. The following meteorological data were derived from the ERA5 Land dataset for the selected study area: the sum of precipitation 12 hours prior to each SAR acquisition, and the temperature at the time of SAR acquisition.

Three land cover datasets, specifically ESA WorldCover v200 (ESA WC) for 2021 with a spatial resolution of 10 m (Zanaga et al. 2022), Corine Land Cover (CLC) for 2018 with a spatial resolution of 100 m and a minimal mapping unit of 25 ha (Kosztra et al. 2019), Copernicus Global Land Cover Layers Collection 3 (GLCL) (Buchhorn et al. 2020) with a spatial resolution of 100 m, and a forest-oriented dataset, the Hansen Global Forest Change v1.10 (GFC) with a spatial resolution of 30 m (Hansen et al. 2013) were used for forest mask generation.

1.2 Study areas and methods

Study Areas

Czechia was selected as a case study. Czechia has a relatively high share of forests with heterogeneous species composition. In 2021, forests represented 34% of the total area of Czechia. The coniferous species represented 70% of the total forest cover, while the most populous species are *Norway spruce* (68% of all conifers), followed by pines (23%) and larch (6%). Broad-leaved species are represented mainly by beech (32% of all broad-leaved species), oak (27%) and birch (10%) (Ministry of Agriculture of the Czech Republic 2022).

Automatic Forest Dataset Generation

Coniferous and broad-leaved forest areas were selected in the entire Czechia for this study. Healthy forest masks were created based on an enhanced pipeline from (Paluba et al. 2021; Onačillová, Krištofová, and Paluba 2023), where an intersection of three land cover datasets (ESA WC, CLC and GLCL) and a forest-oriented dataset (GFC) was utilized. In the first step, pixels with a canopy closure greater than 50% in the base layer, as recorded in the GFC dataset for the year 2000, were selected. Pixels where a forest loss occurred between 2000 and 2021 (*forest_loss* band) were further masked out. The CLC and GLCL datasets allowed differentiation between coniferous and broad-leaved forests; therefore, based on their intersection, broad-leaved and coniferous forest masks were created. Consequently, around 1000 random points with a 20-m buffer, entirely located inside the forest masks, were generated for the whole of Czechia for both forest types.

Validation of automatically generated forest areas

In the next step, a verification of automatically generated healthy forest areas (~1000 from each class) was carried out to include only pure forest areas throughout the observed period. They were verified using a visual analysis with high-resolution images in Google Earth Pro (GEP). GEP provides satellite images with medium to very high spatial resolution, including providers such as NASA / USGS with Landsat data (30 m), CNES with SPOT data (10–1.5 m) or DigitalGlobe/Maxar with IKONOS and QuickBird data with sub-meter resolution (Bey et al. 2016). To differentiate between broad-leaved and coniferous forests, images that capture both leaf-on (summer) and leaf-off (winter) conditions of the forests were used. The *European Larch* (*Larix decidua*), a coniferous tree that loses its needles in autumn, was excluded from both the broad-leaved and coniferous input datasets to avoid discrepancies in the satellite time series. To ensure that the areas did not undergo significant forest changes in 2021 and to eliminate possible errors introduced by the forest masks, only areas with at least 75% tree coverage in their 20 × 20 m buffered areas were left in the final input dataset. Areas located on the borders of different forest growth stages (small young versus high old trees) were excluded to avoid the effects of possible SAR shadowing on young trees caused by higher trees. Areas containing water or paved/concrete roads were also excluded. In the end, 600 coniferous and 600 broad-leaved forest areas were selected for further analysis. Their spatial distribution can be seen in Fig. 1.

S1 and S2 Data Preparation and Pre-Processing

Initially, S2 Surface Reflectance (Level-2A) image tiles with cloud cover higher than 30% were filtered out (resulting in 871 S2 images for the entire Czechia in 2021). It should be noted that the S2 Level-2A data in GEE are already processed using the Sen2Cor processor and are automatically ingested to GEE from the Copernicus Open Access Hub (scihub.copernicus.eu). In the next step, the CloudScore+ approach, using the *cs* band with a default threshold of 0.60 was applied to exclude defected pixels affected by clouds, shadows and haze. CloudScore+ uses a weakly supervised deep learning approach to analyze the quality of each image pixel, while assigning per-pixel quality scores (Pasquarella et al. 2023; Pasquarella 2024). The *cs* band was used rather than the *cs_cdf* due to its higher sensitivity to haze and cloud edges and is recommended for applications where an absolute clear pixel is required (Pasquarella 2024). A threshold of 0.60 was found to have sufficient tradeoff between masking the correct pixels and losing useful information in (Nicolau 2024). After the cloud unmasking, two optical vegetation indices, NDVI and EVI, and two vegetation parameters, LAI and FAPAR, were calculated. More information can be found in Tab. 1.

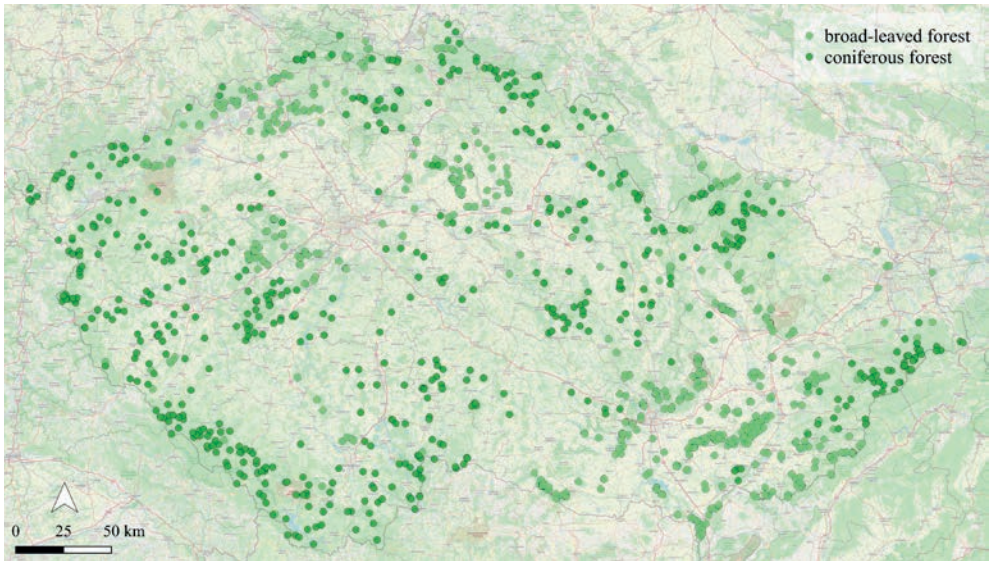

Fig. 1 Spatial distribution of broad-leaved and coniferous forest areas used in this study.

Tab. 1 Target optical vegetation indies.

Name	Abbreviation	Forumula	Source
Normalized Difference Vegetation Index	NDVI	$\frac{NIR - RED}{NIR + RED}$	(Gamon et al. 1995)
Enhanced Vegetation Index	EVI	$2.5 \times \frac{NIR - RED}{NIR + 6 \times RED - 7.5 \times BLUE}$	(Liu and Huete 1995)
Leaf Area Index	LAI	based on (Weiss and Baret 2016)	*
Fraction of Absorbed Photosynthetically Active Radiation	FAPAR	based on (Weiss and Baret 2016)	*

Note: * GEE implementation by Van Tricht (2023).

A total of 1,419 S1 images were acquired and pre-processed for the entire Czechia in 2021. Following Filgueiras et al. (2019), the Lee speckle filter with a window size of 5 × 5 pixels was applied to the S1 data in GEE to reduce the speckle noise, based on the implementation in Mullissa et al. (2021). The Lee filter is one of the most used speckle filters, being computationally efficient while effectively smoothing the speckle effect and preserving the edges or subtle details (Lee 1985). The SAR polarimetric parameters (VV/VH, VH/VV, Radar Forest Degradation Index – RFDI, Radar Vegetation Index – RVI, the original Dual Polarized SAR Vegetation Index – $DPSVI_o$ and its modified version $DPSVI_m$) were then calculated in power/linear units (Tab. 2). The VV and VH polarizations were converted to decibels (dB), to a logarithmic scale.

The final MMTS-GEE pipeline: Image pairing and time series data export

In the next step, the pre-processed S1 and S2 images were temporally and spatially joined and aligned. The joined S1–S2 image collection was created based on a spatial overlap and the 24-hour temporal difference between the pre-processed S1 and S2 images. The S1 images served as master images in image stacking, that is, the S2 images were joined to the S1 images. The temporal difference of 24 hours was selected based on the findings that daily differences in optical VIs, e.g., in NDVI, are negligible (May et al. 2017). In total, 1254 S1–S2 pairs were identified in 2021 in Czechia. The analysis of temporal differences between the S1–S2 pairs resulted in a bimodal distribution. More than half of the pairs (643 images) had differences between 4 and 7 hours, while the second group of the pairs (611 images) had differences between 17 and 20 hours. The mean difference was 12 hours, with the majority of pairs having a difference of 5 (302 images) and 19 hours (288 images).

The ancillary features (DEM and weather data) were then calculated for each pixel and added to the feature space. At the end, an image collection was created, where each image includes spatially and temporally joined and aligned S1 and S2 images, topographic characteristics (elevation, slope, LIA) and weather data (temperature, precipitation). All data are resampled into a 20-m grid using the nearest neighborhood

Tab. 2 Calculated SAR polarimetric features.

Name	Abbreviation	Forumula	Source
Radar Vegetation Index	RVI	$4 \times \frac{VH}{VH + VV}$	[1,2]
Radar Forest Degradation Index	RFDI	$\frac{VV + VH}{VV - VH}$	[3]
Polarimetric Ratio 1	VV/VH	$\frac{VV}{VH}$	[4]
Polarimetric Ratio 2	VH/VV	$\frac{VH}{VV}$	[5]
Normalized Ratio Procedure between Bands	NRPB	$\frac{VH - VV}{VH + VV}$	[6]
Dual Polarized SAR Vegetation Index, original	$DPSVI_o$	$VH \times \frac{VV_{max} \times VH - VV \times VH + VH^2}{1.41421 * VV}$	[7]
Dual Polarized SAR Vegetation Index, modified	$DPSVI_m$	$\frac{VV_{max} - VV + VH}{1.41421 \times ((VV + VH)/VV) \times VH}$	[8]

References: [1]: Kim, van Zyl (2000), [2]: Sahadevan, Sitiraju, Sharma (2013), [3]: Saatchi (2019), [4]: Frison et al. (2018), [5]: Alvarez-Mozos et al. (2021), [6]: Hird et al. (2017), [7]: Periasamy (2018), [8]: dos Santos, Da Silva, do Amaral (2021)

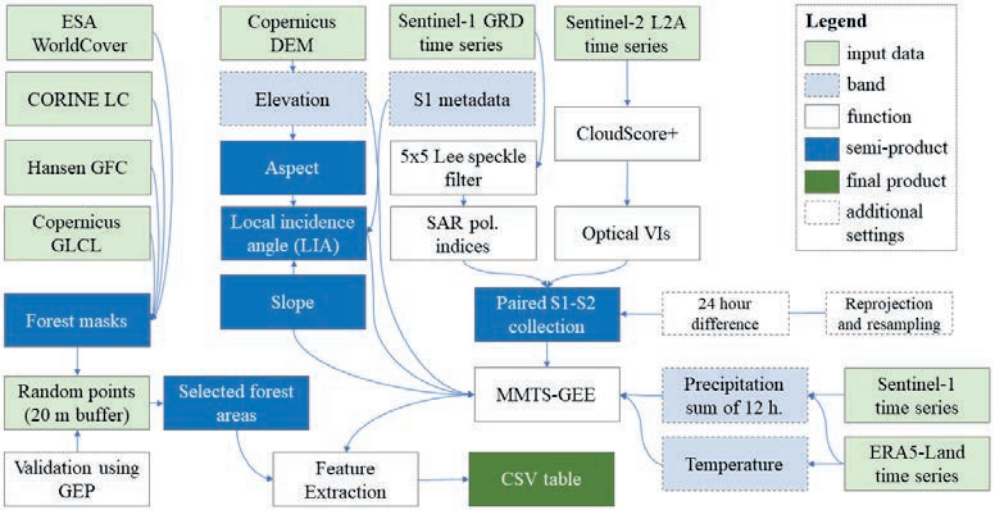

Fig. 2 Data pre-processing and preparation workflow of the MMTS-GEE.

method, while reprojection and resampling in GEE are done automatically on-the-fly.

Multimodal time series were extracted for each selected forest area. Each forest area had its unique ID and the date of SAR image acquisition. As the final step in GEE, each timestep-area combination including values of optical, SAR and ancillary features was exported from GEE in a csv table. The analysis was carried out using the original S1 coordinate system for Czechia (EPSG:32634) and with a spatial resolution of 20 meters, which matches the spatial resolution of the S1 data. The full pipeline of the MMTS-GEE is depicted in Fig. 2.

Pairwise correlation analysis of optical, SAR and ancillary features

In the next step, a pairwise correlation analysis was performed between each SAR feature, to assess similarities between them and to reduce possible data redundancy by excluding features. The second correlation analysis focused on exploring the relationship between SAR features and optical features generated from S2 data. For these analyses, all exported data were used, that is, each time step for each selected point. Pairwise correlation analysis was performed and a Pearson's correlation coefficient (r) was calculated for each combination of features.

To examine seasonality in the optical and SAR domains for both forest classes, a time series analysis was performed on the entire input dataset (600 for each class). Additionally, the mean value for each time step was calculated separately for each class to obtain a complete understanding of the seasonality for each class.

Time series classification on forest type differentiation

To examine the performance of each individual SAR polarimetric parameter (Tab. 2) and both polarizations of S1, a univariate time series classification (TSC) was performed using the Time Series Support Vector Classifier (TS-SVC). The TS-SVC was specifically adopted for time series analysis and is available from the *sktime* Python library (Löning et al. 2022). As the exported time series are based mainly on the availability of S2 data, they are unequal in length for different areas in Czechia. They were first imported into a Python environment and prepared in a Pandas multiindex format (with 'date' and 'ID' as indices), as expected by the *sktime* algorithms. The TS-SVC was selected as the only classifier in the *sktime* library to deal with unequal lengths of time series. Moreover, TS-SVC is considered to be one of the most used algorithms for TSC tasks, while in some cases achieving superior accuracy (Wang et al. 2022; Faouzi 2022). The Radial Basis Function (RBF) was selected as a kernel type due to its general good performance for SVC in RS applications (Thanh Noi and Kappas 2018; Mountrakis, Im, and Ogole 2011; Oliveira, Dutra, Sant'Anna 2023). To find the best performing regularization parameter C, fine-tuning of 11 different values (0.1, 1, 5, 10, 50, 100, 150, 200, 300, 500 and 1000) was performed for VH polarized time series in differentiation between coniferous and broad-leaved forests.

After finding the best C parameter, a univariate time series classification was performed for each S1 SAR polarization and polarimetric parameter (Tab. 2), and the overall accuracy (OA) was calculated. Forest areas were divided into training and testing samples. Time series of 70% of points of each forest type was used in training the TS-SCV, while the remaining 30% was used to test the accuracy for various C parameters and also in accuracy assessment of various SAR features.

2. Results

2.1 Pairwise Correlation Analysis

To explore the proposed SAR polarimetric parameters and other features derived from DEM and weather datasets, a pairwise correlation analysis was performed in the first step. In general, pairwise

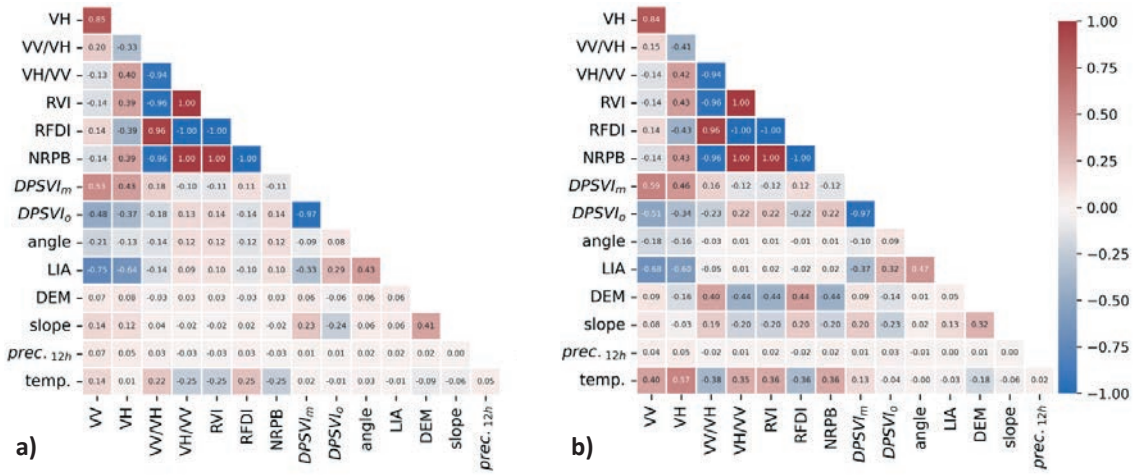

Fig. 3 Pairwise correlation between SAR, DEM and weather features for a) broad-leaved (n = 17303) and b) coniferous forest areas (n = 13070).

correlation analysis indicates a consistent pattern of correlation between certain features for both forest types, while there are features suggesting that some features interact differently for different forest types. A perfect negative or positive correlation (r = +/−1.00) was found for each combination between VH/VV, RVI, RDFI and NRPB for both broad-leaved and coniferous forests (Fig. 3a and Fig. 3b), meaning that they are functions of each other. They also had a very high correlation with VV/VH (|0.94| – |0.96|) and a moderate correlation with VH (~ |0.40|), while the correlation with VV was low (~ |0.15|). The VV/VH and VH/VV had a mutual correlation of 94%, while they had slightly different correlations with other examined features. The $DPSVI_o$ and its modified version ($DPSVI_m$) had a mutual correlation of –0.97 for both forest types, while having a moderate correlation with VV and VH and a low correlation with other SAR parameters.

As expected, a high correlation (−0.60 – −0.75) was found between the LIA and VV and VH polarizations, being stronger for broad-leaved forests, while the SAR parameters had almost no correlation with LIA. The temperature had a moderate correlation with the polarimetric parameters (0.35–0.38) and with VV and VH polarizations (0.40 and 0.57, respectively) for coniferous forests. The correlation for broad-leaved forests was about 0.25 between temperature and SAR features and very low for VV and VH polarizations (0.01 and 0.14, respectively). On the other hand, precipitation showed almost no correlation with SAR or other features. DEM features, slope and elevation, were moderately correlated with polarimetric features only for coniferous forests, while for broad-leaved forests they exhibited almost no correlation.

The pairwise correlation in Fig. 4 demonstrates the varying relationships between SAR and optical features in different forest types. A stronger linear relationship (~0.50) was found for the polarimetric parameters VV/VH and VH/VV in broad-leaved forests compared to coniferous forests. However, coniferous forests exhibited stronger correlations of both S1 polarizations with LAI and EVI. FAPAR achieved the strongest correlation between SAR and optical features for broad-leaved forests, while for coniferous forests it exhibited almost no correlation (Fig. 4b).

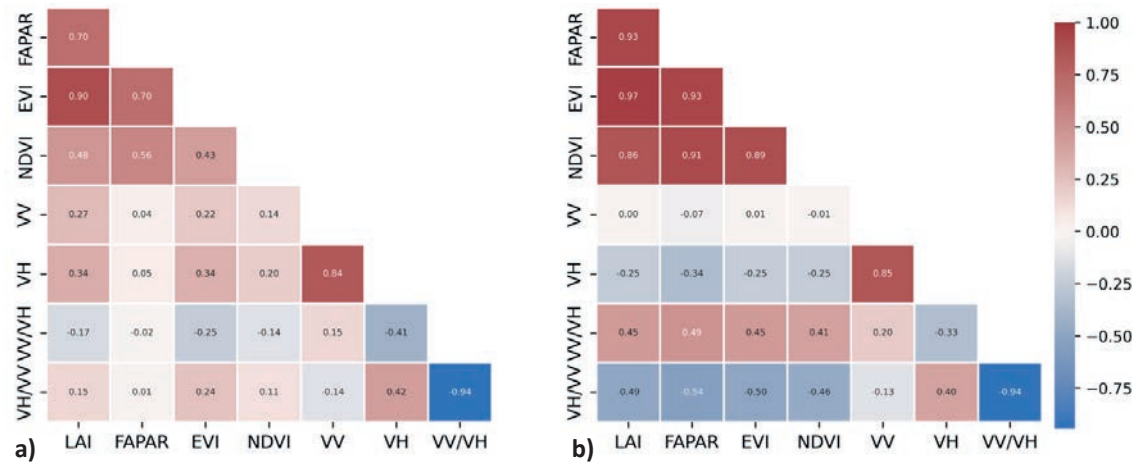

Fig. 4 Pairwise correlation between SAR and optical features for a) broad-leaved (n = 17303) and b) coniferous forest areas (n = 13070).

The strongest correlation for coniferous forests of each SAR feature was found for EVI.

The analysis also shows the correlation between each individual optical vegetation indices and parameters. Generally, the strongest correlation was found for broad-leaved forests: over 0.85 for each combination and a maximum of 0.97 between EVI and LAI. Coniferous forests exhibited a moderate correlation between NDVI and other optical features (~0.50), while the highest correlation was also achieved between EVI and LAI.

Based on the results of the pairwise analysis, some of the tested SAR features (RVI, RFDI, NRPB, and VH/VV) showed perfect correlation with each other; therefore, RVI, RFDI, and NRPB were excluded from further analysis, while VH/VV was retained.

2.2 Time series analysis

Generally, optical vegetation indices and parameters were higher in magnitude for broad-leaved forests in summertime and lower in wintertime compared to coniferous forests, while coniferous forests exhibited a more stable pattern throughout the year. Time series analysis of optical features, showed a clear and expected seasonal pattern for broad-leaved forests with low values in the beginning of the year, peaks in mid-year/summertime and a decrease in late spring with the lowest values during wintertime (Fig. 5a). The optical time series for coniferous forests shows a similar seasonality with peaks in summertime for EVI and LAI (Fig. 5b and 5c) and a rather stable behavior throughout the year with a slight increase toward winter for NDVI and FAPAR (Fig. 5a and 5d). Some areas represent some noise throughout the year, even in the summertime. The lack of data in the wintertime is apparent in the time series, causing a rather noisy behavior of the signal with high fluctuation, especially in NDVI and FAPAR. Certain variability in individual time series, represented by the lighter lines in Fig. 5, can be detected within each forest type.

In the case of SAR time series, clear seasonal behavior was found in both polarizations and ratios (VV/VH and VH/VV) for both forest types, while $DPSVI_o$ and $DPSVI_m$ exhibited a rather noisy behavior throughout the year (Fig. 6). The more apparent differentiation between forest types is enabled by VH polarization and both ratios, while VV showed similar behavior and values for both forest types. The seasonalities found for these features are opposite in nature for the two forest types. For example, the VH backscatter and the VH/VV increase in summertime for coniferous forests, whereas they decrease for broad-leaved forests. An opposite behavior can be observed in VV/VH, which decreases in summertime for coniferous forests and increases for broad-leaved forests. In contrast, VV increases in wintertime for both forest types. Overall, higher values were obtained in the VV polarization compared to those obtained in VH. Higher variation in individual time series can be observed for SAR features compared to optical parameters.

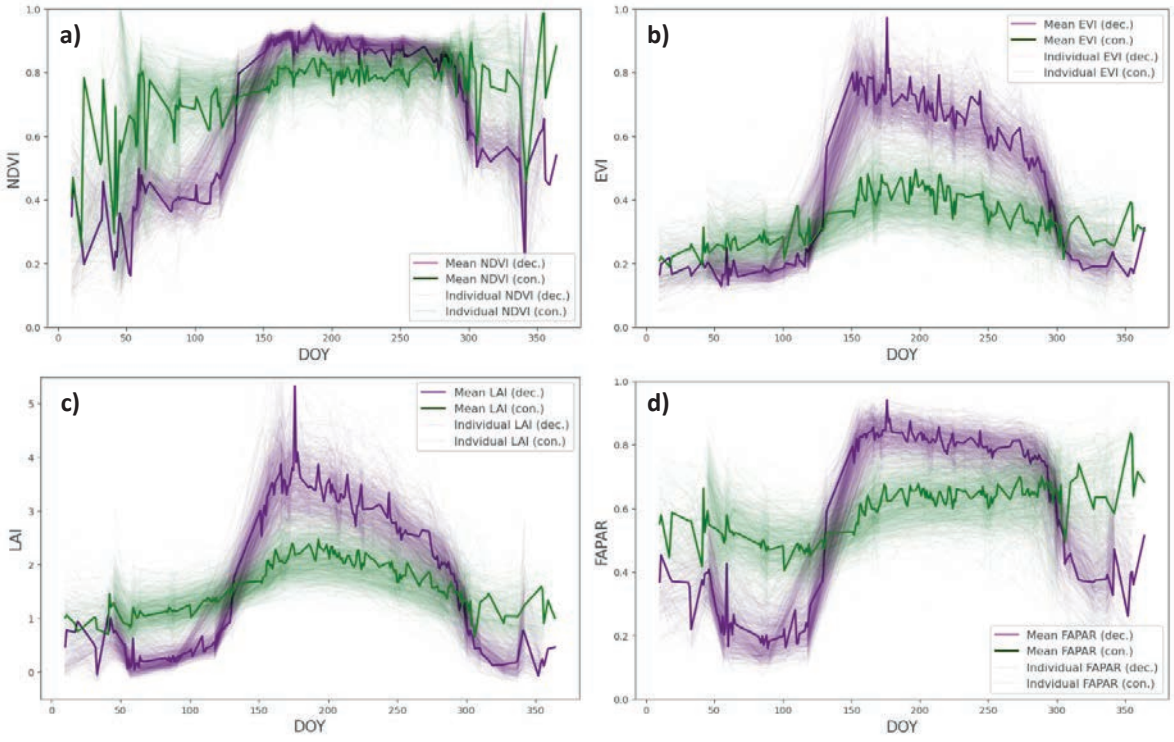

Fig. 5 Average and individual time series for 2021 of a) NDVI, b) EVI, c) LAI and d) FAPAR using all input data for broad-leaved and coniferous forests.

Note: *dec.* = *deciduous forests*, *con.* = *coniferous forests*

2.3 Time series classification

Fine-tuning the TS-SVC model, especially the C parameter yielded expected results: the overall accuracy is increasing with increasing of the C parameter value. An increase from 0.1 to the default C parameter for TS-SVC in sktime (C = 1) showed an increase in OA of 22%. The further increases in OA were slighter, that is, by 2.5% from 1 to 5 and by 0.8% between 5 and 50, 50 and 100 (Fig. 7a). The best OA, 76.12% were achieved with C = 200, 300 and 500, while another increase to 1000 resulted in a decrease of 0.3% in OA (Fig. 7a). This suggests that increasing the C parameter above 200 does not improve the accuracy of the model. For this reason, 200 was set for the regularization parameter C and used in the comparative analysis of the performance of each individual SAR polarization and polarimetric parameter in the differentiation between forest types.

The results of the TSC indicate the highest OA for VH polarization with 76.12%, significantly outperforming other SAR features by at least 11%. The second highest OA was achieved by VH/VV (65.73%), followed by NRPB and RFDI (both 64.89%). Accuracies over 60% were achieved also by VV, VV/VH and RVI (Fig. 7b). Based on the pairwise correlation analysis, where NRPB, RFDI, RVI, and VH/VV each demonstrated a 100% correlation with each other (Fig. 3), VH/VV was identified as the most promising SAR polarimetric parameter for forest monitoring among these four, due to its highest OA in the TSC. The lowest accuracies below 60% were achieved by $DPSVI_m$ and $DPSVI_o$ (53.65% and 47.19%, respectively). These results indicate that the DPSVI indices are less capable of discriminating between forest types. Furthermore, based on the SAR time series analysis (Fig. 6), these features showed a rather noisy behavior throughout the year, which explains the lower accuracy achieved in TSC.

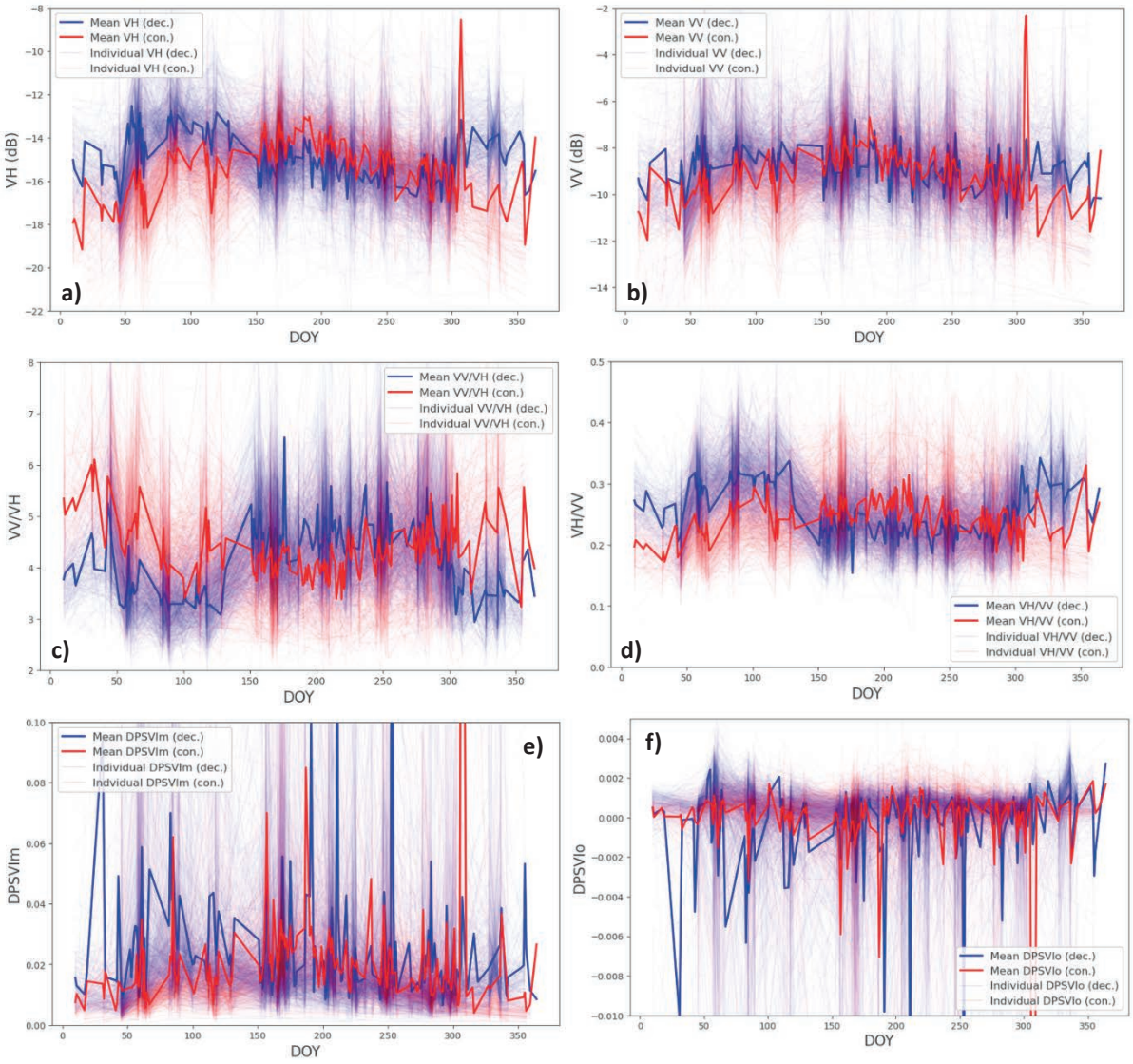

Fig. 6 Average and individual time series of a) VH, b) VV, c) VV/VH d) VH/VV, e) DPSVIm and f) DPSVIo using all input data for broad-leaved and coniferous forests.

Note: *dec.* = *broad-leaved forests*, *con.* = *coniferous forests*

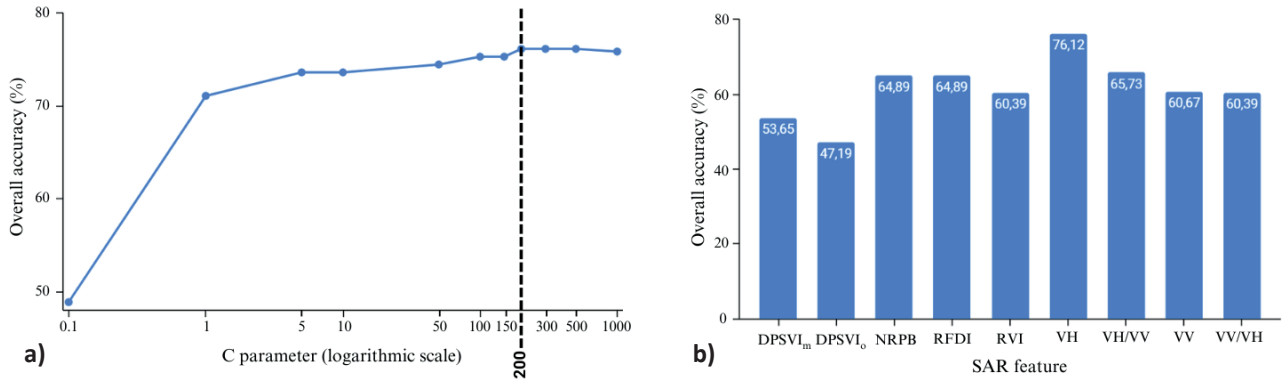

Fig. 7 Fine-tuning of the C parameter for the TS-SVC (a) and results of TSC for SAR polarizations and polarimetric parameters (b).

Therefore, the final selection of the best performing SAR features based on each analysis was VH, VV, VH/VV and VV/VH.

2.4 The MMTS-GEE dataset generation tool

The proposed MMTS-GEE tool, which generates a temporally and spatially paired time series dataset of S1, S2, DEM and weather data, has several parameters, which the user can set to customize the area of interest, time range, the preprocessing pipeline or export settings. The following settings can be set in the GEE environment:

- Time series length: Set the start and end dates to generate time series.
- Random point generation: If enabled, users can specify the type of land cover from the ESA World Cover 2021 to generate random points, the number of these points, and a buffer around each point. Alternatively, users can import their own spatial data as a GEE FeatureCollection and use it in time series generation.
- Geographical coverage: Select a broad geometry like an entire country or manually draw a custom ROI, needed for the initial data assessment.
- Sentinel-2 data preprocessing: Settings to adjust the CloudScore+ algorithm settings for cloud unmasking are available.
- Optical and SAR indices: Choose from a list of predefined optical and SAR polarimetric indices to include in the output.
- Speckle Filtering: There is an option to perform speckle filtering on SAR data using a Lee filter, with configurable kernel window size.
- S1–S2 temporal difference: Set the temporal difference between the S1 and S2 images when pairing them temporally can be set.
- Null Value Handling: Decide how to handle null values in the exported data, with options to exclude all rows with nulls, include only rows where optical indices have nulls, or include all nulls.

It should be noted that the MMTS-GEE code is freely available, therefore, other settings, not included in the recommended user settings listed above, can be adjusted by editing the code. To list a few, users can create their own optical or SAR indices, select a different land cover database for random point generation, set a different speckle filtering approach, or integrate other ancillary data to enhance the multi-modality of the created time series dataset.

3. Discussion

In this study, a tool for creating multi-modal time series datasets, consisting of spatially and temporally aligned and paired preprocessed S1, S2, weather and DEM data was created in GEE (MMTS-GEE). The MMTS-GEE tool is unique because it enables generation of paired time series for any time period (based on data availability) and over any geographic region, both locally and globally. Moreover, customization of data preprocessing pipelines, including cloud masking, speckle filtering and feature extraction, or further extension with other ancillary datasets is possible. This versatility addresses various challenges of the currently used satellite-based datasets, as presented in Schmitt et al. (2023). Therefore, the GEE code for the MMTS-GEE tool has been made publicly available in the GitHub repository of this work at github.com/palubad/MMTSGEE. In the present form, the MMTS-GEE is prepared for export of tabular data, but the next work will focus on improving the MMTS-GEE to export image patches for deep learning (DL) analyzes to fully address the requirements for DL analysis in (Schmitt et al. 2023).

The testing and evaluation of various SAR polarimetric parameters was performed to select the most suitable ones for forest monitoring using both quantitative (pairwise correlation analysis and TSC) and qualitative analysis (time series comparison). For this, time series were generated for 600 broad-leaved and 600 coniferous areas using the MMTS-GEE. Based on the pairwise analysis of mutual correlation between SAR features and the highest achieved OAs in TSC on differentiation of forest types, four SAR features were considered as the most suitable and best performing

ones for forest monitoring: two original S1 polarizations VV and VH and two most commonly used polarization ratios VV/VH and VH/VV. Some of the tested SAR features were excluded due to a perfect correlation between each other (RVI, RFDI, NRPB), while a perfect correlation between RVI and RFDI was also found in Paluba et al. (2023). This suggests that these indices are functions of each other and did not provide new information. $DPSVI_m$ and $DPSVI_o$ were excluded from the final selection due to their low accuracy in TSC and their rather noisy time series behavior for both forest types. Although a high correlation was also found between the VV and VH polarization (0.84–0.85), they were included in the final selection of the most efficient SAR features . With that, the original polarizations of the S1 data were preserved. Moreover, VH polarization achieved the highest OA in TSC, suggesting that it is the most reliable and important SAR feature to distinguish between forest types and for forest monitoring in general.

The basic assumption based on previous studies (Dostálová et al. 2016; Frison et al. 2018), that SAR feature time series have seasonal variations for forests, was confirmed (Fig. 6). Seasonal variations in SAR backscatter have been observed in both coniferous and broad-leaved forests, although their seasonality differs. Coniferous forests exhibit increased backscatter in VV and VH in summer and reduced backscatter during colder conditions, often attributed to loss of moisture content, needle loss and the presence of understory vegetation, which can be formed by broad-leaved plant types (Dostálová et al. 2016; 2018; 2021). Broad-leaved forests, on the other hand, show higher VV and VH backscatter values during leaf-off periods due to decreased attenuation by tree crowns, particularly by leaves with sizes similar to or larger than the C-band wavelength (~5 cm). This leads to a higher received backscatter resulting from multiple scattering between primary and secondary branches, or even between the tree trunk and the ground, depending on tree crown density. Lower backscatter values during hot and dry summer days are associated with a reduced moisture content in vegetation, allowing greater penetration of the SAR signal into the tree crown and less backscatter returning to the SAR sensor. Generally, higher backscatter values are obtained for VV polarization in both forest types, confirming previous findings (Dostálová et al. 2016; 2018; Paluba et al. 2021). A clearer and more distinct seasonality in the VH polarization for both forest types compared to VV can be attributed to the fact that the VH polarization is more strongly affected by volume scattering (Richards 2009; Vreugdenhil et al. 2018). The lower number of observations from wintertime caused a rather noisy behavior, similarly as in optical features. The lack of data in wintertime in the case of SAR data is due to the fact that only unmasked paired S1–S2 observations were considered in the analysis, therefore the number of S1 observations is equal to the number of valid/unmasked observations by S2. Overall, the analysis of these SAR parameters suggests that the SAR backscatter is sensitive to seasonal changes in forest composition.

Topographic properties can significantly alter the backscatter behavior over time, especially when SAR images are combined from ascending and descending orbits (Paluba et al. 2021). A high correlation between the LIA and both S1 polarizations for both forest types can be caused by the fact that the input time series included S1 data derived from every possible acquisition geometry, i.e., both from ascending and descending orbits with variations in LIAs for the same area. The moderate correlation of DEM features (slope and elevation) with SAR features for coniferous forests and almost no correlation for broad-leaved forests can be attributed to the topographical distribution of the input areas. Broad-leaved forest areas had a mean elevation of 417 m with a range of 823 m, while the mean for coniferous forests was 650 m with a range of 1119 m.

Environmental effects, such as precipitation, alter moisture content and consequently the dielectric properties of objects, which typically change throughout the year (Rüetschi, Small, and Waser 2019; Benninga, van der Velde, and Su 2019; Ranson and Sun 2000). However, precipitation had almost no correlation with S1 polarizations and polarimetric parameters. This can be attributed to the high number of observations in which most of the observations (~28 000 out of ~30 000) exhibited less than 1.8 mm of cumulative precipitation in the 12 hours period prior to the S1 acquisition, as defined in (Benninga, van der Velde, and Su 2019). Although a moderate correlation was found between SAR features and temperature in this study, but only for coniferous forests, temperature was found to have a strong correlation with C-band SAR backscatter in other studies, such as in Olesk et al. (2015). Moreover, in previous studies (Rüetschi, Small, and Waser 2019; Benninga, van der Velde, and Su 2019; Ranson and Sun 2000) it was found that freezing conditions and temperatures below 1 °C cause a significant decrease in SAR backscatter over forests. Therefore, the influence of environmental factors, specifically precipitation and low temperatures, on the SAR backscatter in vegetation over time should be further examined in future studies.

Weaker correlations between SAR and optical features were found in this study (with a maximum of 0.54 between FAPAR and VH/VV) compared to previous studies, e.g. 0.63–0.84 in (Jiao, McNairn, and Dingle Robertson 2021), 0.41–0.83 in (Alvarez-Mozos et al. 2021), 0.45–0.74 in (Holtgrave et al. 2020). These studies, however, focused on agricultural areas while performing analysis only on mono-temporal image pairs, using an image-to-image comparison. A correlation of 0.77 between VV/VH and NDVI time series in broad-leaved temperate forests was found in Frison et al. (2018), while almost no correlation was found in coniferous forests. This is in line with

the findings of this study, where a significantly weaker correlation was found between optical and SAR features in coniferous forests. The variability in the individual time series (visualized with lighter lines in Fig. 5 and Fig. 6) for both SAR and optical features suggests that there is variation within both forest types, potentially due to microclimatic or topographic conditions (elevation, slope, aspect), species composition or other ecological factors (Mašek et al. 2023). The noisy behavior of optical TS throughout the year can also be attributed to insufficient haze, cloud and shadow masking.

4. Conclusion

The study aimed to identify the most effective SAR polarimetric parameters for forest monitoring through quantitative and qualitative analyses for Czech forests. The analyses revealed that some of the SAR features exhibit identical behavior, providing no additional information, demonstrated a rather noisy behavior over time, or showed low performance in differentiation of forest types in time series classification. Therefore, the two original S1 polarizations (VV and VH) and two polarimetric parameters (VV/VH and VH/VV) were identified as most suitable and best performing in all the tested aspects and are proposed for further use in forest monitoring. Moreover, in a correlation analysis between SAR and optical features, the strongest correlation was found for broad-leaved forest for VV/VH and VH/VV, while the highest overall accuracy in the time series classification was achieved by VH. As a secondary output, this study introduced the MMTS-GEE tool to generate spatially and temporally aligned multi-modal time series datasets including paired S1 and S2 data, extended with DEM and weather data in GEE. The MMTS-GEE offers high flexibility for users to adopt it for various geographical areas, time frames, adjust processing pipelines or enhance the modality of the tool with additional datasets. This versatility enables its use in time series analyses, intercomparisons and in machine learning applications for tabular time series data. The data generated with MMTS-GEE were used in the case study of Czechia focusing on the identification of the most efficient SAR features for forest monitoring. The public availability of the MMTS-GEE code increases its accessibility and usability for researchers and supports further development and customization of the tool to meet specific research needs. Given its limitation to tabular data, further development of the tool for DL-ready data generation would be important.

Acknowledgements

This work was supported by the Charles University Grant Agency – *Grantová Agentura Univerzity Karlovy (GAUK)* Grant No. 412722 and the European Union's Caroline Herschel Framework Partnership Agreement on Copernicus User Uptake under grant agreement No. FPA 275/G/GRO/COPE/17/10042, project FPCUP (Framework Partnership Agreement on Copernicus User Uptake). Daniel Paluba would like to thank the Erasmus+ programme for the financial support during his research stay at the Φ-lab, European Space Agency (ESA) in Frascati, Italy.

References

Alvarez-Mozos, J., Villanueva, J., Arias, M., Gonzalez-Audicana, M. (2021): Correlation Between NDVI and Sentinel-1 Derived Features for Maize. In: 2021 IEEE International Geoscience and Remote Sensing Symposium IGARSS, 6773–6776, https://doi.org/10.1109/IGARSS47720.2021.9554099.

Bai, Z., Fang, S., Gao, J., Zhang, Y., Jin, G., Wang, S., Zhu, Y., Xu, J. (2020): Could Vegetation Index be Derive from Synthetic Aperture Radar? – The Linear Relationship between Interferometric Coherence and NDVI. Scientific Reports 10: 6749, https://doi.org/10.1038/s41598-020-63560-0.

Bartels, S. F., Chen, H. Y. H., Wulder, M. A., White, J. C. (2016): Trends in Post-disturbance recovery rates of Canada's forests following wildfire and harvest. Forest Ecology and Management 361, 194–207, https://doi.org/10.1016/j.foreco.2015.11.015.

Benninga, H.-J. F., Van Der Velde, R., Su, Z. (2019): Impacts of Radiometric Uncertainty and Weather-Related Surface Conditions on Soil Moisture Retrievals with Sentinel-1. Remote Sensing 11(17): 2025, https://doi.org/10.3390/rs11172025.

Bey, A., Sánchez-Paus Díaz, A., Maniatis, D., Marchi, G., Mollicone, D., Ricci, S., Bastin, J.-F., Moore, R., Federici, S., Rezende, M., Patriarca, C., Turia, R., Gamoga, G., Abe, H., Kaidong, E., Miceli, G. (2016): Collect Earth: Land Use and Land Cover Assessment through Augmented Visual Interpretation. Remote Sensing 8(10): 807, https://doi.org/10.3390/rs8100807.

Buchhorn, M., Smets, B., Bertels, L., Roo, B. D., Lesiv, M., Tsendbazar, N.-E., Herold, M., Fritz, S. (2020): Copernicus Global Land Service: Land Cover 100m: collection 3: epoch 2017: Globe. Zenodo.

Chang, J. G., Shoshany, M., Oh, Y. (2018): Polarimetric Radar Vegetation Index for Biomass Estimation in Desert Fringe Ecosystems. IEEE Transactions on Geoscience and Remote Sensing 56(12), 7102–7108, https://doi.org/10.1109/TGRS.2018.2848285.

Copernicus Climate Change Service (2019): ERA5-Land hourly data from 2001 to present. ECMWF.

Curtis, P. G., Slay, C. M., Harris, N. L., Tyukavina, A., Hansen, M. C. (2018): Classifying drivers of global forest loss. Science 361(6407), 1108–1111, https://doi.org/10.1126/science.aau3445.

De Luca, G., Silva, J. M. N., Modica, G. (2022): Regional-scale burned area mapping in Mediterranean regions based on the multitemporal composite integration of Sentinel-1 and Sentinel-2 data. GIScience & Remote Sensing 59(1), 1678–1705, https://doi.org/10.1080/15481603.2022.2128251.

Didan, K. (2021a): MODIS/Terra Vegetation Indices 16-Day L3 Global 1km SIN Grid V061. NASA EOSDIS Land Processes Distributed Active Archive Center.

Didan, K. (2021b): MODIS/Terra Vegetation Indices 16-Day L3 Global 250m SIN Grid V061. NASA EOSDIS Land Processes Distributed Active Archive Center.

Didan, K., Barreto, A. (2018): VIIRS/NPP Vegetation Indices 16-Day L3 Global 500m SIN Grid V001. NASA EOSDIS Land Processes Distributed Active Archive Center.

dos Santos, E. P., Da Silva, D. D., o Amaral, C. H. (2021): Vegetation cover monitoring in tropical regions using SAR-C dual-polarization index: seasonal and spatial influences. International Journal of Remote Sensing 42(19), 7581–7609, https://doi.org/10.1080/01431161.2021.1959955.

Dostálová, A., Lang, M., Ivanovs, J., Waser, L. T., Wagner, W. (2021): European Wide Forest Classification Based on Sentinel-1 Data. Remote Sensing 13(3): 337, https://doi.org/10.3390/rs13030337.

Dostálová, A., Milenkovic, M., Hollaus, M., Wagner, W. (2016): Influence of Forest Structure on the Sentinel-1 Backscatter Variation – Analysis with Full-Waveform LiDAR Data. In Proceedings of the Living Planet Symposium, Prague, Czech Republic, 9–13 May 2016; Volume 740, p. 202.

Dostálová, A., Wagner, W., Milenković, M., Hollaus, M. (2018): Annual seasonality in Sentinel-1 signal for forest mapping and forest type classification. International Journal of Remote Sensing 39(21), 7738–7760, https://doi.org/10.1080/01431161.2018.1479788.

Dufourg, C., Pelletier, C., May, S., Lefèvre, S. (2024): Satellite Image Time Series Datasets.

European Space Agency, Airbus (2022): Copernicus DEM. European Space Agency.

Faouzi, J. (2022): Time Series Classification: A review of Algorithms and Implementations. Proud Pen. In press, 978-1-83815241-3, hal-03558165.

Filgueiras, R., Mantovani, E. C., Althoff, D., Fernandes Filho, E. I., Cunha, F. F. da (2019): Crop NDVI Monitoring Based on Sentinel 1. Remote Sensing 11(12): 1441, https://doi.org/10.3390/rs11121441.

Forzieri, G., Dakos, V., Mcdowell, N. G., Ramdane, A., Cescatti, A. (2022): Emerging signals of declining forest resilience under climate change. Nature 608, 534–539, https://doi.org/10.1038/s41586-022-04959-9.

Frison, P.-L., Fruneau, B., Kmiha, S., Soudani, K., Dufrêne, E., Le Toan, T., Koleck, T., Villard, L., Mougin, E., Rudant, J.-P. (2018): Potential of Sentinel-1 Data for Monitoring Temperate Mixed Forest Phenology. Remote Sensing 10(12): 2049, https://doi.org/10.3390/rs10122049.

Fuster, B., Sánchez-Zapero, J., Camacho, F., García-Santos, V., Verger, A., Lacaze, R., Weiss, M., Baret, F., Smets, B. (2020): Quality Assessment of PROBA-V LAI, fAPAR and fCOVER Collection 300 m Products of Copernicus Global Land Service. Remote Sensing 12(6): 1017, https://doi.org/10.3390/rs12061017.

Gamon, J. A., Field, C. B., Goulden, M. L., Griffin, K. L., Hartley, A. E., Joel, G., Penuelas, J., Valentini, R. (1995): Relationships Between NDVI, Canopy Structure, and Photosynthesis in Three Californian Vegetation Types. Ecological Applications 5(1), 28–41, https://doi.org/10.2307/1942049.

Global Forest Watch (2014): Forest Monitoring, Land Use & Deforestation Trends | Global Forest Watch. Available online: https://www.globalforestwatch.org/ (accessed on 16. 7. 2024).

Gorelick, N., Hancher, M., Dixon, M., Ilyushchenko, S., Thau, D., Moore, R. (2017): Google Earth Engine: Planetary-scale geospatial analysis for everyone. Remote Sensing of Environment 202, 18–27, https://doi.org/10.1016/j.rse.2017.06.031.

Hansen, M. C., Potapov, P. V., Moore, R., Hancher, M., Turubanova, S. A., Tyukavina, A., Thau, D., Stehman, S. V., Goetz, S. J., Loveland, T. R., Kommareddy, A., Egorov, A., Chini, L., Justice, C. O., Townshend, J. R. G. (2013): High-Resolution Global Maps of 21st-Century Forest Cover Change. Science 342(6160), 850–853, https://doi.org/10.1126/science.1244693.

Harris, N. L., Gibbs, D. A., Baccini, A., Birdsey, R. A., De Bruin, S., Farina, M., Fatoyinbo, L., Hansen, M. C., Herold, M., Houghton, R. A., Potapov, P. V., Suarez, D. R., Roman-Cuesta, R. M., Saatchi, S. S., Slay, C. M., Turubanova, S. A., Tyukavina, A. (2021): Global maps of twenty-first century forest carbon fluxes. Nature Climate Change 11, 234–240, https://doi.org/10.1038/s41558-020-00976-6.

Hird, J. N., Delancey, E. R., Mcdermid, G. J., Kariyeva, J. (2017): Google Earth Engine, Open-Access Satellite Data, and Machine Learning in Support of Large-Area Probabilistic Wetland Mapping. Remote Sensing 9(12): 1315, https://doi.org/10.3390/rs9121315.

Holtgrave, A.-K., Röder, N., Ackermann, A., Erasmi, S., Kleinschmit, B. (2020): Comparing Sentinel-1 and -2 Data and Indices for Agricultural Land Use Monitoring. Remote Sensing 12(18): 2919, https://doi.org/10.3390/rs12182919.

Huang, S., Tang, L., Hupy, J. P., Wang, Y., Shao, G. (2021): A commentary review on the use of normalized difference vegetation index (NDVI) in the era of popular remote sensing. Journal of Forestry Research 32, 1–6, https://doi.org/10.1007/s11676-020-01155-1.

Huete, A., Didan, K., Miura, T., Rodriguez, E. P., Gao, X., Ferreira, L. G. (2002): Overview of the radiometric and biophysical performance of the MODIS vegetation indices. Remote Sensing of Environment 83(1), 195–213, https://doi.org/10.1016/S0034-4257(02)00096-2.

Jiao, X., Mcnairn, H., Dingle Robertson, L. (2021): Monitoring crop growth using a canopy structure dynamic model and time series of synthetic aperture radar (SAR) data. International Journal of Remote Sensing 42(17), 6433–6460, https://doi.org/10.1080/01431161.2021.1938739.

Kim, Y., Van Zyl, J. (2000): On the relationship between polarimetric parameters. GARSS 2000. IEEE 2000 International Geoscience and Remote Sensing Symposium. Taking the Pulse of the Planet: The Role of Remote Sensing in Managing the Environment. Proceedings 3, 1298–1300 (Cat. No.00CH37120), Honolulu, HI, USA, https://doi.org/10.1109/IGARSS.2000.858099.

Kosztra, B., Büttner, G., Hazeu, G., Arnold, S. (2019): Updated CLC illustrated nomenclature guidelines. European Environment Agency. Available online: https://land.copernicus.eu/content/corine-land-cover-nomenclature-guidelines/docs/pdf/CLC2018_Nomenclature_illustrated_guide_20190510.pdf (accessed on 10.4.2024).

Lee, J.-S. (1985): Speckle Suppression and Analysis for Synthetic Aperture Radar Images. Proc. SPIE 0556, Intl Conf on Speckle, https://doi.org/10.1117/12.949537.

Liu, H. Q., Huete, A. (1995): A feedback based modification of the NDVI to minimize canopy background and atmospheric noise. IEEE Transactions on Geoscience and Remote Sensing 33(2), 457–465, https://doi.org/10.1109/TGRS.1995.8746027.

Löning, M., Király, F., Bagnall, T., Middlehurst, M., Ganesh, S., Oastler, G., Lines, J., Walter, M., Viktorkaz, Mentel, L., Chrisholder, Tsaprounis, L., Rnkuhns, Parker, M., Owoseni, T., Rockenschaub, P., Danbartl, Jesellier, Eenticott-Shell, Gilbert, C., Bulatova, G., Lovkush, Schäfer, P., Khrapov, S., Buchhorn, K., Take, K., Subramanian, S., Meyer, S. M., Aidenrushbrooke, Rice, B. (2022): https://github.com/sktime/sktime/releases.v0.13.4. Zenodo.

Ma, J., Li, J., Wu, W., Liu, J. (2023): Global forest fragmentation change from 2000 to 2020. Nature Communications 14: 3752, https://doi.org/10.1038/s41467-023-39221-x.

Mandal, D., Kumar, V., Ratha, D., Dey, S., Bhattacharya, A., Lopez-Sanchez, J. M., Mcnairn, H., Rao, Y. S. (2020a): Dual polarimetric radar vegetation index for crop growth monitoring using sentinel-1 SAR data. Remote Sensing of Environment 247: 111954, https://doi.org/10.1016/j.rse.2020.111954.

Mandal, D., Ratha, D., Bhattacharya, A., Kumar, V., Mcnairn, H., Rao, Y. S., Frery, A. C. (2020b): A Radar Vegetation Index for Crop Monitoring Using Compact Polarimetric SAR Data. IEEE Transactions on Geoscience and Remote Sensing 58(9), 6321–6335, https://doi.org/10.1109/TGRS.2020.2976661.

Mašek, J., Tumajer, J., Lange, J., Kaczka, R., Fišer, P., Treml, V. (2023): Variability in Tree-ring Width and NDVI Responses to Climate at a Landscape Level. Ecosystems 26, 1144–1157, https://doi.org/10.1007/s10021-023-00822-8.

May, J. L., Healey, N. C., Ahrends, H. E., Hollister, R. D., Tweedie, C. E., Welker, J. M., Gould, W. A., Oberbauer, S. F. (2017): Short-Term Impacts of the Air Temperature on Greening and Senescence in Alaskan Arctic Plant Tundra Habitats. Remote Sensing 9(12), 1338, https://doi.org/10.3390/rs9121338.

Ministry of Agriculture of the Czech Republic (2022): Information on forests and forestry in the Czech Republic by 2021. Ministry of Agriculture of the Czech Republic.

Mountrakis, G., Im, J., Ogole, C. (2011): Support vector machines in remote sensing: A review. ISPRS Journal of Photogrammetry and Remote Sensing 66(3), 247–259, https://doi.org/10.1016/j.isprsjprs.2010.11.001.

Mullissa, A., Vollrath, A., Odongo-Braun, C., Slagter, B., Balling, J., Gou, Y., Gorelick, N., Reiche, J. (2021): Sentinel-1 SAR Backscatter Analysis Ready Data Preparation in Google Earth Engine. Remote Sensing 13(10): 1954, https://doi.org/10.3390/rs13101954.

Myneni, R., Knyazikhin, Y. (2018): VIIRS/NPP Leaf Area Index/FPAR 8-Day L4 Global 500m SIN Grid V001. NASA EOSDIS Land Processes Distributed Active Archive Center.

Myneni, R., Knyazikhin, Y., Park, T. (2021): MODIS/Terra+Aqua Leaf Area Index/FPAR 4-Day L4 Global 500m SIN Grid V061. NASA EOSDIS Land Processes Distributed Active Archive Center. Available online: https://doi.org/10.5067/VIIRS/VNP15A2H.001 (accessed on 5.4.2024).

Nicolau, A. P. (2024): Cloud Score+ in Action: Land Cover Mapping in Ecuador, Google Earth and Earth Engine. Available online: https://medium.com/google-earth/cloud-score-in-action-land-cover-mapping-in-ecuador-fd1c5c424317 (accessed on 26. 4. 2024).

Olesk, A., Voormansik, K., Põhjala, M., Noorma, M. (2015): Forest change detection from Sentinel-1 and ALOS-2 satellite images. IEEE 5th Asia-Pacific Conference on Synthetic Aperture Radar (APSAR), 522–527, https://doi.org/10.1109/APSAR.2015.7306263.

Oliveira, W. V. De, Dutra, L. V., Sant'anna, S. J. S. (2023): A Comparison Of Multi-Class Svm Strategies And Kernel Functions For Land Cover Classification. Available online: https://proceedings.science/sbsr-2023/trabalhos/a-comparison-of-multi-class-svm-strategies-and-kernel-functions-for-land-cover-c?lang=en (accessed on 17. 4. 2024).

Onačillová, K., Krištofová, V., Paluba, D. (2023): Automatic forest cover classification using Sentinel-2 multispectral satellite data and machine learning algorithms in Google Earth Engine. Acta Geographica Universitatis Comenianae 67(2), 163–185.

Paluba, D., Laštovička, J., Mouratidis, A., Štych, P. (2021): Land Cover-Specific Local Incidence Angle Correction: A Method for Time-Series Analysis of Forest Ecosystems. Remote Sensing 13(9): 1743, https://doi.org/10.3390/rs13091743.

Paluba, D., Papale, L. G., Perivolioti, T.-M., Štych, P., Laštovička, J., Kalaitzis, P., Karadimou, G., Papageorgiou, E., Mouratidis, A. (2023): Unsupervised Burned Area Mapping in Greece: Investigating the Impact of Precipitation, Pre- and Post-Processing of Sentinel-1 Data in Google Earth Engine. IGARSS 2023 – 2023 IEEE International Geoscience and Remote Sensing Symposium, Pasadena, CA, USA, 2520-2523, https://doi.org/10.1109/IGARSS52108.2023.10283130.

Pasquarella, V. (2024): All Clear with Cloud Score+, Google Earth and Earth Engine. Available online: https://medium.com/google-earth/all-clear-with-cloud-score-bd6ee2e2235e (accessed on 26. 4. 2024).

Pasquarella, V. J., Brown, C. F., Czerwinski, W., Rucklidge, W. J. (2023): Comprehensive quality assessment of optical satellite imagery using weakly supervised video learning. IEEE/CVF Conference on Computer Vision and Pattern Recognition Workshops (CVPRW), Vancouver, BC, Canada, 2125-2135, https://doi.org/10.1109/CVPRW59228.2023.00206.

Periasamy, S. (2018): Significance of dual polarimetric synthetic aperture radar in biomass retrieval: An attempt on Sentinel-1. Remote Sensing of Environment, 217, 537–549, https://doi.org/10.1016/j.rse.2018.09.003.

Pinheiro, M., Miranda, N., Recchia, A., Cotrufo, A., Franceschi, N., Piantanida, R., Schmidt, K., Gisinger, C., Hajduch, G., Vincent, P. (2022): Sentinel-1 instruments status and product performance update for 2022. In: EUSAR 2022; 14th European Conference on Synthetic Aperture Radar, 1–5.

Ranson, K. J., Sun, G. (2000): Effects of environmental conditions on boreal forest classification and biomass estimates with SAR. IEEE Transactions on Geoscience

and Remote Sensing 38(3), 1242–1252, https://doi.org/10.1109/36.843016.
Reiche, J., Mullissa, A., Slagter, B., Gou, Y., Tsendbazar, N.-E., Odongo-Braun, C., Vollrath, A., Weisse, M. J., Stolle, F., Pickens, A., Donchyts, G., Clinton, N., Gorelick, N., Herold, M. (2021): Forest disturbance alerts for the Congo Basin using Sentinel-1. Environmental Research Letters 16(2): 024005, https://doi.org/10.1088/1748-9326/abd0a8.
Richards, J. A. (2009): The Imaging Radar System In: Remote Sensing with Imaging Radar. Signals and Communication Technology. Springer, Berlin, Heidelberg, https://doi.org/10.1007/978-3-642-02020-9_1.
Rüetschi, M., Small, D., Waser, L. (2019): Rapid Detection of Windthrows Using Sentinel-1 C-Band SAR Data. Remote Sensing 11(2): 115, https://doi.org/10.3390/rs11020115.
Saatchi, S. (2019): SAR Methods for Mapping and Monitoring Forest Biomass. In: SAR Handbook: Comprehensive Methodologies for Forest Monitoring and Biomass Estimation. NASA. Available online: https://ntrs.nasa.gov/api/citations/20190002563/downloads/20190002563.pdf (accessed on 10.4.2024).
Sahadevan, D. K., Sitiraju, S., Sharma, J. (2013): Radar Vegetation Index as an Alternative to NDVI for Monitoring of Soyabean and Cotton. In: Indian Cartographer. Jodhpur, 91–96.
Schmitt, M., Ahmadi, S. A., Xu, Y., Taşkin, G., Verma, U., Sica, F., Hänsch, R. (2023): There Are No Data Like More Data: Datasets for deep learning in Earth observation. IEEE Geoscience and Remote Sensing Magazine 11(3), 63–97, https://doi.org/10.1109/MGRS.2023.3293459.
Senf, C., Seidl, R. (2021): Mapping the forest disturbance regimes of Europe. Nature Sustainability 4, 63–70, https://doi.org/10.1038/s41893-020-00609-y.
Smets, B., Cai, Z., Elkund, L., Tian, F., Bonte, K., Van Hoost, R., Van De Kerchove, R., Adriaensen, S., De Roo, B., Jacobs, T., Swinnen, E. (2023): High resolution vegetation phenology and productivity (HR-VPP), Daily Raw Vegetation Indices. European Union, Copernicus Land Monitoring Service 2021, European Environment Agency (EEA).
Thanh Noi, P., Kappas, M. (2018): Comparison of Random Forest, k-Nearest Neighbor, and Support Vector Machine Classifiers for Land Cover Classification Using Sentinel-2 Imagery. Sensors 18(1): 18, https://doi.org/10.3390/s18010018.
Turubanova, S., Potapov, P. V., Tyukavina, A., Hansen, M. C. (2018): Ongoing primary forest loss in Brazil, Democratic Republic of the Congo, and Indonesia. Environmental Research Letters 13: 074028, https://doi.org/10.1088/1748-9326/aacd1c.
Tyukavina, A., Potapov, P., Hansen, M. C., Pickens, A. H., Stehman, S. V., Turubanova, S., Parker, D., Zalles, V., Lima, A., Kommareddy, I., Song, X.-P., Wang, L., Harris, N. (2022): Global Trends of Forest Loss Due to Fire From 2001 to 2019. Frontiers in Remote Sensing 3: 825190, https://doi.org/10.3389/frsen.2022.825190.
Vreugdenhil, M., Wagner, W., Bauer-Marschallinger, B., Pfeil, I., Teubner, I., Rüdiger, C., Strauss, P. (2018): Sensitivity of Sentinel-1 Backscatter to Vegetation Dynamics: An Austrian Case Study. Remote Sensing 10(9): 1396, https://doi.org/10.3390/rs10091396.
Wang, W. K., Chen, I., Hershkovich, L., Yang, J., Shetty, A., Singh, G., Jiang, Y., Kotla, A., Shang, J. Z., Yerrabelli, R., Roghanizad, A. R., Shandhi, M. M. H., Dunn, J. (2022): A Systematic Review of Time Series Classification Techniques Used in Biomedical Applications. Sensors 22(20): 8016, https://doi.org/10.3390/s22208016.
Weiss, M., Baret, F. (2016): S2ToolBox Level 2 Products: LAI, FAPAR, FCOVER. Version 1.1.
WMO, United Nations Educational, S., C. O. (UNESCO), Programme (UNEP), U. N. E., SCIENCE (ICSU), I. C. for (2011): Systematic Observation Requirements for Satellite-based Products for Climate Supplemental details to the satellite-based component of the Implementation Plan for the Global Observing System for Climate in Support of the UNFCCC. Available online: https://library.wmo.int/records/item/48411-systematic-observation-requirements-for-satellite-based-products-for-climate-supplemental-details-to-the-satellite-based-component-of-the-implementation-plan-for-the-global-observing-system-for-climate-in-support-of-the-unfccc (accessed on12. 9. 2023).
Zanaga, D., Van De Kerchove, R., Daems, D., De Keersmaecker, W., Brockmann, C., Kirches, G., Wevers, J., Cartus, O., Santoro, M., Fritz, S., Lesiv, M., Herold, M., Tsendbazar, N.-E., Xu, P., Ramoino, F., Arino, O. (2022): ESA WorldCover 10 m 2021 v200, https://doi.org/10.5281/zenodo.7254221.
Zeng, Y., Hao, D., Huete, A., Dechant, B., Berry, J., Chen, J. M., Joiner, J., Frankenberg, C., Bond-Lamberty, B., Ryu, Y., Xiao, J., Asrar, G. R., Chen, M. (2022): Optical vegetation indices for monitoring terrestrial ecosystems globally. Nature Reviews Earth & Environment 3, 477–493, https://doi.org/10.1038/s43017-022-00298-5.

Critical issues in undergraduate cartographic education: Analysis of final tests and oral examinations

Jan D. Bláha[1,*], Petr Trahorsch[1,2], Martin Bartůněk[1], Petr Hladík[1]

[1] J. E. Purkyně University in Ústí nad Labem, Faculty of Science, Department of Geography, Czechia
[2] J. E. Purkyně University in Ústí nad Labem, Faculty of Science, Centre for Promotion of Science Education, Czechia
* Corresponding author: jan.d.blaha@ujep.cz

ABSTRACT

This article identifies critical issues in cartographic education based on analysis of more than 1,300 anonymized didactic tests and anonymized results of final oral examinations of university courses since 2010. To analyze the students' results, the tasks in the tests and questions in the oral examination were categorized in the cartographic and didactic aspects based on the revised Bloom's cognitive taxonomy. The quantitative analysis shows that students achieve better results in tasks that test their procedural knowledge compared to tasks in which they must demonstrate a conceptual knowledge dimension. Students achieve the worst results in tasks that test their factual knowledge, while poorer results are also associated with tasks that require mathematical calculations. In the cartographic curriculum categories, the form of their delivery (lectures vs. exercises and seminars) plays a more important role than the nature (e.g. difficulty) of the content. This will undoubtedly place greater demands on the planning of cartographic education in the future.

KEYWORDS

critical issues; cartographic education; students' results; final test; oral examination

Received: 6 July 2024
Accepted: 21 October 2024
Published online: 4 December 2024

Bláha, J. D., Trahorsch, P., Bartůněk, M., Hladík, P. (2024): Critical issues in undergraduate cartographic education: Analysis of final tests and oral examinations. AUC Geographica 60(1), 61–74
https://doi.org/10.14712/23361980.2024.19

1. Introduction

The importance of cartographic knowledge and skills for effective work with cartographic products has been demonstrated by numerous studies in the didactics of geography and cartography (e.g. Čerba et al. 2012; Duffek et al. 2018; Frangeš, Frančula, and Lapaine 2001; Gartner 2022; 2023; Hanus et al. 2020). Therefore, it is essential to integrate work with maps and map-related representations into the curriculum at all levels of education, as well as other learning activities (Wiegand 1993; 2006), to foster the development of these competencies from primary education through secondary to eventual tertiary education.

The next step is the provision of *cartographic education* as part of various university undergraduate programs. The goal of these study programs is to produce experts capable of undertaking the creation, revision and adaptation of cartographic products within the fields of geodesy and civil engineering, geography and regional development, geoinformatics, strategic and spatial planning, military, and other related disciplines. The utilization of cartographic skills by educated experts can be observed in other sectors in which maps are employed, ranging from basic data analysis to advanced interpretation and synthesis of spatial information. The aforementioned areas of expertise include but are not limited to archaeology, agronomy, biology, ecology, geology, historical and social sciences, climatology and urban planning, as well as within the operational centers of the Integrated Rescue System. Finally, the preparation of university students in the field of cartographic skills is aimed at future teachers, with a particular focus on geographic education. The intention is to prepare them to utilize maps, among other things, as tools to develop geographical thought in their pupils (Hanus et al. 2020).

Each graduate should have developed specific cartographic skills. The aforementioned format of cartographic competencies should be integrated into the content of university lectures, exercises and seminars. Additionally, it should be reflected in both continuous testing (testing the results and outputs of students during the semester, i.e. formative assessment) and final testing (after the end of the semester during the examination period, i.e. summative assessment). In many cases, cartographic education is integrated into a comprehensive system of subjects, where objectives and resources are aligned with the specifics of the disciplines.

At this point, it is appropriate to explain what the authors in this study mean by the term critical issues of curriculum. *Critical issues of curriculum* can be understood as areas of the curriculum where students or their teachers are failing for various reasons. The term therefore refers not only to the learning individual, but also to the concept of teaching, content or competences that the teacher understands as essential and tries to pass them on to the students. In this context, it is of particular importance to provide *feedback on student testing results* to teachers (McCarthy 2017; Nicol and Macfarlane-Dick 2006). This type of reflection can uncover critical issues within the educational context, including both the general and specific challenges students encounter (Stacke et al. 2020) and the quality of testing. In particular, it is necessary to determine whether the specific subject matter is effectively assessed during the testing process, what the teachers aim to evaluate, and the reliability of the testing process (validity and reliability of testing; Lane and Bourke 2019). In the educational context, reflecting on the quality of teaching and student assessment is crucial, as it can lead to continuous improvement in the content and design of the educational process (Ottens 2013).

The aim of this paper is to present the findings of a study that examined the results of the end-of-term assessment of students enrolled in a basic cartography course. Through this reflection, the authors contribute to the identification of critical issues in undergraduate cartographic education within geography and geoinformatics–related curricula, similar to how critical issues in the geography curriculum have been identified by geography didacticians (see Duffek et al. 2018). Identifying critical issues can help improve related cartography courses and contribute to addressing these problems effectively.

2. Cartography in university education

Cartography is an integral part of university education in a wide range of disciplines and related study programs. It is most commonly found in technical (examples in Czechia include Brno University of Technology, Czech Technical University in Prague and VSB – Technical University of Ostrava), science and environmental (Charles University, Czech University of Life Sciences Prague, Jan Evangelista Purkyně University in Ústí nad Labem, Masaryk University, Palacký University Olomouc, Technical University of Liberec, University of Ostrava, University of South Bohemia in České Budějovice), socioeconomic (Czech University of Life Sciences Prague, University of Pardubice, University of West Bohemia), education (Masaryk University, Technical University of Liberec, University of South Bohemia in České Budějovice) and military (University of Defense) departments. The characteristics and focus of the study programs determine the profile of their graduates.

Cartography plays different roles in the curricula according to the thematic focus of the study program:

(i) as a key discipline throughout the entire period of study (i.e. from the first to the last year, with a structured progression of acquired knowledge and skills), often in conjunction with geoinformatics;
(ii) as a discipline that is only auxiliary or complementary.

In the latter case, the time allocated to cartography-related courses may be limited to one or two courses in the early phase of the study, or may take the form of elective courses in the later phase of study. When a single course is offered across degree programs at a university, each with diverse graduate profiles, determining the content and organization of teaching becomes inherently more challenging.

The temporal scale aligns with the scope of the transferred knowledge and skills. *Cartographic skills*, as well as map skills, represent a complex set of operations and activities in which map and space still play a central role. Map skills can be categorized in terms of their cognitive complexity, ranging from using maps (reading, analysis, interpretation) to their actual production (Havelková and Hanus 2019). Nevertheless, cartographic skills encompass a range of abilities that are not necessarily directly related to the use or production of maps. These include a variety of data collection techniques and methods, as well as the distribution of cartographic products (Hanus and Marada 2014).

Undergraduate education typically aims to strike a balance between cartographic theory – the necessary minimum of professional knowledge, principles and conventions – and practical cartographic skills, involving the creation of maps or other cartographic products through partial or complex assignments during exercises and seminars. This also aligns with the generally accepted definition of cartography as "art, science and technology of making and using maps" (see, e.g., the 2003–2011 strategic plan of the International Cartographic Association, cited in Kraak and Fabrikant 2017). Here *science* corresponds to the theoretical concepts, principles and rules, while technology encompasses procedures and the integration with information technologies, geographic information systems (GIS) and other innovations in cartographic production (ibid.). Unfortunately, the principle of *art* is often not given sufficient attention in educational practice, particularly in map design and other less technical and structured aspects of map making. These competencies, occasionally referred to as visual talent or the talent component of map making, are more likely to be expected from map makers and professionals, including students.

In today's mainstream map making environment, which includes many individuals lacking the necessary cartographic production background and, regrettably, without the necessary skills (Dodge, McDerby, and Turner 2008), there is a pressing need to prioritize the practical use and creation of maps (*map use* and *map making*) in undergraduate education (MacEachren 2013; Ormeling and Rystedt 2014). The goal of such an educational program should be to equip students with an understanding of the fundamental principles of map design, including its visual elements and compositional structure. Additionally, it should develop practical skills in applying different scales and mathematical parameters (Anderson and Leinhardt 2002; Ooms et al. 2016; Wiegand 2006, 94–98), understanding the planimetric and altimetric components of maps and map lettering, selecting appropriate means of map representation and methods for representing thematic content (Michaelidou, Filippakopoulou, and Nakos 2007), and converting spatial and attribute data into map visualizations. This comprehensive list demonstrates that cartography places significant demands on students due to the inherently complex nature of the discipline. Even when cartography is introduced early in study programs, the demands are heightened due to the unique cross-curricular links it requires. Unlike fields such as statistical methods or spatial data processing, which are relatively universal in content, cartography requires specific knowledge and skills not offered in other courses. In addition, students typically possess a markedly disparate foundation of knowledge and abilities when transitioning from upper secondary education to undergraduate studies. Another significant challenge is the reluctance among successive generations of students, who have grown up in the digital age, to initially develop these skills in the traditional (analogue) form – drawing maps by hand without the use of GIS or other software tools (comp. Solórzano, Comíns, and Sendra 2017; Trahorsch and Reich 2023).

The framework of cartographic education objectives presented above provides the foundation for the *categories of cartographic curriculum* in the university environment. Based on the authors' extensive experience in teaching cartography and subsequent analysis (comp. Bláha 2021; Kůtová 2014), the following categories have been identified:

i) thematic cartography, map and content;
ii) map scale;
iii) map composition and compositional elements;
iv) map lettering;
v) cartographic semiology and linguistics, means of expression;
vi) mathematical principles of maps;
vii) topographic cartography, map and content (planimetric components);
viii) hypsography components – the third dimension in a map;
ix) statistical data processing/statistics;
x) other topics in cartography (cartography as a discipline, map, institutions, generalization, map production, history, evaluation, etc.).

3. Cartographic skills in a university environment and their testing

The development and level of cartographic skills can be influenced by a number of factors, including *the user of the cartographic product*, in this case the student, *the cartographic product* itself and *external factors* (Hanus et al. 2020, 97–102). These factors undoubtedly also influence students' performance in cartographic skills testing. Factors include student

characteristics, such as learning style, cognitive level, age and experience, as well as external factors such as the integration of cartography activities within the study plan, the time allocated for the course, the content and structure of the course syllabus, the teacher, and the teaching and testing methods employed (Havelková and Hanus 2019; Ooms et al. 2016).

In the context of university education, students enrolled in study programs that include cartography typically have an average to slightly above average level of cartographic user skills before they start the study (similarly see studies Havelková and Hanus 2018). However, the level of tested cartographic skill may be significantly influenced by *disciplinary specificities*. For instance, there can be a notable difference between single-discipline geography × geoinformatics students, as well as between teacher × non-teacher students. These variations stem from the prerequisites and motivation of applicants for specific study programs, as well as from the admission procedure. Often, the cartography educator has little influence over these aspects, particularly when cartography is regarded as a mere auxiliary discipline. The aforementioned disciplinary specifics also determine the methods used in teaching cartography (e.g. by incorporating more frequent field exercises in technical or natural science disciplines).

Cartographic products and their quality play a crucial role in university education, serving primarily as examples of good and bad practice. Above all, graduate students should be able to distinguish between these two categories of cartographic products to enhance their effective use in the practice of their respective disciplines (Trahorsch and Bláha 2022).

The testing of cartographic or map *skills* is typically conducted during the course through practical activities. Such activities may focus on either the application of the acquired knowledge within the partial activities (e.g. map scale calculation and compilation, generalization of map content) or creating complete map output of various types (e.g. creating a thematic map). The process of testing also encompasses the evaluation of general competencies (such as the ability to work with visuals), or competencies derived from other subjects (such as mathematical operations, analyzing and processing statistical data).

In particular, in the end-of-term examination, both *knowledge* acquired during the semester and skills are tested, either in written or oral form, depending on the educational policy environment's practices (predominantly summative function of assessment). In certain disciplines, it is common to test knowledge more frequently through continuous written tests, surveys or interviews (predominantly formative function of assessment) (Bijsterbosch, van der Schee, and Kuiper 2017; Weeden and Simmons 2017).

Assessing map skills through a final didactic test or exam can have several dimensions. Generally well-known cognitively demanding tasks (Downs, Liben, and Daggs 1988) range from basic knowledge remembering and understanding to the application of learned information in analysis, evaluation and creation. In the former scenario, students typically exhibit passive learning, passing on what they have learned without significant cognitive activity. In the latter, the student is required to engage in higher cognitive processes, such as actively applying learned knowledge to new contexts and relationships and drawing informed conclusions (Anderson and Krathwohl 2001). Another cognitive didactic level relates to the type of knowledge (according to the Revised Bloom's taxonomy; Anderson and Krathwohl 2001). On the one hand, the evaluation may emphasize factual knowledge, which is the initial prerequisite for effective work and creation with map products. However, this emphasis may result in a lack of attention to the application level.

The second dimension of evaluation is conceptual knowledge, which is of a more general nature; this dimension contextualizes factual knowledge, which includes knowledge and understanding of theories, models, patterns and generalizations. The procedural knowledge dimension includes familiarity with widely accepted procedures and conventional practices within the field of cartography, e.g., using the correct rules for creating a map legend (de Almeida 2012). The final dimension of knowledge is metacognitive knowledge, which encompasses the understanding of one's own learning practices and processes.

Apart from the student's attributes, *the nature of the final examination*, particularly its format – written in the form of a didactic test, oral in the form of an interview or a combination of the two – undoubtedly influences the results of the final examination (Aljazairi et al. 2022). If the testing is conducted over a longer period (2010–2023 in the presented case study), among others, the following factors should be considered:

a) variants of the didactic test (historical and contemporary);
b) characteristics of the didactic test – reliability, validity, sensitivity of tasks, etc.;
c) the nature and content of the tasks in terms of didactics, or in terms of the categories of the cartographic curriculum.

It can be assumed that synthesis and consideration of the aforementioned approaches and factors may provide insights into the following questions:

a) in the didactic aspect: To what extent are students' results influenced by the nature of the written test tasks (e.g. dimensions of knowledge, cognitive demand, presence of visuals)? To what extent are students' results influenced by the need to apply specific competencies (e.g. mathematical or linguistic operations)?
b) in the cartographic aspect: What mistakes do university students make? What are the critical issues in the cartographic curriculum? To what extent

does study discipline influence overall performance or results within the different categories of the cartographic curriculum?

4. A case study from a Czech regional university

The case study presented below comes from the Jan Evangelista Purkyně University in Ústí nad Labem, a typical example of a Czech regional university. Cartography is an auxiliary discipline within the study programs, and it is taught in the first semester of study for three diverse groups of students with different graduate profiles:

a) single-discipline students of geography;
b) double-discipline students of geography and other disciplines, many of whom expect to work in geography education in primary and secondary schools;
c) single-discipline students of geoinformatics, applied mainly to the environment.

The testing process during the semester is based on the fundamental principle of learning by doing and learning from mistakes. Students are guided through the sub-activities of map making, where their acquired knowledge and skills are demonstrated in their map outputs. These outputs are continuously corrected by the lecturer, with students revising their maps based on the teacher's feedback to improve their work. The number of map outputs has evolved over the study period (2010–2023), with the initial five outputs being replaced by the three outputs that are currently in use. The first of the retained map outputs focuses on thematic cartography, the second on topographic cartography. In the third, students demonstrate their own map productions, incorporating not only their interests but also all the cartographic skills they have acquired so far. In addition to the presentation of the third output, the seminar also includes a peer evaluation of another student's map output, followed by a discussion. The number of attempts and the results of the student's efforts are reflected in the final evaluation, which uses a nominal (output submitted in an acceptable × unacceptable form) and interval scale (scoring). If all outputs are submitted in an acceptable form, and the student also obtains a minimum of 24 out of 46 points (approximately 52%), the student may proceed to the end-of-term examination. Considering the difficulties in analyzing the results of a continuous assessment, including various external factors, the authors decided not to prioritize this aspect of testing, instead focusing solely on the analysis of the students' end-of-term testing, namely its written form. However, based on the teachers' experience, it is evident that the ongoing assessment and its formative role in these tasks is likely to be reflected in the results of didactic tests.

The final testing of students' cartographic skills is conducted through an exam in written (for double-discipline students) or combined form (i.e. written and oral form; for single-discipline students of geography and geoinformatics). The written exam consists of a didactic test comprising 12 tasks of varying types. Each task is scored based on its significance, ranging from 1 to 3 points, for a maximum total of 20 points. Scoring is to the nearest 0.25 points, which allows for the recognition of differences, particularly in the responses to open-ended questions. A score of at least 11 points is required to pass the test. Grades are then derived from the scores obtained according to the system used at certain Czech universities: 1–3 are passing grades, grade 4 is a failing grade (0–10 points corresponds to grade *4*, 11–13 points correspond to grade *3,* 14–16 points correspond to grade *2* and 17–20 points correspond to grade *1*). For borderline scores of 10.5, 13.5 or 16.5, additional questions are provided for the failed tasks in the test. In light of the longer time horizon (2010–2023), the didactic test has a total of four historical variants (A–D). Each historical variant contains different contemporary sub-variants: 1–8 for the first three variants and 1–6 for the last variant.

5. Methodology

The presented research is semi-longitudinal and is based on the collection of the results of final tests and oral examinations in a basic cartography course. The study employs a quantitative approach, utilizing statistical procedures to identify the critical points of the curriculum and the factors that the student in the given example navigates with no difficulty. The results are interpreted using classical test theory (CTT), which has the potential to identify the level of ability and skills of the respondents.

5.1 Structure of didactic tests used

Tab. 1 and 2 illustrate the test structure and the various tasks that were expertly analyzed by the members of the research team, (a) the didactics aspects (Tab. 1), and (b) the categories of the cartographic curriculum (Tab. 2). The coding of the tasks was carried out by two members of authors' collective, independently of each other and then they compared and discussed their results. As an example, we present two tasks that were conceptually quite different in the tests (comp. with Tab. 1 and 2):

a) U1 – "Circle the appropriate thematic mapping techniques for the map topic below (there may be one or more correct answers): *Religious denominations* in Asia: (a) cartogram, (b) area-class map, (c) choropleth map, (d) dasymetric map, (e) diagram map;"
b) U9 – "Briefly but clearly explain in your own words the terms below from the field of cartography. Please provide examples if appropriate. Terms: (i) reference surface, (ii) UTM, (iii) isochrones."

Tab. 1 Structure of the test with tasks assessed from the didactic perspective.

Didactic aspects	U1	U2	U3	U4	U5	U6	U7	U8	U9	U10	U11	U12
Cognitive Process Dim.	App.	App.	App.	Anal.	App.	App.	Anal.	App.	Und.	App.	Rem.	Crea.
Knowledge Dimension	Proc.	Proc.	Proc.	Conc.	Proc.	Proc.	Proc.	Proc.	Fact.	Proc.	Fact.	Proc.
Type of Task	CMCA	OBRS	OBRS	OSSA	OBRS	OBRS	OBRD	OBRU	OBRU	OBRS	OSPA	OBRS
Working with Visuals	No	No	Yes	Yes	No	No	Yes	No	No	No	No	Yes
Mathematical Operations	No	Yes	No	No	No	No	No	Yes	No	Yes	No	No

Cognitive Process Dimension

Rem.	remember
Und.	understand
App.	apply
Anal.	analyze
Crea.	create

Knowledge Dimension

Fact.	factual
Conc.	conceptual
Proc.	procedural

Type of Task

OBRD	open-ended with broad response structure defined
OBRS	open-ended with broad response structure given by convention
OBRU	open-ended with broad response unstructured
CMCA	closed with multiple choice answers
OSPA	open-ended with brief response production
OSSA	open-ended with brief response completion

Notes for Tab. 1 and Tab. 2: U1–U12 are individual tasks, with task U4 having three sub-questions U41–U43 in the historical version of Test D, I–X are individual categories of the cartographic curriculum (see Part 2); for certain tasks, multiple categories are represented in varying proportions.

The oral part of the exam is conducted through an interview over two randomly selected topics and focuses mainly on the student's knowledge, or the analysis, interpretation and conceptual design of maps. Performance on the oral part of the examination is evaluated solely based on the aforementioned marking system, whereas the written test serves as the primary input parameter.

In the 2010–2023 period, the anonymized results of the scores and marks were stored in the database of written test results and the database of oral examination results. However, for a detailed analysis of the final assessment, only the database of written test results was used (monitored variables see Part 5.3). Due to incomplete records in the database, it is impossible to ascertain whether the first or second randomly selected topics influenced the outcome of the oral examination.

5.2 Methodological attributes of the tests used

From a methodological perspective, the authors examined the attributes of test tasks and historical test variants. Initially, it was necessary to unify the individual tasks according to their thematic focus into tasks under the U1–U14 label (Tab. 1). In each of these tasks, both the didactic and cartographic attributes, as well as the sensitivity and difficulty of each task, were monitored. *Task sensitivity* is defined as the extent to which a given task measures what the whole test measures and is calculated using the *ULI* and *RIT* coefficients. All the tasks fall within the range of <0.10–0.66>, indicating sufficient sensitivity for individual tasks (or at least tolerable, for those slightly above 0.10), specifically, the U4 and U9 tasks (Štuka and Vejražka 2021). *Task difficulty* measures how challenging a task is for students. The index used in this case ranges from 0 to 100, with higher values indicating easier tasks. All the tasks observed in each historical variant had values <25; 80>, indicating that none of the tasks were inappropriately easy or difficult (ibid.).

The reliability of the individual historical variants of the test, calculated using Cronbach's alpha, ranges from 0.57 (historical variant C) to 0.74 (historical variant A). It should be noted that variant C has the smallest number of records ($N = 119$), however, when converted to values per 250 (like the other historical variants), the reliability is close to 0.70. In general, the reliability of the individual tests can be considered sufficient, but slightly lower for historical variants B (0.62) and C (0.57). Based on methodological studies, the reliability can be described as acceptable, sufficient and satisfactory (Taber 2017).

These data show that the tests used are reliable and, in terms of their properties, applicable in practice (none of the questions deviates significantly from the testing objective). The presented tool (didactic test) can thus be used to answer research questions.

5.3 Structure of the results database

The total *number of monitored tests* (the number of processed written tests) is 1,315. Each submitted test corresponds to exactly one record in the database, which has the following structure:

a) information about the test (test ID, year and date of the test, historical variant and contemporary sub-variant of the test, total score, total test score marked with a grade);

Tab. 2 Structure of the test with tasks assessed from the perspective of the cartographic curriculum.

Historical variant	Sub-variant	U1	U2		U3			U41	U42	U43	U5		U6		U7		U8	U9			U10			U11	U12	
A	1	I	II	III	IV	V		VI			III	V	V	I	VII	VIII	II	V	X	I	IX	I	V	X		
	2	I	II	III	IV	V		VI			III	V	V	I	VII	VIII	II	VIII	X	X	IX	I		III		
	3	I	II	III	IV	V		VI			III	V	V	VII	VII	VIII	II	X	V	X	IX	I	V	X		
	4	I	II	III	IV	V		VI			III	V	V	VII	VII	VIII	II	V	VIII	VI	IX	I		III		
	5	I	II	III	IV	V	VIII	VI			III	V	V	I	VII	VIII	II	VI	X	X	IX	I		V		
	6	I	II	III	IV	V		VI			III	V	V	VII	VII	VIII	II	III	X	V	IX	I	V	V		
	7	I	II	III	IV	V		VI			III	V	V	I	VII	VIII	II	VI	VI	X	IX	I	V	X		
	8	I	II	III	IV	V		VI			III	V	V	I	VII	VIII	II	VI	X	V	IX	I		X		
B	1	I	II	III	IV	V		VI			III	V	V	I	VII	VIII	II	V	X	VI	IX	I	V	V		
	2	I	II	III	IV	V		VI			III	V	V	I	VII	VIII	II	V	I	X	IX	I		III		
	3	I	II	III	IV	V		VI			III	V	V	I	VII	VIII	II	VI	X	X	IX	I	V	X		
	4	I	II	III	IV	V		VI			III	V	V	I	VII	VIII	II	V	VIII	VI	IX	I		V		
	5	I	II	III	IV	V		VI			III	V	V	I	VII	VIII	II	VI	VI	I	IX	I	V	X		
	6	I	II	III	IV	V	VIII	VI			III	V	V	VII	VII	VIII	II	VI	X	V	IX	I		V		
	7	I	II	III	IV	V		VI			III	V	V	I	VII	VIII	II	X	X	VIII	IX	I	V	X		
	8	I	II	III	IV	V		VI			III	V	V	I	VII	VIII	II	III	VI	V	IX	I		X		
C	1	I	II	III	IV	V		VI			III	V	V	I	VII	VIII	II	V	X	VI	IX	I	V	V	III	V
	2	I	II	III	IV	V		VI			III	V	V	I	VII	VIII	II	V	I	X	IX	I		V	III	V
	3	I	II	III	IV	V		VI			III	V	V	I	VII	VIII	II	VI	X	X	IX	I	V	X	III	V
	4	I	II	III	IV	V		VI			III	V	V	I	VII	VIII	II	V	VIII	VI	IX	I		V	III	V
	5	I	II	III	IV	V	VIII	VI			III	V	V	I	VII	VIII	II	VI	VI	I	IX	I	V	X	III	V
	6	I	II	III	IV	V		VI			III	V	V	VII	VII	VIII	II	VI	X	V	IX	I		V	III	V
	7	I	II	III	IV	V		VI			III	V	V	I	VII	VIII	II	X	X	VIII	IX	I	V	X	III	V
	8	I	II	III	IV	V		VI			III	V	V	I	VII	VIII	II	III	VI	V	IX	I		X	III	V
D	1	I	II	III	IV	V		VI	VI	VI	III	V	V	I	VII	VIII	II	V	X	VI	IX	I	V	V	III	V
	2	I	II	III	IV	V		VI	VI	VI	III	V	V	I	VII	VIII	II	V	I	X	IX	I		V	III	V
	3	I	II	III	IV	V		VI	VI	VI	III	V	V	I	VII	VIII	II	VI	X	X	IX	I	V	X	III	V
	4	I	II	III	IV	V		VI	VI	VI	III	V	V	I	VII	VIII	II	V	VIII	VI	IX	I		V	III	V
	5	I	II	III	IV	V	VIII	VI	VI	VI	III	V	V	I	VII	VIII	II	VI	VI	I	IX	I	V	X	III	V
	6	I	II	III	IV	V		VI	VI	VI	III	V	V	VII	VII	VIII	II	VI	X	V	IX	I		V	III	V

Categories of cartographic curriculum

- I – thematic cartography, map and content
- II – map scale
- III – map composition and compositional elements
- IV – map lettering
- V – cartographic semiology and linguistics, means of expression
- VI – mathematical principles of maps
- VII – topographic cartography, map and content (planimetric components)
- VIII – hypsography components – the third dimension in a map
- IX – statistical data processing/statistics
- X – other topics in cartography (cartography as a discipline, map, institutions, generalization, map production, history, evaluation, etc.)

b) information about the student (student ID, specialization – discipline, number of testing attempts to date – maximum of six attempts during one study period);
c) information on the results in individual tasks (scores for individual tasks, which have been standardized for the purposes of subsequent statistical analysis and standardized on a scale of 0–100, corresponding to the percentage of successful solutions).

In cases where a student completes both the written and oral parts of an examination, a record is included detailing the topics selected for the oral interview and the final grade awarded. This enables comparisons between the results of the written and oral examinations.

5.4 Statistical analysis of the results

The results database is the primary input material for statistical analysis. To perform the statistical analysis, classical measures of central tendency (modus, median – *M*, mean), measures of variability (mainly

standard deviation – *SD*) and inferential statistical procedures were utilized. The authors followed the recommendations of Rabušic, Soukup and Mareš (2019) in assessing the normal distribution of the data.

Normality tests (Shapiro–Wilk, Kolmogorov–Smirnov) indicated that the observed sample did not exhibit a normal distribution of data. However, the authors emphasize that these tests are unreliable in numerically large samples and that normality can be assessed by examining skewness and kurtosis values, assessing differences between mean and median values, or analyzing the shape of the histogram. In accordance with these criteria and recommended procedures, the authors subsequently applied parametric statistical tests. These included the comparison of two or more means, followed by a post hoc analysis (*t*-test for the comparison of two means; ANOVA test for the comparison of multiple means and Bonferroni's post hoc test) and calculating product–moment correlation coefficient. Subsequently, the assessment of statistical significance was enhanced by examining *effect size* indicators (η^2), which gauge the significance and practical importance of the results. The interpretation of these indicators is based on the recommendations of Cohen (1988) and Soukup, Trahorsch and Chytrý (2021).

6. Results

6.1 Testing results in overall terms

In the observed tests, students achieved an average score of 9.2 points (*SD* = 3.3), with a success rate of 46%. There is a minimal difference between the median and the mean (*M* = 9.25). The mode of the sample corresponds to a score of 10.75 points (students achieved this score 42 times), which is interesting considering that a score of 11.00 points (55%) is required to pass the written exam or proceed to the oral part of the exam. During the monitoring period (2010–2023), no student achieved the maximum score of 20.00 points.

All the primary measures of central tendency demonstrate that the students' scores fluctuate around the 50% success rate, which is near or just below the threshold for obtaining credits or being admitted to the oral exam. This fact is also illustrated by the histogram (Fig. 1). The observed mode (value of 10.75) and the apparent shift in the histogram around the values of 9.00–10.00 points can be attributed to the subsequent evaluation of the written tests by the lecturer. Despite the implementation of objective assessment criteria, the teacher tries to differentiate between the performance of those who failed the test and those who succeeded. This procedure leads to a reduction in the total number of tests with a score of 9.50–10.00. The rationale behind this scoring system is twofold. Firstly, it aims to eliminate debates about narrowly missed passing grades. Secondly, it ensures that students who only take the written exam achieve the lowest passing score, 10.75, which is rounded up to meet the minimum threshold.

The overall results demonstrated how the success rate of the test varied depending on *the students' attempts*. In this case, the analysis of variance revealed that there was no statistically significant difference (p = 0.182) in success rates between attempts. For the first through fifth attempts, the average success rate was just above 9.00 points, while the first attempt exhibited the lowest success rate. Considering the aforementioned result, it is not surprising that the effect size of the sequence of attempts on the overall test score is minimal (η^2 = 0.006). Unfortunately, this indicates a minimal practical impact on improving student performance with repeated attempts. Consequently, the number of attempts explains only 0.6% of the overall test score. This may be due to a lower degree of student motivation in studying the field (in the case of this study geography) or very low study prerequisites of students who may not yet have been assessed and selected in other courses (students are still at the beginning of their studies).

As previously stated, students from different study groups may exhibit disparate outcomes due to their varying profiles and the *targeted focus of their respective study programs*. It was not confirmed that there

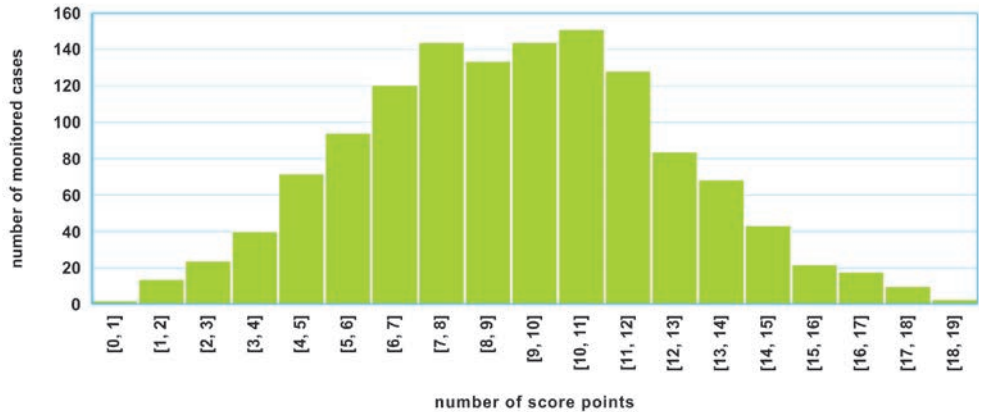

Fig. 1 Histogram of scores of the didactic test.

was a statistically significant difference (p = 0.08) among the various disciplines of study (i.e. applied geoinformatics, single-discipline specialized geography, double-discipline with geography, geography teaching). Additionally, the effect size indicates that the influence of the discipline of study on the results is minimal, practically zero (η^2 = 0.04). In the next phase of the analysis, the authors proceeded to a more in-depth examination of the results by discipline, dividing them into groups with similar skills and fields (disciplinary grouping). These groups included applied geoinformatics, single-discipline geography, geography combined with physical education, geography combined with social sciences, geography combined with science (excluding biology), and geography combined with biology. Even using this division of disciplines, a statistically significant difference between them was not confirmed (p = 0.08). The only additional information available is that the highest mean scores were achieved by students in applied geoinformatics, which may be due to the smaller sample size (see e.g. Soukup, Trahorsch, and Chytrý 2021) and different characteristics of the historical version of the test (see Methodology).

6.2 Student results in the didactic aspects of the tasks

In tasks involving *visuals*, the results were found to be slightly worse (47%) than in tasks lacking visual elements (48%). Two-sample t-test showed a statistically insignificant difference between the two types of tasks (p = 0.08; d = 0.21; r = 0.05), indicating that the inclusion of visuals had a minimal effect on task achievement – according to r, only 5%. This may be because students have already developed the requisite skills to work with different types of visuals, leading to an insignificant difference in the success rate of solving problems with and without visuals. The students' own production of maps during the semester may also be a factor.

In tasks requiring *complex mathematical operations*, students achieve worse results than in tasks without such operations (45% vs. 49%). The difference between the results of these two types of tasks is statistically significant (two-sample t-test; p < 0.01; d = 0.23; r = 0.10). Although the result is statistically significant, the effect of mathematical skills on solving tasks is only about 10%, indicating a small effect. Students achieve higher success rates in tasks that do not require more complex mathematical operations. However, there was no association between success rates in tasks requiring mathematical operations and the discipline of study (p = 0.45; η^2 = 0.001). This may be related to students' lack of mathematical skills, as mathematics is often not an elective subject for graduating from high school. On the contrary, geography is frequently selected as an "escape" from disciplines in which mathematical skills are applied more frequently.

An analysis of student results in terms of *Bloom's taxonomy of cognitive goals* (Fig. 2) reveals some interesting patterns. Students achieve the highest success rate in tasks requiring application (53%), while showing the same success rate (40%) in tasks with both low and high cognitive demands. The difference in success rate across different cognitively demanding tasks is statistically significant (analysis of variance; p < 0.01; η^2 = 0.06). In terms of substantive significance, the result can be assessed as moderately important. Bonferroni's post hoc test showed a statistically significant difference between the lower cognitive level tasks (knowledge, understanding) and the application (p < 0.01) as well as between the application and the higher cognitive level tasks (analysis, evaluation, creation; p < 0.01); a statistically significant difference between the lowest and highest cognitive operations was not identified by a post hoc test (p = 1). In contrast, no statistically significant difference was found between the lower and higher cognitive level tasks. One potential explanation for these results may lie in the teaching approach, which prioritizes the practical application of cartographic skills over the mere rote memorization of definitions. The difficulty of the higher cognitive functions, and therefore the low success rate, correlates with the overall proficiency level of geography students (as seen in other studies), potentially influenced by the rigorous testing and assessment of these cognitive abilities.

In the context of higher success rates in application tasks, and in consideration of the nature of cartography, the authors conducted further research into the extent to which students are successful in *understanding and applying the of conventions*. In tasks where students are required to demonstrate understanding of conventions and their application, they achieve a higher success rate (56% vs. 42%) than in other tasks. The observed difference in success rates

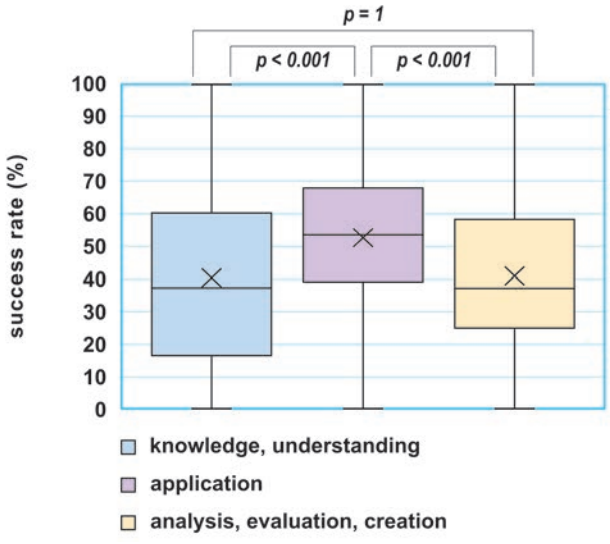

Fig. 2 Comparison of success rates between the different cognitive dimensions of the didactic test.

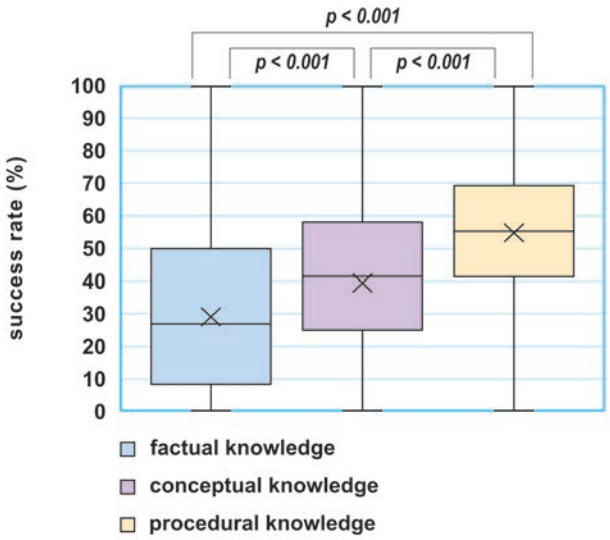

Fig. 3 Comparison of success rates between different types of knowledge in the didactic test.

between the two types of tasks is statistically significant (two-sample t-test; $p < 0.01$; $d = 0.73$). This may be beneficial for future studies, as the results show that students have demonstrated an understanding of fundamental cartographic procedures and conventions. The result is of medium significance and has the highest impact on task success compared to the other factors.

In terms of the *knowledge dimension* (Fig. 3), students achieve the highest success rate in procedural knowledge (55%), and the lowest success rate in factual knowledge (29%). The differences in success rates for tasks requiring different types of knowledge are statistically significant (analysis of variance; $p < 0.01$; $\eta = 0.189$). The effect size indicates that the knowledge dimension of the task has a considerable impact on the success rate, affecting the result by almost 20%. Bonferroni's post hoc test showed a statistically significant difference between all dimensions (in all cases $p < 0.01$). This may be due to the prevailing teaching methods, which place a significant emphasis on procedural knowledge (i.e., the procedures for creating maps and their component parts). This is evidenced by the fact that students are able to infer conceptual knowledge during the tests. In contrast, students demonstrate low levels of factual knowledge, struggling to derive independently, with effective memorization and repetition of learning required for its reproduction.

6.3 Students' results in the cartographic aspects of the tasks and the oral examination

The results of the descriptive statistics (Fig. 4) show that students achieve the highest success in map composition (Category III) and the lowest success in Category X (other topics of cartography – see Part 2) and to a lesser extent in statistics (Category IX), which is a specific category and has a higher degree of variability (see below). This is consistent to a certain extent with the results of the previous analysis, in which the problematic tasks were those in which students were required to solve mathematical operations. A greater variability in the results was evident in the categories focusing on map lettering (Category IV) and topographic cartography (Category VII). Conversely, a low variability of results was observed for cartographic semiology and linguistics (Category V) and thematic cartography (Category I). These findings may be caused by the form in which the information is presented; much of the information that students find difficult is presented in lectures (frontally, without practical application), while much of the knowledge and skills students find easier are discussed in seminars with practical applications (e.g., creating the maps, among others).

The differences in success rates observed between the various cartographic aspects are statistically significant (analysis of variance; $p < 0.01$), indicating that students achieve significantly different results in the different categories. Bonferroni's post hoc showed that there is a statistically significant difference ($p < 0.05$) between the success of most cartographic aspects.

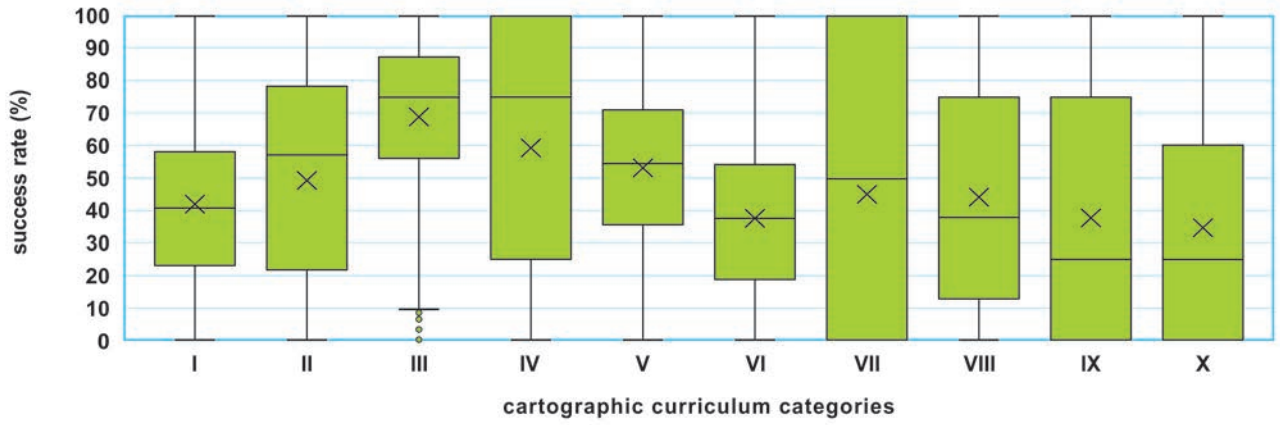

Fig. 4 Success rate by individual cartographic aspects of the tasks.

Tab. 3 Pearson correlation coefficients between individual cartographic aspects of the tasks.

	I	II	III	IV	V	VI	VII	VIII	IX	X
I	×	0.22	0.08	0.05	0.25	0.15	0.05	0.08	0.36	0.12
II		×	0.14	0.09	0.21	0.15	0.00	0.05	0.24	0.12
III			×	0.29	0.42	0.15	0.07	0.11	0.11	0.16
IV				×	0.30	0.06	0.09	0.16	0.03	0.18
V					×	0.26	0.21	0.25	0.23	0.35
VI						×	0.13	0.16	0.11	0.34
VII							×	0.92	−0.04	0.19
VIII								×	−0.02	0.24
IX									×	0.11
X										×

Notes: $p < 0.05$ shown in red.

If we select exemplary examples of cartographic aspects between which no statistically significant difference was identified, it is Category I – thematic cartography aspect with Category VII – topographic cartography aspect ($p = 1$) and Category VIII – hypsography aspect ($p = 1$). Furthermore, there are thematically and competently similar thematic categories, namely Category IX – statistical data processing and Category VI – mathematical foundations of maps ($p = 1$) or Categories VII–VIII – topographic cartography and hypsography ($p = 1$), in which it is necessary to demonstrate logical reasoning and more complex mathematical calculations. There was also no statistically significant difference between Category II – map scale and Category V – cartographic semiology ($p = 0.1$).

Tab. 3 demonstrates this association between the different cartographic aspects of the tasks. Categories VII (topographic cartography aspect) and VIII (hypsography aspect) demonstrate a highly significant correlation, indicating their close interconnection. Moreover, higher correlations are evident in those aspects that are practiced in the seminars, specifically Categories III, IV and V (map composition and compositional elements, map lettering, and cartographic semiology and linguistics, respectively). In general, the statistical data processing aspect (Category IX) shows a comparatively weaker correlation with other aspects, likely due to its specific knowledge and skill requirements.

A statistical analysis of the average success rate of students divided according to the individual disciplines (see Part 6.1) reveals relatively minor differences in the cartographic aspects of the tasks. Students of biology and science have a higher success rate than those studying physical education. In Categories VII and VIII (topographic cartography including planimetric and hypsography components), biology students have the highest success rates, while students of other science disciplines have the greatest difficulties with these categories. In contrast, science students have the highest success rates in Categories II and III (map scale calculation and map composition including compositional elements). Applied geoinformatics students have the highest success rates in Category VI (mathematical principles of maps). Category V (cartographic semiology and linguistics) exhibits minimal variability in success rates across disciplines. This may be because the subject matter is largely specific and novel to the majority of students.

The results of the oral and written parts of the exam in the records containing information from the oral examination (over 330 records) are correlated, and the correlation is statistically significant (rank correlation coefficient; $r = -0.55$, $p = < 0.01$). In the context of the oral examination, the procedure for selecting thematic areas for students is structured so that they must choose three topics guaranteed by random selection of numbers. They are permitted to answer only two of their own choice. Although a detailed analysis of the results is not possible due to the aforementioned reasons (see Part 4), it is at least possible to observe the frequency of popular or unpopular topics in cartography. It can be hypothesized that preference or dislike is primarily influenced by the subjective perception of difficulty, specifically in identifying critical aspects within the cartography curriculum.

The frequency analysis revealed the most commonly answered and eliminated topics. This analysis demonstrates that the aforementioned categories of cartographic curriculum do not, in themselves, play a significant role in the formation of positive or negative attitudes. Rather, it is the forms of transfer of the individual content that are of greater importance. While the topics practiced in the seminars and individual exercises (e.g. map symbols, thematic maps and thematic mapping techniques, placement of lettering) were favored by the students, the fact-based topics (history of cartography, state and military maps) were not as popular. Students tend to favor relatively simple definitions (cartography, cartographic product, plan, etc.), yet their explanations often lead to numerous errors.

In certain categories of cartographic curricula (e.g. mathematical cartography), contradictions can be identified (cf. relatively popular reference surfaces vs. unpopular coordinate system conversions). This may be due to the presence of different forms of spatial imagination and visualization possibilities. In general, topics in which the student can apply certain easier forms of visualization (e.g. cartographic generalization methods, placement of lettering, map symbols) are preferred.

Finally, students tend to avoid topics with a greater degree of uncertainty resulting from the on-site assignment (selection of the method of thematic cartography according to the given topic, choice of cartographic projection for the given territory) or the need to follow current trends (private production, work on the map including data acquisition and distribution of cartographic products). An exception to this is the evaluation of the cartographic product given during the oral exam, which appears to reflect the experience of the activity that students attempt during the seminars.

7. Discussion

The analysis of the students' scores on both the didactic and cartographic aspects of the written test tasks indicates that their performance is significantly influenced by the curriculum content covered in seminars, practical activities and through frontal teaching – lecture or open discussions during lectures. The analysis of the most/least favorite topics during the oral examination showed similar results. Therefore, the overall results cannot be solely attributed to specific categories of the cartographic curriculum. Identifying critical issues is more complex and likely depends significantly on the teaching approach, including the distribution and content of lectures and seminars.

In terms of the didactic aspects, the statistical analysis revealed a *hierarchy of influences on student performance*. The incorporation of visuals in the test tasks has a relatively low impact on students' success, but simple visualization techniques can motivate students in oral examinations to select a particular topic over others that are more challenging to visualize. As the long-term experience of the examiner shows, students prefer during the oral examination precisely those questions where it is possible to apply visualization or where visuals are present.

The presence of more complex mathematical operations has a slightly greater impact on students' success rate. Finally, varying levels of cognitive complexity and different dimensions of knowledge (factual vs. procedural) have the greatest impact on success rates. From the analysis, it can be concluded that students are prepared for the application of knowledge and procedural knowledge, meaning that they have developed adequate cartographic skills. Conversely, students often lack sufficient development in fact-based information, leading to gaps in their performance on the final test. University curricula are heavily fact-based, and mastering this information requires time, ongoing repetition, and consistent effort. When procedural knowledge involves mathematical competence, students are more likely to fail compared to tasks that do not require the application of more complex mathematical operations.

In considering the role of cartography in the curricula of the Jan Evangelista Purkyně University in Ústí nad Labem as an auxiliary or complementary discipline, the results of this study can be viewed positively. It is crucial for students to master the fundamental practical procedures of map creation and understand the associated concepts and conventions, such as creating diagram scales within diagram maps, determining intervals for dataset values, and designing a graphical scale. Graduates can acquire this factual knowledge, including terminology, through the repetitive process of map production and further professional communication practice.

7.1 Limitations of the study

The present study has a number of limitations that could have affected its results. Limits can be divided from the point of view of the actors of the educational process into limits on the side of students (e.g. the predominant type of study, anxiety about a written test or, conversely, of exams, dropping out of studies and entering another field) and limits on the side of teachers (staffing of exercises, representation of teaching methods, changes in the assignment and scoring of tasks). Furthermore, limits related to changes in the organization of the course can be reflected in the results (changes in the content concept of the test – Tab. 2, partial changes to the curriculum in response to changes in study plans and current trends in the field). Nevertheless, we believe that the presented study tried to present maximally comparable data and results based on them.

8. Conclusion

The summative evaluation of student achievement in cartographic education represents a key feedback tool not only for cartography educators but also for all cartographers in general. As shown in this study, such evaluations have the long-term potential to identify a number of critical issues within the curriculum of a given subject (discipline). Addressing these issues can lead to enhanced teaching quality, with the aim of eliminating these weaknesses over time. The case study revealed that students encounter difficulties with tasks requiring factual knowledge, complex mathematical operations, statistics, or other topics in cartography, such as the history of the discipline.

Conversely, students had fewer difficulties with aspects of the curriculum that were covered extensively during the seminars, due to the course design and the summative assessment. This is valuable information to a certain extent, as it shows that content taught more practically can eliminate critical issues in the cartography curriculum. However, it is interesting to note that the variations between study programs (in terms of students' disciplinary differences) are not significant, underscoring that the teaching approach is likely a key factor in the final testing.

Nevertheless, the following suggestions or modifications are proposed regarding the teaching of cartography at this institution:

a) place even more emphasis on the mathematical background of operations. Reinforce the practice of mathematical operations when a separate course is not available and encourage more collaboration between teachers of courses in which these competencies are promoted (e.g. applying statistical methods to real data, which are then used in GIS teaching);
b) incorporate fact-based tests into the exercises during the semester to help students learn factual knowledge gradually and continuously;
c) consider including a glossary of key terms or linking seminar activities more closely to existing didactic tools, such as textbooks, which frequently emphasize these terms.

However, within diversely designed study plans featuring distinct graduate profiles, expectations and needs may vary, necessitating a detailed analysis specific to each university.

This paper contributes to the ongoing discussion among cartography educators regarding how teaching strategies can be applied across various study programs and graduate profiles. Future research should explore similar analyses of summative assessments at other universities to compare whether critical issues vary significantly across different disciplines and universities.

Acknowledgements

This work was supported by the Internal Grant Agency of the Jan Evangelista Purkyně University in Ústí nad Labem under Grant UJEP-SGS-2023-53-001-2: "*Critical spots in undergraduate cartographic education: analysis and initial interpretation of the results of a longitudinal study*".

References

Aljazairi, S., Salcedo-Bellido, I., Barrios-Rodríguez, R., Requena, P. (2022): Comparison of two online university examination modalities in Didactics of Sciences. ReiDoCrea 11, 245–254, https://doi.org/10.30827/Digibug.74685.

Anderson, K. C., Leinhardt, G. (2002): Maps as Representations: Expert Novice Comparison of Projection Understanding. Cognition and Instruction 20(3), 283–321, https://doi.org/10.1207/S1532690XCI2003_1.

Anderson, L. W., Krathwohl, D. R. (Eds.) (2001): A Taxonomy for Learning, Teaching, and Assessing: A Revision of Bloom's Taxonomy of Educational Objectives. Allyn & Bacon: Boston, MA.

Bijsterbosch, E., van der Schee, J., Kuiper, W. (2017): Meaningful learning and summative assessment in geography education: an analysis in secondary education in the Netherlands. International Research in Geographical and Environmental Education 26(1), 17–35, https://doi.org/10.1080/10382046.2016.1217076.

Bláha, J. D. (2021): Vybrané okruhy z geografické kartografie, 2nd ed.; Univerzita J. E. Purkyně v Ústí nad Labem: Ústí nad Labem, Czechia.

Cohen, J. (1988): Statistical Power Analysis for the Behavioral Sciences, 2nd ed.; Erlbaum: New York, NY.

Čerba, O., Čada, V., Vichrová, M., Jedlička, K., Janečka, K., Šilhavý, J., Ježek, J. (2012): Cartographic Education in Geomatics Curriculum. Proceedings of AutoCarto 2012 – Columbus, OH.

de Almeida, R. D. (2012): Research on Cartography for School Children. In: Zentai, L., Reyes Nunez, J. (Eds.) Maps for the Future: Children, Education and Internet. Springer: Berlin, Germany, pp. 219–227, https://doi.org/10.1007/978-3-642-19522-8.

Dodge, M., McDerby, M., Turner, M. (2008): Geographic Visualization: Concepts, Tools and Applications. Wiley: Hoboken, NJ, https://doi.org/10.1002/9780470987643.

Downs, R. M., Liben, L. S., Daggs, D. G. (1988): On Education and Geographers: The Role of Cognitive Developmental Theory in Geographic Education. Annals of the Association of American Geographers 78(4), 680–700, https://doi.org/10.1111/j.1467-8306.1988.tb00238.x.

Duffek, V., Pluháčková, M., Stacke, V., Mentlík, P. (2018): Kritická místa ve výuce zeměpisu na 2. stupni základní školy. Západočeská univerzita v Plzni: Plzeň, Czechia.

Frangeš, S., Frančula, N., Lapaine, M. (2001): Cartographic education at the Institute for Cartography, Faculty of Geodesy, University of Zagreb. E-mail Seminar of Cartography 2000–2001.

Gartner, G. (2022): Underpinning Aspects of Developing a Cartographic Curriculum. Journal of Geodesy and Geoinformation Science 5(3), 41–50, https://doi.org/10.11947/j.JGGS.2022.0305.

Gartner, G. (2023): Activating students in cartographic education. Abstracts of the ICA 6(68), 2 p, https://doi.org/10.5194/ica-abs-6-68-2023.

Hanus, M., Havelková, L., Kocová, T., Bernhäuserová, V., Štolcová, K., Fenclová, K., Zýma, M. (2020): Práce s mapou ve výuce. Certifikovaná metodika. P3K: Prague, Czechia.

Hanus, M., Marada, M. (2014): Mapové dovednosti: vymezení a výzkum. Geografie 119(4), 406–422, https://doi.org/10.37040/geografie2014119040406.

Havelková, L., Hanus, M. (2018): The Impact of Map Type on the Level of Student Map Skills. Cartographica 53(3), 149–170, https://doi.org/10.3138/cart.53.3.2017-0014.

Havelková, L., Hanus, M. (2019): Map Skills in Education: A Systematic Review of Terminology, Methodology and Influencing Factors. Review of International

Geographical Education Online 9(2), 361–401, https://doi.org/10.33403/rigeo.591094.
Kraak, M.-J., Fabrikant, S. I. (2017): Of maps, cartography and the geography of the International Cartographic Association, International Journal of Cartography, 3(sup1), 9–31, https://doi.org/10.1080/23729333.2017.1288535.
Kůtová, E. (2014): Analýza středoškolských a vysokoškolských učebnic kartografie od počátku 20. století. Bachelor thesis. Univerzita J. E. Purkyně v Ústí nad Labem.
Lane, R., Bourke, T. (2019): Assessment in geography Education: a systematic review. International Research in Geographical and Environmental Education 28(1), 22–36, https://doi.org/10.1080/10382046.2017.1385348.
MacEachren, A. M. (2013): Map Use and Map Making Education: Attention to Sources of Geographic Information. The Cartographic Journal 23(2), 115–122, https://doi.org/10.1179/caj.1986.23.2.115.
McCarthy, J. (2017): Enhancing feedback in higher education: Students' attitudes towards online and in-class formative assessment feedback models. Active Learning in Higher Education 18(2), 127–141, https://doi.org/10.1177/1469787417707615.
Michaelidou, E., Filippakopoulou, V., Nakos, B. (2007): Children's Choice of Visual Variables for Thematic Maps. Journal of Geography 106(2), 49–60, https://doi.org/10.1080/00221340601188686.
Nicol, D. J., Macfarlane-Dick, D. (2007): Formative assessment and self-regulated learning: a model and seven principles of good feedback practice. Studies in Higher Education 31(2), 199–218, https://doi.org/10.1080/03075070600572090.
Ooms, K., Maeyer, P. D., Dupont, L., Veken, N. V. D., de Weghe, N. V., Verplaetse, S. (2016): Education in cartography: what is the status of young people's map-reading skills? Cartography and Geographic Information Science 43(2), 134–153, https://doi.org/10.1080/15230406.2015.1021713.
Ormeling, F. J., Rystedt, B. (Eds.) (2014): The World of Maps. International Cartographic Association: Stockholm.
Ottens, H. (2013): Reflections on Geography Education in Europe. Journal of Research and Didactics in Geography 2, 97–100, https://doi.org/10.4458/2379-09.
Rabušic, L., Soukup, P., Mareš, P. (2019): Statistická analýza sociálněvědních dat (prostřednictvím SPSS), 2nd ed.; Masarykova univerzita: Brno, Czechia.
Solórzano, L. S. G., Comíns, J. S., Sendra, J. B. (2017): Atlas Design: A Usability Approach for the Development and Evaluation of Cartographic Products. The Cartographic Journal 54(4), 343–357, https://doi.org/10.1080/00087041.2017.1393189.
Soukup, P., Trahorsch P., Chytrý, V. (2021): Míry věcné významnosti s intervaly spolehlivosti a ukázky jejich využití v pedagogické praxi. Studia paedagogica, 26(3), 131–165, https://doi.org/10.5817/SP2021-3-6.
Stacke, V., Duffek, V., Pluháčková Kuberská, M., Vočadlová, K. Mentlík, P. (2020): Jak na kritická místa ve výuce zeměpisu? Geografická revue 16(1), 4–24, https://doi.org/10.24040/GR.2020.16.1.4-24.
Štuka, Č., Vejražka, M. (2021): Testování a hodnocení studentů na VŠ. Karolinum, Univerzita Karlova: Prague, Czechia, https://doi.org/10.14712/9788024651088.
Taber, K. S. (2017): The Use of Cronbach's Alpha When Developing and Reporting Research Instruments in Science Education. Research in Science Educartion 48, 1273–1296, https://doi.org/10.1007/s11165-016-9602-2.
Trahorsch, P., Bláha, J. D. (2022): The Influence of Textbook Visual Quality of Geographical Phenomena on Children's Conceptions. Journal of Geography 121(3), 100–114, https://doi.org/10.1080/00221341.2022.2088828.
Trahorsch, P., Reich, J. (2023): Problem-solving procedures in spatially explicit tasks: comparing procedures with printed and digital cartographic documents. GeoScape 17(1), 34–46, https://doi.org/10.2478/geosc-2023-0003.
Weeden, P., Simmons, M. (2017): Formative assessment. Chapter of book: Debates in Geography Education, 2nd ed., Routledge: Abingdon-on-Thames, UK.
Wiegand, P. (1993): Children and Primary Geography. Cassell: London, UK.
Wiegand, P. (2006): Learning and Teaching with Maps. Routledge: Abingdon-on-Thames, UK, https://doi.org/10.4324/9780203477793.

Landslide disaster risk perception in times of COVID-19: A student's perspective

Karla María Hernández-Cadena[1], Irasema Alcántara-Ayala[2,*]

[1] National Autonomous University of Mexico (UNAM), Postgraduate Program in Geography, Mexico
[2] National Autonomous University of Mexico (UNAM), Institute of Geography, Mexico
* Corresponding author: ialcantara@geografia.unam.mx

ABSTRACT

This study aimed to understand landslide risk perception among 15 to 20-year-old students in Teziutlán, Puebla, from 2018 to 2022 during the COVID-19 pandemic, a period in which communicating risks and providing information to the public were of utmost significance. The research involved a quantitative approach, using structured questionnaires to measure the level of risk perception within a specific population of young people residing in mountainous regions prone to landslides. A representative sample of 77 students from Antonio de Mendoza High School was interviewed using intentional sampling based on location and age. The study followed a comprehensive, multi-phase approach, which included developing indicators, obtaining informed consent, administering the questionnaire, ensuring voluntary participation, and data analysis. Young individuals interviewed showed a higher level of knowledge about the occurrence of landslides than what previous studies had reported. However, the global crisis resulting from the COVID-19 pandemic overshadowed the dissemination of information about landslides and other hazards.

KEYWORDS

landslides; disaster risk; risk perception; COVID-19; landslide disaster risk reduction

Received: 16 July 2024
Accepted: 11 November 2024
Published online: 21 January 2025

Hernández-Cadena, K. M., Alcántara-Ayala, I. (2024): Landslide disaster risk perception in times of COVID-19: A student's perspective. AUC Geographica 60(1), 75–93
https://doi.org/10.14712/23361980.2025.1

1. Introduction

1.1 The COVID-19 pandemic and its impact on disaster risk perception

The COVID-19 pandemic, which dominated global attention from 2020 to 2022, exposed societal vulnerabilities across multiple sectors, including health, economy, education, and governance. Beyond its immediate health impacts, the pandemic disrupted daily life and altered how individuals and communities perceived various risks, including those unrelated to the virus. This unprecedented crisis highlighted the interconnectedness of global disasters and revealed the cascading impacts across societal systems (Maskrey et al. 2023).

While the pandemic brought attention to global health vulnerabilities, it inadvertently overshadowed the ongoing risks of other hazards. Previous studies showed that during crises, financial and immediate survival concerns often overshadow the perception of other risks, including environmental hazards (Kirsch-Wood et al. 2022). This shift in risk priorities during the pandemic led to a diminished focus on preparedness for other types of hazards, such as landslides, which remain a critical issue in regions like Teziutlán, in the state of Puebla.

1.2 The Mexican experience with COVID-19

In Mexico, the COVID-19 pandemic had a devastating impact, with millions of confirmed cases and hundreds of thousands of deaths. As of March 10, 2023, the pandemic has had a devastating effect on Mexico, with official data reporting over 7,483,444 infections and 333,188 deaths (Johns Hopkins University 2023). However, additional sources claimed a more significant impact. Wang et al. (2022) estimated 798,000 excess deaths in Mexico by December 2021, while 600,590 deaths in excess were estimated by Palacio-Mejía et al. (2022). Both estimates placed it among the seven countries with the highest excess mortality in the world.

The country's healthcare and economic systems struggled under the weight of the crisis, revealing pre-existing inequalities and structural issues (Arellano Morales 2022). The education sector was particularly affected, with many students, especially those from disadvantaged backgrounds, forced to abandon their studies due to a lack of resources and infrastructure for remote learning (OECD 2022; INEGI 2021).

These disruptions to education and daily life had significant consequences for young people, who faced economic and social instability. Still, they were also exposed to new forms of vulnerability, including mental health challenges (Glowacz and Schmits 2020). For communities already at risk of natural hazards, such as landslides, this period further complicated efforts to maintain awareness and preparedness for these threats.

1.3 Landslide risk perception during the COVID-19 pandemic

Despite the global focus on the pandemic, natural hazards posed significant community risks. Landslides, which frequently affect Teziutlán, Puebla, are a persistent threat, particularly during intense rainfall. However, during the COVID-19 pandemic, attention to such hazards diminished as the global health crisis consumed public discourse and governmental resources.

Between 2018 and 2022, Teziutlán experienced several significant landslide events, with notable incidents in 2018, 2020, and 2021 (El Sol de Puebla 2018, 2020; Zepeda 2021). These events caused infrastructure damage and disrupted local communities, including schools and public facilities, which often serve as emergency shelters (Hassan et al. 2020). However, the pandemic made it more challenging to address these events effectively, as disaster response systems were stretched thin, and public attention was diverted.

Understanding how young people perceive landslide risks during such complex crises is essential for designing effective disaster risk reduction strategies. The educational disruptions caused by the pandemic and the overshadowing of local hazards by the global health emergency may have altered students' awareness and preparedness for landslides.

This study explores how young students aged 15 to 20 in Teziutlán, Puebla, perceived the risk of landslides between 2018 and 2022, a period heavily influenced by the COVID-19 pandemic. The goal is to highlight the importance of maintaining disaster risk communication on various hazards, even during global crises, and to identify potential gaps in students' understanding of local environmental risks. This research seeks to contribute to more resilient disaster preparedness frameworks that address health-related and environmental vulnerabilities by analyzing the intersection of pandemic-related disruptions and landslide risk perception.

2. Landslide risk perception

2.1 Risk perception: a brief introduction

Although the Sendai Framework for Disaster Risk Reduction (UNISDR 2015) does not include the concept of risk perception, the Global Assessment Report 2022 (Kirsch-Wood et al. 2022) states that it is essential to evaluate and study it in different social contexts and with different age groups because, in risk situations, risk perception can become a cognitive bias that influences decision-making in the face of disasters.

Risk perception involves various cognitive factors, such as information selection, organization, and

interpretation. It is a measurable concept that can be evaluated psychometrically. Risk perception also involves heuristics and cognitive biases that affect how we think about and understand risk, especially in uncertain situations (Slovic 2016).

As a multifaceted process, risk perception considers individual and collective factors. These aspects work together to understand the danger and give it meaning. According to this approach, risk perception encompasses nine dimensions: whether the risk is voluntary or involuntary, how immediate its effects are, the level of personal and scientific knowledge about the risk, the risk potential, the type of risk (including the level of fear it generates), the perceived severity or potential for disaster, the level of exposure to the risk, and how new or unfamiliar the risk is (Fischhoff et al. 1978).

Risk perception is rooted in the influence of cultural norms, values, and practices on how different social groups perceive risk. Risk perception is shaped by the beliefs and practices established and exemplified by diverse cultural groups during specific historical periods (Douglas and Wildavsky 1983).

How people perceive risks can be influenced by various factors, including the type of information or experiences and the social and cultural context in which they live. Those with firsthand disaster experience tend to have a more nuanced understanding of potential risks. In contrast, those with less experience may rely on sources like the media, social networks, or intuition to form their opinions and judgments (Wachinger et al. 2010).

Studying risk perception can provide insights into how various cultures and groups of people perceive risk and help develop better strategies for managing risk in different situations. Research on disasters has incorporated the concept of risk perception to highlight the gaps in disaster risk management and the limited understanding of these risks among the general public and government officials. This lack of knowledge often leads to inadequate mitigation and prevention measures.

2.2 Landslide risk perception

Mountain regions are vital for sustainable development and climate stability, offering essential resources, biodiversity, and cultural richness. However, they are often exposed to landslide risks, severely affecting local populations (Adler et al. 2022). Reducing landslide risk requires strategies based on the community's perception of these risks (Alcántara-Ayala and Moreno 2016).

Landslide disaster risk awareness, preparedness, and knowledge

Numerous studies have highlighted various factors that influence landslide risk perception. For example, in Bangladesh, Alam (2020) found that communities in landslide-prone areas are often unaware of the risks, which leads to inadequate preparedness and resistance to relocation. Development levels, property ownership, ethnicity, gender, and economic status shape these behaviors. The study underscores the importance of considering livelihood and social dynamics when planning relocation strategies.

In La Paz, Bolivia, residents, local leaders, and planners often underestimate or deny the risk of landslides, complicating efforts to implement prevention strategies. Nathan (2008) pointed out that risk perceptions are multifaceted and cannot be addressed through a singular approach, illustrating the complexity of community attitudes toward landslide threats.

Chinese farmers, for example, are vulnerable to landslides due to limited disaster preparedness and a lack of access to information. Gao et al. (2020) emphasized that these farmers need training in terrace restoration and conservation, which is essential for building long-term resilience and fostering trust in local authorities. Similar dynamics are found in other rural areas worldwide, where access to education and resources is critical in shaping risk perception.

Education also plays a critical role in landslide risk perception. In Pakistan's Murree area, Qasim et al. (2018) found that residents' awareness of landslide risks is closely tied to their social and economic conditions and past experiences. The study identified education as a key factor influencing household preparedness and attitudes toward risk.

In contrast, residents in Frosinone, Italy, despite being aware of landslide risks, do not view them as a significant threat. Gravina et al. (2017) highlighted a critical gap in preparedness, driven by a lack of knowledge about prevention and protection measures, reflecting a common issue where perceived risks do not translate into actionable preparedness.

In Malaysia, public concern is higher for technological hazards than natural disasters, though floods and landslides are frequent concerns. Sim et al. (2023) observed that socioeconomic factors like gender, education, and occupation influence risk perception, particularly regarding landslides. While floods are considered more widespread, landslides tend to be perceived as localized, affecting how people assess their risk.

Landslide disaster risk communication

Effective communication is essential to ensure public safety from landslide risks (Alcántara-Ayala and Moreno 2016). Examining landslide risk perception can help develop strategies to convey information about hazards and risks to the public clearly and comprehensively. Clear and accurate communication can motivate people to take preventive measures. People's perception of risk directly influences their behavior. Gaining insights into how individuals are likely to respond to warnings, evacuation orders, or other risk mitigation measures can help tailor educational

programs and outreach efforts, ultimately minimizing the impact of potential landslides.

Also, in Italy, Calvello et al. (2016) stated that Sarno residents are not aware of the risks of landslides despite recently experiencing a landslide disaster. Better communication strategies are needed to improve their knowledge of measures to minimize regional landslide risk.

Yik et al. (2023) conducted a study to understand the public's knowledge of landslides and their perception of the Landslip Early Warning System (LEWS). They also explored the usefulness of the multi-tiered LEWS concept. Accordingly, only 37% of the participants linked landslides to global warming. Most believed slope safety improved (88%), and landslides were rare (91%). 90% knew about LEWS, but only 28% were concerned as it did not affect them. The idea of a multi-tiered LEWS was well-received, but the study suggested that more research is needed to ensure public awareness about landslides improves.

Understanding how communities perceive the risks of landslides is crucial in making informed decisions on urban planning and land use management. Proper planning can minimize the impact of landslides. Early warning systems aligned with people' s perceptions can aid in timely responses. The study of landslide risk perception can help develop strategies to enhance community resilience. Insights from these studies can shape land use, building standards, and emergency management policies to reduce vulnerability and exposure to landslide events.

Landslide disaster risk governance

A study by Finlay and Fell (1997) found that people in Australia and Hong Kong underestimate the impact of landslides. They support regulating development on landslide-vulnerable land and believe that experts and the government should set acceptable standards for landslide risk. Vulnerable groups are anxious about landslides, which are seen as uncontrollable and deadly.

Landslide-related disasters expose the inadequacy of disaster risk reduction policies in many countries. A recent study by Barreto de Mendonca and Gullo (2020) found that effective communication between government agencies and local residents in Brazil is crucial. Residents often assess the risk of landslides alongside other hazards and opportunities and tend to underestimate their ability to mitigate landslide risks.

Landslides in southeast Bangladesh have caused over 700 deaths since 2000, with informal settlements being the most affected. Despite government claims to implement risk reduction, the number of deaths is increasing due to political-economic factors such as land management, illegal deforestation, and unplanned development activities. A study was conducted by Alam and Islam (2023) to identify shortcomings in early warning systems and suggest ways to improve evacuation procedures, rescue operations, relief efforts, and risk reduction strategies. The findings culminated in recommendations for effectively implementing landslide risk reduction measures in the country.

3. Methodology

3.1 Methodological approach

This study employed a quantitative approach, using structured Likert-type questionnaires with dichotomous and open-ended questions to measure and assess landslide risk perception among young students. The focus on this demographic stemmed from their vulnerability to disaster events due to their developmental stage and potential lack of experience, as well as their critical role as future leaders and community members who can champion disaster risk reduction efforts. Several key factors guided the decision to survey students aged 15 to 21:

1. Youth as a Target Population: This age group is significant due to its high capacity for learning and adaptation, particularly regarding environmental and risk-related education. Furthermore, as students in this region have lived through multiple landslide events during their lifetime, they are likely to have formed perceptions of risk. Specific recall questions were designed to assess whether they had clear memories of significant regional landslide events. This ensured that their responses reflected either direct experience or knowledge gained through their community, school, or media.

2. Access and Representativeness: The Antonio de Mendoza High School was chosen because it is located in a landslide-prone area (Murillo-García and Alcántara-Ayala 2017), making its students an ideal population for this research. Although convenience sampling was employed due to the school's proximity to landslide-prone zones, selecting participants was intentional (Fig. 1). It aimed to ensure that the respondents had experiential exposure to landslides and ongoing educational engagement. This dual criterion maximizes the relevance of their risk perception in the study context.

3. Previous Knowledge and Recall of Events: Special attention was given to whether the respondents could recall past landslides. This was tested through specific questions to evaluate their direct or indirect exposure to landslide events. These questions assessed their ability to describe particular incidents or express knowledge acquired through various sources, ensuring that their responses were grounded in tangible experiences.

77 students were surveyed in June 2023, and the process was carried out in several phases. First, indicators were prepared based on previously validated landslide risk factors, as outlined in comparable studies (Hernández-Moreno and Alcántara-Ayala 2017).

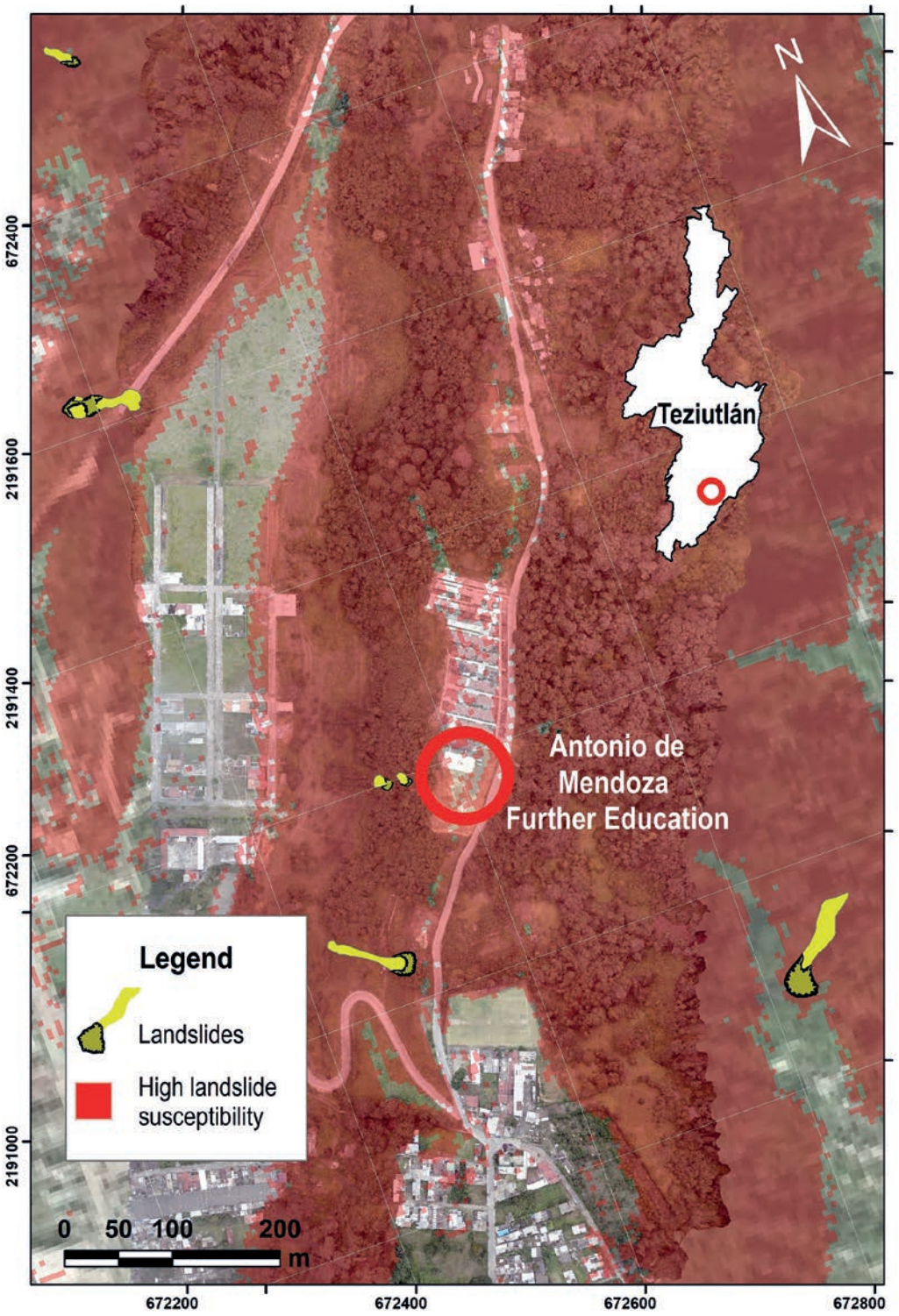

Fig 1. Landslide context in which Antonio de Mendoza High School is located.

Second, the study's objectives were communicated to the students, and informed consent was obtained from all participants to ensure ethical research standards were met. Third, the questionnaires were administered in person at Antonio de Mendoza High School, providing an opportunity for direct engagement with the students (Fig. 2) (Table 1). Fourth, participation was voluntary, and no incentives were offered, ensuring the responses remained unbiased. Finally, the collected data was analyzed using SPSS 21 statistical software. This allowed for both descriptive statistics and analyses, such as cross-tabulation, which helped evaluate patterns in risk perception across different age groups and levels of prior experience.

The decision to use SPSS 21 enabled a data analysis, offering significant insights into the relationships between variables such as age, prior knowledge, and

Fig. 2 Application of the questionnaire at the Antonio de Mendoza High School, Teziutlán, Puebla, México.

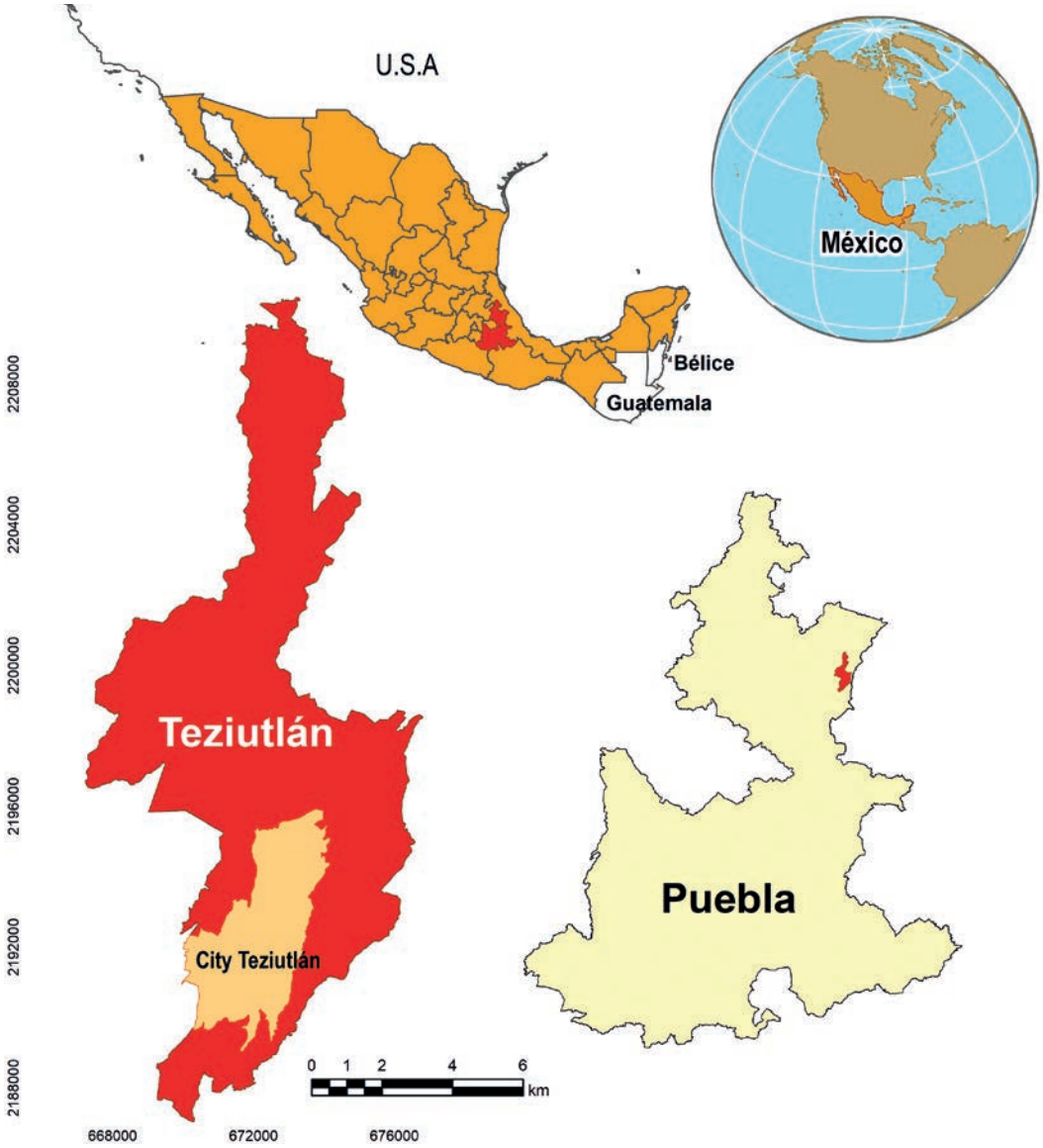

Fig. 3 Location of the study site.

Tab. 1 Description of the parameters included in the surveys.

Sociodemographic data	Age	Open answer
	Occupation (employee or student only)	
	School grade	
	The neighborhood where the interviewee lives	
Knowledge and risk identification	Knowledge about the occurrence of different hazards	Dichotomous scale
	Knowledge about the most frequently occurring hazards	Multiple choice
	Knowledge about the occurrence of a landslide	Dichotomous scale
	Situations that could trigger a landslide	Multiple choice
	Colony that is considered to be of highest risk	Open answer
Disaster Response Preparedness	Information about disaster response preparedness measures before the pandemic	Likert scale
	Information about disaster response preparedness measures during the pandemic	Likert scale
Experience with landslides	Personal experiences with landslides before or during the pandemic	Dichotomous scale and open answer
	Indirect experiences with landslides before or during the pandemic	Dichotomous scale and open answer
COVID-19 experience	Direct or indirect experience with COVID-19 infection	Dichotomous scale and open answer
	Perception of access to medical services	Likert scale
	Perception of the level of contagion by COVID-19 in the area where you live	Likert scale
	Action measures taken during the pandemic	Likert scale
Information and media	Perception of the quality of information received from the authorities through the media about COVID-19	Likert scale
	Perception of the quality of the information received from the authorities through the media about hazards that occurred before and during the pandemic	Likert scale
Landslide Preparedness in Time of COVID-19	Perception of the degree of risk that homes have in the face of landslides	Likert scale
	Perception of the degree of risk that students and others have in the face of landslides	Likert scale
	The frequency with which landslide preparedness actions were undertaken during the pandemic	Likert scale
	Preparedness actions in case landslides occurred during the pandemic	Likert scale
	The frequency with which preparedness actions against COVID-19 were undertaken during the pandemic	Likert scale
Communication of the population with stakeholders	Identifies the authorities responsible for risk management	Dichotomous scale
	Receive information on what to do in case of landslides from the authorities	Dichotomous scale
	Perception of the degree of responsibility of the actions of authorities in case of risk due to landslides	Likert scale
	Perception of the degree of responsibility of the actions of authorities to prevent COVID-19 infections	Likert scale
	Perception of the degree of responsibility of authorities when they responded to a landslide before the pandemic	Likert scale
	Perception of the degree of responsibility of authorities when they responded to a landslide during the pandemic	Likert scale

exposure to educational interventions. Future stages of the study, with a larger sample, will incorporate additional statistical tests to assess whether these factors significantly influence landslide risk perception.

3.2 Study design and area selection

Teziutlán is a municipality in the northeastern Sierra of Puebla, with an altitude range of 1221 m to 2660 m (Fig. 3). The region's climate is warm and temperate, with an average temperature of 15.5°C and precipitation of around 1658 mm (INEGI 2010). The area is part of the Trans-Mexican Volcanic Belt, an east-west-oriented volcanic arc produced by the subduction of the Cocos tectonic plate beneath the North American tectonic plate.

The geology of Teziutlán is directly linked to Los Humeros, a central Mexican caldera volcano and one of the Pleistocene silica centres. The Xaltipan ignimbrite was formed due to the final activity of the first active phase and the Los Humeros caldera subsidence. Most of the ignimbrite deposits found in the study area are non-welded and composed of aphyric high-silica rhyolite material, which can be explicitly identified as ash-pumice flow deposits (Alaniz-Álvarez et al. 1998; Alva-Valdivia et al. 2000; Dávila-Harris

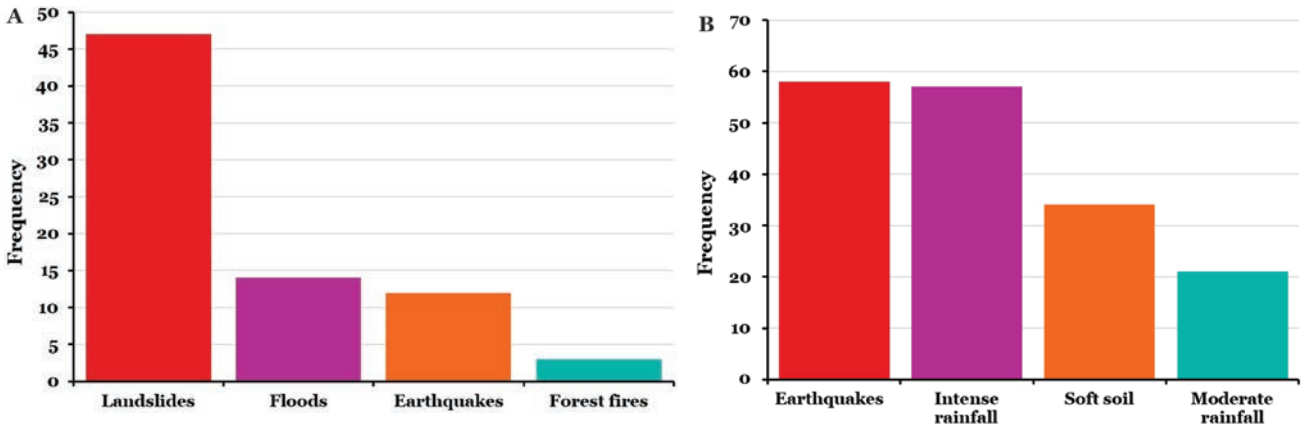

Fig. 4 Knowledge and risk identification: Hazard occurrence (A) and landslide triggering mechanisms knowledge (B).

and Carrasco-Núñez 2014). Residual shallow soils associated with the Xaltipan ignimbrite are formed on steep slopes by decomposing poorly consolidated rock materials with high clay content and high-water retention capacity, leading to mass movement processes (Flores and Alcántara-Ayala 2002).

The municipality is home to a population of 103,583 inhabitants. Of this population, 48,649 are men (47%) and 54,934 are women (53%). It encompasses 34 localities, with five being urban areas. The population can be categorized by age range as follows: 16.8% of the population is between the ages of 0 and 9, 18.2% belong to the age group of 10 to 19 years old, 24.2% are between 20 to 34 years old, 19.5% are aged 35 to 49, and 20.1% of the population is 50 years old or older. As for education, in 2020, 23% of the population had completed primary education, 25.8% had completed secondary education, and 23.2% had finished high school or higher education (INEGI 2020).

The urban locality of Teziutlán presents levels of marginalization from very low to medium, depending on the type of community. As the municipality's social and economic conditions differ, vulnerability and landslide exposure vary (Alcántara-Ayala et al. 2018; González-Sánchez et al. 2017).

Landslides are frequent in Teziutlán due to heavy rainfall. Flows and complex movements are the most common types of landslides. Notable events from 1944, 1955 and 1999 stand out in particular due to their severity and the socio-economic impact they caused. Large landslides occur after one day of cumulative precipitation with over 300 mm of rain, while smaller ones happen during the rainy season (Murillo-García and Alcántara-Ayala 2017).

4. Results

4.1 Sociodemographic data

The samples consisted of 34 males and 43 females. Among the total, 58 (71.6%) were between 15 and 17 years old, while 17 (21%) were 18 to 20. Six interviewees did not provide an answer regarding their age. 31.2% (N = 24) of the students were in 1st grade at the time of the survey, while 29.9% (N = 23) were in 2nd grade and 39% (N = 30) were in 3rd grade. Apart from being students, 25 also reported having a job. According to the updated landslide susceptibility map created by Murillo-García and Alcántara-Ayala (2017), 42 interviewees resided in areas highly prone to landslides, while 28 individuals lived in unsusceptible areas. Seven students did not provide any response regarding their respective areas.

4.2 Knowledge and risk Identification

Out of the entire sample, 83.1% of the respondents stated that they were aware of the potential hazards in their municipality. 94.8% of the respondents knew what a landslide is, and 61% of the participants believed that landslides are the most common hazard in their area. In contrast, floods and earthquakes were considered more frequent hazards by only 18.2% and 15.6% of the respondents, respectively (Fig. 4A).

Likewise, 71.6% of those surveyed believe that earthquakes have the potential to set off landslides, while 70.3% identified heavy rainfall as another contributing factor. Only 25.9% of those surveyed believed moderate rainfall could lead to landslides. Furthermore, 42% of respondents reported that areas with soft or weak soil are more prone to landslides (Fig. 4B).

The participants' perceptions of neighborhood risk show some alignment with the actual hazard profile, though differences are evident. Of the 77 students surveyed, 20 (25.97%) identified La Aurora, the site of a significant 1999 landslide, as the most susceptible neighborhood, while 17 (22.08%) viewed Xoloco as the area most at risk. Eleven students (14.28%) considered La Cantera the most concerning despite its lower historical landslide incidence than La Aurora and Xoloco. In contrast, only four students (5.19%) mentioned Taxcala, and two (2.59%) identified the city center as high-risk zones, with minimal records

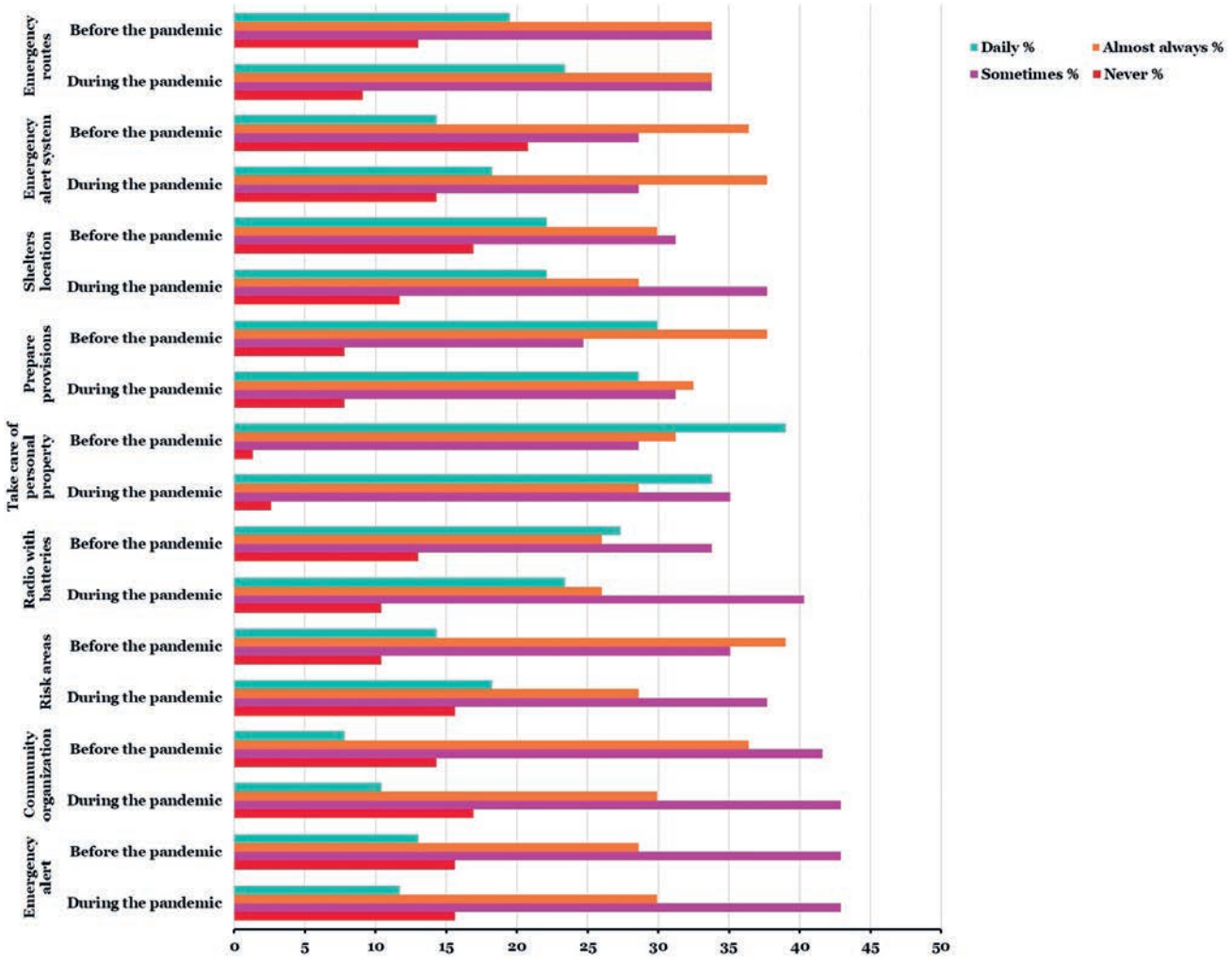

Fig. 5 Information regarding disaster response preparedness before and during the pandemic.

of landslide activity. This indicates that while student perceptions generally align with documented risk areas, some discrepancies likely stem from varying levels of awareness or differing interpretations of risk.

4.3 Disaster response preparedness

Access to information by inhabitants regarding reading or hearing recommendations to respond to disasters associated with any hazard was also heterogeneous. The highest scores, 39% and 34%, corresponded to the interviewees' information on how to take care of their personal property daily before and during the pandemic, respectively. Daily information concerning knowledge of emergency routes increased from 19.5% to 23.4% during the pandemic. Likewise, information about emergency alert systems also increased for the same period from 14.3% to 18.2%.

During the pandemic, the percentage of students who reported sometimes receiving information about the location of shelters increased from 31% to 38%. Perceptions on preparing provisions, the need for radios with batteries, how to organize the community, and emergency alerts remained unchanged. Daily information on areas at risk increased from 14% to 18% during the pandemic (Fig. 5).

The findings derived from a cross-tab analysis of responses concerning the frequency of exposure to emergency preparedness recommendations before the pandemic revealed significant gender disparities and varying levels of awareness among participants. In emergency routes, women reported higher frequencies of daily or almost daily engagement with this information, reflecting a proactive stance toward emergency preparedness. In contrast, a considerable proportion of men indicated that they access such information only occasionally, suggesting a less consistent awareness of emergency protocols. When examining alert systems, men demonstrated a greater tendency for daily engagement, indicative of their familiarity with these mechanisms; however, a notable percentage of women reported never encountering such recommendations, underscoring a potential gap in effective communication tailored to this demographic. Regarding safe places, men again reported more frequent daily engagement, while women exhibited

a more balanced distribution across the response categories, suggesting a nuanced understanding of safety protocols. The data on provisions preparation further accentuates these trends, with women displaying greater preparedness and awareness, particularly in the "daily" and "almost always" categories.

Likewise, the analysis of responses during the pandemic unveiled significant gender differences and varying levels of awareness among participants. Women exhibited higher daily engagement rates with emergency routes, constituting 66.7% of those accessing this information regularly, suggesting a proactive approach to preparedness. Similarly, women reported more significant engagement with alert systems, with 64.3% indicating daily exposure. At the same time, a notable percentage of women also reported never encountering such recommendations, indicating potential gaps in targeted communication strategies. Regarding safe places, men displayed a higher frequency of daily engagement (58.8%), yet many women indicated they had never received information, highlighting the need for improved outreach. The data on provisions preparation further underscores these trends, with 68.2% of women engaging daily compared to their male counterparts, reflecting heightened vigilance during the pandemic.

A comparison of responses regarding exposure to emergency preparedness recommendations before and during the pandemic showed significant shifts in engagement levels and gender dynamics. Overall, while women maintained higher levels of engagement before and during the pandemic, the crisis context amplified their proactive approach to preparedness, underscoring the need for targeted outreach and education to address communication gaps and enhance community preparedness.

4.4 Experience with landslides

Before the COVID-19 pandemic, 32.5% of participants reported having direct experience with landslides, while 22.1% indicated indirect experience. These figures decreased significantly during the pandemic, with only 6.5% reporting direct experience and 5.2% reporting indirect experience. This decline likely reflects reduced exposure and mobility due to pandemic-related restrictions, limiting interactions with landslide-prone areas.

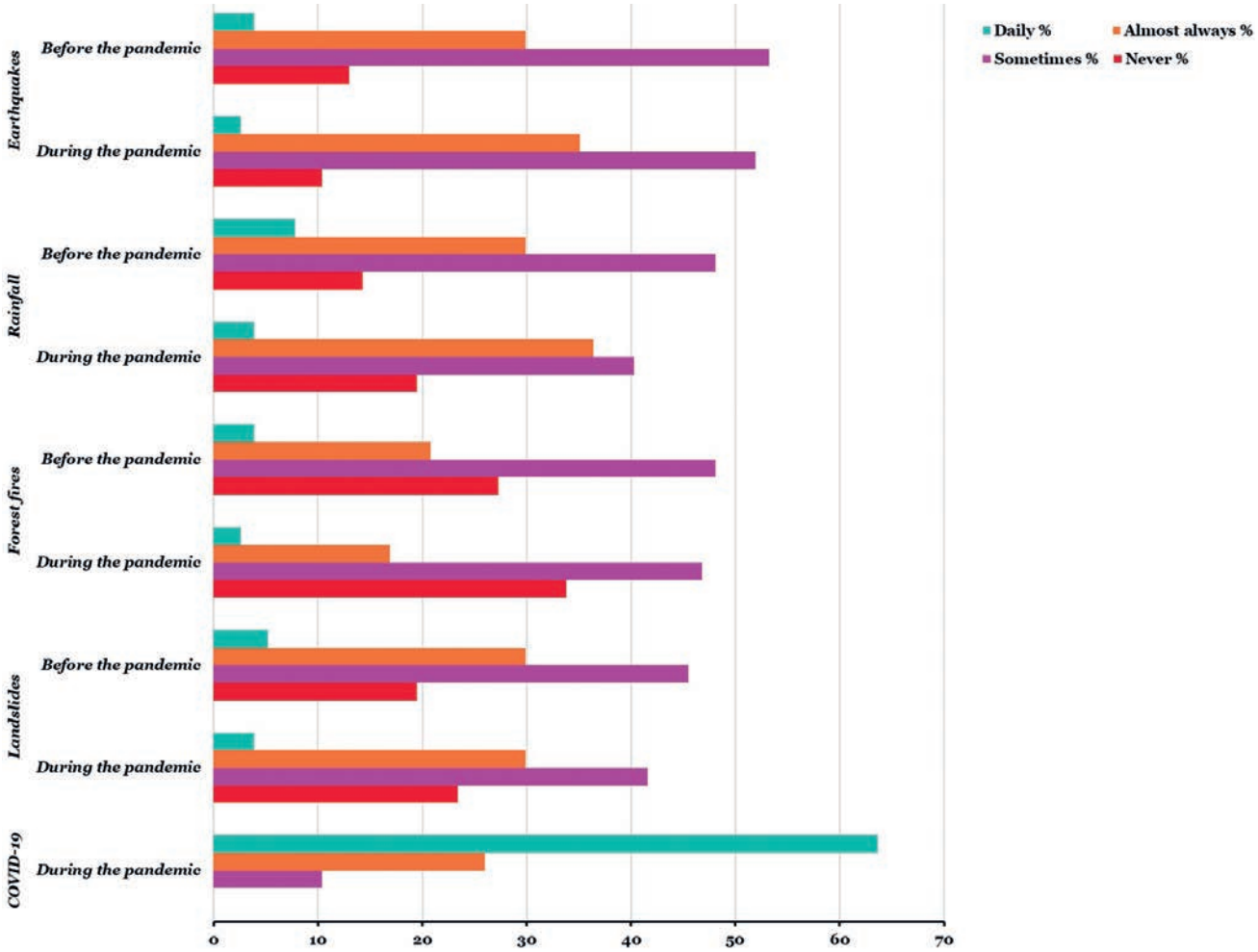

Fig. 6 Perception of the quality of information received from the authorities through the media about hazards that occurred before and during the pandemic.

4.5 COVID-19 experience

It was found that 76.6% of the students who participated knew someone who had contracted COVID-19. Out of the respondents, 61% reported that access to health services was sometimes available, while 35.1% indicated they had permanent access. Only 3.9% of the respondents reported that they had no access to health services at all. Likewise, 76.6% of respondents believed COVID-19 infections were low in their neighborhood. 66.2% reported visiting family sometimes during the pandemic, 31.2% visited friends, 28.6% visited their neighbors, and 32.5% organized parties or gatherings.

During the pandemic, 14.3% of students gave up studying due to various reasons such as job search (2.6%), lack of motivation (3.9%), lack of concentration (2.6%), inaccessibility to the internet (1.3%), inaccessibility to a computer or telephone (3.9%), and little space inside their homes to take online classes (1.3%).

4.6 Information and media

The survey also showed that 19.5% of respondents found the information provided by authorities on what to do in case of COVID-19 infection excellent, 50.6% found it good, and 28.6% regular. Similarly, 22.1% found information on where to go if infected was excellent, 48.1% found it good, 22.1% found it regular, and only 6.5% found it inadequate.

53.2% of respondents indicated that before the pandemic, they sometimes received information on earthquakes from the authorities, while 13% indicated they never received it. Regarding rainfall, 48.1% sometimes got the information, while 14.3% never received it. Similar numbers were reported for forest fires, with 48.1% and 27.3%. In terms of landslides, 45.5% of respondents indicated they sometimes received information, 27.3% never, and 20.8% reported almost always receiving information (Fig. 6).

Participants received inconsistent information involving preventive measures for different hazards during the pandemic. Concerning COVID-19, 63.6% of respondents received daily updates, 26% received them almost constantly, and 10.4% received them sometimes. In the case of earthquakes, only 2.6% received daily information, 35.1% almost always, 51.9% sometimes, and 10.4% never received any information. For rainfall, 3.9% received daily updates, 36.4% almost always, 40.3% sometimes, and 19.5% never received any information. Regarding forest fires, 2.6%, 16.9%, 46.8%, and 33.8% of participants reported receiving updates, respectively. Lastly, for landslides, 3.9% received daily information, 29.9% almost always, 41.6% sometimes, and 23.4% never received any information (Fig. 6).

The cross-tab analysis showed significant gender disparities in awareness and engagement with preventive measures before the pandemic. For earthquakes, while 29.9% of participants reported accessing information "almost always," a higher proportion of women (65.2%) engaged consistently compared to men (34.8%). This trend is further evidenced by the fact that women comprised 90% of those who reported never receiving information. In the context of rainfall, women exclusively reported daily access to preventive measures, indicating a notable gap in information access for men, who predominantly indicated "almost always" (47.8%) and "sometimes" (51.4%). Similar patterns emerged for fires, with women accounting for all daily information recipients and men reporting higher engagement in the "almost always" and "sometimes" categories. Regarding landslides, women again exhibited greater daily engagement (100%), while a significant proportion of men reported never receiving information (40%).

Moreover, the same analysis during the pandemic revealed significant gender differences in engagement with various safety protocols. For COVID-19, most respondents indicated daily access to information, with women constituting 63.3% of this group compared to 36.7% of men. While 55% of men reported receiving information "almost always," women's engagement in this category was lower at 45%. In the context of earthquakes, most participants indicated they received information "almost always," with 59.3% of women compared to 40.7% of men; however, daily access was minimal, with only women reporting such access. In terms of rainfall prevention, women exclusively reported daily access to information. Fire prevention responses were more balanced, yet a significant percentage of women reported never receiving information (65.4%). For landslide prevention, women represented 66.7% of those receiving daily information, further indicating their engagement in safety measures.

The comparison of responses on receiving information about preventive measures before and during the pandemic revealed changes in gender engagement and awareness. The findings showed that even though the pandemic increased awareness and access to important safety protocols, there are still disparities in how information is shared, especially among men in certain situations. This highlights the urgent need for communication strategies that are inclusive and ensure that everyone, regardless of gender, has equal access to information. This will help improve preparedness and response to different emergencies.

4.7 Landslide preparedness in time of COVID-19

The survey results revealed that respondents generally had good knowledge about the risk of homes being affected by landslides. According to the survey, 35% and 38% of respondents considered areas located in downtown Teziutlán to be very low and low risk, respectively. Houses built with sun-dried bricks or

Tab. 2 Perception of the degree of risk homes have of being affected by landslides.

Homes	Perceived risk of homes being affected by landslides			
	Very low risk (%)	Low risk (%)	Moderate risk (%)	High risk (%)
They are located in downtown Teziutlán	35.1 (N = 27)	37.7 (N = 29)	19.5 (N = 15)	7.8 (N = 6)
They are built with sun-dried bricks or sheet materials	9.1 (N = 7)	28.6 (N = 22)	48.1 (N = 37)	14.3 (N = 11)
They are near the river	10.4 (N = 8)	6.5 (N = 5)	32.5 (N = 25)	49.4 (N = 38)
They are built by the government	6.5 (N = 5)	39.0 (N = 30)	44.2 (N = 34)	10.4 (N = 8)
They are at the foot of the slope	5.2 (N = 4)	13.0 (N = 10)	28.6 (N = 22)	53.2 (N = 41)
They are located in areas where landslides have already occurred	10.4 (N = 8)	3.9 (N = 3)	23.4 (N = 18)	58.4 (N = 45)
They are relocated	6.5 (N = 5)	44.2 (N = 34)	39.0 (N = 30)	7.8 (N = 6)
They are next to roads	10.4 (N = 8)	42.9 (N = 33)	35.1 (N = 27)	10.4 (N = 8)
They are on the edge of slopes	6.5 (N = 5)	11.7 (N = 9)	32.5 (N = 25)	48.1 (N = 37)
They are reinforced with columns, walls	9.1 (N = 7)	41.6 (N = 32)	36.4 (N = 28)	10.4 (N = 8)
They are at the top of the slope	3.9 (N = 3)	7.8 (N = 6)	36.4 (N = 28)	49.4 (N = 38)
Trees surround them	7.8 (N = 6)	20.8 (N = 16)	45.5 (N = 35)	24.7 (N = 19)

sheet materials were perceived as a moderate risk by 48% of the interviewees. In comparison, those near the river were considered moderate and high risk by 32% and 49%, respectively, while those at the foot of the slope were perceived as moderate and high risk by 29% and 53% of the students. Additionally, 44% believed that the risk of government-built houses was moderate. Relocated houses were perceived as low and moderate risk by 44% and 39%, respectively, while those in areas that have already experienced landslides were considered moderate (23%) and high (58%). Housing on the edge and at the top of the slopes was conceived of as high risk by 48% and 49%, respectively. Interestingly, houses located next to roads were perceived as low risk by 43%, while those surrounded by trees were considered moderate (45%) and high risk (25%) (Table 2).

Based on the interviewees' responses, individuals residing in Puebla (57%) and Teziutlán (54%) are considered at moderate risk during a landslide. Similarly, residents of other neighborhoods (56%) are also perceived to face moderate risk. In contrast, participants rated the risk to themselves (27.3%) and their families (19.5%) as very low (Fig. 7).

During the pandemic, students infrequently engaged in landslide preparedness actions. Nevertheless, some reported occasionally noticing signs indicative of potential landslide risks, such as cracks in the ground (52%), leaning poles and trees (52%), and evidence of prior landslides (52%). They also paid attention to the accumulation of rainwater (48%), signs of humidity (37%), and improperly closing doors and windows (34%). More than 50% of respondents indicated that they had never observed the river rising (Fig. 8).

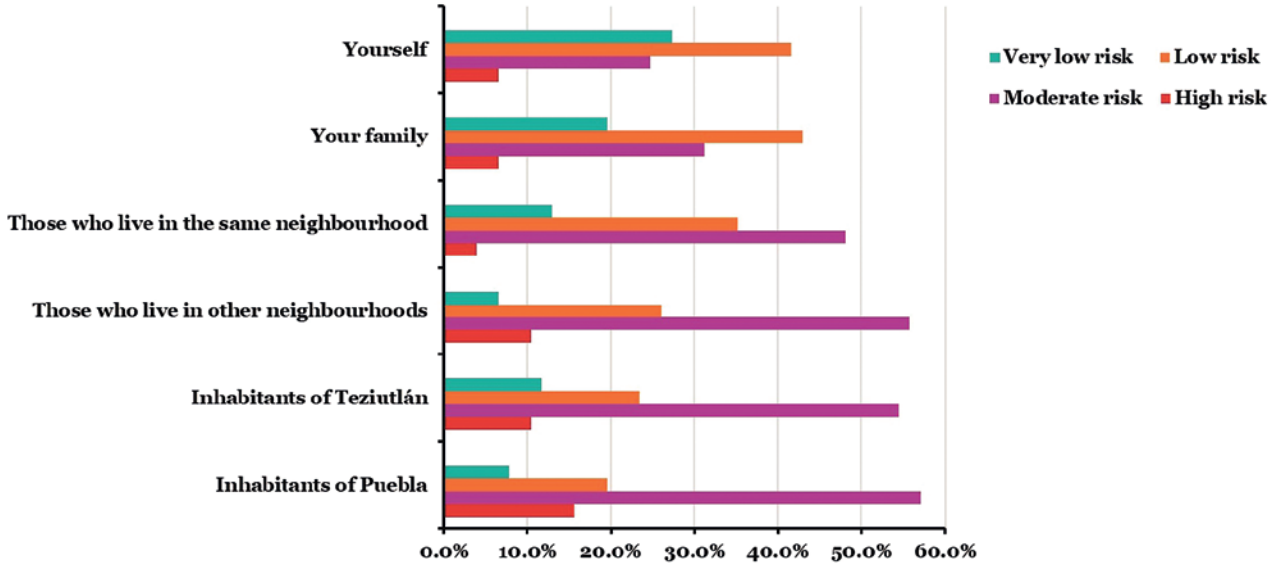

Fig. 7 Perception of the degree of risk students and others have in the face of landslides.

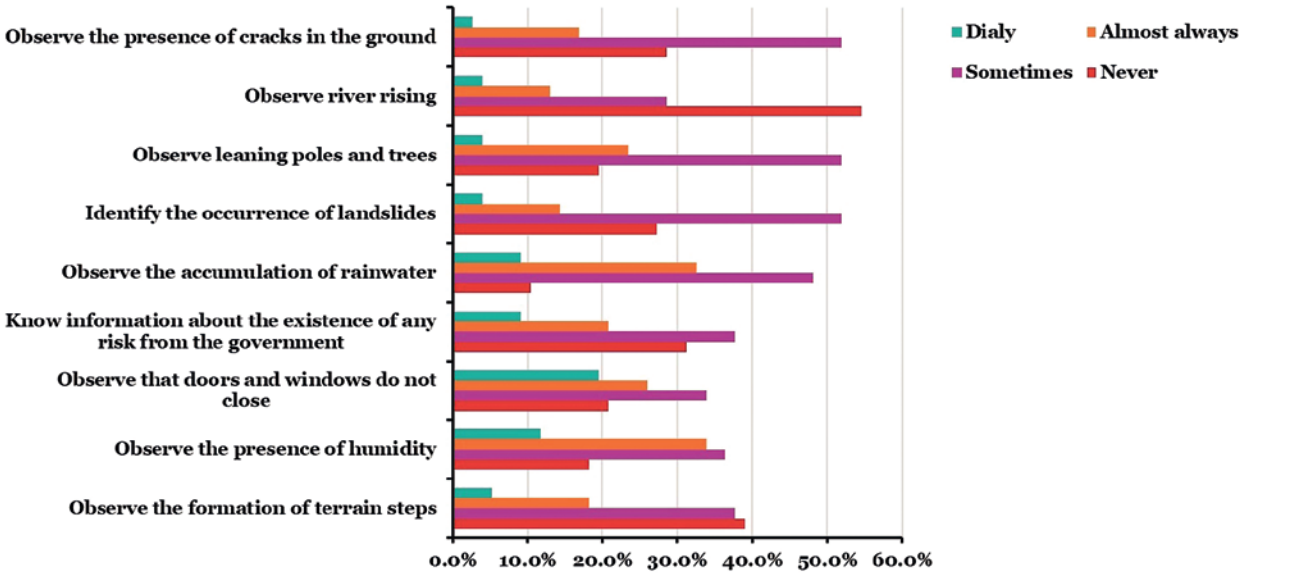

Fig. 8 Frequency with which landslide preparedness actions were undertaken during the pandemic.

Regarding preparedness actions for potential landslides during the pandemic, students agreed on several key areas: 61% reported knowing how to protect themselves. In comparison, 67% felt confident in their ability to ensure their safety. Additionally, 51% acknowledged the importance of preparedness prior to an emergency, 64% recognized the need to maintain their homes in good condition, and 44% were aware of the locations of safe places (Fig. 9).

The study unveiled that 71% of the interviewees reported washing their hands daily, while 64% consistently wore face masks in public settings. When authorities mandated stay-at-home orders, 44% of respondents adhered to this directive. Additionally, 56% indicated that they remained at home if they exhibited symptoms of COVID-19. Notably, 42% of those who experienced symptoms did not seek medical attention at a hospital (Fig. 10).

4.8 Communication of the population with stakeholders

It was found that 70.1% of those interviewed were familiar with the civil protection personnel of their municipality or neighborhood. Additionally, 49.4% of respondents had received information from civil protection authorities or the municipality on identifying symptoms before a landslide. Furthermore, 54.5% had received information from these authorities on what to do during a landslide.

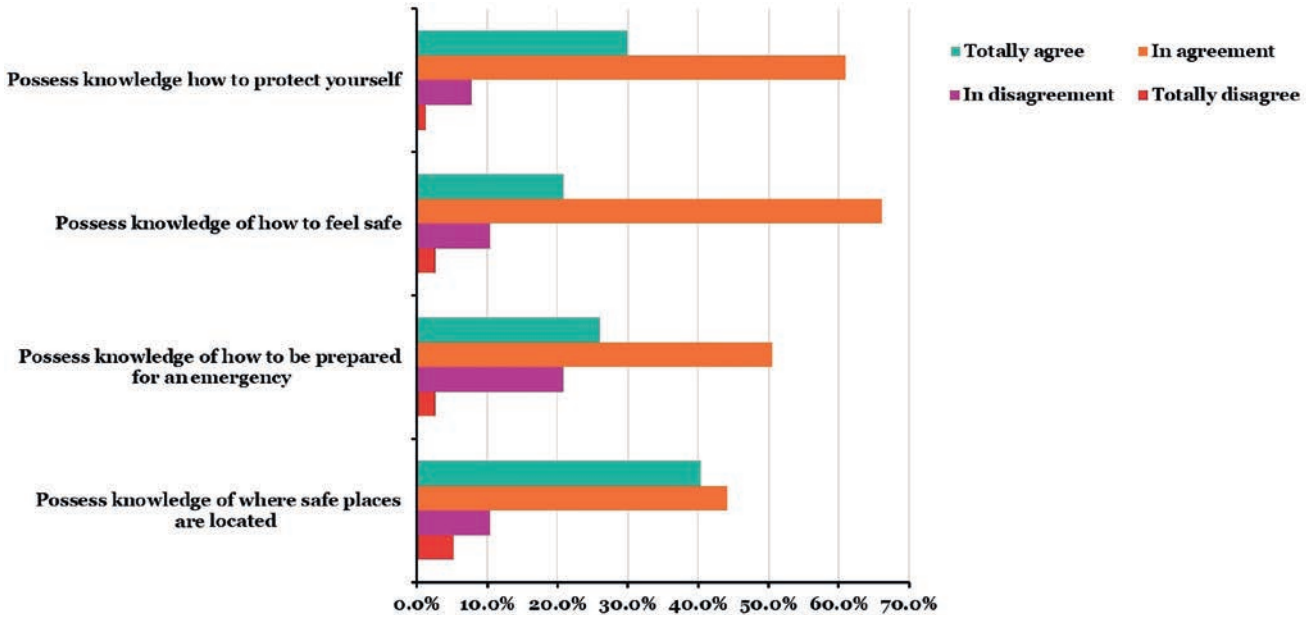

Fig. 9 Preparedness actions in case landslides occurred during the pandemic.

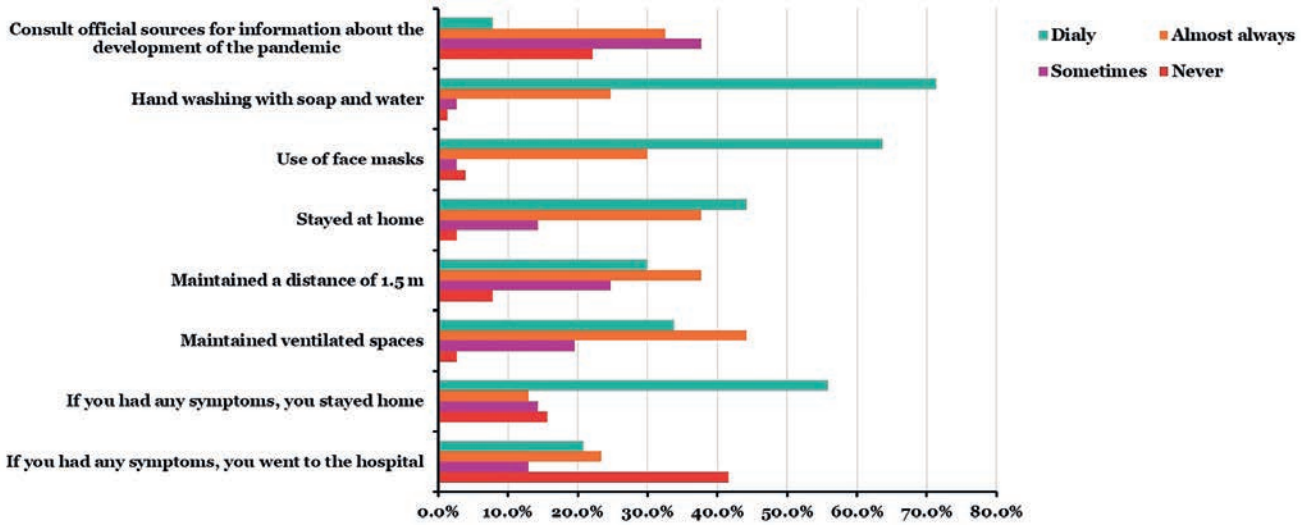

Fig. 10 Frequency with which preparedness actions against COVID-19 were undertaken.

When experiencing the appearance of cracks, floods, or rivers rising near the area in which they live, 58.4% of those surveyed go to the civil protection unit, while 24.7% contact the municipal government.

Perception of the degree of responsibility of diverse actors in the event of a landslide was also evaluated. Before the pandemic, civil protection and the Red Cross were considered very good by 23% and 21% of the respondents, respectively. During the pandemic, municipal government and health personnel were considered good by 52% and 48%, respectively. They were followed by civil protection, the Red Cross, the Mexican army (47%), scientists (42%), and the community (40%). Mexico Lions Club was the worst evaluated, as 30% and 34% of the interviewees considered their performance bad before and during the pandemic (Fig. 11).

Before the pandemic, the cross-tab analysis revealed notable gender differences in perceived responsibility among students regarding various management actors' responses during or after a landslide. Women generally viewed the response of the municipal government, civil protection, local police, health personnel, and the Red Cross more positively than men. For instance, women were more likely to rate the performance of the municipal government, civil protection, and local police as "very good." At the same time, men tended to assess these actors' responses as "acceptable" or "bad." The same trend is seen with health personnel and the Red Cross, where women overwhelmingly viewed their efforts as "very good," and men were more represented in the lower categories, particularly "acceptable."

Similarly, in the context of the pandemic, the same analysis showed a generally positive sentiment towards their responses. Notably, the Municipal Government and Civil Protection received high ratings, with most respondents indicating "very good" or "good" evaluations. The data suggests that women tended to rate these entities more favorably than men, highlighting a possible greater trust or reliance on these institutions during crises. Similarly, the Local Police, Health Personnel, and the Red Cross also garnered pżredominantly positive assessments. However, there were noteworthy discrepancies, particularly with Health Personnel receiving a significant portion of "very good" ratings predominantly from female respondents.

The analysis of perceptions concerning the responses of different management personnel during and after landslides indicated a consistent impact of gender in both pre-pandemic and pandemic scenarios. These findings suggest that positive sentiments towards management actors have remained stable across both periods. However, the pandemic has amplified recognition of their essential roles in crisis management, particularly among female respondents. This underscores the importance of considering gender dynamics in evaluating disaster response effectiveness and suggests implications for enhancing disaster management strategies to meet the needs of diverse populations better.

5. Discussion

Perceived risk significantly influences protective actions in response to disaster warnings. Effective warning systems rely on the quality and quantity of information provided, directly and indirectly influencing risk perception. Understanding disaster risk before a hazard event enhances community response to warnings, and demographic factors—such as age, gender, and ethnicity—can also affect perceptions (Mileti and O'Brien 1992).

In Teziutlán, previous research analyzed landslide risk perception through experience, awareness,

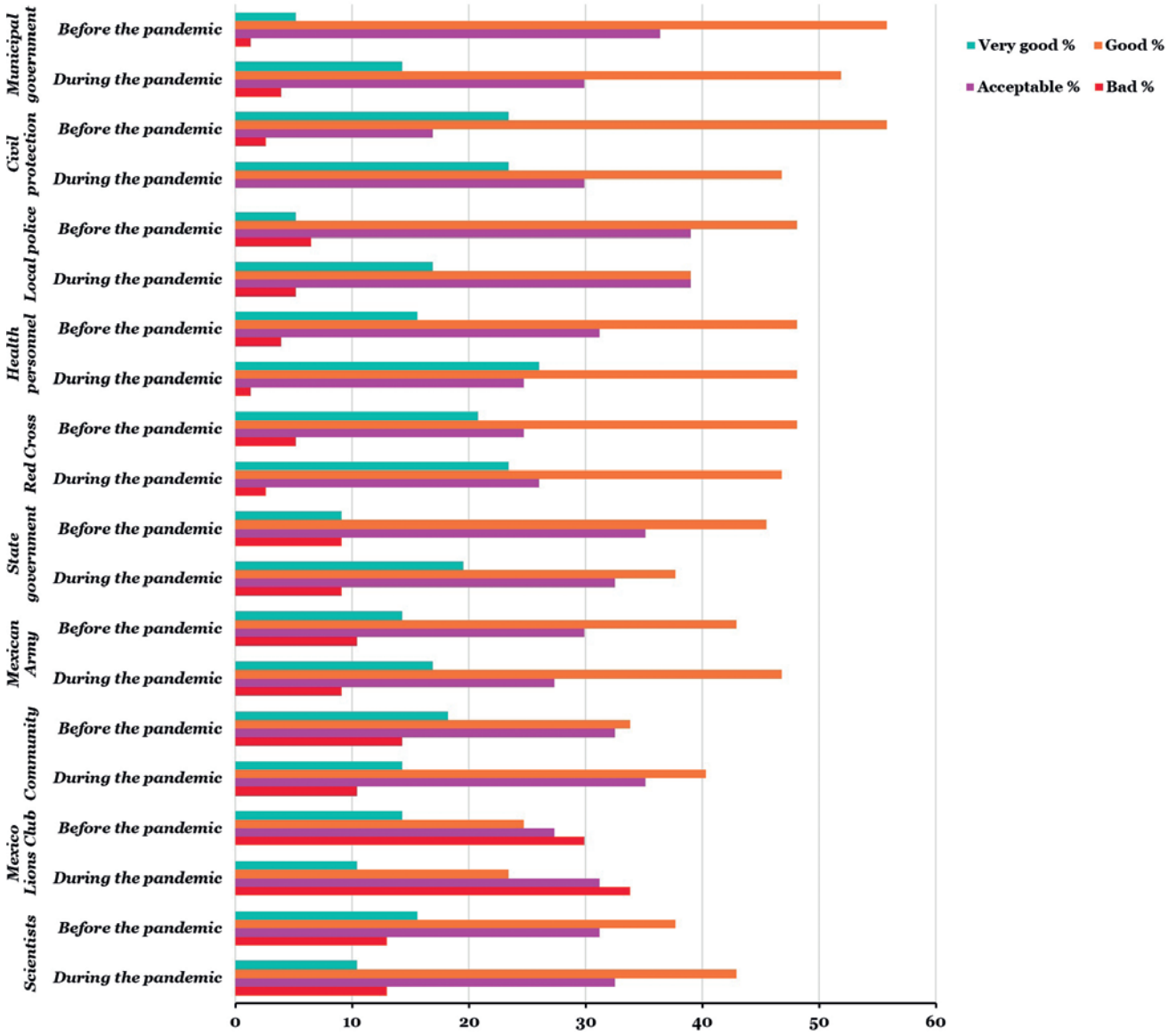

Fig. 11 Perception of the degree of responsibility of diverse actors in a landslide event.

exposure, preparedness, communication, and trust. Findings indicated that not all community members had direct experiences with landslides, and there was a notable lack of information on management strategies, revealing gaps in institutional coordination (Alcántara-Ayala and Moreno 2016).

Residents who experienced landslides exhibited heightened awareness of potential risks, often accepting higher levels of risk due to perceived benefits, such as better access to resources (Landeros-Mugica et al. 2016). Furthermore, while community members recognized landslide risks, they deemed homes in the city center as safer, emphasizing a need for initiatives focused on disaster risk reduction (Hernández-Moreno and Alcántara-Ayala 2017).

Soft soils are a critical precondition for landslides, significantly influencing their occurrence and severity. In the study area, the prevalence of soft soils creates conditions conducive to slope failure, particularly when combined with additional factors such as rainfall and seismic activity. Furthermore, anthropogenic activities, including deforestation, urban development, and land-use changes, can influence landslides. These human interventions often destabilize slopes, exacerbating the susceptibility to landslides. By recognizing the interplay between soft soil conditions and human activities, a more comprehensive understanding of landslide risk can be achieved, underscoring the need for targeted disaster risk reduction strategies.

During the COVID-19 pandemic, disasters continued, as evidenced by severe flooding in September 2021 (Castañeda-Ovando et al. 2022). Valverde and Valverde (2022) noted that COVID-19 outcomes in Puebla were linked to factors like marginalization and social resilience.

This research aimed to assess landslide risk perception among young people in Teziutlán before and during the COVID-19 pandemic, a demographic notably affected during the health crisis. Understanding how these experiences shape perceptions is essential for updating risk reduction strategies.

Young individuals today have greater access to information about potential hazards, yet community engagement in preparedness remains critical. Findings showed that Antonio de Mendoza High School students recognized landslides as common hazards. They received more information about COVID-19 prevention measures (63.6%) than other risks, underscoring the need for broader educational initiatives.

Awareness of emergency routes increased from 19.5% before the pandemic to 23.4% during it, alongside rising awareness of community disaster organization efforts and evacuation risk areas. Students perceived the authorities' responses positively, noting improvements in the perceived effectiveness of municipal and state governments and local organizations during the pandemic.

Examining landslide risk perception in the context of COVID-19 highlights the intersection of disaster management and public health. This research contributes to understanding how these domains inform one another, revealing the complex relationships between societal responses and environmental hazards.

Given the pandemic's effects on daily life, social interactions, and information access, people's attitudes towards natural hazards may experience notable changes. Risk perception studies can examine these shifts to reveal the interplay between psychological influences, societal responses, and environmental hazards, providing valuable insights into risk perception dynamics, disaster preparedness, and resilience strategies.

6. Concluding remarks

The COVID-19 pandemic underscored the urgent need for clear risk communication, yet its global scale overshadowed the communication of risks related to hazards like earthquakes, floods, and landslides. In Teziutlán, Puebla, as in many places, the pandemic diluted focus on disaster risk management, particularly concerning these hazards. This research highlights the importance of investigating how young people perceive such risks during the pandemic, as this insight is vital for developing disaster risk reduction strategies.

This study found that despite young people in Teziutlán showing greater awareness of landslide risks than reported in previous studies, information about these hazards was often minimized by the pandemic. The research highlights that disaster risk management remains overly reactive, focusing on emergency response rather than prospective risk mitigation and public awareness of preventive measures. Better communication and trust between authorities and the community is crucial, as this bond forms the foundation for effective disaster risk management strategies and emergency responses.

Effective risk communication is pivotal in shaping public perception and decision-making regarding landslides. However, young individuals often rely on intuition and cognitive shortcuts, leading to poor decision-making (Kirsch-Wood et al. 2022; Gravina et al. 2017). Addressing this through improved communication offers an opportunity to enhance disaster resilience at the community level.

The analysis found gender differences in engagement with emergency preparedness. Women show higher awareness and involvement than men, emphasizing the need for tailored communication strategies to improve overall community preparedness. By recognizing these gender-based engagement patterns, stakeholders can develop more effective outreach initiatives. Furthermore, the pandemic has raised awareness of emergency protocols, but there are still gaps in information, especially among men. Inclusive outreach programs are needed to ensure equal access to crucial emergency information for all genders, improving preparedness and response effectiveness in crisis situations.

This study has several limitations. The focus on young students in Teziutlán, Puebla, from 2018 to 2022 limits the generalizability of the findings, as the sample may not represent broader populations. The reliance on self-reported data introduces potential biases, including recall bias, which may affect the accuracy of participants' recollections. The broad focus on multiple hazards could also dilute specific insights into landslide risk.

Additionally, the research provides a snapshot of perceptions during the pandemic without tracking changes over time. These elements limit understanding of how perceptions evolve, particularly about preparedness actions. Future studies could expand the sample, focus more on specific hazards, and adopt a longitudinal approach for deeper insights.

While this research cannot be generalized, it offers valuable insights into youth perceptions of government responsibility in managing local hazards. This opens pathways for engaging young people in innovative disaster risk reduction strategies. Further interdisciplinary collaboration is essential to developing comprehensive risk management approaches that integrate scientific and local knowledge. Future research should focus on refining these strategies and addressing this study's limitations.

By aligning risk communication with public perceptions, policymakers can enhance the effectiveness of disaster risk management efforts and ensure more resilient communities.

Acknowledgements

We thank DGAPA-UNAM for providing financial support to conduct landslide risk research through Project PAPIIT IN300823. Thanks to the National Council of Humanities, Sciences, and Technologies (CONAHCYT), who provided a student fellowship for Karla María Hernández-Cadena. We would like to express our gratitude to two anonymous reviewers for providing valuable feedback on earlier versions of this paper, which significantly enhanced the article.

References

Adler, C., Wester, P., Bhatt, I., Huggel, C., Insarov, G. E., Morecroft, M. D., Muccione, V., Prakash, A. (2022): Cross-chapter paper 5: Mountains, In: Climate change 2022 – Impacts, adaptation, and vulnerability. Contribution of Working Group II to the Sixth Assessment Report of the Intergovernmental Panel on Climate Change. Cambridge University Press, 2273–2318, https://doi.org/10.1017/9781009325844.022.

ADN 40 (2020): Desalojan viviendas en Álvaro Obregón por riesgo de derrumbe. Available online: https://www.adn40.mx/noticia/ciudad/notas/2020-06-12-13-46/desalojan-viviendas-en-alvaro-obregon-por-riesgo-de-derrumbe (In Spanish Accessed on 29 January 2024).

Alam, E. (2020): Landslide hazard knowledge, risk perception and preparedness in Southeast Bangladesh. Sustainability 12 (16): 6305, https://doi.org/10.3390/su12166305.

Alam, E., Ray-Bennett, N. S. (2021): Disaster risk governance for district-level landslide risk management in Bangladesh. International Journal of Disaster Risk Reduction 59: 102220, https://doi.org/10.1016/j.ijdrr.2021.102220.

Alam, E., Islam, M. K. (2023): Enhancing landslide risk reduction strategies in Southeast Bangladesh. Jàmbá: Journal of Disaster Risk Studies 15(1), 1–12, https://doi.org/10.4102/jamba.v15i1.1541.

Alaniz-Álvarez, S., Nieto-Samaniego, Á. F., Ferrari, L. (1998): Effect of strain rate in the distribution of monogenetic and polygenetic volcanism in the Transmexican volcanic belt. Geology 26(7), 591–594, https://doi.org/10.1130/0091-7613(1999)027<0571:EOSRIT>2.3.CO;2.

Alcántara-Ayala, I., Moreno, A.R. (2016): Landslide risk perception and communication for disaster risk management in mountain areas of developing countries: a Mexican foretaste. Journal of Mountain Science 13, 2079–2093. https://link.springer.com/article/10.1007/s11629-015-3823-0.

Alcántara-Ayala, I., Garnica-Peña, R. J., Murillo-García, F. G., Salazar-Oropeza, M. O., Méndez-Martínez, A., Coll-Hurtado, A. (2018): Landslide disaster risk awareness in México: community access to mapping at local scale. Landslides 15, 1–14, https://doi.org/10.1007/s10346-018-1010-4.

Alcántara-Ayala, I., Burton, I., Lavell, A., Mansilla, E., Maskrey, A., Oliver-Smith, A., Ramírez-Gómez, F. (2021): Root causes and policy dilemmas of the COVID-19 pandemic global disaster. International Journal of Disaster Risk Reduction 52: 101892), https://doi.org/10.1016/j.ijdrr.2020.101892.

Arellano, M. A. (2022): Consecuencias de la covid-19 en la economía y las finanzas públicas en México: más allá de la pandemia. El trimestre económico 89(355), 829–864, https://doi.org/10.20430/ete.v89i355.1307. (In Spanish)

Alva-Valdivia, L. M., Goguitchaichvili, A., Ferrari, L., et al. (2000): Paleomagnetic data from the Trans-Mexican Volcanic Belt implications for tectonics and volcanic stratigraphy. Earth, Planets and Space 52, 467–478, https://doi.org/10.1186/BF03351651.

Barreto de Mendonca, M., Gullo, F. T. (2020): Landslide risk perception survey in Angra dos Reis (Rio de Janeiro, southeastern Brazil): A contribution to support planning of non-structural measures. Land Use Policy 91: 104415, https://doi.org/10.1016/j.landusepol.2019.104415.

Castañeda-Ovando, E. P., Mendoza-Tolentino, Y., Añorve-Morga, J., Nieto-Velázquez, S., Castañeda-Ovando, A. (2022): Desbordamiento del Río Tula: más allá de las Lluvias. Pädi Boletín Científico de Ciencias Básicas e Ingenierías del ICBI 10(19), 23–29, https://doi.org/10.29057/icbi.v10i19.8987. (In Spanish)

Calvello, M., Papa, M. N., Pratschke, J., Crescenzo, M. N. (2016): Landslide risk perception: a case study in Southern Italy. Landslides 13, 349–360, https://doi.org/10.1007/s10346-015-0572-7.

Corriero, A. C., Khan, F. M. A., Bassey, E. E., Bouaddi, O., dos Santos Costa, A. C., Outani, O., Hasan, M. M., Ahmad, S., Essar, M. Y. (2022): Floods, landslides and COVID-19 in the Uttarakhand State, India: impact of ongoing crises on public health. Disaster medicine and public health preparedness 16(6), 2279–2282, https://doi.org/10.1017/dmp.2021.373.

Dávila-Harris, P., Carrasco-Núñez, G. (2014): An unusual syn-eruptive bimodal eruption: the Holocene Cuicuiltic Member at Los Humeros caldera, Mexico. Journal of Volcanology and Geothermal Research 271, 24–42, https://doi.org/10.1016/j.jvolgeores.2013.11.020.

Douglas, M., Wildavsky, A. (1983): Risk and culture: An essay on the selection of technological and environmental dangers. Berkeley: University of California Press, https://doi.org/10.1525/9780520907393.

El Sol de Puebla (2018): Deslave obstruye tramo carretero en Xiutetelco y Teziutlán. Available online: https://www.elsoldepuebla.com.mx/local/estado/deslave-obstruye-tramo-carretero-en-xiutetelco-y-teziutlan-puebla-lluvia-sierra-norte-2185084.html (In Spanish. Accessed on 29 January 2024).

El Sol de Puebla (2020): [Fotos] Dejan lluvias por depresión tropical dos deslaves en Teziutlán. Available online: https://www.elsoldepuebla.com.mx/local/estado/fotos-dejan-lluvias-por-depresion-tropical-dos-deslaves-en-teziutlan-5324317.html (In Spanish. Accesed on 29 January 2024).

Esquivel, G. (2020): Los impactos económicos de la pandemia en México. Economía UNAM 17(51), 28–44, https://doi.org/10.22201/fe.24488143e.2020.51.543 (In Spanish).

Finlay, P. J., Fell, R. (1997): Landslides: risk perception and acceptance. Canadian Geotechnical Journal 34(2), 169–188, https://doi.org/10.1139/t96-108.

Fischhoff, B., Slovic, P., Lichtenstein, S., Read, S., Combs, B. (1978): How safe is safe enough? A psychometric study of attitudes towards technological risks and benefits. Policy Sciences 9, 127–152. https://link.springer.com/article/10.1007/BF00143739.

Flores, P., Alcántara-Ayala, I. (2002): Cartografía morfogenética e identificación de procesos de ladera en Teziutlán, Puebla. Investigaciones geográficas 49, 7–26. Available online: https://www.scielo.org.mx/pdf/igeo/n49/n49a2.pdf (In Spanish. Accesed on 29 January 2024).

Gao, X., Roder, G., Jiao, Y., Ding, Y., Liu, Z., Tarolli, P. (2020): Farmers' landslide risk perceptions and willingness for restoration and conservation of world heritage site of Honghe Hani Rice Terraces, China. Landslides 17, 1915–1924, https://doi.org/10.1007/s10346-020-01389-4.

Glowacz, F., Schmits, E. (2020): Psychological distress during the COVID-19 lockdown: The young adults most at risk. Psychiatry Research 293: 113486, https://doi.org/10.1016/j.psychres.2020.113486.

González-Sánchez, J., MacGregor, M. T., Coll-Hurtado, A., et al. (2017): El municipio de Teziutlán (mapas a escala 1:62,000). Factores inductores de la vulnerabilidad. En: Alcántara-Ayala I, et al. (2017) Inestabilidad de Laderas en Teziutlán, Puebla. Factores inductores del riesgo. UNAM: Instituto de Geografía. (In Spanish)

Gravina, T., Figliozzi, E., Mari, N., De Luca Tupputi Schinosa, F. (2017): Landslide risk perception in Frosinone (Lazio, Central Italy). Landslides 14, 1419–1429, https://doi.org/10.1007/s10346-016-0787-2.

Guzmán, O., Santiago, V. (2021): Corriente Alterna UNAM. Tragedia en el cerro del Chiquihuite: La Zona del Derrumbe estaba catalogada como de Muy alto Riesgo. Available online: https://corrientealterna.unam.mx/territorios/cerro-del-chiquihuite-tlalnepantla-derrumbe-falla-geologica-expansion/ (In Spanish. Accessed on 29 January 2024)

Hassan, E. M., Mahmoud, H. N., Ellingwood, B. R. (2020): Resilience of school systems following severe earthquakes. Earth's Future 8(10): e2020EF001518, https://doi.org/10.1029/2020EF001518.

Henríquez, E. (2021): Se desgaja ladera en Unión Juárez, Chiapas: dos atrapados Available online: https://www.jornada.com.mx/notas/2021/09/13/estados/se-desgaja-ladera-en-union-juarez-chiapas-dos-atrapados/ (In Spanish. Accessed on 29 January 2024).

Hernández-Moreno, G., Alcántara-Ayala, I. (2017): Landslide risk perception in Mexico: a research gate into public awareness and knowledge. Landslides 14, 351–371, https://doi.org/10.1007/s10346-016-0683-9.

Ibarra-Nava, I., Cardenas-de la Garza, J. A., Ruiz-Lozano, R. E., Salazar-Montalvo, R. G. (2020): Mexico and the COVID-19 Response. Disaster Medicine and Public Health Preparedness 14(4), e17–e18, https://doi.org/10.1017/dmp.2020.260.

INEGI (2010): Compendio de información geográfica municipal de los Estados Unidos Mexicanos. Teziutlán: Instituto Nacional de Geografía y Estadística. 1–10. Available online: https://www.inegi.org.mx/contenidos/app/mexicocifras/datos_geograficos/21/21174.pdf (In Spanish. Accessed on 29 January 2024).

INEGI (2020): México en cifras. Teziutlán, Puebla. Available online: https://www.inegi.org.mx/app/areasgeograficas/?ag = 070000210174#collapse-Indicadores (In Spanish. Accessed on 29 January 2024).

INEGI (2021): Encuesta para la Medición del Impacto COVID-19 en la Educación (ECOVID-ED) 2020 (Survey for Measuring the Impact of COVID-19 on Education (ECOVID-ED). Available online: https://www.inegi.org.mx/investigacion/ecovided/2020/ (In Spanish. Accessed on 29 January 2024).

Jaziri, R., Miralam, M. S. (2021): The impact of crisis and disasters risk management in COVID-19 times: Insights and lessons learned from Saudi Arabia. Ethics, Medicine and Public Health 18: 100705, https://doi.org/10.1016/j.jemep.2021.100705.

Johns Hopkins University (2023): COVID-19 Case Tracker. Coronavirus Resource Center. Available online: https://coronavirus.jhu.edu/map.html (Accessed on 29 January 2024).

Kawasaki, H., Yamasaki, S., Rahman, M. M., Murata, Y., Iwasa, M., Teramoto, C. (2020): Teachers-parents cooperation in disaster preparation when schools become as evacuation centers. International Journal of Disaster Risk Reduction 44: 101445, https://doi.org/10.1016/j.ijdrr.2019.101445.

Kirsch-Wood, J., Katsanakis, R., Giradet Hieber, L., Kumar, A., Mena, R., Cook, R., et al. (2022): In: Global Assessment Report United Nations Office for Disaster Risk Reduction (UNDRR), Geneva, Switzerland.

Landeros-Mugica, K., Urbina-Soria, J., Alcántara-Ayala, I. (2016): The good, the bad and the ugly: on the interactions among experience, exposure and commitment with reference to landslide risk perception in México. Natural Hazards 80, 1515–1537, https://doi.org/10.1007/s11069-015-2037-7.

Maskrey, A., Jain, G., Lavell, A. (2023): The social construction of systemic risk: towards an actionable framework for risk governance. Disaster Prevention and Management: An International Journal 32(1), 4–26, https://doi.org/10.1108/DPM-07-2022-0155.

Mileti, D. S., O'Brien, P. W. (1992): Warnings during disaster: Normalizing communicated risk. Social problems 39(1), 40–57, https://doi.org/10.1525/sp.1992.39.1.03x0062j.

Murillo-García, F. G., Alcántara-Ayala, I. (2017): Landslide inventory, Teziutlán Municipality, Puebla, México (1942–2015). Journal of Maps 13(2), 767–776, https://doi.org/10.1080/17445647.2017.1381194.

Nandi, S. (2022): Chapter Fourteen: Disaster risk management during COVID-19 pandemic. In COVID-19 and the Sustainable Development Goals. Elsevier-PMC COVID19 Collection. 325–348, https://doi.org/10.1016/B978-0-323-91307-2.00013-4.

Nathan, F. (2008): Risk perception, risk management and vulnerability to landslides in the hill slopes in the city of La Paz, Bolivia. A preliminary statement. Disasters 32(3), 337–357, https://doi.org/10.1111/j.1467-7717.2008.01043.x.

OECD (2022): Estudios Económicos de la OCDE México. Resumen Ejecutivo. OCDE Mejores Políticas para una vida mejor 1:8. Available online: https://www.gob.mx/cms/uploads/attachment/file/704552/Mexico-2022-OECD-economic-survey-executive-summary-Spanish.pdf (In Spanish. Accessed on 29 January 2024).

Palacio-Mejía, L. S., Hernández-Ávila, J. E., Hernández-Ávila, M., Dyer-Leal, D., Barranco, A., Quezada-Sánchez, A. D., Alvarez-Aceves, M., Cortés-Alcalá, R., Fernández-

Wheatley, J. L., Ordoñez-Hernández, I., Vielma-Orozco, E., de la Cruz Muradás-Troitiño, M., Muro-Orozco, O., Navarro-Luévano, E., Rodriguez-González, K., Gabastou, J. M., López-Ridaura, R., López-Gatell, H. (2022): Leading causes of excess mortality in Mexico during the COVID-19 pandemic 2020–2021: A death certificates study in a middle-income country. The Lancet Regional Health – Americas 13: 100303, https://doi.org/10.1016/j.lana.2022 .100303.

Patwary, M. M., Rodriguez-Morales, A. J. (2022): Deadly flood and landslides amid COVID-19 crisis: a public health concern for the world's largest refugee camp in Bangladesh. Prehospital and disaster medicine 37(2), 292–293, https://doi.org/10.1017 /S1049023X22000164.

PNUD (2023): Reducción del impacto económico del covid-19 y fomento a la recuperación temprana resiliente en comunidades de México. Available online: https://www.undp.org/es/mexico/projects /reducci%C3%B3n-del-impacto-econ%C3%B3mico -del-covid-19-y-fomento-la-recuperaci%C3%B3n -temprana-resiliente-en-comunidades-de-m%C3% A9xico (In Spanish. Accessed on 29 January 2024).

Qasim, S., Qasim, M., Shrestha, R. P., Khan, A. N. (2018): Socio-economic determinants of landslide risk perception in Murree hills of Pakistan. AIMS Environmental Science 5(5), 305–314, https:// doi.org/10.3934/environsci.2018.5.305.

Sim, K. B., Lee, M. L., RemeytePrescott, R., Wong, S. Y. (2023): Perception on landslide risk in Malaysia: a comparison between communities and experts' surveys. International Journal of Disaster Risk Reduction 95: 103854, https://doi.org/10.1016/j.ijdrr.2023 .103854.

Slovic, P. (2016): The perception of risk. Earthscan: New York, USA, https://doi.org/10.4324/9781315661773.

UNISDR (2015): Sendai framework for disaster risk reduction 2015–2030. United Nations International Strategy for Disaster Reduction. Available online: http:// www.wcdrr.org/uploads/Sendai_Framework_for_ Disaster_Risk_Reduction_2015-2030.pdf. Accessed Jan 24 2024 (Accessed on 29 January 2024).

UNICEF (2008): Desarrollo positivo adolescente en América Latina y el Caribe. Unicef/Unidad de Desarrollo y Equidad de Género. Temas de Políticas Públicas 1:16. Available online: https://www.unicef.org/venezuela /media/941/file/UNICEF%20Oficina%20Regional%20 para%20Am%C3%A9rica%20Latina%20y%20el%20 Caribe.pdf (Accessed on 29 January 2024).

UNICEF (2009): Albergues en Escuelas, ¿Cuándo? ¿Cómo? ¿Por qué? Red Interinstitucional para la Educación en Situaciones de Emergencia (INEE) 1–68. Available online: https://inee.org/sites/default/files/resources /UNICEF_Albergues_en_escuelas.pdf (Accessed on 29 January 2024).

Valverde, G. R., Valverde, B. R. (2022): Impacto del COVID-19 por marginación y rezago social en el estado de Puebla, México. Regiones y Desarrollo Sustentable 22(43), 1–31. Available online: http://www.coltlax.edu .mx/openj/index.php/ReyDS/article/view/243/pdf (Accessed on 29 January 2024).

Wachinger, G., Renn, O., Bianchizza, C., et al. (2010): Risk perception and natural hazards. CapHaz-Net WP3 Report. p. 112. Available online: http://caphaz-net.org /outcomes-results/CapHaz-Net_WP3_Risk-Perception .pdf (Accessed on 29 January 2024).

Wang, H., Paulson, K. R., Pease, S. A., et al. (2022): Estimating excess mortality due to the COVID-19 pandemic: a systematic analysis of COVID-19-related mortality, 2020–21. The Lancet 399(10334), 1513–1536, https://doi.org/10.1016 /S0140-6736(21)02796-3.

World Bank (2022): World Development Report 2022, Finance for an equitable recovery, Chapter 1. The economic impacts of the COVID-19 crisis. Available online: https://www.worldbank.org/en/publication /wdr2022/brief/chapter-1-introduction-the-economic -impacts-of-the-covid-19-crisis (Accessed on 29 January 2024).

Yik, M., Pun, W. K., Kwok, F. H., Pho, J., Ng, C. W. W. (2023): Perceptions of landslide risks and warnings in Hong Kong. Landslides 20, 1211–1224, https://doi.org /10.1007/s10346-022-02021-3.

Zepeda, G. (2021): Uno TV.com. ¿Y la carretera? Socavón devora este tramo en Puebla. Available online: https:// www.unotv.com/estados/puebla/puebla-socavon -destruye-carretera-de-teziutlan/ (In Spanish. Accessed on 29 January 2024).

Assessing small-holder coffee farmers' awareness and choice of climate change/variability adaptation strategies in Mattu Woreda, southwestern Ethiopia

Leta Jima Desta[1], Mengie Belayneh[2,*], Bijiga Emiru[3]

[1] Department of Geography and Environmental Studies, Oda Bultum University, Chiro, Ethiopia
[2] Department of Geography and Environmental Studies, Mattu University, Mettu, Ethiopia
[3] Department of Civics and Ethical Studies, Mattu University, Mettu, Ethiopia
* Corresponding author: mengie1980@yahoo.com

ABSTRACT

It is advocated that smallholder coffee farmers' characteristics and perceptions strongly affect the use and selection of climate variability/change response mechanisms. Therefore, we investigated the climate change/variability perceptions and determining factors of the selection of smallholder coffee farmers' adaptation strategies over the period 1992–2022 in Mattu woreda, Ethiopia. This study used cross-sectional research design as the data was collected from different groups (adaptor and non-adaptor) at a time. A sample of 325 coffee farmers were randomly selected for a self-administered questionnaire supplemented with face-to-face interviews and focus group discussions. A multinomial logistic regression model was used for statistical analysis. The findings of the study showed that 79% of coffee farmers are conscious of the prevailing climate change and related consequences on coffee growth, production, productivity, and quality. Coffee farmers practiced planting coffee under shade, close spacing, mulching, and irrigation, developing an adaptable coffee variety, developing disease and heat-tolerant varieties, changing the location and planting date, and pruning as strategies to lessen the influence of climatic change on coffee production. However, most coffee farmers prefer to plant coffee under shade and pruning. The selection of climate change/variability adaptation strategies among coffee farmers is significantly influenced by age, family size, coffee farm experience, land holding size, income of HHs, distance to coffee farm plots, access to climate information, and training and TLU ($P < 0.05$). Therefore, provision of climate information, extension services, and seed varieties to farmers, and improving social and physical infrastructures are recommended to better adapt and mitigate the effect of climate change/variability.

KEYWORDS

adaptation strategies; climate change/variability; determinants; multinomial logistic regression model

Received: 30 April 2024
Accepted: 14 December 2024
Published online: 31 January 2025

Desta, L. J., Belayneh, M., Emiru, B. (2025): Assessing small-holder coffee farmers' awareness and choice of climate change/variability adaptation strategies in Mattu Woreda, southwestern Ethiopia. AUC Geographica 60(1), 94–104
https://doi.org/10.14712/23361980.2025.2

1. Introduction

Climate change (hereafter CC) was an environmental problem since the Industrial Revolution, and currently a critical universal challenge, as industries have been the main contributors to the increasing trend of atmospheric greenhouse gases (Zandalinas et al. 2021). It causes an increasing temperature, flooding, drought, and depletion of environmental resources (Naqvi and Sejian 2011; Parry et al. 2004). Climate change is predicted to cause significant (3–30%) crop yield and 15–37% of fauna and flora species loss by 2050 if no adaptive measures are taken (Nelson et al. 2009). Africa's smallholder farmers are more vulnerable to the influences of climate change/variability ([hereafter CCV]; Mubiru et al. 2018; Makate 2019; Naab et al. 2019). The problem is predominantly serious within the smallholder societies (Hein et al. 2019); whose livings are deeply reliant on the healthiness of seasonal climatic situations (Gemeda et al. 2021).

It is estimated that 62.8% of Ethiopia's workforce is employed in agriculture (African Economic Outlook 2024), which also provides more than 85% of the country's foreign exchange earnings and accounts for 32.4% of Ethiopia's GDP (National Bank of Ethiopia 2022). However, it is anticipated that Ethiopia's agricultural output will decline by 50% in the near future related to CCV (FDRE 2011). It has therefore been shown to have potentially serious effects on development and livelihood (Mengestu 2011).

Recent reports indicated that eastern Africa is experiencing severe drought and wet scenarios currently. Ethiopia as a typical East African nation, experiences severe fluctuations in the trend of rainfall and even temperature in different areas. Several recent research reports documented a decreasing (Asfaw et al. 2019; Hill and Porter 2017), increasing (Gemeda 2019; Tesfamariam et al. 2019; Wedajo et al. 2019), and both (Gebrechorkos et al. 2018; Degefie et al. 2019) annual and seasonal rainfall trends in different parts of Ethiopia.

As part of southwestern Ethiopia, the Illu Aba Bora zone (in which Mattu woreda is its part) is a moist evergreen Afromontane forest area (Friis et al. 2010) with high potential for wild Coffea arabica production, but starting from the recent past it has been influenced by recurrent CCV (Desta and Belayneh 2023). It is documented that the highest reduction in rainfall (Gemeda et al. 2021) and increase in temperature (Desta and Belayneh 2023; Gemeda et al. 2021) is observed. Besides, rainy days in the high coffee-growing region of the southwestern parts of Ethiopia declined from 9 to 5.5 months (almost by 39% the previous; Fekadu et al. 2020). Similarly, the projected information depicted that an increasing trend (2.2 °C rise annually) of temperature in all regions is expected by the 2050s (Conway and Schipper 2011).

Climate variability/change pointedly affects the valuable cash crops in southwestern Ethiopia (Gemeda et al. 2021). For instance, a study by Desta and Belayneh (2023) reported that the rise in temperature significantly affected coffee production in southwestern Ethiopia. The deteriorating bioclimatic suitability for Coffea arabica in the coffee-growing wettest topography of Ethiopia is an alerting climate change-linked negative effect (Davis et al. 2012; Moat et al. 2017). Coffee-growing landscapes are projected to decline to nearly 100% in 2080 (Davis et al. 2012).

Adaptation, therefore, remains among the list of policy and implementation options to better prepare and respond to climatic change challenges that prevail in the agrarian population such as coffee farmers. There are several causes and compelling arguments for a more general consideration of CCVAS (Amare et al. 2018). For instance the world has experienced some degree of CC due to past greenhouse gas emissions, which cannot be prevented even by the most ambitious reductions in emissions (Füssel and Klein 2006). The effects of emissions reductions will take decades to fully manifest, but most adaptation measures have more immediate and lasting benefits (Rahman 2013). Adaptations can be effectively implemented on a local or regional scale and most adaptations reduce climate variability-associated risks, which cause frequent hazards in different parts of the world (Amare et al. 2018). Similarly, smallholder Ethiopian coffee farmers have practiced adaptation techniques to resist extreme events and high inter-annual climate variability, despite their high level of vulnerability to climate change. Furthermore, farmers have been practicing, evaluating, and embracing a variety of coping techniques (AEO 2016). Nevertheless, still, coffee production has shown a reduction mainly related to climate change-associated consequences (Desta and Belayneh 2023).

In these regards, understanding farmers' knowledge of CCVAS is important to better prepare them to respond to the upcoming negative consequences of CCV on coffee production and smallholder coffee farmers. However, studies conducted in the wettest landscapes; particularly in southwestern Ethiopia are very limited (Gemeda et al. 2021). This is mainly related to aligning the effect of CCV to the past drought and famine scenarios in the dry lands of Ethiopia. The thoughtfulness of smallholder coffee farmers about CCV and the determinants of the selection of responding mechanisms is noteworthy; take lessons and immediately respond to it as a precautionary measure. Therefore, the main purposes of this study were to 1) assess the perception of coffee farmers about climate change and variability and 2) identify the main determining factors of selection and use of different climate change adaptation strategies among smallholder coffee farmers. This study presents smallholder coffee farmers' knowledge of CCV and determinants of the choice of effective adaptation strategies, which is expected to give scientific evidence for policymakers for intervention.

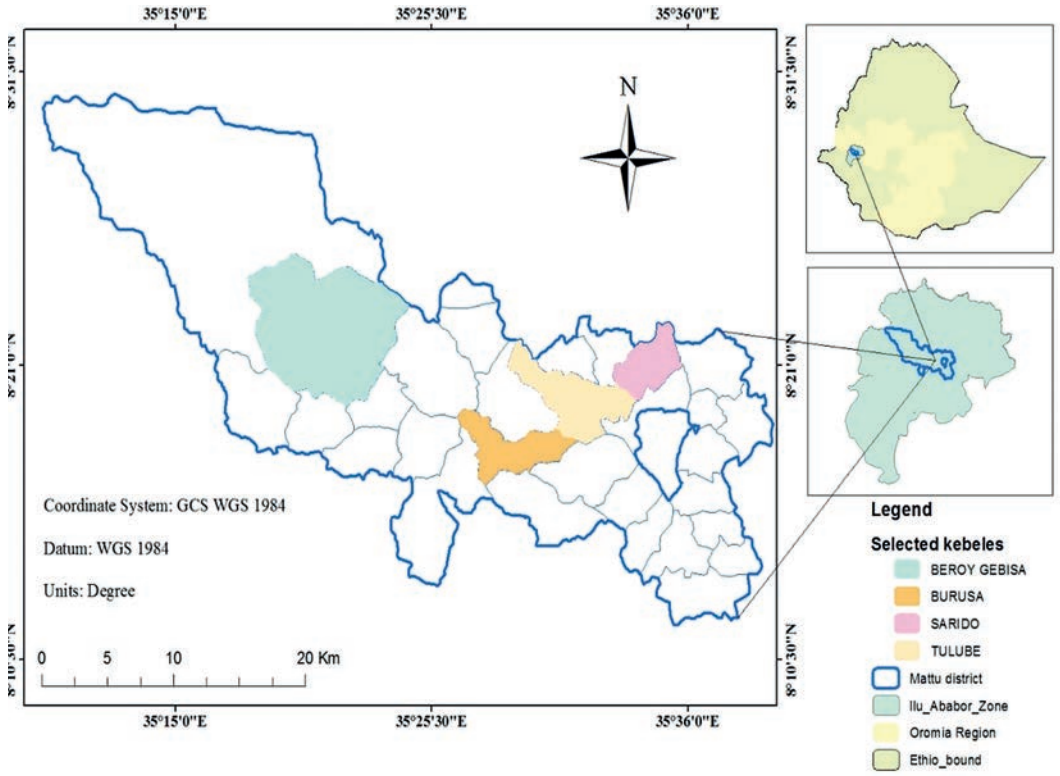

Fig. 1 Mattu woreda and study kebeles in Illu Aba Bor zone, southwestern Ethiopia.

2. Materials and methods

2.1 The study site

Mattu woreda[1] is found in the wettest highland landscapes of southwestern highlands, Oromia National Regional State, Ethiopia (Fig. 1). It is located between 8°11′20″ to 8°30′12″ latitude and 35°10′20″ to 35°40′12″ longitude. Mattu woreda covers a total area of 1452 km^2. The major city (Mattu), is situated about 600 km southwest of the country's capital (Addis Ababa) via the Addis-Mattu-Gambella road.

The area is described by diverse landscapes typically called the wettest highland of Ethiopia. The area is dominated by wet Woina Dega/Sub-tropical and Kolla/tropical agroecological zones. The area receives rainfall almost year-round (6 to 9 months), although recently declined to 5.5 months (Fekadu et al. 2020). The long-term mean total rainfall of the woreda is 1,408.6 mm (thirty years of yearly rainfall data). The area's temperature increased over time, reaching an average of 19.67 °C.

The area is a typical coffee crop production area, specifically the wild Coffea Arabica in Ethiopia. Subsistence mixed crop and livestock farming is the key means of livelihood for the community. The predominant cash crop of the area is coffee, which plays a significant role in smallholder farmers' source of cash and the local economy. It is reported that approximately 60% of the local community directly depends on coffee-based livelihoods (Mattu woreda agricultural office 2021).

2.2 Research design and approach

The study used a cross-sectional research design. Cross-sectional research design was used in this study because the data were collected from two groups (both the CCSAS adaptors and non-adaptors) at a time. Creswell (2012) states that a mixed research approach yields a more comprehensive understanding of the research problem and questions than either method alone. For this reason, mixed research approach was employed for this study. Simultaneous collection of data is the hallmark of concurrent parallel mixed research strategy was adopted for this study. The combined data sets are then analyzed to reinforce the limitations of the quantitative data and provide a more comprehensive understanding of the research problem.

2.3 Sources of data

Data concerning smallholder coffee farmers' knowledge about CC were collected from small-holder coffee farmers' HHs, developmental agents (DAs) working in each kebele[2], woreda, and zonal experts.

1 *Woreda* is the second lowest administrative division in the Ethiopian current administration tiers (five tiers).

2 Kebele is the lowest administrative division in the Ethiopian current administration tiers.

2.4 Sample size determination

Among 30 kebeles in the woreda, four (Beroy Gebisa, Tulube, Burusa, and Sardo) were selected purposely considering their high coffee-producing trends and better experience of farmers' use of CCVAS. Then, 325 smallholder coffee farmers were selected using systematic random sampling. Kothari (2004) formula was used for sample size determination from the target population (2256 HHs). A proportional sample allocation technique was applied to get a representative sample from the selected kebeles (Tab. 1).

Tab. 1 Sampled kebeles, total HHs, and samples.

No.	Name of Kebeles	Total HHs			Sample HHs
		Male	Female	Total	
1	Beroy Gebisa	391	38	429	62
2	Burusa	606	105	711	102
3	Tulube	506	108	614	89
4	Sardo	420	82	502	72
Total		1923	333	2256	325

Source: Mattu *Woreda* Administration Office, 2022.

$$\frac{Z^2pqN}{e^2\,(N-1)+Z^2pq},$$

where n = sample size
Z = the standard variant at 95% confidence interval (Z = 1.96)
N = total population (2256)
P = proportion of sampled population (0.01)
e = 0.01 (since the estimate should be within 1% of the true values)

$$q = 1 - p$$

Using their knowledge, experience, and expertise of CCVAS in the area as a criterion, five model farmers, two agricultural officers, two developmental agents (DAs), and two natural resource management offices were chosen for in-person interviews. Four focus group discussions each consisting of seven farmers from each sample kebele were conducted.

2.5 Data collection instruments

Data were gathered using a questionnaire that included both open-ended and closed-ended questions. Questions were prepared in Afan Oromo (local language) for a simple understanding of the questionnaire by the respondent households. Professionals from the offices of climate, agriculture, and natural resource management as well as woreda administration were interviewed in person. Due to their close interactions with coffee growers, these individuals are more knowledgeable about the issues of climate change and variability. For this purpose, open-ended, semi-structured interview questions were used. Additionally, focus group discussions were held with seven specifically chosen HHs from each kebele. A total of four focus group discussions were made. It will be crucial to gather diverse opinions and data regarding CC and adaptation techniques from smallholder coffee farmers. Lastly, the researcher made direct, firsthand observations at the study site to observe conservation practices related to climate variability/change adaptation practices.

2.6 Method of data analysis

The textual organization and analysis of the qualitative data took the shape of narratives and descriptions. Both descriptive and inferential statistics were applied to the analysis of quantitative data. Descriptive statistics including percentage, and frequency of occurrence were used and presented in the form of tabulations, graphs, and charts. A multinomial logistic regression model was employed with the help of Statistical Package for Social Sciences (SPSS) version 26.

A multinomial logit was utilized to ascertain the determinant variables affecting the selection of adaptation tactics used by smallholder coffee farmers. With six possible outcomes (planting coffee under shade, close spacing, mulching, and irrigation; using adaptable coffee varieties; applying disease- and heat-tolerant varieties; altering the location, planting date, and pruning), dependent variables are different strategies used by coffee farmers to adapt CCV.

Therefore, for this study, HHs' selection of adaptation strategy (Yi) is determined by various explanatory variables X_1, X_2, X_3, X_4, X_5, X_n, which can be formulated as:

$$Y = \beta_0 + \beta_1X_1 + \beta_2X_2 + \ldots + \beta_nX_n + \varepsilon$$

Where; Yi: Is HH participation in adaptation strategies to CCV X_1, X_2, X_n: are explanatory variables that are related to adaptation strategies, **ε** is the error term, followed by B_1 and B_2, B_n: are the slopes of the model's explanatory variable coefficients (Tab. 2).

Log likelihood ratio (LR), Chi-square (X^2), and Pseudo R^2 goodness-of-fit tests were performed to assess the predicting ability of the model. Multi-collinearity describes the correlation between multiple independent variables in a model. When two variables have a correlation of +/−1, they are said to be perfectly collinear. Menard (2000) explained that there is no multi-collinearity if the tolerance value is >0.25 and the VIF value for each variable is <10. It is calculated as:

$$VIF_i = \frac{1}{1-Ri^2}$$

Tab. 2 Independent variables and their expected effect on the choice of climatic variability/change adaptation practices among smallholder coffee farmers in Mattu woreda.

Variables	Variable type	Description	Exp. sign
Sex	Dummy	1 = Male; 2 = Female	+*
Age	Continuous	Age of the HH	+
Coffee Farm exp.	Continuous	Coffee farm experience of the HH	+
Landholding size	Continuous	Total land owned by the HH in hectares	+
Credit access	Dummy	0 = No; 1 = Yes	+
Family size	Continuous	Number of family members per HH	+/−
Educational level	Continuous	The education level of HH	+
Climate information	Dummy	1, if a HH has access to climate information; 0 otherwise.	+
Extension service	Dummy	HH head access to extension advice and training per year [0 = No; 1 = Yes]	+
Income of HHs	Continuous	HH farm income	+
Incentives	Dummy	Incentives are given while participating in adaptation practices [0 = No; 1 = Yes]	+
Livestock holding (Tropical Livestock Unit (TLU))	Continuous	Number of livestock the HH owned in TLU	+/−
Distance to farm plot	Continuous	Accessibility of farm plots in kilometers	−

* refers if the household is male headed it will have an expected positive effect on the adoption decision.

3. Results and discussion

3.1 Sample HHs characteristics

As shown in Tab. 3, males were the predominant HHs (hereafter HHs; 84.7%), while the remaining 15.3% were females. Several authors argue that male-headed HHs have access to new technologies and take more appropriate actions than female-headed HHs (Asfaw et al. 2019; Deressa et al. 2011). Usually under the agrarian economy of rural Ethiopia, women HHs are classified under poor wealth rank.

The majority of the HHs were between 56 and 65 years old, which accounts for 31.4%. Among the total households considered in this study, 35.6% and 28.8% of them were having a family size ranging from 7 to 9 and 4 to 6, respectively. Therefore, large numbers of the HHs were within the active age group. It is known that these groups are the most productive forces that can play a decisive role in generating appropriate and suitable responses to CC for their locality and these people are ready and fit to take responsibility just to cope with the challenges paused due to CC.

The majority (69.5%) of the households' received no formal schooling. On the other hand, about 23.7% and 6.8% of them completed primary and secondary education, respectively. It is understood that education is considered central in determining the readiness to adopt new ideas, and enables people to realize the diversification or specialization of livelihood activities and technology. Indeed, HHs better literacy level was assumed to have a positive impact on their involvement to use and better accept adaptation mechanisms. Household heads higher levels of education increase the opportunity and access to information, better understanding and application of new technologies as well as better ability to withstand climatic risks (Belay et al. 2017; Hadgu et al. 2015). Furthermore, according to Ndambiri et al. (2013), education improves farmers' capacity to accept, understand, and realize information necessary to make creative decisions on their farmland.

Tab. 3 Descriptive statistics of sex, age, marital status, family size, and educational levels.

Descriptive variables	Description	Frequency (f)	Percentage (%)
Sex	Male	275	84.70
	Female	50	15.30
Age	26–35	77	23.70
	36–45	80	24.60
	46–55	36	11.00
	56–65	102	31.40
	> 65	30	9.30
Family size	1–3	44	13.60
	4–6	94	28.80
	7–9	116	35.60
	10–12	52	16.10
	None	19	5.90
Marital status	Single	19	5.90
	Married	278	85.60
	Divorced	25	7.60
	Widowed	3	0.80
The educational level of respondents	Cannot read and write	226	69.50
	Primary education (1–8)	77	23.70
	Secondary education (9–12)	22	6.80

3.2 Coffee farmers' perception of climate change/variability

About 60.2% of the coffee farmers explained that the trend of temperature in the last three decades was increasing, but 33.1% perceived it is constant and the remaining 6% perceived decreasing (Tab. 4). Similarly, 82.2% of stallholder farmers explained a decrease in rainfall, while 17% did not over the period 1992-2022. Farmers' perception has a greater role in being prepared and withstand in the changing climatic situation (Wagesho and Yohannes 2016).

Before ~20 years, most farmers' land was covered with dense plant forests, and this was also essential to their means of sustenance, especially when it came to producing coffee. However, the forest cover had declined due to the growing human population and their desire to expand land for the production of crops and other uses like building materials and various furniture, charcoal, and wood. The FGD participants also mentioned that although the number of coffee growers has occasionally increased, the yield of coffee has decreased due to diseases and climate change/variability.

A five-point Likert scale rating was employed to gauge the sample respondents' perceptions of a few chosen CC attributes. Farmers who choose to simply agree or strongly agree are thought to perceive change differently than those who do not. The results showed that most respondents (79%) thought there was less rainfall and that it was insufficient to sustain crops during their whole growing season. The findings of this study were similar to those of Tesfaye and Seifu (2016) and Belay et al. (2017), which claimed that 79.1% of farmers believed rainfall could not sustain production. The results of the FGD verified that the rainfall usually ends before or after the crop-growing season. In a similar vein, 90% of the participants noted a rise in the quantity of hot spots. Eighty percent of respondents reported seeing an early end to the rainy season, and eighty-two percent reported that the start of the rainy season was later than usual (Tab. 5). The belg (spring) season production in the woreda, which typically produces a sizable amount of output, abruptly declined. The research reports of Tesfaye and Seifu (2016) corroborate the results, which also showed that farmers acknowledged the rise in crop disease and pest infestation that had previously become an issue.

Tab. 4 Coffee farmers' perception of rainfall/temperature change trends over the period 1992–2022 (n = 325).

Descriptive variables	Description	Frequency (f)	Percentage (%)
Temperature trend	Increases	196	60.2
	Decreases	22	6.8
	Constant	107	33.1
	I don't know	–	–
Rainfall trend	Increases	–	–
	Decreases	267	82.2
	No change	58	17.8
	I don't know	–	–

3.3 Smallholder Coffee farmers adaptation strategies to climate change/variability

The study result revealed that 28 and 24.6% of the HHs use planting coffee under shade and pruning as a prime strategy to cope with CCV by coffee farmers, respectively (Tab. 6). Besides, 17 and 14.4% of coffee farmers used heat-tolerant varieties and diseases, and altered the planting date and location as a strategy, respectively.

Farmers reported planting coffee under shade regulates light penetration to coffee plants (91.5%) and increases coffee yields and quality (79.7%). Others experienced climate adaptation strategies to improve

Tab. 5 A Likert scale-based measurement of small-holder farmers' perception of CC in the Mattu woreda. Note: 1 = strongly disagree, 2 = disagree, 3 = undecided, 4 = agree, and 5 = strongly agree.

CC signals and pattern of changes	Farmers perception (n = 325)				
	1	2	3	4	5
Rainfall unable to support a full growing period	–	21.00	–	62.90	16.10
Increase in the number of hot days	10.00	–	–	62.80	27.20
Early cessation of rainfall	–	20.00	–	34.40	45.60
Delay of the onset of rainfall	–	10.00	–	7.25	82.75
The community is aware of the effect of CC on coffee yield	27.00	56.70	–	7.30	9.00
Rise of the price of coffee due to low productivity caused by CC	43.30	30.00	3.00	–	23.70
High deforestation to compensate the income and livelihoods losses from coffee	11.80	–	6.20	28.50	53.50
Change of livelihood due to CC	31.00	16.50	–	18.50	34.00
High fluctuation of temperature and rainfall	5.90	–	5.00	24.10	65.00
Crop disease and pests increase over time	–	–	–	32.60	67.40

Tab. 6 Climate variability/change adaptation strategies practiced by coffee-producing rural farmers in Mattu woreda.

Strategies practiced	Frequency (f)	Percentage (%)
Planting coffee under the shade	91	28.0
Close spacing, mulching, and irrigation	36	11.0
Developing an adaptable coffee variety	28	8.5
Use of disease and heat-tolerant varieties	22	6.8
Changing the location and planting date	39	11.9
Pruning	80	24.6
No adaptation	30	9.3

Farmers' coffee yield suddenly decreased as a result of frost and lack of rain. Climate change/variability caused a strong impact on coffee production in the Mattu woreda (Desta and Belayneh 2023).

soil moisture and fertility, increase coffee yields and quality, and reduce soil erosion in the woreda. Local farmers cultivate a variety of coffee varieties, some of which become poor in their resistance to disease and pests and tolerant of drought shock. These coffee varieties have variable yields and remain with the farmer for a long time. The agricultural experts noted that the productivity of coffee occasionally declined because of challenges to the traditional coffee production systems, where the absence of attention is significant in terms of technical assistance and extension, a lack of improved varieties, and an inadequate supply of input for coffee productivity package enhancement. The primary issues facing farmers were the layout of the coffee plantations and the replacement of older coffee trees in the new plantation. Experts retorted that adopting and utilizing new technologies is difficult for farmers. Besides, the extension service, awareness and capacity-building training program, and agricultural input availability are very limited.

3.4 Determinants of choice of climate change/variability adaptation strategies among smallholder coffee farmers

The statistical analysis result implies that the model displays a good fit. The Pseudo R^2 was 0.2279, implying that 22.79% of the variation in the selection of climate variability/change adaptation techniques was explained by the 14 explanatory variables (Tab. 7). There is no multi-collinearity among variables because the tolerance value is >0.25 and the VIF value for each variable is <10.

HH age

HH age is a key explanatory factor with a positive coefficient. When all other factors are held constant, there is a 73.7% increase in the likelihood that farmers will employ close spacing, mulching, and irrigation as an adaptation strategy when the age of the HH head rises (P-value = 0.029). This suggests that as the HH's age increases there will be an increase in the probability

Tab. 7 Variance inflation factor (VIF) analysis results for explanatory variables (n = 325).

Variables	Multi-collinearity statistics		
	R-squared	Tolerance	VIF
Sex	0.273	0.727	1.376
Age	0.386	0.614	1.620
Marital Status	0.272	0.728	1.373
Family size	0.328	0.672	1.488
Educational level	0.334	0.667	1.500
Land Holding Size	0.226	0.774	1.291
Coffee farm experience	0.469	0.531	1.883
Income of HHs	0.347	0.653	1.531
Distance to coffee farm	0.433	0.567	1.763
Climate information	0.637	0.363	2.754
Credit access	0.131	0.869	1.150
Extension Services	0.091	0.909	1.100
Training	0.380	0.620	1.612
Tropical Livestock Units	0.547	0.453	2.207

of implementing close spacing, mulching, and irrigation. This could be related to more experienced farmers having a better sense of CCV and related effects on coffee production.

The study's finding is consistent with the results of Nhemachena et al. (2014), who showed that farming experience raises the likelihood that people will use adaptation strategies. Age influences farmers' decisions to select the type of adaptation strategies to use. But, on the contrary, Deressa et al. (2011) found an undetermined impact of age on adaptation decisions.

Family size

This variable has a positive and significant impact on CCVAS. The likelihood that farmers will use close spacing, mulching, and irrigation as adaptation techniques increased by 75.1% with every unit increase in family size while maintaining the same levels of other variables (P = 0.015). One argument is that having a higher family size allows for the easier adoption of new technologies by providing the necessary labor force.

Landholding size

Land holding size positively and significantly increases the likelihood of farmers' adoption of CCVAS. For instance, if one-hectare increases in farm size, the chance of coffee farmers using disease and heat-tolerant varieties as an adaptation strategy increased by 92% (P = 0.03) holding other variables constant (Tab. 8). Landholding size is mostly linked to better wealth and may lead to better implementation of adaptation strategies.

Therefore, the amount of land allotted for various crop varieties as farmers' likely adaptation strategies increase with the size of the farm. The likelihood of

Tab. 8 Factors determining the selection of climate variability/change adaptation strategies: multinomial logistic regression model result.

Explanatory variables	Dependent variable (adaptation strategies)											
	Planting coffee under shade		Close, spacing, mulching, and Irrigation		Use an adaptable coffee variety		Apply disease and heat-tolerant varieties		Changing the location and planting date		Pruning	
	β	P	β	P	β	P	β	P	β	P	β	P
Sex	.306	.824	.878	.513	1.006	.488	.494	.734	.416	.753	.148	.863
Age	.281	.388	.737	.029*	.268	.409	.185	.422	.219	.334	−.281	.388
Marital status	−.594	.602	1.238	.202	−1.350	.301	.130	.986	.236	.760	.594	.602
Family size	−.825	.104	.751	.015*	−.821	.085	−.140	.647	−.419	.139	.825	.104
Educational level	−1.363	.213	−.804	.249	.888	.163	.110	.831	.141	.775	1.363	.213
Landholding size	−.0840	.859	.071	.842	−.387	.393	.920	.030*	.356	.222	.084	.859
Coffee farming experience	.994	.044*	−1.612	.060	1.184	.270	1.292	.032*	−1.797	.054	1.142	.018*
HHs income	1.215	.025*	−1.275	.071	.177	.743	.264	.509	.041	.920	−1.405	.724
Distance to coffee farmland	.371	.083	−.521	.043*	.036	.827	−.147	.254	−.384	.006*	−.371	.083
Climate-related information	.758	.090	.427	.180	.129	.739	−.362	.145	.577	.024*	−.758	.090
Credit access	.921	.116	.236	.667	−546	.342	.801	.253	−.309	.714	.311	.593
Extension services	−1.004	.404	.146	.899	.794	.505	−.818	.561	.113	.940	−.731	.544
Training	.800	1.677	−2.458	.120	−2.980	.160	−2.875	.270	−1.807	.145	−1.177	.720
Tropical livestock unit	−.379	.046*	.318	.445	.141	.780	.637	.067	.571	.097	−.822	.126

Base category = No adaptation; N = 118; Log likelihood = −153.7985; LR Chi2 (50) = 90.80; Probability > Chi^2 = 0.04*; Pseudo R^2 = 0.2279; *, **, significant at 0.01 (1%) and 0.05 (5 %), probability level of significance.

a farmer's adaptation decision to CC increases with the size of their farm because larger farms are invariably linked to higher wealth, capital, and resources. This result also agrees with the finding of Tessema et al. (2013). However, some research documented that farm size influences adoption in both positive and negative ways, indicating that there is conflicting evidence regarding farm size's impact on technology adoption (Bradshaw et al. 2004).

HH income

HH farm income is another statistically significant variable that exerts influence on planting coffee under shade as a means of CCVAS. Holding other factors constant, the likelihood that farmers would use planting coffee under shade as an adaptation strategy increased by 12.15% (P = 0.025; Tab. 8) with a one Ethiopian birr (ETB) increase in HH farm income. Deressa et al. (2011) reported a positive co-variation between farmers' income and the use of adaptation strategies. When farming becomes their primary source of income, farmers typically invest in options that smooth productivity, like irrigation. This finding is consistent with studies by (Ahmed and Bogale 2021; Mengistu and Haji 2015).

Coffee farm experience

This variable had a strong correlation with practices related to climate adaptation, as indicated by the model's result. The analysis's result shows that the HH's prior experience on the farm had a favorable and significant impact on the use of shade-grown coffee plants as a method of adaptation to CC, increasing their use by 99.4% (P = 0.044). Smallholder farmers' use of disease and heat-tolerant varieties and pruning increased by 12.9% (P = 0.032) and 11.42% (P = 0.018), respectively.

Distance from coffee farmland

The distance of the HHs place of residence from his/her coffee farm plot negatively affected the adaptation strategies for improving coffee production. Farmers are less likely to employ irrigation, mulching, and close spacing as adaptation techniques when it takes them longer to travel from their home to the cultivated area, holding all other variables constant (P = 0.043). Holding all other factors constant, the likelihood of farmers to use location and planting date changes as an adaptation strategy dropped by 38.4% (P = 0.06), due to an increased distance between their home and coffee plot. Minwuye (2017) also argued that the distance of plots from the homestead may influence HH investment in time lost traveling to and from a plot, and plots located far from farmers' residences are a high-risk investment as the chance of losing these plots is higher in the event of land distribution.

Farmers' access to climate-related information

Farmers' decisions to use location and planting date changes as a strategy for climate variability were

positively impacted, and this effect was significant at 5% probability levels (P = 0.024). When other factors were held constant, the multinomial logistic regression model's result showed that farm HHs with access to climate information were more likely than their counterparts to use location and planting date changes as a strategy for climate variability. By using climate information practices to adjust planting dates and locations, smallholder farmers can increase yields by 57% while mitigating the effects of climate variability. The study's conclusions were validated by Minwuye (2017).

Livestock size (TLU)

In this study, one important explanatory variable was the farmer's livestock count. Its indication was having a detrimental effect on farmers' decisions to adopt new crop varieties and enhance livestock and crop adaptation strategies. Keeping all other factors equal, the likelihood of adopting coffee under shade as an adaptation strategy drops by 37.9% for every unit of livestock the HH owns. In this instance, livestock was viewed as a resource by the farmers and was crucial because it provided cash for the purchase of better crop varieties. However, having a lot of livestock can make it harder for farmers to adapt to CC because they need a lot of grazing land, which limits their ability to use coffee land for grazing. However, one aspect of agricultural activity that is also impacted by CC is the raising of livestock. As a result, farmers will become less interested in seeking out adaptation strategies to protect their assets from climate-related issues as the number of livestock increases. This result is against the research reported by Tazeze et al. (2012).

4. Conclusions and policy implications

The study examined the smallholder coffee farmers' perception and determinants of the adaptation choices to climate variability/change using cross-sectional data employing a multinomial logistic regression model. Coffee farmers were requested to reflect on their awareness of the changes in climatic elements and the main factors determining the use and selection of CCVAS. About 79% of coffee farmers were aware of the effects of a changing climate on coffee growth, productivity, and quality. The majority of farmers were also aware of the trends in rising temperatures and falling rainfall during the study period. Farmers who perceived changes practiced different adaptation strategies including planting coffee under shade, close spacing, mulching, and irrigation, developing an adaptable coffee variety, adopting disease and heat-tolerant varieties, changing the location and planting date, and pruning. However, we found diverse preferences for adaptation strategies among smallholder farmers. Field-based assessments on farmers' experience of using multiple adaptation choices were done and the result showed that nearly 52% of the farmers were found to use planting coffee under shade and pruning.

The study's conclusions showed that the age, family size, land holding size, income, experience on the coffee farm, distance to the coffee farm plot, availability of information about climate change, training, and TLU of the HHs significantly (positively/negatively) influenced the adaptation strategies chosen by the coffee farmers (P < 0.05). The primary obstacles to coffee farmers using various adaptation strategies were a lack of funding, a labor shortage, and a lack of training regarding the impact of climate change and coping mechanisms as well as extension services.

Therefore, it is recommended to design early warning policy systems that target to make farmers aware of future CCV and potential impacts so as to take proactive measures in different agro-climatic conditions. The government and other stakeholders should assist more vulnerable smallholder coffee farmers in terms of training, financing (credit service), and identifying and suggesting agroecological suitable CCVAS. In this regard, we suggest further research to identify and recommend evidence and agroecology-based, cost and labor-effective, and sustainable adaptation strategies for coffee farmers.

Acknowledgements

We would like to thank Mattu Woreda Agricultural office experts, extension workers as well as local farmers for their willingness and cooperation during fieldwork. We have benefited a lot from the editor's comments, editing, and recommendations as well as the anonymous reviewers. Thanks for your constructive and insightful comments on our manuscript.

References

African Economic Outlook (2024): Recent macroeconomic and financial developments. Available online: https://www.afdb.org/en/countries/east-africa/ethiopia/ethiopia-economic-outlook#:~:text = Ethiopia's%20structural%20transformation%20has%20been,(7.8%25%20in%201990) (accessed on 5. 2. 2024).

Ahmed, N. M., Bogale, A. P. (2021): Determinants of smallholder farmer's adaptation strategies to climate change: the case of haramaya woreda, eastern hararghe, oromia, ethiopia (doctoral dissertation).

Amare, M., Jensen, N. D., Shiferaw, B., Cissé, J. D. (2018): Rainfall shocks and agricultural productivity: Implication for rural HH consumption. Agricultural Systems 166, 79–89, https://doi.org/10.1016/j.agsy.2018.07.014.

Amare, Z. Y., Ayoade, J. O., Adelekan, I. O., Zeleke, M. T. (2018): Barriers to and determinants of the choice of crop management strategies to combat climate change in Dejen District, Nile Basin of Ethiopia. Agriculture and Food Security 7: 37, https://doi.org/10.1186/s40066-018-0188-y.

Asfaw, A., Simane, B., Bantider, A., Hassen, A., (2019): Determinants in the adoption of climate change adaptation strategies: evidence from rainfed-dependent smallholder farmers in north-central Ethiopia (Woleka sub-basin). Environment, Development and Sustainability 21, 2535–2565, https://doi.org/10.1007/s10668-018-0150-y.

Belay, A., Recha, J. W., Woldeamanuel, T., Morton, J. F. (2017): Smallholder farmers' adaptation to climate change and determinants of their adaptation decisions in the Central Rift Valley of Ethiopia. Agriculture and Food Security 6, 1–13, https://doi.org/10.1186/s40066-017-0100-1.

Bradshaw, B., Dolan, H., Smit, B. (2004): Farm-level adaptation to climatic variability and change: Crop diversification in the Canadian prairies. Climatic Change 67, 119–141, https://doi.org/10.1007/s10584-004-0710-z.

Conway, D., Schipper, E. L. F. (2011): Adaptation to climate change in Africa: Challenges and opportunities identified from Ethiopia. Global Environmental Change 21(1), 227–237, https://doi.org/10.1016/j.gloenvcha.2010.07.013.

Creswell, J. W. (2012): Qualitative Inquiry Research Design: Choosing among Five Approaches (4th ed.). Thousand Oaks, CA: Sage.

Davis, A. P., Gole, T. W., Baena, S., Moat, J. (2012): The impact of climate change on indigenous Arabica coffee (Coffea arabica): Predicting future trends and identifying priorities. PloS ONE 7(11): e47981, https://doi.org/10.1371/journal.pone.0047981.

Degefie, D. T., Seid, J., Gessesse, B., Bedada, T. B. (2019): Agricultural drought projection in Ethiopia from 1981 to 2050: Using coordinated regional climate downscaling experiment climate data for Africa, 311–323. In Extreme hydrology and climate variability. Elsevier, https://doi.org/10.1016/B978-0-12-815998-9.00024-5.

Deressa, T. T., Hassan, R. M., Ringler, C. (2011): Perception of and adaptation to climate change by farmers in the Nile basin of Ethiopia. The Journal of Agricultural Science 149(1), 23–31, https://doi.org/10.1017/S0021859610000687.

Desta, L. J., Belayneh, M. (2023): Analysis of climatic change and variability and its effect on coffee production in Mattu Woreda, Southwest Ethiopia. Sustainability and Climate Change 16(6), 461–479, https://doi.org/10.1089/scc.2023.0091.

Ethiopia Climate-Resilient Green Economy (2011): Ethiopia's Climate-Resilient Green Economy: Green Economy Strategy. Federal Democratic Republic of Ethiopia.

Fekadu, A., Soromessa, T., Dullo, B. W. (2020): GIS-based assessment of climate change impacts on forest habitable *Aframomum corrorima* (Braun) in Southwest Ethiopia coffee forest. Journal of Mountain Science 17, 2432–2446, https://doi.org/10.1007/s11629-019-5722-2.

Feleke, F. B., Berhe, M., Gebru, G., Hoag, D. (2016): Determinants of adaptation choices to climate change by sheep and goat farmers in Northern Ethiopia: the case of Southern and Central Tigray, Ethiopia. SpringerPlus 5: 1692, https://doi.org/10.1186/s40064-016-3042-3.

Friis, I. B., Demissew, S., van Breugel, P. (2010): Atlas of the Potential Vegetation of Ethiopia. Det Kongelige Danske Videnskabernes Selskab.

Füssel, H. M., Klein, R. J. (2006): Climate change vulnerability assessments: an evolution of conceptual thinking. Climatic Change 75(3), 301–329, https://doi.org/10.1007/s10584-006-0329-3.

Gebrechorkos, S. H., Hülsmann, S., Bernhofer, C. (2018): Evaluation of multiple climate data sources for managing environmental resources in East Africa. Hydrology and Earth System Sciences 22(8), 4547–4564, https://doi.org/10.5194/hess-22-4547-2018.

Gebreegziabher, Z., Stage, J., Mekonnen, A., Alemu, A. (2016): Climate change and the Ethiopian economy: a CGE analysis. Environment and Development Economics 21(2), 205–225, https://doi.org/10.1017/S1355770X15000170.

Hadgu, G., Tesfaye, K., Mamo, G., Kassa, B. (2015): Farmers' climate change adaptation options and their determinants in the Tigray region, northern Ethiopia. African Journal of Agricultural Research 10 (9): 956–964, https://doi.org/10.5897/AJAR2014.9146.

Gemeda, D. O. (2019): Climate change variability analysis in and around Jinka, Southern Ethiopia. With special emphasis on temperature and rainfall. The Journal of Agricultural Sciences – Sri Lanka 14(4), 145–153, https://doi.org/10.4038/jas.v14i3.8598.

Gemeda, D. O., Korecha, D., Garedew, W. (2021): Evidences of climate change presences in the wettest parts of southwest Ethiopia. Heliyon 7(9): e08009, https://doi.org/10.1016/j.heliyon.2021.e08009.

Hassan, R., Nhemachena, C. (2008): Micro-Level Analysis of Farmers' Adaptation to Climate Change in Southern Africa, IFPRI Discussion Paper 00714, August 2008.

Hein, A., Weking, J., Schreieck, M., Wiesche, M., Böhm, M., Krcmar, H. (2019): Value co-creation practices in business-to-business platform ecosystems. Electronic Markets 29, 503–518, https://doi.org/10.1007/s12525-019-00337-y.

Hill, R. V., Porter, C. (2017): Vulnerability to drought and food price shocks: evidence from Ethiopia. World Development 96, 65–77, https://doi.org/10.1016/j.worlddev.2017.02.025.

Huber, E., Stephens, J. (1995): Applied logistic regression analysis: sage university series on quantitative applications in the social sciences. Acta Sociologica 36(4), 309–325, https://doi.org/10.1177/000169939303600401.

IPCC (2007): Summary for policymakers: Climate Change published for the inter-governmental Panel on Climate Change. Cambridge: Cambridge University Press.

IPCC (2014): Climate Change: Synthesis Report. Contribution of Working Groups I, II and III to the Fifth Assessment Report of the IPCC [Core Writing Team, Pachauri RK, Meyer LA, (eds.)], IPCC, Geneva, Switzerland.

Kothari, C. R. (2004): Research methodology: methods and techniques.(2nd edition). New Age International (P) Ltd. Publishers. New Delhi.

Makate, C. (2019): Effective scaling of climate smart agriculture innovations in African smallholder agriculture: A review of approaches, policy and institutional strategy needs. Environmental Science Policy 96, 37–51, https://doi.org/10.1016/j.envsci.2019.01.014.

Menard, S. (2000): Coefficients of determination for multiple logistic regression analysis. The American

Statistician 54(1), 17–24, https://doi.org/10.1080/00031305.2000.10474502.

Mengistu, D. K. (2011): Farmers' perception and knowledge on climate change and their coping strategies to the related hazards: case study from Adiha, central Tigray, Ethiopia. Agricultural sciences 2(2), 138–145, https://doi.org/10.4236/as.2011.22020.

Mengistu, D., Haji, M. (2015): Factors affecting the choices of coping strategies for climate extremes: the case of Yabello District, Borana zone, Oromia National Regional State, Ethiopia. Science Research 3(4), 129–136, https://doi.org/10.11648/j.sr.20150304.11.

Mattu woreda agricultural office (2021): Annual report. (unpublished document), Mattu, Ethiopia.

Minwuye, B. (2017): Farmers' perception and adaptation strategies to climate change: the case of Wore Illu district of Amara region, northeastern Ethiopia.

Moat, J., Williams, J., Baena, S., Wilkinson, T., Gole, T. W., Challa, Z. K., Demissew, S., Davis, A. P. (2017): Resilience potential of the Ethiopian coffee sector under climate change. Nature plants 3(7), 1–14, https://doi.org/10.1038/nplants.2017.81.

Mubiru, D. N., Radeny, M., Kyazze, F. B., Zziwa, A., Lwasa, J., Kinyangi, J., Mungai, C. (2018): Climate trends, risks and coping strategies in smallholder farming systems in Uganda. Climate Risk Management 22, 4–21, https://doi.org/10.1016/j.crm.2018.08.004.

Naab, F. Z., Abubakari, Z., Ahmed, A. (2019): The role of climate services in agricultural productivity in Ghana: The perspectives of farmers and institutions. Climate Services 13, 24–32, https://doi.org/10.1016/j.cliser.2019.01.007.

Naqvi, S. M. K, Sejian, V. (2011): Global climate change: role of livestock. Asian Journal of Agricultural Sciencee 3, 19–25.

National Bank of Ethiopia (2022): National Bank of Ethiopia annual bulletin. Available online: https://nbe.gov.et/wp-content/uploads/2023/07/2021-22-Annual-report.pdf (accessed on 5. 2. 2024).

Ndambiri, H. K., Ritho, C. N., Mbogoh, S. G. (2013): An evaluation of farmers' perceptions of and adaptation to the effects of climate change in Kenya. International Journal of Food and Agricultural Economics (IJFAEC), Alanya Alaaddin Keykubat University, Department of Economics and Finance 1(1), 1–22, https://doi.org/10.22004/ag.econ.156144.

Nelson, G. C, Rosegrant, M. W., Koo, J., Robertson, R., Sulser, T., Zhu, T., Ringler, C., Msangi, S., Palazzo, A., Batka, M., Magalhaes, M., Valmonte-Santos, R., Ewing, M., Lee, D. (2009): Climate change: Impact on agriculture and costs of adaptation. International Food Policy Research Institute, Food policy reports :21 Washington, DC.

Nhemachena, C., Hassan, R., Chakwizira, J. (2014): Analysis of determinants of farm-level adaptation measures to climate change in Southern Africa. Journal of Development and Agricultural Economics 6(5), 232–241, https://doi.org/10.5897/JDAE12.0441.

Parry, M. L., Rosenzweig, C., Iglesias, A., Livermore, M., Fischer, G. (2004): Effects of climate change on global food production under SRES emission and socio-economic scenarios. Global Environmental Change 14(1), 53–67, https://doi.org/10.1016/j.gloenvcha.2003.10.008.

Rahman, M. I. U. (2013): Climate change: A theoretical review. Interdisciplinary Description of Complex Systems 11(1), 1–13, https://doi.org/10.7906/indecs.11.1.1.

Rahman, M. S. (2013): Climate change, disaster and gender vulnerability: A study on two divisions of Bangladesh. American Journal of Human Ecology 2(2), 72–82, https://doi.org/10.11634/216796221302315.

Tazeze, A., Haji, J., Ketema, M. (2012): Climate change adaptation strategies of smallholder farmers: the case of Babilie Woreda, East Harerghe Zone of Oromia Regional State of Ethiopia. Journal of Economics and Sustainable Development 3(14), 1–12.

Tesfamariam, B. G., Gessesse, B., Melgani, F. (2019): Characterizing the spatiotemporal distribution of meteorological drought as a response to climate variability: The case of rift valley lakes basin of Ethiopia. Weather and Climate Extremes 26: 100237, https://doi.org/10.1016/j.wace.2019.100237.

Tesfaye, W., Seifu, L. (2016): Climate change perception and choice of adaptation strategies: Empirical evidence from smallholder farmers in east Ethiopia. International Journal of Climate Change Strategies and Management 8(2), 253–270, https://doi.org/10.1108/IJCCSM-01-2014-0017.

Tessema, Y. A., Aweke, C. S., Endris, G. S. (2013): Understanding the process of adaptation to climate change by small-holder farmers: the case of east Hararghe Zone, Ethiopia. Agricultural and Food Economics 1: 13, https://doi.org/10.1186/2193-7532-1-13.

Wagesho, N., Yohannes, E. (2016): Analysis of rainfall variability and farmers' perception towards it in agrarian community of Southern Ethiopia. Journal of Environment and Earth Science 6(4), 99–107.

Wedajo, G. K., Muleta, M. K., Gessesse, B., Koriche, S. A. (2019): Spatiotemporal climate and vegetation greenness changes and their nexus for Dhidhessa River Basin, Ethiopia. Environmental Systems Research 8:31, https://doi.org/10.1186/s40068-019-0159-8.

Loneliness and the changing care landscape for the elderly in Albania

Majlinda Nesturi[1,*], Irida Agolli Nasufi[2]

[1] Charles University, Faculty of Science, Department of Demography and Geodemography, Czechia
[2] University of Tirana, Social Science Faculty, Department of Social Work and Policy, Albania
[*] Corresponding author: majlindanesturi@gmail.com

ABSTRACT

Albania is currently experiencing a notable demographic shift marked by a substantial increase in its aging population, aligned with the theory of demographic transition. With an emphasis on senior care processes and the prevalence of loneliness among the elderly, this paper explores the difficulties presented by this demographic transition. Key factors of loneliness, such as age, health status, frequency of social interactions, internet access, and the presence of close social ties, were discovered using logistic regression analysis on data from the "Elderly and Loneliness" survey carried out in Albania. As conventional family structures deteriorate and migration continues to influence care dynamics, the results highlight the vital role that comprehensive care systems play in reducing loneliness. To enhance the well-being of Albania's senior citizens, the report emphasizes the urgent need for legislative changes that prioritize digital inclusion, long-term care infrastructure, and community-based social support networks. This study offers an approach for tackling the dual issues of loneliness and caregiving in an aging society by tying empirical findings to practical suggestions.

KEYWORDS

aging population; elderly care; loneliness; long-term care; care drain

Received: 19 September 2024
Accepted: 10 January 2025
Published online: 6 February 2025

Nesturi, M., Nasufi, I. A. (2025): Loneliness and the changing care landscape for the elderly in Albania. AUC Geographica 60(1), 105–114
https://doi.org/10.14712/23361980.2025.3

1. Introduction

Albania is undergoing a significant shift marked by a decline in the overall population and a simultaneous rise in the elderly, challenging the country's social fabric. By 2050, the percentage of people 65 and older is expected to increase from 16% in 2022 to about 29% (IOM 2022). The social fabric of Albania faces significant challenges because of this change, as well as falling fertility rates, younger generations leaving the country, and the breakdown of traditional family caregiving systems. In Albanian society, elderly people are among the most vulnerable groups due to the growing problems of social isolation, economic instability, and insufficient care services. One of the most pressing issues among the elderly is loneliness, which has been widely recognized as a significant risk factor for mental and physical health problems, as well as a barrier to successful ageing (Holt-Lunstad et al. 2015). In Albania, approximately 24% of elderly individuals experience severe or extreme loneliness, with this figure expected to grow as the population continues to age (Keck 2022). While the problem of loneliness is well-documented globally, there is limited research that explores its specific determinants within Albania's unique socio-economic and cultural context.

The results of the 2021 "Elderly and Loneliness" survey, which first used a linear regression model to pinpoint broad risk factors for loneliness among the elderly, are the foundation of this study. This study uses logistic regression to provide a more comprehensive examination of the factors that contribute to severe loneliness.

Furthermore, Albania, a country going through major demographic changes that have significantly altered traditional caregiving methods, is the focus of this study.

The aim of this study is to investigate the interplay between demographic aging, caregiving practices, and loneliness among Albania's elderly population. Using data from the "Elderly and Loneliness" survey, this study identifies key determinants of loneliness, including health status, age, and social interactions, and examines their implications for senior care policies. By bridging empirical insights with theoretical frameworks like the life course approach and successful aging model, this paper aims to provide actionable recommendations for addressing Albania's evolving care challenges while also examining the relationship between demographic ageing, caregiving practices, and loneliness among the country's elderly population.

This paper is structured as follows: the next section provides an overview of Albania's demographic development and the socio-economic conditions of its elderly population. This is followed by a detailed discussion of caregiving practices and their gendered dimensions, with an emphasis on how migration and socio-cultural changes have disrupted traditional support systems. The empirical findings, based on logistic regression analysis, are presented to highlight the key determinants of loneliness among elderly Albanians. Finally, the paper concludes by proposing policy interventions to mitigate loneliness and improve care for Albania's aging population.

2. Background and context

2.1 Demographic development

Albania, as one of the last countries in Europe, is now experiencing the impact of population aging, a phenomenon characterized by a progressively larger proportion of older individuals within the overall population. Over the past two decades, the country has undergone an unprecedented demographic shift, witnessing a notable increase in the proportion of elderly individuals, defined as those aged 65 years and older. Simultaneously, there has been a corresponding decline in the proportion of children and young adults.

The demographic transition signals a significant change in the age distribution, necessitating policymakers to foresee and tackle the far-reaching consequences that will materialize over the coming decades. This demographic shift affects political, social, and economic domains, presenting both opportunities and challenges for the country's future. Policymakers must strategically plan and adopt flexible policies to address these changes, ensuring the requirements of various age groups are met. Between 2011 and 2022, the total population in Albania decreased by approximately 130,000 inhabitants, reflecting a decline of nearly 4.4% (INSTAT 2023). This period marked a reduction of 5.5% among males and 3.3% among females, underscoring the dynamic nature of Albania's population landscape.

Over the same period, the median age increased significantly from 32.6 years in 2011 to 38.8 years in 2022, reflecting the country's demographic aging dynamics. The life expectancy trend has also shifted, with a slight initial increase before the COVID-19 pandemic reduced empirical values. While the proportion of children (0–14 years) decreased from 21.1% in 2011 to 16.2% in 2022, the elderly population (65+) increased from 11.2% to 16.1%. Projections indicate that by 2050, the elderly population will increase to 29% of Albania's total population (IOM 2022). These trends show the urgency of addressing the needs of an aging population through good planning and proactive policy interventions.

The shifting age structure is reflected in Albania's dependency ratios. While the young-age dependency ratio declined from 31.2% in 2011 to 23.9% in 2022, the old-age dependency ratio increased from 16.5% to 23.8% over the same period. Projections for 2050 suggest that the young-age dependency ratio will

continue to decrease, while the old-age dependency ratio will rise sharply to 46.9% (IOM 2022). This transition highlights the closing of Albania's demographic window of opportunity and emphasizes the critical need for policies that address the social and economic implications of an aging population.

2.2 Albanian care practices and gender roles

Complex dynamics influenced by social, cultural, and historical aspects are revealed when the care practices of Albanian households are examined. Strong ties between generations and extended family structures have long been features of Albania, and they have historically encouraged elder care. However, this paradigm has been upset by huge emigration, especially among younger generations, which has left many older people living alone and at higher risk of social isolation.

Since women have traditionally performed the majority of unpaid caregiving duties, the care industry is still strongly gendered. Even though women's rights made great strides under communism, traditional gender norms still hold sway in the post-communist era. The state's role in providing social aid was greatly reduced, and the family was repositioned as the main social network. Consequently, women are disproportionately responsible for providing care, which exacerbates gender inequality (Gjonca, Aassve, and Mencarini 2008).

Caregiving methods and family structures have been further altered by migration. Emigrants' remittances are an important source of revenue that support "transnational caring practices" such as frequent trips back to the place of origin, long-distance communication, and financial support (Baldassar 2007). These methods, however, frequently can't fully replace providing direct care. According to De Soto et al. (2002) and King and Vullnetari (2006), many elderly Albanians, especially those living in rural regions, have become "orphan pensioners," abandoned by emigrant children and left with little social support.

Albanian family structures are changing from extended to nuclear, bringing with them both new potential and challenges. Even if it's becoming more and more necessary, outsourcing elder care frequently goes against the norm. According to research, between 85 and 90 percent of older people want to age in place (AARP 2021), but there are still few official long-term care options available. Women caregivers, especially older women themselves, are disproportionately affected by this dependence on family care, which prolongs stress and task imbalances (HelpAge International 2017).

2.3 Situation of the elderly in Albania

The elderly population of Albania is particularly vulnerable due to their socioeconomic and health situations. The number of elderly people in Albania is expected to almost double by 2050, which will make the sustainability of the nation's social structures difficult to maintain (IOM 2022). Many older people have financial instability and are frequently unable to meet their fundamental necessities, such as having access to prescription drugs. Hospitalization is common for people with serious illnesses, but without family caregivers, they experience social and physical isolation (ASAG 2015).

Elderly people get much lonelier when their children migrate and leave them behind. According to a 2017 Albanian Network of Ageing survey, 8% of senior citizens reported no interaction with friends or relatives, with social isolation being more common among women and the extremely old (UNFPA 2019). The psychological effect that loneliness takes on people's health and well-being is shown by these findings. The elderly are further marginalized by social isolation, which is exacerbated by the ending of job relationships. This reduces their prospects for meaningful engagement in society.

Interventions to improve chances for voluntary labor and encourage community involvement are crucial, even while state services are still insufficient to meet these issues. Comprehensive policy initiatives that incorporate social, economic, and health dimensions are necessary to address loneliness and enhance caring systems (UNFPA 2019).

3. Introduction to the theoretical framework

A solid theoretical basis is necessary to comprehend the factors that contribute to loneliness in the elderly. This study conceptualizes and analyzes loneliness in the Albanian context using three major frameworks: the life course approach, the theory of successful aging, and attribution theory. Together, these ideas shed light on the behavioral, psychological, and social elements that contribute to loneliness. They also serve as a framework for interpreting research results and developing policy recommendations.

In their idea of successful aging, Rowe and Kahn (1997) highlight the difference between "usual ageing" and "successful ageing." The latter is characterized as a process by which people preserve their cognitive and physical abilities, resist off illness, and actively participate in life. This biological paradigm emphasizes that retaining independence and leading a healthy lifestyle are essential elements of aging successfully. According to effective aging theory, loneliness in the elderly is influenced by social interaction and physical health in the context of this study. More social isolation and less social engagement are frequently linked to poor health, less mobility, and impaired cognitive functioning, which increases one's vulnerability to loneliness. This study supports

the ideas of successful aging by identifying important factors of loneliness, such as health and social interaction frequency, and emphasizes the necessity of interventions that support active and independent living among Albania's senior citizens.

According to the life course theory, aging is a dynamic process that is influenced by a person's lifetime interactions with social, economic, and biological elements (Dannefer 2003). This viewpoint questions fixed ideas of "natural stages of life" and emphasizes how aging outcomes are influenced by a combination of experiences, such as social settings, personal habits, and life events (Townsend 2007). This approach is especially pertinent in the Albanian setting, where conventional caregiving practices have been significantly altered by migration, demographic shifts, and socioeconomic changes. For instance, many older people are socially isolated as a result of the dissolution of intergenerational housing patterns and the emergence of transnational caregiving practices. The life course approach emphasizes how critical it is to address loneliness risk factors at an early age because they build up and become apparent as people age. Later in life, policies that promote healthy behaviors and enhance social networks in order to reduce risk factors in childhood and middle age are likely to improve mental and physical health (Walker 2002).

Attribution theory (Lunt 1991) provides a psychological lens to understand how loneliness may become chronic. According to this theory, lonely individuals often attribute their loneliness to uncontrollable external causes, which perpetuates dysfunctional attitudes such as fear of rejection, social embarrassment, and high levels of social anxiety (Marangoni and Ickes 1989). These negative attributional styles can create a cycle of avoidance and further isolation, exacerbating loneliness. Attribution theory clarifies how psychological elements interact with sociocultural shifts to impact loneliness in the Albanian setting, where social and familial bonds are rapidly changing. One potential strategy to lessen social isolation among older persons is the usage of the internet. By creating a sense of connection and belonging, online relationships can help fight loneliness, especially for older people who are not physically close to their family and friends. How these virtual encounters could lessen negative self-perceptions and encourage constructive social participation is explained by attribution theory.

The three theories provide a framework for comprehending loneliness among the elderly in Albania. While the life cycle approach stresses the cumulative impact of behavioral and socioeconomic factors over time, successful aging theory places more emphasis on the importance of health and social engagement. From a psychological point of view, attribution theory explains how unhelpful cognitive habits can contribute to loneliness. These frameworks work together to direct the study of loneliness and provide guidance for the formulation of policy suggestions intended to reduce social isolation and enhance the welfare of Albania's elderly population.

4. Data and method

This study is based on individual-level data collected through the "Elderly and Loneliness" survey conducted in 2021. The survey was a collaborative effort between University College London (UCL), UNFPA Albania, and the Institute of Statistics (INSTAT), which oversaw its implementation and data collection. The primary objective of the survey was to establish a standardized methodology for generating, analyzing, and disseminating indicators to enhance understanding of Albania's elderly population (refer to Keck for the technical report).

The target population consisted of individuals aged 65 to 85 years, with an equal gender distribution. A multi-stage stratified sampling approach was used to ensure representativeness at the national level, with stratification by region and proportional allocation based on population size. The sample consisted of 1,106 respondents, carefully selected to ensure national-level representativeness through a multi-stage stratified sampling approach. Key demographic characteristics of the sample are:

- sex distribution: 50% females and 50% males
- median age: 71 years old

By delineating these indicators across demographic and social dimensions, the survey seeks to provide a comprehensive and nuanced perspective on the circumstances of the elderly population in Albania, contributing valuable insights to address and improve their overall well-being.

In order to go deeper to the factors and specificities of the factors that the elderly in Albania face for being or feeling lonely. Logistic regression analysis is used to statistically explain the factors of feeling lonely. Our dependent variable is Loneliness, which was derived using 11 items on the De Jong Gierveld Loneliness Scale. This was collapsed into a binary variable distinguishing between those who feel moderately lonely (58%) or do not feel lonely at all (18.5%) and those who feel severely (19%) and extremely lonely (4.3%). Self-perceived health status, which was measured categorically and collapsed into three answer options: good and very good (35%), fair (45.5%), and bad (22.1%). The availability of an internet connection at home, which is a binary variable, yes (45.5%) or no (54.5%).

As explanatory variables we took some specific questions which shown to be significant when explaining the dependent variable. The explanatory variables are:

1. Age
2. Frequency of meeting friends and family members
3. Health status
4. Availability of internet connection

5. Results

According to the findings of the report (Keck 2022), variables such as: age, frequency of interactions with friends and family members, and having friends and family members to talk to were significant in our analysis. Tab. 1 provides bivariate evidence supporting the hypotheses that elderly individuals who experience loneliness are more likely to report poor health, lack internet access, have fewer close friends and family members to talk to, and engage less frequently in social interactions with friends. Additionally, as highlighted in the report by Keck (2022), the analysis reveals that the median age of elderly individuals who feel lonely is higher compared to those who do not experience loneliness, aligning with expectations.

The control variables show the expected associations, indicating that they represent alternative influences on loneliness. Specifically, we used the level of satisfaction with the financial situation and the marital status (married or not married/widowed, divorced or single) as control variables. Previous studies have repeatedly shown that financial instability and marital status are important factors influencing older individuals' feelings of loneliness. Higher degrees of loneliness are closely associated with marital status, especially being widowed or divorced, as a result of the loss of the social and emotional support that a partner used to provide. For instance, Essex and Nam (1987) pointed out that elderly women's loneliness is significantly influenced by their marital status, especially when they don't have close family or friends. According to Victor, Scambler, and Bond (2009), widowed or single people are more prone to feel lonely in later life, but marriage acts as a buffer against social isolation. Since it restricts older persons' capacity to participate in social activities and uphold meaningful connections, financial instability has also been recognized as a significant driver. In their meta-analysis, Pinquart and Sörensen (2010) discovered that loneliness is significantly predicted by economic insecurity, especially for people who have little access to resources or community services.

Multivariate analysis was conducted using logistic regression to examine the independent effects of various predictors on loneliness. This approach allowed us to assess the contribution of each variable (e.g., age, health status, internet access, social interaction) while controlling for the influence of others. The analysis was conducted in three steps, starting with core predictors in Model 1, followed by the inclusion of financial satisfaction in Model 2, and finally adding marital status variables in Model 3. The results are presented as odds ratios, with decreasing -2 Log-Likelihood values across models indicating improved model fit.

As illustrated in Model 1 below, an increase in age is associated with higher odds of feeling lonely. Specifically for each additional year of age, the odds of feeling lonely increase by 1.419 times. Moreover, our analysis revealed that individuals who reported meeting friends or family members less frequently were more likely to feel lonely. Individuals who do not interact at all with friends and family members have a 5.6 times higher probability of feeling lonely compared to those who meet daily. Health status is a crucial factor that influences feelings of loneliness. It affects various aspects of an individual's life, including their quality of life, social interactions, and social support, which in turn can impact feelings of loneliness. In your analysis, health status was assessed using a question that asked individuals to evaluate their general health. The results indicate that individuals who rated their health status as poor were 6.2 times more likely to feel lonely. These findings suggest that there is a significant association between health status and loneliness, with poorer health status being associated with higher odds of feeling lonely. In our study on loneliness among the elderly in Albania, we investigated the impact of having an internet connection at home on feelings of loneliness. The availability of internet connection was seen as a facilitator for staying in touch with friends and family members, potentially mitigating feelings of social isolation.

Our findings revealed that individuals who reported not having an internet connection at home were 1.67 times more likely to feel lonely compared to those who had access to the internet. This suggests that internet connectivity plays a significant role in shaping social interactions and support networks, particularly among the elderly population. These results underscore the importance of digital connectivity in combating loneliness, especially in contexts where physical interactions may be limited. Policies and interventions that promote internet access and

Tab. 1 The incidence of feeling lonely by health status, internet access, frequency of meeting friends and family members and median age.

	Good and very good health	Fair health	Poor health	Internet connection at home (yes)	Internet connection at home (no)	Meet friends frequently (yes)	Meet friends frequently (no)	Median age
No Lonely	92%	76%	55%	85%	69%	81%	59%	70 years
Lonely	8%	24%	45%	15%	31%	19%	41%	74.5 years
Total	100%	100%	100%	100%	100%	100%	100%	

Note: all differences are statistically significant at $p < 0.01$, N = 1106.

Tab. 2 Loneliness: Odds ratios from logistic regression models.

	Model		
	1	2	3
Age	1.419	1.510	1.371
Health status (good and very good)			
Fair	3.443	2.723	2.864
Poor	6.208	4.585	4.721
Internet connection at home (no)	1.672	1.515	1.423
Family and friends interactions (daily)			
Once or twice a week	2.705	2.543	2.447
Once a month or less	4.695	4.216	4.162
No friends or family members	5.628	4.912	4.662
Satisfied with financial situation (no)		2.004	1.973
Not married (widowed, divorced or single)			1.623
−2LL	991.012	978.479	966.067
Nagelkerke R Square	0.247	0.262	0.271
N	1106	1106	1106

Note: The dependent variable is Loneliness. In the table are given the odds ratios. All coefficients are significant at $p < 0.05$.

digital literacy among the elderly could help enhance social connectedness and reduce feelings of loneliness in this vulnerable population.

Models 2 and 3 in Tab. 2 add an additional control variable each to demonstrate the robustness of the findings. The addition of these variables does not increase the model fit significantly, nor are the explanatory variables affected in a substantive way. The reduction factors calculated between Model 1 and the subsequent models (Model 2 and Model 3) indicate that the odds ratios for the primary predictors of loneliness, such as age, health status, internet connection, and social interactions, experience only minor changes after adding control variables. Specifically, the reductions in odds ratios for key variables, such as health status (fair and bad), internet access, and family and friends' interactions, remain modest, ranging between approximately 5% and 27%. These changes are within acceptable limits and do not alter the direction or significance of the predictors.

Variables like financial satisfaction and marital status refine the model by explaining additional variance in loneliness. However, they do not fundamentally alter the relationships observed in Model 1. The reduction in likelihood values (−2LL) indicates a slight improvement in model fit with the addition of controls without fundamentally altering the primary findings.

For reasons of multicollinearity and lack of strong theoretical reasons we have refrained from adding additional variables in the models presented here; the models presented in Tab. 2 have a VIF less than 1.3 suggesting that multicollinearity is not a concern. Additional tables presenting the significance of the variables in the models are provided in Appendix 1 and Appendix 2 for further reference.

6. Limitations

A number of limitations should be noted, even if the survey offers insightful information about the variables affecting loneliness among Albania's senior citizens. First, the study's cross-sectional design limits the capacity to draw conclusions about the causal relationship between loneliness and the factors that were found. To determine causal linkages and look at changes over time, longitudinal studies would be required.

Second, using self-reported measures raises the possibility of response bias. Due to personal views or social desirability bias, loneliness and health status are subjective experiences that may be overstated or underreported. This is especially true for sensitive topics like loneliness, which in some cultural contexts may be stigmatized and cause respondents to give responses they feel are more acceptable in the eyes of others.

Third, some qualitative aspects of loneliness and caregiving that could offer a deeper understanding of the underlying social and emotional dynamics are not included in the study. For example, the study does not adequately address the role of informal caregiving arrangements, personal coping strategies, and cultural norms.

7. Discussion

7.1 Key determinants of loneliness

This study demonstrates the complex connection between demographic aging, loneliness, and caregiving challenges in Albania. The results highlight several important factors that contribute to loneliness among the elderly, such as age, social interaction frequency, health status, internet access, and the availability of close social connections. Although these findings are consistent with findings on loneliness in aging populations around the world, they also highlight difficulties that are specific to Albania's sociocultural and economic context, especially regarding caregiving practices.

Our analysis of loneliness among the elderly in Albania highlights several significant factors. Age was found to be positively associated with loneliness, with each additional year of age increasing the odds of feeling lonely. Frequency of interactions with friends and family members also played a crucial role, with less frequent interactions leading to higher odds of loneliness. Furthermore, having close friends and family members to talk to was found to be protective against loneliness, findings which are in line with the study report on Loneliness and Social Isolation in Eastern Europe and Central Asia.

Even though health status and availability of internet connection at home seemed to be insignificant to explain the loneliness, for Albania these factors turned up to be significant. According to a number of studies

older adults who use the internet report feeling less lonely (Cotten, Anderson, and McCullough 2013; Morris et al. 2014). Elderly people now have a new means of communication with their peers, families, and the wider community – the internet (Khvorostianov 2016). A study by Sum et al. (2008) reports that seniors who use the internet more frequently for communication report that they feel less socially isolated.

When it comes to helping older people who are less mobile because of their health issues maintain social connections, the internet can be especially helpful (Heo et al. 2015). Unfortunately, having physical health problems can lead to loneliness as well as be a cause of it. This is especially true if those problems make it difficult for a person to engage in social activities. When taken as a whole, these detrimental impacts on physical health could help to explain why loneliness raises the risk of dying (HoltLunstad et al. 2015). Living alone and having poor health makes it 10 times more likely to feel lonely than living with someone and having good health (Sundström et al. 2008).

Health status emerged as a key factor influencing loneliness, with individuals reporting fair or poor health status being significantly more likely to feel lonely compared to those with good or very good health, while the availability of internet connection at home was found to be associated with lower odds of loneliness, highlighting the importance of digital connectivity in combating social isolation among the elderly.

7.2 Challenges in caregiving practices

Economic constraints have further compounded the lack of formal care systems, as many elderly people lack the financial means to access private care services or the digital tools necessary to stay connected with family members. According to the empirical findings, there is a significant gap in the availability of formal long-term care services in Albania. The lack of a robust care infrastructure places an overwhelming burden on families, especially women, who continue to handle the majority of caregiving responsibilities. However, migration and the resulting "care drain" have weakened the capacity of families to provide consistent support, leaving many elderly people at risk of social marginalization and neglect. Albania lacks an official definition of long-term care, resulting in no formal system. Provisions are found in various laws, but they do not establish a comprehensive, complementary system. In Albania, older people's long-term care heavily relies on informal care, with working adult children hiring informal workers.

7.3 Policy implications

The results point to several legislative measures that could close the gap between the infrastructure and the needs of caregiving:

1. Creating a formal long-term care system: The development of an integrated care system that offers senior citizens accessible and affordable care must be a top priority for policymakers. This covers residential facilities, day centers, and home-based care.
2. Strengthening community-based support: By encouraging social interaction and relationships, community-based activities like volunteer programs and senior activity centers may reduce loneliness.
3. Encouraging digital inclusion: Programs that improve seniors' digital literacy and offer reasonably priced internet services ought to be put into place, as internet access plays a crucial part in reducing loneliness.
4. Addressing gendered caregiving burdens: By encouraging fair caregiving behaviors and offering official support networks, policies must recognize and reduce the unequal burden that women bear when providing care. Caregivers' physical and mental well-being and skills-based care competencies are crucial for older people's care, as they often form a critical part of the unpaid workforce.

7.4 The link between loneliness and care systems

This study clearly shows the link between loneliness and providing care. Loneliness is significantly predicted by both poor health and a lack of social connections, which are indicative of larger issues with Albania's care system. The results emphasize the necessity of a comprehensive approach to caregiving that promotes social inclusion, emotional well-being, and physical health. This necessitates a change from depending on family care to a more structured system that can sustainably and fairly address the requirements of Albania's aging population.

While this study provides important insights, future research should explore the intersection of caregiving and loneliness in greater depth. Longitudinal studies are needed to assess the impact of emerging care policies and interventions on the well-being of Albania's elderly population.

8. Conclusions

The aging dynamics of Albania's population are considerably high, even though we are not too far from the beginning of this unavoidable long-term process. The observed changes are entirely in line with the theory of demographic transition. The demographic process of population ageing poses a strong task to policy makers and civil society organisations to address such issues and to create opportunities for the increasing shares of elderly to participate in today's and tomorrow's society in an active and productive way. The landscape of care practices among

Albanian households is shaped by the complex interactions between historical legacies, cultural norms, migratory patterns, and economic realities. Comprehending these relationships is crucial in tackling the obstacles encountered by the elderly and cultivating more just and encouraging caring structures.

Research revealed that the lack of a formal long-term care system puts elderly people in an unsafe and vulnerable condition that is seriously dangerous for their physical and mental health, even with the new legislative measures in the social and protective system (Jorgoni and Musabelliu 2021). An important social and economic role is played by long-term care. It helps safeguard the basic rights of individuals in need of care and ensures their well-being and life in dignity. Additionally, it lessens inequality, enhancing social justice and generational unity. Family members may be forced to provide care when there is insufficient formal long-term care, which may have a detrimental effect on their health and general well-being.

Having into consideration the changing family structures and the demographic projections on population decline, the importance to establish a Long-Term Care system has become a priority. The weakening of traditional family links and bottlenecks of social and protection welfare systems, place a great burden on care delivery for elder populations who are faced with socio-economic constraints and social isolation. Older people in Albania are excluded from the opportunity to have a decent life, due to their inability to afford their daily life expenses, social exclusion and isolation. Therefore, due to recent social and demographic changes, and inadequacies of care infrastructure, Albania is faced with the "care drain" phenomenon, which has led to increased demand for an efficient and integrated care system for elder persons. Having in mind the decentralization reform and the fact that services should be closer to citizens, there is a need for enhancing community-based social care and healthcare services for elderly people.

A thorough, multidimensional approach to senior care that incorporates social, economic, and digital aspects is necessary to meet these issues. Priority should be given to the establishment of a formal long-term care system that provides accessible and reasonably priced residential, community-based, and home-based care options. By encouraging relationships among the elderly, community assistance services like senior activity centers and volunteer programs can encourage social inclusion and lessen loneliness. Programs for digital inclusion that improve internet access and digital literacy are also essential for increasing social involvement and opening up new channels for interaction and communication. In addition, gender-sensitive policies are necessary to provide a more equitable distribution of caregiving obligations and lessen the burden of caregiving on women.

From a broader perspective, this study emphasizes how Albania must move away from an excessive dependence on unofficial caregiving and toward a more organized and long-lasting care system. Designing and implementing policies that meet the needs of an aging population while advancing social justice and generational parity requires cooperation from local communities, civil society organizations, and policymakers. Building resilience in the face of demographic changes and creating an atmosphere that allows the elderly to age with health, dignity, and active engagement in society must also be the main goals of such initiatives.

Future research should use longitudinal methods to examine the long-term effects of new policies and interventions, even if this study offers insightful information on the factors that contribute to loneliness and caregiving difficulties in Albania. Furthermore, more research into technology's involvement in managing loneliness and community-based solutions may provide creative avenues for enhancing senior citizens' quality of life.

In conclusion, there are opportunities as well as challenges associated with Albania's demographic shift. Albania can create a more welcoming and encouraging care system by addressing the social, emotional, and physical needs of the elderly through comprehensive policies and initiatives. In order to guarantee the health and dignity of its aging population in the years to come, proactive steps to improve social inclusion, advance digital literacy, and create official caring structures are essential.

References

AARP Study (2021): Home and community preferences survey. Available online https://www.aarp.org/pri/topics/livable-communities/housing/2021-home-community-preferences/ (accessed on 5.3.2024).

ASAG (2015): Older persons are an asset to and make a significant contribution to global development [Press release].

Baldassar, L. (2007): Transnational families and the provision of moral and emotional support: The relationship between truth and distance. Identities 14(4), 385–409, https://doi.org/10.1080/10702890701578423.

Bart de Bruijn, G., Filipi, G., Nesturi, M., Galanxhi, E. (2015): Population ageing: The elderly situation in Albania. Tirana: INSTAT. Available online: https://www.instat.gov.al/media/3550/population_ageing_situation_of_elderly_people_in_albania.pdf (accessed on 5. 3. 2024).

Carreiro, S. (2012): Gender differences and perspectives on elderly care in China. Undergraduate Review 8, 145–151. Available online: https://vc.bridgew.edu/undergrad_rev/vol8/iss1/26 (accessed on 10. 2. 2024).

Cotten, S. R., Anderson, W. A., McCullough, B. M. (2013): Impact of internet use on loneliness and contact with others among older adults: Cross-sectional analysis.

Journal of Medical Internet Research 15(2): e39, https://doi.org/10.2196/jmir.2306.
Dannefer, D. (2003): Cumulative advantage and the life course. Journal of Gerontology: Series B 58(6), S327–S337, https://doi.org/10.1093/geronb/58.6.S327.
Danaj, E. (2014): Family in Albania as a primary solidarity network. In R. Pichler (Ed.), Legacy and Change: Albanian transformation from multidisciplinary perspective 117–134. LIT Verlag.
De Soto, H., Gordon, P., Gëdeshi, I., Sinoimeri, Z. (2002): Poverty in Albania: A qualitative assessment. World Bank technical Paper WTP 520 Washington, D.C.: World Bank Group, https://doi.org/10.1596/0-8213-5109-5.
Essex, M. J., Nam, S. (1987): Marital Status and Loneliness among Older Women: The Differential Importance of Close Family and Friends. Journal of Marriage and Family 49(1), 93–106, https://doi.org/10.2307/352674.
Gjonca, A., Aassve, A., Mencarini, L. (2008): Albania: Trends and patterns, proximate determinants and policies of fertility change. Demographic Research 19(11), 283–284, https://doi.org/10.4054/DemRes.2008.19.11.
Heo, J., Chun, S., Lee, S., Lee, K. H., Kim, J. (2015): Internet use and well-being in older adults. Cyberpsychology, Behavior and Social Networking 18(5), 268–272, https://doi.org/10.1089/cyber.2014.0549
HelpAge International (2017): Investing in an ageing world: Shifting debates from costs to investments. London: HelpAge International. Available online: https://www.helpage.org/silo/files/investing-in-an-ageing-world-.pdf (accessed on 5. 2. 2024).
Holt-Lunstad, J., Smith, T. B., Baker, M., Harris, T., Stephenson, D. (2015): Loneliness and Social Isolation as Risk Factors for Mortality: A Meta-Analytic Review. Perspectives on Psychological Science 10(2), 227–237, https://doi.org/10.1177/1745691614568352.
ILO (2023): Long-term care for the elderly in Albania: Challenges and key policy issues. Available online: https://www.ilo.org/publications/long-term-care-elderly-albania-challenges-and-key-policy-issues (accessed on 5. 3. 2024).
INSTAT (2023): Population data. Available online: https://databaza.instat.gov.al:8083/pxweb/en/DST/START__DE/NewPOP_0001/table/tableViewLayout1/ (accessed on 5. 3. 2024).
Jorgoni, E., Musabelliu, E. (2021): ESPN thematic report on long-term care for older people – Albania. European Social Policy Network (ESPN), Brussels: European Commission. Available online: https://ec.europa.eu/social/BlobServlet?docId=24029andlangId=en (accessed on 5. 3. 2024).
Keck, T. (2022): Loneliness and social isolation among older people in the Eastern Europe and Central Asia region. Available online: https://eeca.unfpa.org/sites/default/files/pub-pdf/loneliness_study_english.pdf (accessed on 15. 2. 2024).
King, R., Vullnetari, J. (2006): Orphan pensioners and migration grandparents: The impact of mass migration on older people in rural Albania. Ageing and Society 26(5), 783–816. Cambridge University Press, https://doi.org/10.1017/S0144686X06005125.
Khvorostianov, N. (2016): "Thanks to the Internet, We Remain a Family": ICT Domestication by Elderly Immigrants and their Families in Israel. Journal of Family Communication 16(4), 355–368, https://doi.org/10.1080/15267431.2016.1211131.
Lerch, M. (2016): Internal and international migration across the urban hierarchy in Albania. Population Research and Policy Review 35(6), 851–876, https://doi.org/10.1007/s11113-016-9404-2.
Lunt, P. K. (1991): The perceived causal structure of loneliness. Journal of Personality and Social Psychology 61(1), 26–34, https://doi.org/10.1037/0022-3514.61.1.26.
Marangoni, C., Ickes, W. (1989): Loneliness: A theoretical review with implications for measurement. Journal of Social and Personal Relationships 6(1), 93–128, https://doi.org/10.1177/026540758900600107.
Morris, M. E., Adair, B., Ozanne, E., Kurowski, W., Miller, K. J., Pearce, A. J., Said, C. M. (2014): Smart technologies to enhance social connectedness in older people who live at home. Australasian Journal on Ageing 33(3), 142–152, https://doi.org/10.1111/ajag.12154.
Musabelliu, M. (2022). Albania social briefing: The hardships of the elderly in Albania. China CCE Institute 50(3), Budapest. Available online: https://china-cee.eu/wp-content/uploads/2022/12/2022s12_Albania.pdf (accessed on: 15. 3. 2024).
Podgorica, N., Zenelaj, B., Deufert, D., Ganner, M., Flatscher-Thöni, M. (2020): A Narrative Review on Legal Aspects of Older People in Albania. Journal of Educational and Social Research, 10(5): 88, https://doi.org/10.36941/jesr-2020-0090.
Pinquart, M., Sorensen, S. (2010): Influences on Loneliness in Older Adults: A Meta-Analysis. Psychology and Aging 23(4), 245–266, https://doi.org/10.1207/1532483017 53225702.
Rowe, J. W., Kahn, R. L. (1997): Successful Aging. The Gerontologist 37(4), 433–440, https://doi.org/10.1093/geront/37.4.433.
Sundström, G., Fransson, E., Malmberg, B., Davey, A. (2008): Loneliness among older Europeans. European Journal of Ageing 6, 275–267, https://doi.org/10.1007/s10433-009-0134-8
Sum, S., Mathews, R. M., Hughes, I., Campbell, A. (2008): Internet use and loneliness in older adults. Cyberpsychology and Behavior 11(2), 208–211, https://doi.org/10.1089/cpb.2007.0010.
Townsend, P. (2007): Using human rights to defeat ageism: Dealing with policy-induced structured dependency. In M. Bernard and T. Scharf (Eds.), Critical Perspectives on Ageing Societies 27–44. Polity Press, https://doi.org/10.2307/j.ctt9qgpgh.9.
UNFPA (2019): The national action plan on aging 2020–2024. Available online: https://acpd.org.al/wp-content/uploads/2021/01/PLANI-KOMBËTAR-I-VEPRIMIT-MBI-MOSHIMIN-Anglisht.pdf (accessed on 20. 2. 2024).
Victor, C., Scambler, S., Bond, J. (2009): The Social World of Older People: Understanding Loneliness and Social Isolation in Later Life. Maidenhead: Open University Press.
Walker, A. (2018): Why the UK Needs a Social Policy on Ageing. Journal of Social Policy 47(2), 253–273, https://doi.org/10.1017/S0047279417000320.

Appendix 1 Logistic regression results for predictors of loneliness among elderly in Albania.

	B	S.E.	Wald	df	Sig.	Exp(B)	95% C.I. for EXP(B)	
							Lower	Upper
Age	0.316	0.135	5.507	1	0.019	1.371	1.053	1.786
Health status (good and very good)			37.306	2	0.000			
Fair	1.052	0.234	20.300	1	0.000	2.864	1.812	4.527
Bad	1.552	0.254	37.265	1	0.000	4.721	2.868	7.771
Internet connection at home (no)	0.353	0.175	4.085	1	0.043	1.423	1.011	2.004
Family and friends' interactions (daily)			36.547	3	0.000			
Once or twice a week	0.895	0.213	17.652	1	0.000	2.447	1.612	3.715
Once a month or less	1.426	0.246	33.602	1	0.000	4.162	2.570	6.741
No friends or family members	1.539	0.445	11.952	1	0.001	4.662	1.948	11.159
Satisfied with financial situation (no)	0.680	0.202	11.318	1	0.001	1.973	1.328	2.932
Not married (widowed, divorced or single)	0.484	0.171	7.994	1	0.005	1.623	1.160	2.270
Constant	−4.237	0.330	165.287	1	0.000	0.014		

Appendix 2 Collinearity diagnostics for predictors in logistic regression model.

Collinearity test			Standardized coefficients	t	Sig.	Collinearity statistics	
			Beta			Tolerance	VIF
(Constant)	−0.338	0.081		−4.180	0.000		
Age	0.051	0.021	0.073	2.424	0.016	0.841	1.189
Health status	0.119	0.018	0.210	6.673	0.000	0.766	1.305
Internet connection at home	0.052	0.025	0.061	2.104	0.036	0.897	1.114
Interactions with friends and family members	0.098	0.016	0.181	6.269	0.000	0.910	1.099
Satisfaction with financial situation	0.090	0.027	0.104	3.360	0.001	0.793	1.261
Marital status	−0.078	0.026	−0.086	−2.939	0.003	0.893	1.120

Note: Dependent variable: LONELINESS

Analysis of watercourses on Aretin's Map of the Bohemian Kingdom from 1619

Miroslav Čábelka*, Tomáš Bayer

Charles University, Faculty of Science, Department of Applied Geoinformatics and Cartography, Czechia
* Corresponding author: miroslav.cabelka@natur.cuni.cz

ABSTRACT
Historic maps provide evidence of landscape development, including the shape of watercourses in the past. Aretin's map of the Bohemian Kingdom (contemporary Czechia) from 1619 is Bohemia's third-oldest map. In this analysis of Aretin's map, we aimed to create an overview of watercourses at the beginning of the 17th century. We used MapAnalyst software to perform cartometric analyses and plotted watercourses on a contemporary map. Special interest was given to watercourses outside of the Bohemian Kingdom, which have not been included in previous analyses of the map. Content, semiotic, and cartometric analyses focusing on watercourses and on changes in the depiction of rivers over the four editions of Aretin's map were performed to identify and label the previously unnamed rivers.

KEYWORDS
old map; Aretin; watercourses; cartometric analysis; 17th century; Bohemia

Received: 25 July 2024
Accepted: 21 January 2025
Published online: 18 February 2025

Čábelka, M., Bayer, T. (2025): Analysis of watercourses on Aretin's Map of the Bohemian Kingdom from 1619.
AUC Geographica 60(1), 115–133
https://doi.org/10.14712/23361980.2025.4

1. Introduction

Cartographic sources, primarily old maps and plans are among the most valuable sources of information about the past. They illustrate development and landscape changes over the defined territory, inform about the geopolitical situation, etc. (Trpáková 2009; Hvizdák 2023). An important part of their content are hydrographic elements, represented by all natural and artificial water areas, watercourses, and surrounding objects.

Watercourses were essential for transport and strategic planning of settlement establishment, but they are skewed and distorted on the old maps (Gregory 2014). The style, completeness, and accuracy of the cartographic representation of watercourses provide evidence of their importance to our ancestors.

The article focuses on analyzing watercourses on Aretin's map of Bohemia, the third oldest cartographic depiction of Bohemia (1619) and its subsequent editions.

It is the first map on which watercourses are comprehensively shown. However, the analyzed map is not based on precise geodetic measurements, so their locations or shapes are distorted and skewed, which was common at the time.

The analyses focused on finding geometrical discrepancies in the hydrographic elements depiction and unnamed watercourses identification, were performed on four copies of Aretin's map from 1619, 1632, 1665, and before 1747, obtained from the Map Collection of the Faculty of Science of Charles University and the National Archives in Prague.

The analyses of rivers on old maps were presented in several papers. Gatta used old georeferenced maps to compare the historical landscape of Bologna with the current state (Gatta 2020). The possibilities of identification and interpretation of cartographic symbols on old maps were described in Gašperič (2023).

The first study of Aretin's map of Bohemia from 1619, was presented by Kuchař and Roubík (1936). Later on, for example, Roubík (1951), Bayer (2009), Semotanová (2001, 2008), Novotná et al. (2022), were focused on cartometric and semiotic analyses, but watercourses were mentioned marginally. Some topographic inaccuracies, especially regarding water-

Fig. 1 Aretin's map of Bohemia, 2nd edition of 1632. Source: Map Collection of the Faculty of Science, Charles University.

courses in eastern Bohemia and the Erzgebirge (Kuchař 1936; Roubík 1951; Novotná et al. 2022) were found.

We generally assume, that the depiction of the watercourses at this time is very general or inaccurate. This paper concentrates on watercourses and water areas analyses in order to find positional inaccuracies in their depiction and identify unknown river names.

Are there some regions on the map, that were more accurately depicted than the others and why? Does it somehow correlate with Aretins experience – e.g. are the regions, where he surely lived and work, more detailed than the others? Georeferenced digital copies of maps and vector layers of watercourses were used for the analyses.

2. Aretin's map of Bohemia

Aretin's map of Bohemia from 1619 is the third oldest map of the Bohemia territory, with four known editions (1619, 1632, 1665, and before 1747). The first two editions are assigned to Paulus Aretin of Ehrenfeld (active between the years 1608 and 1632) Between 1600 and 1608, he worked as a junior scribe in Klatovy. In 1609, he became secretary to the aristocrat Peter Wok of Rosenberg (1539–1611). After three years, he moved to Prague and was awarded the title of Prague burgher.

The third edition of Aretin's map (which was issued after Aretin's death) is assigned to Daniel Wussin (1621–1691), and the fourth (and undated) edition is assigned to his son Kaspar Wussin (1664–1747). The famous Aretin family of engravers, publishers, and booksellers was established in the 17th century by Daniel Wussin, who came from Graz and moved to Prague (Kuchař 1936). The first analysis of Aretin's map of Bohemia (see Fig. 1) entitled "Regni Bohemiae Nova et Exacta Descriptio" (New and Exact Description of the Bohemian Kingdom) presented Kuchař (1959).

The rectangular map frame oriented to the north has dimensions of 574 × 766 mm, its approximate scale is 1 : 504,000 (Kuchař 1936). A detailed explanation of the map symbols was also presented. The settlements depicted by a circle with a dot, emphasized by a silhouetted mask, containing 1157 items (Kuchař 1936), are differentiated into the following categories: free royal towns, towns of the Bohemian king, manorial towns, and villages. Moreover, different map symbols were used to depict fortresses, castles, chateaux, and monasteries. The map also shows relief, vegetation, and water supplies, as well as map labels. The terrain is represented by the hill method with shading; see Fig. 2.

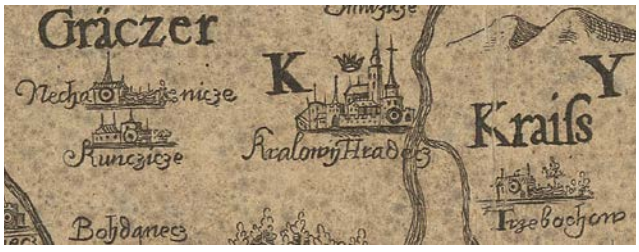

Fig. 2 An example of the representation of the royal town of Hradec Králové, settlements and relief on the 2nd edition of Aretin's map of Bohemia. Source: Map Collection of the Faculty of Science, Charles University.

Compared to the previous maps of Bohemia (Klaudyán's, 1518, and Criginger's, 1568), watercourses are depicted in more detail. Although many rivers are drawn, they remain unnamed. Rivers in Bohemia are connected to foreign streams, but there are many inaccuracies and errors (Novotná et al. 2022). The most visible changes between the fourth editions of Aretin's map refer to the depiction of rivers in eastern Bohemia.

Only two roads are depicted: The Golden Trail, leading through Prachatice, and the New Trail, leading through Český Krumlov. Aretin's map of Bohemia is the first map showing the borders of the 15 regions in Bohemia. The graphic decoration consists of two columns placed next to the left and right frames of the map; they show six male and female figures wearing historical clothing.

The map was engraved and published using the copperplate technique. Kuchař (1958) supposed that all editions were printed from two identical printing plates; differences in topographical content are evident.

The original edition of Aretin's map of Bohemia from 1619 is owned by the National Archives of the Czech Republic, located in Prague, under the inventory number NAD 0324/1256. The other three editions of Aretin's map are part of the Map Collection of the Faculty of Science, Charles University.

3. Methods

The article aimed to perform complex content-based and fundamental cartometric analyses of watercourses on Aretin's map of Bohemia from 1619 and its subsequent editions. Descriptive, comparative, and analytical methods were used to analyze the map content and evaluate the correctness of the watercourses depiction. More specifically, we can determine how watercourses are drawn and described on the map, compare their depiction with the current state, and determine their positional accuracy.

3.1 Content analysis

The map content includes all the objects, phenomena, and their relationships. Contemporary cartography classifies map elements according to their origin,

character, and meaning into four categories: mathematical, physical-geographical, socio-economic, complementary, and semiotic elements (Voženílek 2004).

3.1.1 Mathematical elements

Mathematical elements represent the structural foundation of the map. They include geodetic bases, cartographic representation, map scale, coordinate system, map frame, sheet layout, and map composition (Voženílek 2004).

3.1.2 Socio-economic elements

Settlements are essential elements, often used to localize and identify rivers on the map. According to the map scale, they can be represented in two ways – by point or area cartographic symbols. For the oldest maps of Bohemia territory, the most common representation of settlements uses point symbols (Semotanová 2001); see Fig. 2. Roads joining different locations are represented by linear symbols (Voženílek 2004).

3.1.3 Physical-geographical elements

Physical-geographical elements are objects of living and non-living nature: relief, watersheds, and vegetation cover. Watercourses involve all standing and flowing waters on and under the Earth's surface (oceans and seas, lakes, artificial reservoirs, watercourses, and springs). Flowing watercourses are represented by continuous lines from their confluences to the sources; their thicknesses correspond to the widths. On some old maps, it is possible to see watercourses drawn with the same wide line. For example, Klaudyan's map of Bohemia from 1518.

As mentioned above, the content-based analyses concerned watercourses, water areas, and bridges. The goal was to find and identify all rivers and water areas on Aretin's map of Bohemia in all four editions. Moreover, the topographic accuracy of the watercourses and water areas was also examined.

A specific feature of watercourses on old maps is their linear character. For content-based analysis, it is necessary to georeference the analyzed map and vectorize the watercourses so that the data can easily be overlaid with the current base map. This helps to identify the location and direction of watercourses and water areas (Farooqi 2023; Tsorlini 2014).

3.2 Semiotic analysis

Subsequently, semiotic analysis, focusing on cartographic symbols and their use forming the map language, was performed.

Cartographic symbols can be divided into three categories according to their geometry (point, line, and areal). They have different properties, such as shape, size, structure, filling or orientation.

Linear and areal cartographic symbols are essential for analyzing the watercourses. Linear symbols are used for objects of linear shapes, especially rivers, roads, and streets. Single, double, dotted, or dashed lines and their combinations are frequently used for their graphic representation. Areal symbols, consisting of two components (contour and fill), are suitable for water area representation (Medyńska-Gulij 2013). Regarding Aretin's map, the depiction of watercourses, water areas, and bridges is analyzed in all four editions of the map.

3.3 Description analysis

Object labels are an essential part of the map content, clarifying the qualitative and quantitative features of the map objects. Old maps use various font styles, sizes, and languages. The geographical names of watercourses are generally called hydronyms. The analyses of watercourses, water areas, and bridge labels on Aretin's map of Bohemia is involved.

3.4 Cartometric analyses

Using modern tools, cartometric analyses of old maps allow verification and evaluation of their geometric accuracy. They provide helpful information about map construction, geodesic bases, and cartographic processing (Bayer 2009; Jenny 2011; Aguilar-Camacho 2022).

The cartometric analyses are based on a comparison of the old and reference (i.e., current) maps in order to detect and interpret their changes. A fundamental step affecting the results is the proper choice of identical points used for the transformation key calculation. Aretin's map of Bohemia does not contain a geographic grid. Therefore, easily identifiable points assumed not to have changed significantly in space and time are used. Typically, we prefer historical centers of villages, castles, chateaux, religious buildings, and confluences of rivers.

A first-degree affine transformation was applied to prevent geometric distortion of objects. It has several benefits, such as keeping the spatial relationships between map objects, eliminating the sheet shrinking, but it is not conformal. Transformations of higher degrees causing unnatural twisting of the map content, were not used in the analyses (Bayer 2009).

The equations of the affine transformation can be written in the form

$$X = m_x \cos(\alpha) x - m_y \sin(\alpha) y + \Delta x,$$
$$Y = m_x \sin(\alpha) x + m_y \cos(\alpha) y + \Delta y,$$

where x, y represent the coordinates in the local coordinate system (the old map), X, Y the coordinates in the global coordinate system (the reference map), m_x, m_y are scale factors in the x, y directions, α is the rotation angle (Bayer 2009).

Results include estimating the map scale and rotation, displacement vectors and their changes depending on the geographic position. Displacement vectors

with the given size and direction are a simple but efficient graphical technique. Deviations from the median suspected of being outliers caused by positional errors can easily be identified. The results are visualized using various methods of thematic cartography, such as isolines or deformation grid (Jenny 2011). Beineke (2001, 2007) presented a comprehensive mathematical background based on multiquadratic interpolation (Hardy 1972). The proposed technology for evaluating maps was fully automated in MapAnalyst software (Jenny 2006), which was also used in this paper.

4. Results

The results of analyses involving the four editions of Aretin's map of Bohemia (1619, 1632, 1665, and before 1747) will be presented. Digitized maps in the tiff format (resolution 400 dpi) were provided by the Map Collection of the Faculty of Science of Charles University and the National Archives of the Czech Republic. Initially, the maps were georeferenced in QGIS software, and a complete vector model of the watercourses was created. Subsequently, semiotic analyses of the watercourses (see Sec. 3.2) and map labels (see Sec. 3.3) were performed. Finally, the depicted watercourses, areas, and bridges were compared with the base map, and a content analysis was carried out (see Sec. 3.1).

4.1 Semiotic analysis and description of watercourses

On Aretin's map of Bohemia, watercourses are depicted using line symbols, the size of which corresponds to the dominance of the river. The space between the riverside lines is longitudinally hatched. The water areas are visualized using the area symbols, with the boundaries (simple contour) and the interior parts (fill combined with hatching and dots); see Tab. 1.

Drawn with the graduated line symbols, the rivers Labe ("Elbe") and Vltava are dominating. Regarding the ponds, there are two unnamed ponds in South Bohemia near Třeboň and the Jordán pond. At the confluence of rivers, the line symbol thickness is adjusted, so the tributary has a narrower representation.

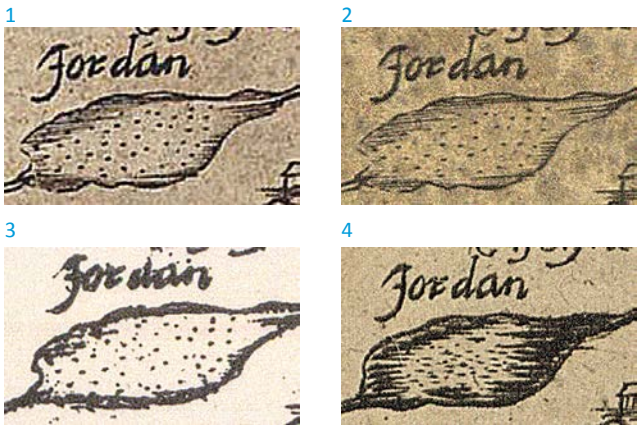

Fig. 3 Change in areal symbol intensity on the Aretin map (1st, 2nd, 3rd and 4th editions). Source: National Archives of the Czech Republic, Map Collection of the Faculty of Science, Charles University.

Aretin's map was printed on paper using hand-engraved copper plates. Therefore, the saturation of line features does not indicate a particular river attribute (such as its importance). Regarding area symbols depicting ponds, their edges are highlighted. Because the fourth edition of the map has been overprinted, the linear and areal water features are more intense and darker. See Jordan Pond on the fourth edition map in Fig. 3.

The river symbols are filled with longitudinal hatches following the flow direction. It is apparent that the area symbols of the ponds are exaggerated, their edges highlighted by extended hatches, which are either horizontal or have a slight gradient as the river flows into/out of the pond; the center of the pond is filled with dots. The specific edition of the map is also reflected – the newer the map, the more hatching on line and area features. This phenomenon is present in all water areas and is particularly evident at the Jordan Pond (Fig. 3), which has longer lines with lower spacing on the eastern shore.

The watercourse labels are on all editions of Aretin's map of Bohemia in German, Czech, and Latin languages. For example, the Labe river in Latin is *Albis* or

Tab. 1 Map symbols of Aretin's map of Bohemia.

Content of the map field	Element	Type of map symbol	Map symbol
watercourses	river	line symbol	
	pond	area symbol	

Source: Map Collection of the Faculty of Science, Charles University.

Tab. 2 Descriptions of watercourses on Aretin's maps of Bohemia.

Language of description	Map edition	Object name
Latin	First edition, 1619	
Czech	Fourth edition, before 1747	
German	Fourth edition, before 1747	

Source: National Archives of the Czech Republic, Map Collection of the Faculty of Science, Charles University.

Fig. 4 Situation around the spring of the Vltava river in Šumava. The angel with a compass in the 2nd edition (left) was removed on the 4th edition of Aretin's map (right). In the 4th edition, the spring of the Vltava river was redrawn, signs for the forest and the inscription "*Passauer Wald*" were added. Source: Map Collection of the Faculty of Science, Charles University.

Labe in Czech. The watercourse labels are handwritten (serif, italic font) with calligraphic tendencies; see Tab. 2. Behind the river names, the suffix "fl" or "flu" has been added, identifying the abbreviation from the Latin word "*fluvius*".

4.2 Content analysis

The location and identification of all rivers and water areas depicted on four editions of Aretin's map, as well as the geometric and topographic accuracy with respect to the present, were analyzed.

4.2.1 Watercourses on Aretin's map

In total, 121 watercourses on the four editions of Aretin's map of Bohemia were identified, of which 41 were described, and 17 water areas, including 2 described ponds (Bethlehem, Jordan) and 2 described springs (Labe, Morava).

The dominant river is Vltava. The fourth edition of Aretin's map omits the sketch of a cherub with a compass near the Vltava spring. Instead, its upper flow is depicted and labeled as Passauer Wald; see Fig. 4. The first right-side tributary of Vltava is the Malše river, but with a reduced flow length. According to Aretin's opinion, the river starts at the village of Dolní Dvořiště (*Dworzisste*). However, forming the Czech-Austrian border, its source is located in Austria near the Viehberg hill. A spring of an unnamed river non-corresponding with the current state of the watercourses, later flowing into Lužnice, is depicted near Dolní Dvořiště. The river flows through the cities of Gmünd and Weitra, which is correct given the course of the river. However, these cities are shifted on Aretin's map, Weitra is depicted north of Gmünd, but in reality, Gmünd is located further north.

The right tributary of Lužnice flowing through the Gmünd is the Braunaubach. Subsequently, the Lužnice river turns incorrectly to the east of Třeboň and flows through the village of Kunžak, where it may be confused with the Nežárka river (or another minor tributary of the Lužnice river).

The Otava river flows into Vltava near the village of Zvíkov (*Zwikow*). Its flow starts at Sušice, while, in reality, the Otava springs southwest of Rejštejn, as a result of the confluence of the Křemelná and Vydra rivers.

The Sázava river is not drawn along the entire length of its course, which is missing in Žďár nad Sázavou (*Zdiar*) and Přibyslav (*Przibislaw*). From Havlíčkův Brod has the same course and direction as at present.

The biggest left-side tributary of Vltava is the Berounka river. It is emerging in Pilsen as the confluence of four rivers: Mže, Radbuza, Úhlava, and Úslava. Compared to present, the course of the Mže river is mirror-reversed; see Fig. 5. It rises south of Bärnau (*Bernau*), while the Meuse originates in Germany in the Griesbach Forest, which is located north of Bärnau. Then, it flows southeast from Tachov (*Tachow*) and continues through the Stráž (*Straz*) village. At present, the flow direction is somewhat northeast, and it does not pass through Stráž. On Aretin's map, the spring of Radbuza is depicted near the village of Zelena Lhota in Nýrsko (*Zelena Lhota*). However, the right-side tributary of Radbuza, the Úhlava river, originates here; its spring was moved east of the village of Velhartice (*Welhartice*). From its spring, the Radbuza river continues through the villages of Dešenice (*Dessenice*) and Janovice nad Úhlavou (*Janowice*), following the present-day riverbed of Úhlava. The river then turns west towards Domažlice. From Horšovský Týn (*Teÿn Horssonoskÿ*), its course is identical to the present.

The Úhlava river flows from the west around the villages of Čachrov (*Czachrow*) and Strážov (*Strazow*). From Klatovy (*Klatowy*), its course is correct. The first tributary of Berounka is the Úslava river; its source is drawn in the Blatno region in the pond area. The river continues through Březnice (*Bréznice*), then turns west to the village of Blovice (*Hradisste*). Subsequently, it continues northwards through Starý Plzenec (*Plzenecz*), where it flows into the Berounka river, see Fig. 5. The river rises to the southwest at Číhaň and flows around the eastern edge of the town of Plánice.

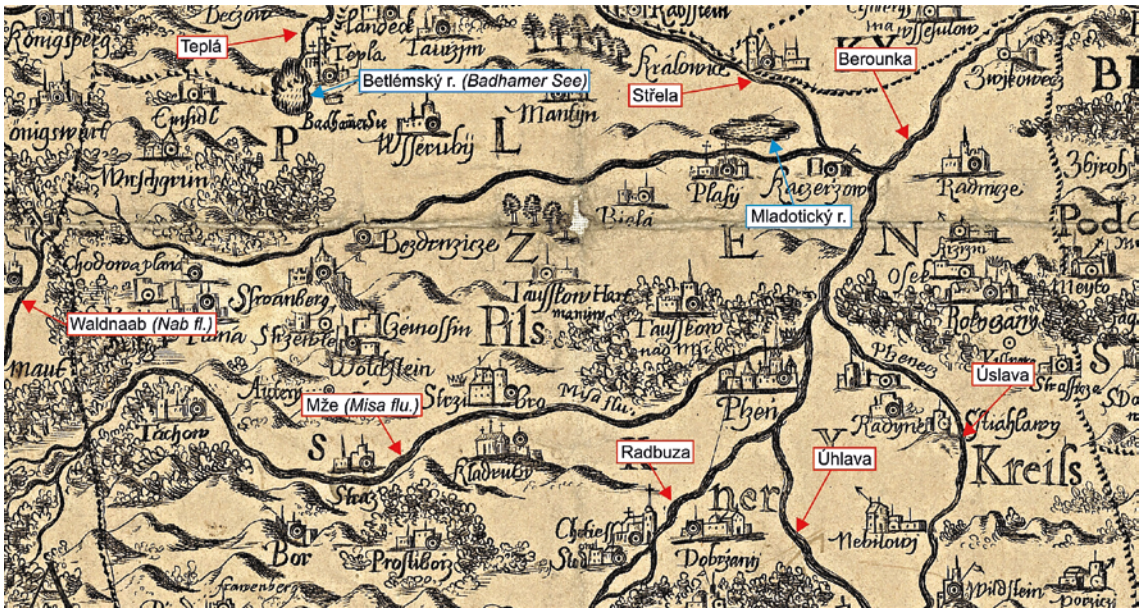

Fig. 5 Watercourses around Pilsen on the 4th edition of Aretin's map. Source: Map Collection of the Faculty of Science, Charles University.

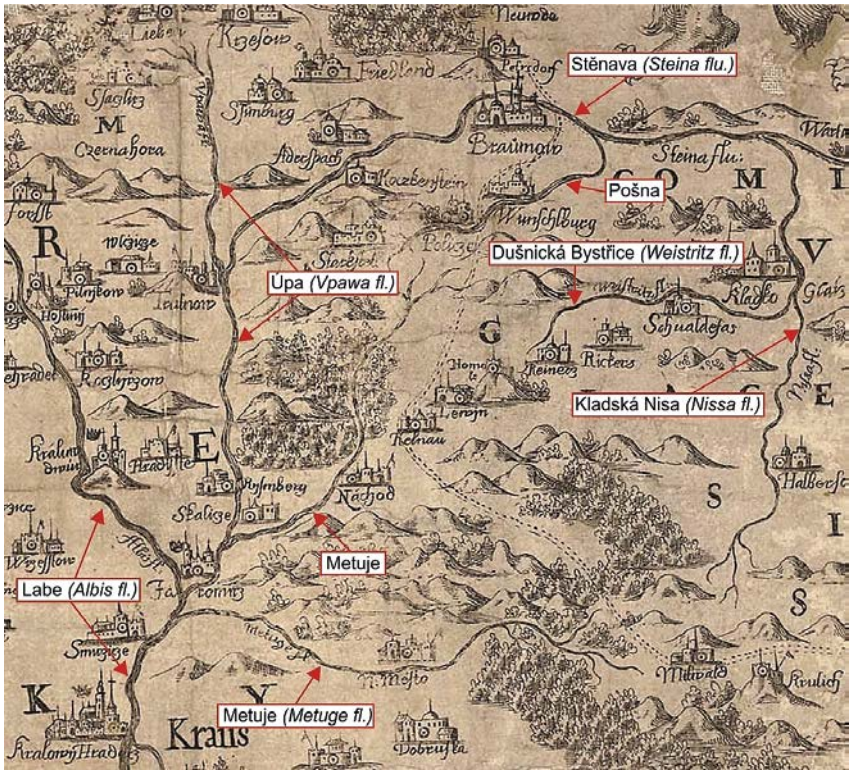

Fig. 6 Twice drawn Metuje river in East Bohemia on the 1st edition of Aretin's map. Source: National Archives of the Czech Republic.

Behind the village of Žinkovy it turns east and continues north through Blovice, Starý Plzenec to Plzeň, where it flows into Berounka.

The rivers in the northeastern part of the map area are, in many cases, incorrectly depicted. At present, the Metuje river rising in Adršpach, flows through Teplice nad Metují, Hronov, Náchod, Nové Město nad Metují and in Jaroměř, it flows into the Labe river. The part of its course from Jaroměř (*Jaromirz*) to Nové Město nad Metují (*N. Město*) is shown correctly. After that, however, the river continues further east, where it rises at the Polish village of Międzylesie (*Mitvald*). In Jaroměř, another stream with an unknown name besides Úpa flows into Labe. It flows through Náchod (*Náchod*) and rises near Police nad Metují (*Policze*). This might be the Metuje river again, as it follows the course of Metuje to some extent. The situation is shown in Fig. 6.

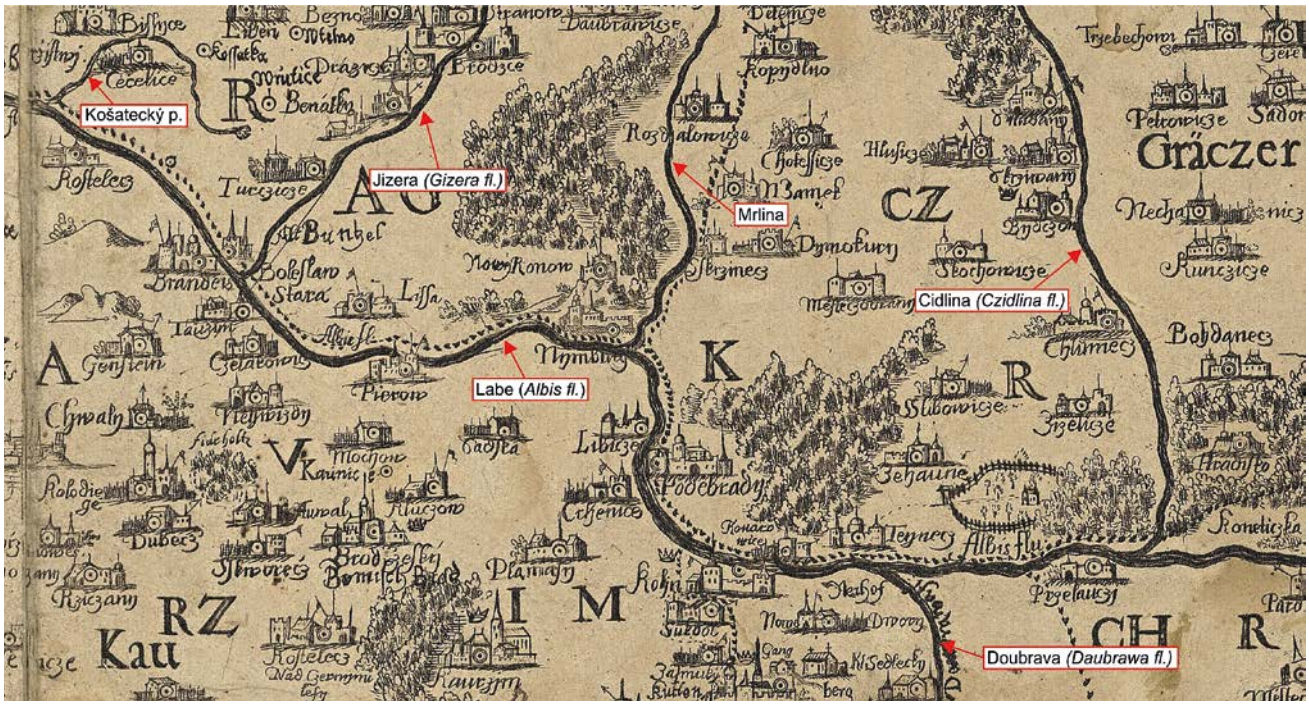

Fig. 7 The Labe river and incorrectly plotted the Cidlina river, 1st edition of Aretin's map. Source: Map Collection of the Faculty of Science, Charles University.

Other tributaries of Labe are Orlice, Loučná and Chrudimka. The course of Chrudimka is depicted from its spring in a northeastern direction, then it turns north and flows into Labe near the village of Stolany. At present, the river flows north-west from its spring to the village of Seč, then turns east, and beyond the village of Nasavrky it continues north through Slatiňany and Chrudim to Pardubice, where it flows into Labe. Then, near the village of Chrast, the Novohradka river flows into the Loučná river instead of the Chrudimka river in Úhřetice.

The spring of the Cidlina river is depicted near Lomnice nad Popelkou. Then, the river continues south through Jičín (*Giczin*), Nový Bydžov (*Bydczow*),

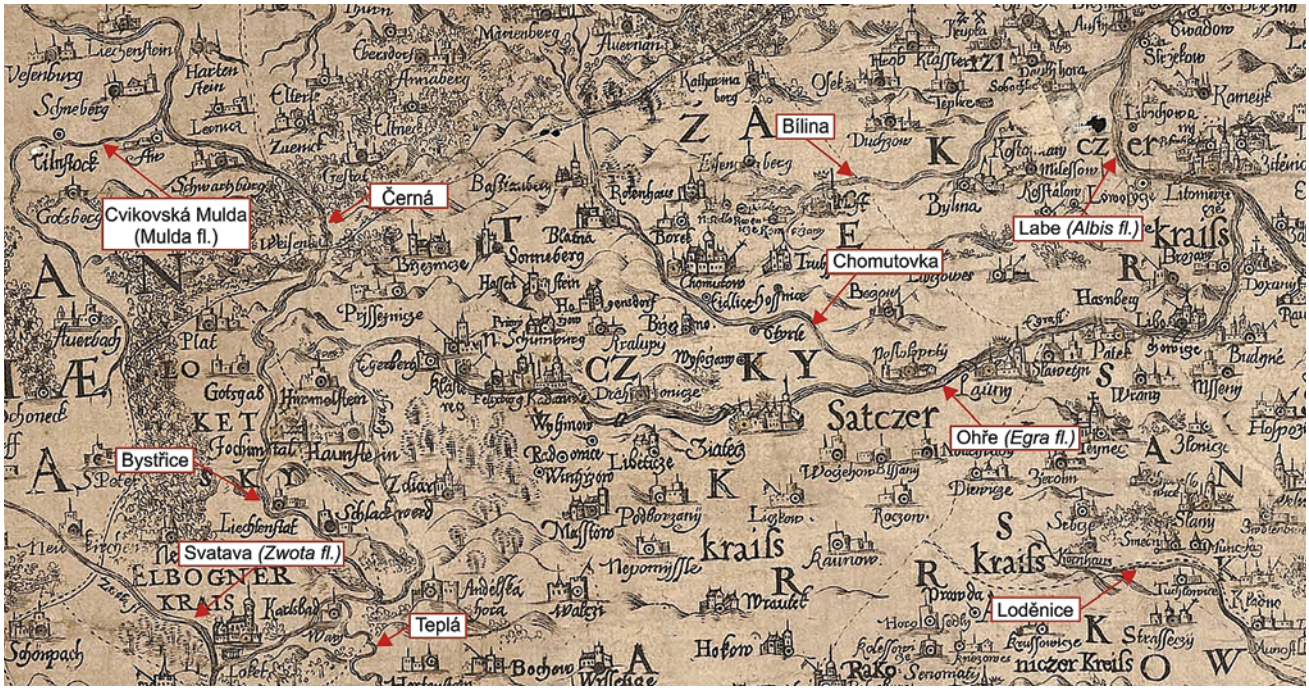

Fig. 8 Connection of the two rivers Černá and Bystřice and the Ohře river on the 1st edition of Aretin's map. Source: National Archives of the Czech Republic.

Chlumec nad Cidlinou (*Chlumecz*) and flows into Labe; see Fig. 7. Today, the river creates a large arc from Chlumec nad Cidlinou through Žíželice, towards the west. At the village of Chotěboř (*Chotěborz*) the spring of the Doubrava river is located. However, it rises near the village of Radostín, which is less than twenty kilometers southeast of Chotěboř, and west of Týnec nad Labem (*Teynecz*), it proceeds to Labe. In Nymburk, the Mrlina river flows into Labe. It runs through Křinec (*Sskrzinecz*), continues to Rožďalovice (*Rozdalowice*), and further north. However, it does not turn east to Kopidlno (*Kopydlno*) but flows around Libáň (*Libaně*) from the west, instead of the east. The spring of the Mrlina river is depicted southwest of Staré Hrady, with Mrlina rising in the village of Příchvoj. The Jizera river and its right-side tributary might be confused, as the river marked as Jizera follows the present course of the Kamenice river closely.

Another right-side tributary of Labe is the Košátky stream. It rises in Mšeno (*Msseno*), where on Aretin's map the stream is shown as far as Kropáčova Vrutice (*Wrutice*). The Vltava river flows into the Labe river in Mělník.

The confluence of the Labe and Ohře rivers, depicted in Litoměřice, corresponds to the current state; see Fig. 8. In Postoloprty (*Postoloprtij*) the Chomutovka river flows into the Ohře river. Its spring is located at the southern tip of the Marienberg instead of the Krušné ("Ore") Mountains. Then, the river flows around the village of Blatno (*Blatná*) from the east instead of the west. At Karlovy Vary (*Karlsbad Wary*) the rivers Teplá and Bystřice flow into Ohře. The Bystřice river was probably connected with the Černá river, as this river is also drawn as a right-side tributary of Cvikovská Mulda, which would correspond to Černá. The situation is illustrated in Fig. 8. Another tributary of Ohře is the Svatava river, which was probably joined to Bílý Halštrov. Svatava actually rises south of the town of Schöneck, i.e. north-east of Adorf (*Adorff*), where Bílý Halštrov flows.

The spring of the Jihlava river is depicted in the Pelhřimov region. Then, the river flows through Třebíč

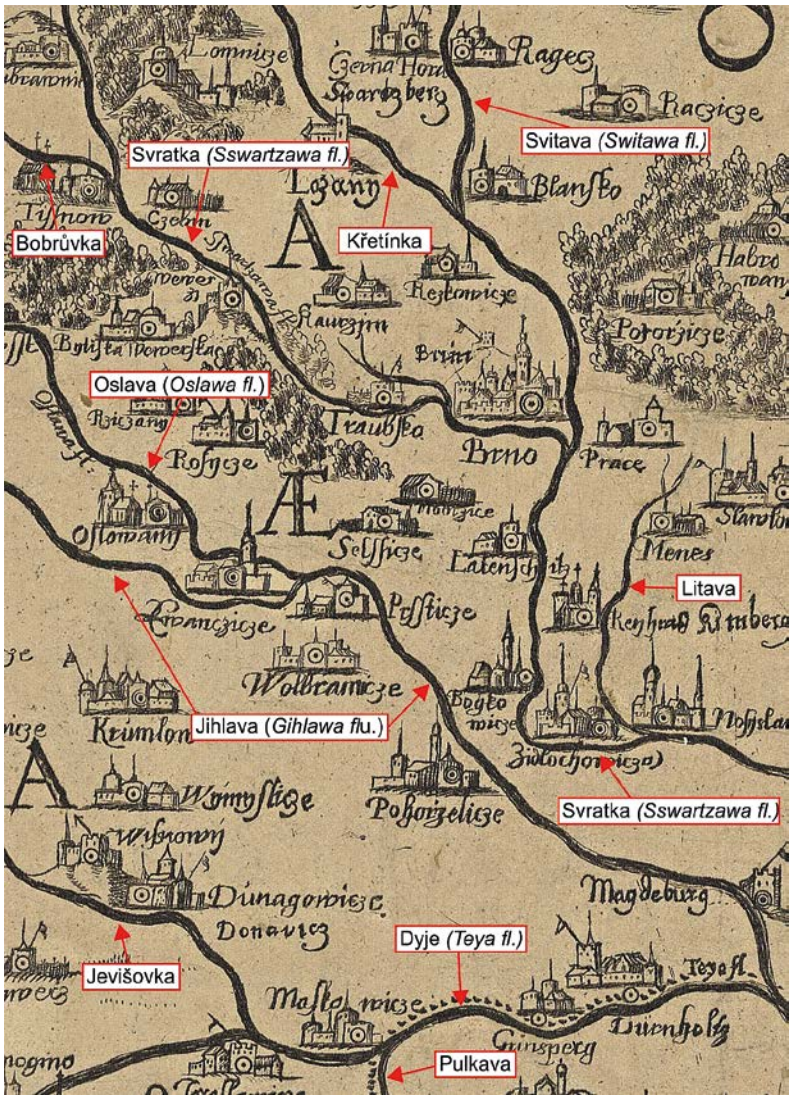

Fig. 9 Watercourses around the Jihlava river, 1st edition of Aretin's map. Source: Map Collection of the Faculty of Science, Charles University.

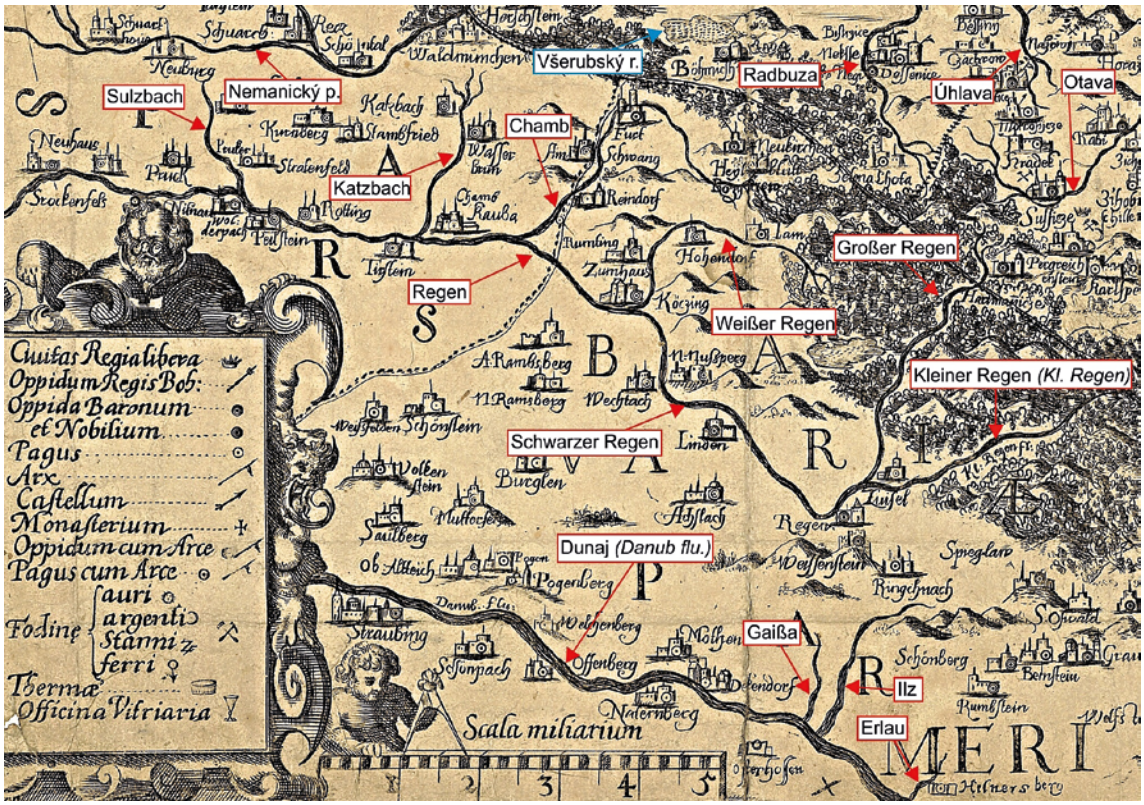

Fig. 10 Identification of German watercourses on the 4th edition of the Aretin map. Source: Map Collection of the Faculty of Science, Charles University.

(*Trzebitz*) and Vladislav (*Wladislaw*). At Ivančice (*Iwanczice*) the Oslava river flows into the Jihlava river, which then flows into the Dyje river. Just before the outflow to the Nové Mlýny reservoir on Dyje, Svratka flows into Jihlava; see Fig. 9. It rises northeast of Žďár nad Sázavou in the Ždárské vrchy Hills. In the map, its source is marked at the village of Swoys, south of Svojanov (*Swoganow*). Instead of passing through Nedwedicze, the river flows around it in the west direction. The Bobrůvka river, sometimes marked as the Loučka river, flows into it at Tišnov (*Tissnow*). Then, Svratka continues through the village of Veverská Bítýška (*Bytiska Wewerska*), which is depicted southeast, but the river passed it.

In Brno, the Svitava river flows into the Svratka river, and its source is correctly depicted north of the village of the same name (*Switawy*). The river Svitava bypasses Boskovice (*Bozkowice*) from the west (instead of the east), with an unnamed river inflowing in Blansko. Probably, given the spring in the surroundings of Polička (*Policzka*), it is the Křetínka river. It proceeds through Svojanov (*Swoganow*), while it continues south past Kunštát (*Kunstat*), and then flows around Černá Hora from the west. The confluence of Křetinka and Svitava should be located in Letovice instead of Blansko. Behind Brno, Svratka continues south to Židlochovice (*Zidlochowicze*), where another inflow, probably the river Litava, is depicted. While it rises southeast of Cetechovice, continues west, and turns southwest to Židlochovice near Slavkov u Brna, its flow is south on the map; see Fig. 9.

The rivers in the south part of the map do not have assigned names. The Pulkava spring is also missing. It rises at the village of Ludweishofen, north of Horn, and its course turns southwest from its outflow to Pulkau (*Pulka*). Three right-hand tributaries join it and further flows south from Eggenburg (*Egenborg*). On the map's boundary, it probably flows into the Kamp river. An unnamed river, entering the map area west of the cartouche, flows through Hollabrunn (*Hollbrun*) and Gollersdorf (*Gellersdorf*). It is probably the Göllersbach river, which flows through the villages mentioned above. On the map, the river does not aim eastwards, where it should pass through Enzerdorf im Thale (*Enczendorf*), but instead it flows around from the west and proceeds north-westwards towards Pulkava.

In the Southwest (above the map scale), the Danube river with its three left-side inflows (Gaißa, Ilz and Erlau from the West) is depicted. An unnamed watercourse flows east of Danube, bypassing the town of Freyung (*Freiung*) from the west; this could be the Erlau river. Towns are depicted inaccurately in this part of the map; for example, Aigen-Schlägl (*Sslegel*) is located southeast of Freyung and Fürholz (*Furholtz*), while the map shows this town northeast. This river probably represents Große Mühl – it flows through Aigen-Schlägl and then continues into Danube. The situation is shown in Fig. 10.

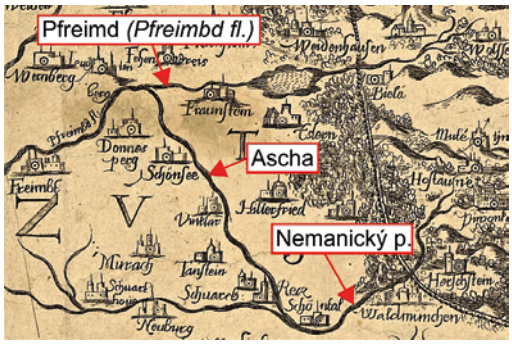

Fig. 11 Incorrect connection of watercourses on the 4th edition of Aretin's map. Source: Map Collection of the Faculty of Science, Charles University.

Above the legend, we can find the Regen river. It rises in the Šumava region as the Großer Regen river. At Zwiesel, it continues to the Kleiner Regen river and then into the Schwarzer Regen river. From the city of Regen, it turns northwest. In Bad Kötzting (*Köczing*), the Weißer Regen river flows through and continues as the Regen river; see Fig. 10. Behind Nittenau (*Nitnau*), it turns south to Regensburg, where it flows into Danube. North of Regen in the Bohemian Forest it joins Nemanice stream. The Ascha river flows into it at Rötz (*Recz*), their confluence should be west of Neunburg vorm Wald (*Neuburg*). The spring of Ascha is missing from the map. Instead, the river continues incorrectly to the Pfreimd river, see Fig. 11.

The flow of Cvikovská Mulda follows the current watercourse, but the river is interrupted at the village of Penig (*Penig*), with a sword held by an imperial eagle in the gap. The confluence of Cvikovská Mulda and Kamenice is located north of Wechselburg, but the correct place is two kilometers to the south. To the east of the Kamenice river, the Sapava river is drawn, but its shape is skewed. Aretin probably merged two rivers Flája and Sapava. From Flöha, the Sapava river continues northwards, and it later flows into the Freiber Mulde river.

The Smědá and Lužická Nisa rivers are depicted north of the spring of the Ploučnice river. Smědá follows the border between Germany, Poland, and Czechia, while Lužická Nisa actually forms this border. Its course has been shortened, and instead of Lučany nad Nisou, its source is drawn at the town of Zittau (*Zitawa*).

The Bobr river rises northeast of the spring of the Úpa river above the village of Krzeszów (*Krzesow*). Its source should be locted towards the town of Žacléř. On the map, the river continues through Kowary (*Schmidberg*) and Miedzianka (*Kupferberg*) and turns west. Another name for this river is Kamienna. However, the Kamienna river is a left-hand inflow river of the Bóbr river. Aretin joined two different watercourses into one.

As mentioned above, Aretin made a mistake in the northeastern part of the map field. Another inaccurately depicted river is Stěnava, which flows into the Úpa river. It should rise south of Wałbrzych, where the river continues southeast to Broumov, and an unnamed tributary, probably the Pośna, flows into Stěnava from the right. The Kladská Nisa river is depicted as a left-side tributary of the Stěnava river as well as the left-hand tributary of the Kladská Nisa river, the Dušnická Bystřice river. Its source is near the village of Duszniki-Zdrój (*Reinecz*), but it rises north of Velká Deštná, near the Eagle Mountain.

The spring of the Morava river is west of the springs of the Divoká and Tichá Orlice rivers, but in reality, it is further north, below the top of Králický Sněžník. The river flowing through Moravská Třebová (*Trzebowa Morawska*) is probably the Třebůvka river. However, it rises to the southwest, not to the north of the town.

An overview of all named watercourses on Aretin's map of Bohemia is shown in the Appendix 1.

4.2.2 Water areas on Aretin's map

A total of 19 water areas are drawn on Aretin's map, while only two are described. The first is the Jordan pond, created in 1492 by damming the Košín stream, the oldest dam reservoir in Czechia (Krajíc 2019). The pond is part of the Tábor city but is plotted easter.

Fig. 12 The Betlém pond (*Badhamer See*) on Aretin's map (2nd and 4th editions). Source: Map Collection of the Faculty of Science, Charles University.

Fig. 13 Water areas in the Třeboň region (4th edition of Aretin's map). Source: Map Collection of the Faculty of Science, Charles University.

The second labeled water area is the Betlém pond (*Badhamer See*), located on the Teplá river near the village of the same name; see Fig. 12.

There are also eight unnamed water areas in the Třeboň region; see Fig. 13. The largest one could be the Rožmberk pond, according to its position to Lomnice nad Lužnicí (*Lomnicze*) and Třeboň as well as due to Lužnice river flowing through it. The history of fish farming in the Třeboň region refers to the 15th century when already 20 ponds in the Třeboň region were established. Unfortunately, the remaining seven water areas have not successfully been identified; see Fig. 13.

Northern the village of Plasy (*Plasij*) the Střela river is shown with a water area (Mladotice pond) founded already in the 14th century (Jánský 2010), but it is now defunct. Its existence was confirmed by the maps of the Second military mapping, where the pond near Mladotice was depicted. Fig. 14 shows the difference in the landscape in the 19th century and today.

The water area near the village of Všeruby (Böhmicsh Weijer) refers to the pond of the same name. The spring of the Úslava river near Blatná, as well as the pond system established in the 15th century, are depicted.

Fig. 14 The Mladotice pond on maps of the 2nd military mapping (top left), at present and on Aretin's map (2nd and 4th edition). Source: Map Collection of the Faculty of Science, Charles University; State Administration of Land Surveying and Cadastre.

Fig. 15 Examples of bridges in Louny, Libochovice and Roudnice on Aretin's map (1st edition). Source: National Archives of the Czech Republic.

Another pond is located north of Eslarn (Eslern) on the Pfreimd river. The larger water area is Železná pond, but instead of being north of Eslarn, it lies western the village of Bělá nad Radbuzou (Bielá). The last unnamed water area is located at the spring of Labe and could represent the Labe meadow in the vicinity of the Labe spring.

4.2.3 Bridges on Aretin's map

All four editions of Aretin's map of Bohemia show the same amount of bridges, eight in total. The bridges are depicted over the Vltava river in Prague, Labe river in Mělník, Roudnice n. Labem and Litoměřice and over the Ohře river in Libochovice, Louny, Žatec and Drahonice. The bridges are drawn simply, using two thicker unfilled lines, either closed at the end, forming a rectangle, or open and stretching across the hatched river; see Fig. 15.

4.3 Cartometric analysis of watercourses on Aretin's map

Cartometric analyses of the first edition of Aretin's map of Bohemia provided in TIFF format with a resolution of 400 DPI, were performed in the MapAnalyst software. While the analyzed map does not have any cartographic projection, the OpenStreetMap layer used as the reference map utilized the Web Mercator coordinate system (EPSG: 3857). Georeferencing was performed using the affine transformation, which is non-conformal but removes the map sheet distortions efficiently. In total, 70 identical points evenly covering the whole map area, respecting the historical and social development of the territory, were collected. The analyses provided the following results. The estimated scale of the Aretin map is 1 : 544,000; the map is rotated by 9° to the east, Its standard deviation on the identical points is ±5,322 m, and the average positional error is ±7,526 m. Based on the calculation of displacement vectors, the least accurately drawn towns are Jihlava (18 km), Bad Kötzing (15.0 km), Dobruška (14.3 km), Domažlice (13.7 km) and Polná (13.0 km). On the contrary, the most accurately depicted are Mšeno (0.9 km), Znojmo (1.5 km), and Petrovice (1.6 km). Fig. 16 shows a deformation grid illustrating the local geometric distortions of the Aretin's map.

The results are in accordance with previous works. Kuchař (1936) estimated the scale as 1 : 504,000, Vejrová (2008) as 1 : 510,000, Bayer (2009) as 1 : 544,766. He also identified the town of Jihlava (18 km) as the most inaccurately depicted and determined the mean positional error of the map as ±7,860 m.

5. Conclusion

The paper is focused on comprehensive content and basic cartometric analyses of watercourses on four known editions of Aretin's map of Bohemia from 1619, 1632, 1665, and before 1747. Several unnamed watercourses and areas were identified using modern computational and geoinformation tools. Furthermore, the graphical representation of hydrographic elements has been analyzed.

In general, we assume that the depiction of watercourses on maps from the 16th and 17th centuries was rather vague or even inaccurate. This reflects the state of knowledge, the quality and quantity of available sources and the limited mobility of people.

While previous maps of the Bohemian Kingdom recorded 9 watercourses on Klaudyan's map of Bohemia (1518) and 61 watercourses on Criginger's map of Bohemia (1568), Aretin's map shows a total of 194 watercourses. Of these, 41 are described on the map and 97 have been newly named in the process of this work.

The results clearly show that the number of watercourses plotted on these maps increases very significantly over time as the map becomes more detailed.

Regarding old maps, no supplementary information about their creation is currently available. For

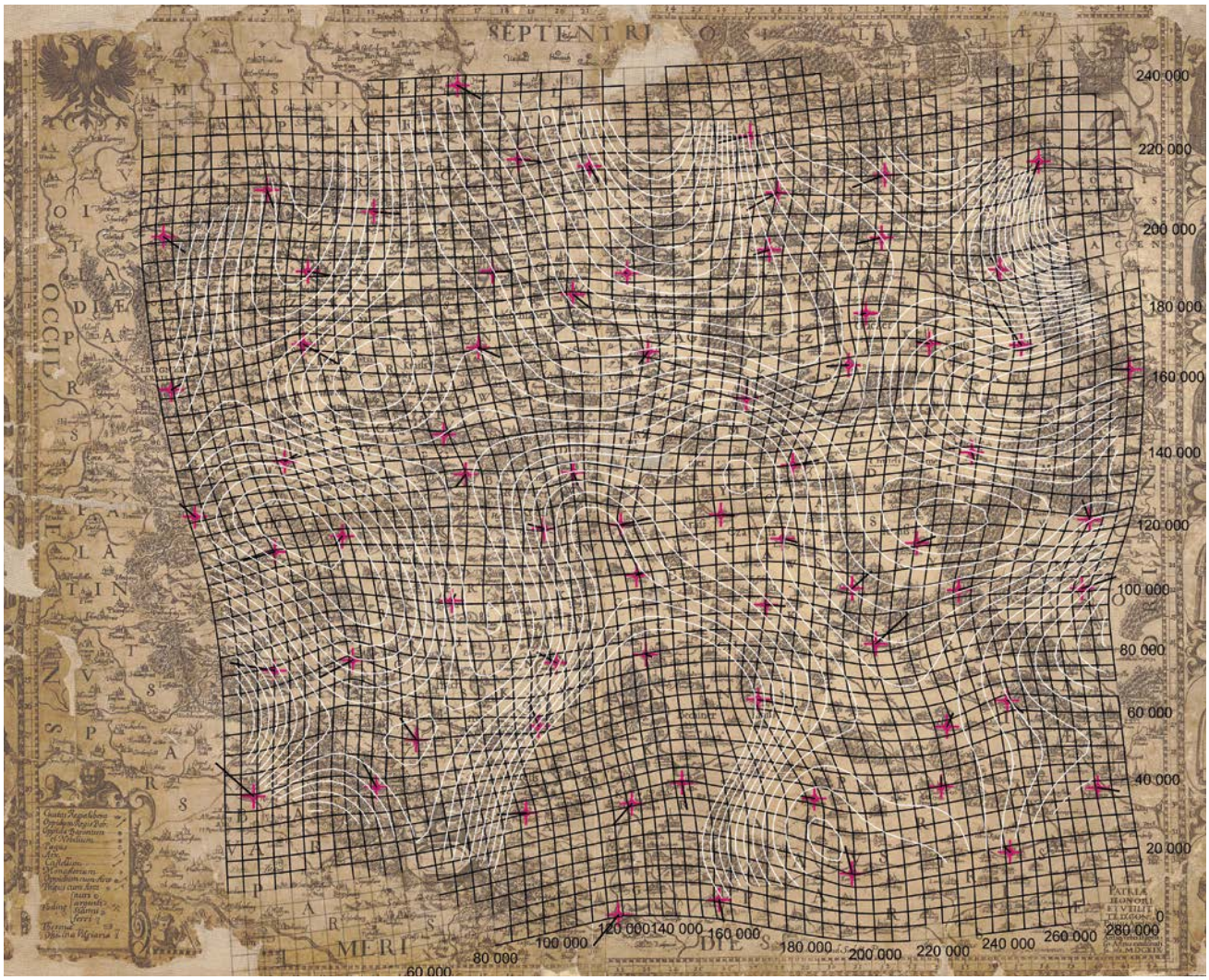

Fig. 16 Deformation grid with identical points and their displacement vectors on the Aretin's map. Source: National Archives of the Czech Republic.

Aretin's map, it cannot be proven whether it is based on the field measurements. Aretin was not a surveyor, but he might, at least partially, use measurements made by the surveyor Simon Podolsky (Kuchař 1936). The lack of map projection may cause graphical errors in drawing watercourses (especially Chrudimka or Saxon rivers).

It has been confirmed that all analyzed editions of Aretin's map of Bohemia contain many graphical errors. In some cases, a watercourse was assigned by two names since its topography corresponded partly to more rivers (Bóbr+Kamienna, Bystřice+Černá, Flöha+Zschopau). Two watercourses were also identified as Metuje. A significant error was found in the depiction of the Labe and Cidlina rivers confluence. Pavel Aretin worked as an tutor of Hynek Březnicky from Náchod. It is therefore interesting that in this locality, i.e. in East Bohemia, there are most errors in the drawing of watercourses.

All 138 identified water features (including their names in all map editions) were summarized in a table; see Appendix. The attached table shows that in terms of the number of watercourses drawn, the individual editions differed only slightly from each other. In particular, there are differences in the drawing of the course of some watercourses; see chapter 4.2.1.

This paper provided new findings about the four editions of Aretin's map. Most watercourses and water areas were identified, their positional inaccuracies were estimated. It is remarkable, that of the 70 longest current Czech rivers, only 11 are not drawn on the map. These rivers are Želivka, Rokytná, Blanice (a tributary of Sázava), Bystřice (a tributary of Cidlina), Lomnice, Stropnice, Dědina, Trnava, Nežárka, Skalice and Klabava. Only two water areas were labeled, four were identified by the authors as Rožmberk, the Všeruby pond, Bílý Halštrov and the Mladotice pond. Of the remaining 13 water areas, 7 are located in the Třeboň region, where the history of fish farming dates back to the middle of the 15th century. In 1609–1611 Aretin worked in the Třeboň region as a secretary of Peter Wok of Rosenberg. It appears very likely that he

knew the locality well and plotted the local pond system on the map. However, adequate sources clearly identifying the depicted water areas in this location have not be found. Based on the results of analyses, comparative methods are suitable for assessing the content of old maps.

Basic cartometric analyses were carried out on the first edition of the map; its scale 1 : 544,000 was determined and compared with the previous results. With an average positional error of ±7,526 m, the most considerable positional errors were found in southern, south-eastern, and northeastern Bohemia. The least accurately depicted city is Jihlava (18 km). The results of the cartometric analyses illustrate the well- known fact, the lack of solid geodetic bases. Thanks to the application of digital technology (MapAnalyst), the results can easily be visualized.

Summarizing the above-mentioned facts, the main contribution of the paper was the identification, recognition, and description of all the watercourses and water areas. This process was considerably simplified and accelerated by the use of modern software tools.

Table containing a list of watercourses including their labels in the individual editions of Aretin's map of Bohemia can be found in Appendix.

Acknowledgements

We would like to thank the Map Collection of the Faculty of Science of Charles University and and the National Archives in Prague for providing the digital copies of the originals of Aretin's map of Bohemia Kingdom.

References

Aguilar-Camacho, J., Granado-Castro, G., Cabrera-Revuelta, E. (2022): Visualization of the Local Distortions on the Oldest Known Urban Map of Seville (1771). In: Ródenas-López, M. A., Calvo-López, J., Salcedo-Galera, M. (eds) Architectural Graphics. EGA 2022. Springer Series in Design and Innovation, vol. 21. Springer, Cham, https://doi.org/10.1007/978-3-031-04632-2_46.

Beineke, D. (2001): Verfahren zur Genauigkeitsanalyse für Altkarten. Studiengang Geodäsie und Geoinformation. München, Universität der Bundeswehr.

Beineke, D. (2007): Zur Bestimmung lokaler Abbildungsverzerrungen in Altkarten mit Hilfe der multiquadratischen Interpolationsmethode. Allgemeine Vermessungsnachrichten, 1/2007, 19–27.

Bayer, T., Potůčková, M., Čábelka, M. (2009): Cartometric analysis of old maps of Czech Lands: map of Bohemia and map of Moravia by Petrus Kaerius. Geografie 114, 230–243, https://doi.org/10.37040/geografie2009114030230.

Čapek, R., Mikšovský, M., Mucha, L. (1992): Geografická kartografie. Státní pedagogické nakladatelství, Praha.

Farooqi, J. A., Ono, H. (2024): A comparative analysis of two century-old historical map and satellite images for assessing land use transformation and preservation of the historical monuments of the Ahmad Shahi old city, Kandahar. Japan Architectural Review 7: e12428, https://doi.org/10.1002/2475-8876.12428.

Gašperič, P. (2023): A new standardized methodology for analyzing cartographic information on old maps. Acta geographica Slovenica 63(2), 23–49, https://doi.org/10.3986/AGS.10867.

Gatta, G., Bitelli, G. (2020): A HGIS for the study of waterways: the case of Bologna as ancient city of waters. IOP Conference Series: Materials Science and Engineering 949: 012051, 1–7, https://doi.org/10.1088/1757-899X/949/1/012051.

Gregory, I., Geddes, A. (2014): Toward Spatial Humanities: Historical GIS and Spatial History; Indiana University Press: Bloomington, USA.

Hardy, R. L. (1972): Geodetic application of multiquadratic analysis. Allgemeine Vermessungsnachrichten, 79, 398–406.

Hanušík, V. (2017): Laborec riverine landscape between Brekov and Michalovce from the half of 18th century to the half of 19th century. Geographia Cassoviensis 11(1), 5–21. Available online: https://uge-share.science.upjs.sk/webshared/GCass_web_files/articles/GC-2017-11-1/2017_1-Hanusik_final.pdf (accessed on 5. 5. 2024).

Hvizdák, L., Tometzová, D., Iannaccone, B., Šoltésová, M., Domaracká, L., Kyšeľa, K. (2023): Old Mine Map Georeferencing: Case of Marsigli's 1696 Map of the Smolník Mines. ISPRS International Journal of Geo-Information 12(8): 345, https://doi.org/10.3390/ijgi12080345.

Jánský, B., Schulte, A., Česák, J., Escobar, V. R. (2010): The Mladotice Lake, western Czechia: The unique genesis and evolution of lake basin. Geografie 115, 247–265, https://doi.org/10.37040/geografie2010115030247.

Jenny, B. (2006): MapAnalyst – A digital tool for the analysis of the planimetric accuracy of historical maps. e-Perimetron 1(3), 239–245. Available online: https://www.e-perimetron.org/Vol_1_3/Jenny.pdf (accessed on 5. 5. 2024).

Jenny, B., Hurni, L. (2011): Studying cartographic heritage: Analysis and visualization of geometric distortions. Computers & Graphics 35(2), 402–411, https://doi.org/10.1016/j.cag.2011.01.005.

Krajíc, R. (2019): Medieval waterworks in Tábor: archaeological research into the Jordán reservoir. Archeologia historica 44(2), 1001–1027, https://doi.org/10.5817/AH2019-2-21.

Krejčí, J., Cajthaml, J. (2022): Historical Vltava River Valley–Various Historical Sources within Web Mapping Environment. ISPRS International Journal of Geo-Information 11(1), 35, https://doi.org/10.3390/ijgi11010035.

Krejčí, J., Cajthaml, J. (2009): Müller's maps of the Czech lands and their analysis. Acta Geodaetica et Geophysica Hungarica 44(1), 27–38, https://doi.org/10.1556/AGeod.44.2009.1.4.

Kuchař, K. (1959): Vývoj mapového zobrazení Československé republiky I. – Mapy českých zemí do pol. 18. století. Ústřední správa geodézie a kartografie, Praha.

Kuchař, K. (1958): Naše mapy odedávna do dneška. Nakladatelství Československé akademie věd, Praha.

Kuchař, K., Roubík, F. (1936): Regni Bohemiae Nova et Exacta Descriptio MDCXIX. Monumenta Cartographica

Bohemiae. Text k listu 3 a 3a. Geografický ústav Karlovy university, Praha.
Medyńska-Gulij, B. (2013): How the Black Line, Dash and Dot Created the Rules of Cartographic Design 400 Years Ago. The Cartographic Journal 50(4), 356–368, https://doi.org/10.1179/1743277413Y.0000000035.
Miklín, J., Dušek, R., Krtička, L., Kaláb, O. (2018): Tvorba map. Ostrava: Ostravská univerzita.
Novotná, E., Tröglová Sejtková, M., Čábelka, M., Paták, J. (2022): Aretin's Map of the Bohemian Kingdom. Praha: Karolinum. Monumenta Cartographica Bohemiae.
Roubík, F. (1951): Soupis map českých zemí, I. Přehled vývoje kartografického zobrazení Čech, celkové mapy Čech, mapy krajů v Čechách, mapy Zemí Koruny české, historické mapy českých zemí. Praha: Státní nakladatelství učebnic, 306 s.
Semotanová, E. (2001): Mapy Čech, Moravy a Slezska v zrcadle staletí. Libri, Praha.
Semotanová, E. et al. (2008): České země na starých mapách. Praha: Ministerstvo obrany ČR, Geografická služba AČR.
Stachoň, Z., Konečný, M. (2014): Certified methodology for map objects cataloguing. Brno: Masaryk University, Department of Geography. 47 s. Project Identification DF11P01OVV003.
Trpáková, I. (2009): The use of historical sources and their ecological interpretation in the course of almost two centuries – a literature review. Journal of Landscape Studies – online version, 3(2), 97–119.
Tsorlini, A., Iosifescu, I., Iosifescu, E. C., Hurni, L. (2014): A methodological framework for analyzing digitally historical maps using data from different sources through an online interactive platform. e-Perimetron. 9(4), 153–165. Online at www.e-perimetron.org.
Vejrová, L. (2008): Visualization of Cartometric Characteristics of the Czech Oldest Maps in Software MapAnalyst. Bachelor thesis. Faculty of Civil Engineering, Czech Technical University in Prague, Prague.
Voženílek, V. (2004): Applied cartography I. – Thematic maps. Palacký University Olomouc, Olomouc.

Map sources

Pavel Aretin of Ehrenfeld: Regni Bohemiæ Nova et Exacta Descriptio. Patriae Honori et Utilitati D(at) Cons(ecra) t Paulus Aretinus ab Ehrenfeld, Civis Antiq: Urbis Pragensis: Paulus Bayard Sculpsit, scale 1 : 504 000, Pragae: Paulus Aretinus ab Ehrenfeld, 1619, copper engraving, 57,4 × 76,6 cm. The National Archives of the Czech Republic, inventory number NAD 0324/1256.
Pavel Aretin of Ehrenfeld: Regni Bohemiæ Nova et Exacta Descriptio. Ab auctore recognita et aucta Anno Salutis 1632. Patriae Honori et Utilitati D(at) Cons(ecra)t Paulus Aretinus ab Ehrenfeld, Civis Antiq. Urbis Pragensis: Paulus Bayard Sculpsit, scale 1 : 504 000, [Pragae]: Paulus Aretinus ab Ehrenfeld, 1632, copper engraving, taped canvas; 51,6 × 61,4 cm on the shet 76 × 98 cm. The Map Collection of the Faculty of Science, Charles University.
Pavel Aretin of Ehrenfeld: Regni Bohemiæ Nova et Exacta Descriptio. Prostat apud Daniel Wussim Civem Neo-Pragensem. Qui pro honore ac Utilitate Patriae opus hoc renovauit et excudit, scale 1 : 504 000, Pragae: Daniel Wussim, 1665, copper engraving; 51,6 × 61,4 cm. The Map Collection of the Faculty of Science, Charles University.
Pavel Aretin of Ehrenfeld: Haec tabula Regni Boemiae: Prostat Pragae apud Casparu Wussin, scale 1 : 504 000, Pragae: Casparus Wussin, 1690–1720, copper engraving, taped canvas; 52 × 62 cm. The Map Collection of the Faculty of Science, Charles University.

Appendix 1 List of hydronyms on Aretin's map of Bohemia Kingdom.

	Aretin 1st edition, 1619	Aretin 2nd edition, 1632	Aretin 3rd edition, 1665	Aretin 4th edition, before 1747	Current name	State
Rivers						
1	–	–	–	–	Ascha	DE
2	–	–	–	–	Berounka	CZ
3	–	–	–	–	Bílá Řezná / Weißer Regen	DE
5	–	–	–	–	Bílina (CZ)	CZ
6	–	–	–	–	Bílý Halštrov / Weiße Elster	CZ, DE
7	–	–	–	–	Bílý p.	CZ
8	Blánice fl	Blánice fl	Blánice fl	Blánice fl	Blanice	CZ
9	–	–	–	–	Bobrůvka	CZ
10	Bober fl	Bober fl	Bober fl	Bober fl	+Bóbr	CZ, PL
11	–	–	–	–	Borecký p.	CZ
12	–	–	–	–	Braunaubach	AT
13	–	–	–	–	+Bystřice	CZ
14	X	–	–	–	Cerhovka	CZ
15	Czidlina fl	Czidlina fl	Czidlina fl	Czidlina fl	Cidlina	CZ
16	–	–	–	–	Cikánský p.	CZ
17	Mulda fl	Mulda fl	Mulda fl	Mulda fl	Cvikovská Mulda / Zwickauer Mulde	DE
18	–	–	–	–	+Černá / Schwarzwasser	CZ, DE
19	–	–	–	–	Černá Řezná / Schwarzer Regen	DE
20	–	–	–	–	Červený p.	CZ
21	X	–	–	–	Divoká Orlice	CZ
22	X	Daubrawa fl	Daubrawa fl	Daubrawa fl	Doubrava	CZ
23	Danub fl	Danub fl	Danub fl	Danub fl	Dunaj / Donau	DE
24	Weistritz fl	Weistritz fl	Weistritz fl	Weistritz fl	Dušnická Bystřice / Bystrzyca Dusznicka	PL
26	Teya fl	Teya fl	Teya fl	Teya fl	Dyje / Thaya	AT, CZ
27	–	–	–	–	Erlau	DE
28	Ssopa fl	Ssopa fl	Ssopa fl	Ssopa fl	+Flöha / Fláje	CZ, DE
29	–	Mulda fl	Mulda fl	Mulda fl	Freiberská Mulda / Freiberger Mulde	CZ, DE
30	–	–	–	–	Frombach	DE
31	–	–	–	–	Gaißa	DE
32	–	–	–	–	Gmoosbach	AT
33	–	–	–	–	Göllersbach	AT
34	–	–	–	–	Große Mühl	DE
35	–	–	–	–	Große Taffa	AT
36	–	–	–	–	Großer Kamp	AT
37	–	–	–	–	Großer Regen	DE
38	Kempnitz fl	Kempnitz fl	Kempnitz fl	Kempnitz fl	Chemnitz	DE
39	–	–	–	–	Chomutovka	CZ
40	Chrudimka	X	X	–	Chrudimka	CZ
41	–	–	–	–	Ilz	DE
42	–	–	–	–	Jevišovka	CZ
43	Gihlawa fl	Gihlawa fl	Gihlawa fl	Gihlawa fl	Jihlava	CZ
44	Gizera fl	Gizera fl	Gizera fl	Gizera fl	Jizera	CZ
45	–	–	–	–	Kamenice	CZ
46	Zak fl	Zak fl	Zak fl	Zak fl	+Kamienna / Zacken	PL
47	–	–	–	–	Chuba / Kamp	AT

	Aretin 1st edition, 1619	Aretin 2nd edition, 1632	Aretin 3rd edition, 1665	Aretin 4th edition, before 1747	Current name	State
48	–	–	–	–	Katzbach	DE
49	Nissa fl	Nissa fl	Nissa fl	Nissa fl	Kladská Nisa / Nysa Kłodzka	CZ, PL
50	–	–	–	–	Košatecký p.	CZ
51	–	–	–	–	Kouba / Chamb	DE
52	X	X	X	–	Krounka	CZ
53	–	–	–	–	Křemenný p.	CZ
54	–	–	–	–	Křemžský p.	CZ
55	–	–	–	–	Křetínka	CZ
56	Albis, Labe fl	Albis, Labe fl	Albis, Labe fl	Albis, Labe fl	Labe	CZ, DE
57	Albis, fons	Albis, fons	Albis, fons	Albis, fons	Labe – pramen	CZ
58	–	–	–	–	Litava	CZ
59	–	–	–	–	Litavka	CZ
60	–	–	–	–	Loděnice	CZ
61	X	–	–	–	Loučná	CZ
62	Neise fl	Neise fl	Neise fl	Neise fl	Lužická Nisa	CZ
63	Lusnicze fl	Lusnicze fl	Lusnicze fl	Lusnicze fl	Lužnice	AT, CZ
65	Kl[einer] Regen fl	Kl[einer] Regen fl	Kl[einer] Regen fl	Kl[einer] Regen fl	Malá Řezná / Kleiner Regen	CZ, DE
67	Maltz fl	Maltz fl	Maltz fl	Maltz fl	Malše / Maltsch	AT, CZ
68	Metuge fl	Metuge fl	Metuge fl	Metuge fl	Metuje	CZ
69	–	–	–	–	Mezný p.	CZ, DE
70	–	–	–	–	Mödringbach	AT
71	–	–	–	–	Morava	CZ
72	Moraviae, fons	Moraviae, fons	Moraviae, fons	Moraviae, fons	Morava – pramen	CZ
73	–	–	–	–	Moravská Dyje / Mährische Thaya	AT, CZ
74	–	–	–	–	Mrlina	CZ
75	Misa fl	Misa fl	Misa fl	Misa fl	Mže / Mies	CZ, DE
76	X	X	X	–	Novohradka	CZ
77	–	–	–	–	Odrava	CZ, DE
78	Egra fl	Egra fl	Egra fl	Egra fl	Ohře / Eger	CZ, DE
79	Orlicze fl	Orlicze fl	Orlicze fl	Orlicze fl	Orlice	CZ
80	Oslawa, Woslawa fl	Oslawa, Woslawa fl	Oslawa, Woslawa fl	Oslawa, Woslawa fl	Oslava	CZ
81	Ottawa fl	Ottawa fl	Ottawa fl	Ottawa fl	Otava	CZ
82	Czirla fl	Czirla fl	Czirla fl	Czirla fl	Pe□cznica	PL
83	Pf[reimbd] fl	Pfreimbd fl	Pfreimbd fl	Pfreimbd fl	Pfreimd	CZ, DE
84	Pleisa fl	Pleisa fl	Pleisa fl	Pleisa fl	Pleißenbach	DE
85	Pulsnicz fl	Pulsnicz fl	Pulsnicz fl	Pulsnicz fl	Ploučnice	CZ
86	–	–	–	–	Pośna	PL
87	–	–	–	–	Pulkava / Pulkau	AT
88	–	–	–	–	Purzelkamp	AT
89	–	–	–	–	Radbuza	CZ
90	Teya	Teya	Teya	Teya	Rakouská Dyje	AT
91	–	–	–	–	Rakovnický p.	CZ
92	–	–	–	–	Retzbach	AT
93	Rosla fl	Rosla fl	Rosla fl	Rosla fl	Reslav / Röslau	CZ, DE
94	–	–	–	–	Řezná / Regen	CZ, DE
95	Sazawa fl	Sazawa fl	Sazawa fl	Sazawa fl	Sázava	CZ
96	–	–	–	–	Schmida	AT

	Aretin 1st edition, 1619	Aretin 2nd edition, 1632	Aretin 3rd edition, 1665	Aretin 4th edition, before 1747	Current name	State
97	–	–	–	–	Nemanický p. / Schwarzach	DE
98	–	–	–	–	Smědá / Witka	CZ, PL
99	–	Spre fl	Spre fl	Spre fl	Spréva / Spree	CZ, DE
100	Steina fl	Steina fl	Steina fl	Steina fl	Stěnava / Ścinawka	CZ, PL
101	–	–	–	–	Střela	CZ
102	–	–	–	–	Sulzbach	DE
103	Zwota fl	Zwota fl	Zwota fl	Zwota fl	Svatava / Zwota	CZ, DE
104	Switawa fl	Switawa fl	Switawa fl	Switawa fl	Svitava	CZ
105	Sswartzawa fl	Sswartzawa fl	Sswartzawa fl	Sswartzawa fl	Svratka	CZ
106	–	–	–	–	Šlapanka	CZ
107	–	–	–	–	Taffa	AT
108	–	–	–	–	Teplá	CZ
109	–	–	–	–	Tichá	CZ
110	Orlicze fl	Orlicze fl	Orlicze fl	Orlicze fl	Tichá Orlice	CZ
111	–	–	–	–	Tismenický p.	CZ
112	–	–	–	–	Trojanský p.	CZ
113	–	–	–	–	Třebovka	CZ
114	–	–	–	–	Třebůvka	CZ
115	–	–	–	–	Úhlava	CZ
116	–	–	–	–	Úslava	CZ
117	Vpawa fl	Vpawa fl	Vpawa fl	Vpawa fl	Úpa	CZ
118	Wltawa, Wulda fl	Wltawa, Wulda fl	Wltawa, Wulda fl	Wltawa, Wulda fl	Vltava	CZ
119	Nab fl	Nab fl	Nab fl	Nab fl	Lesní Nába / Waldnaab	DE
120	Ssopa fl	Ssopa fl	Ssopa fl	Ssopa fl	+Zschopau	DE
121	–	–	–	–	Zwettl	AT
Water areas						
1	Badhamer See	Badhamer See	Badhamer See	Badhamer See	Betlémský	CZ
2	–	–	–	–	Bílý Halštrov	CZ
3	Jordan	Jordan	Jordan	Jordan	Jordán	CZ
4	–	–	–	–	Mladotický r.	CZ
5	–	–	–	–	Rožmberk	CZ
6	–	–	–	–	u Blatné	CZ
7	–	–	–	–	u Eslarn	CZ?
8	–	–	–	–	u Lam	DE
9	–	–	–	–	u pramene Labe	CZ
10	–	–	–	–	u Třeboně	CZ
11	–	–	–	–	u Třeboně	CZ
12	–	–	–	–	u Třeboně	CZ
13	–	–	–	–	u Třeboně	CZ
14	–	–	–	–	u Třeboně	CZ
15	–	–	–	–	u Třeboně	CZ
16	–	–	–	–	u Třeboně	CZ
17	–	–	–	–	Všerubský r.	CZ

Notes to table:
fl, flu from Latin fluvius, a river; – unnamed watercourse; X watercourse is not plotted; AT watercourse flows through Austria; CZ watercourse flows through the Czechia; DE watercourse flows through Germany; PL watercourse flows through Poland; + two watercourses are connected into one (Bóbr+Kamienna, Bystřice+Černá, Flöha+Zschopau)

River channel stability assessment under flow alteration: The Brda River case study (Poland)

Dawid Szatten[1,*], Alberto Bosino[2]

[1] Kazimierz Wielki University, Faculty of Geographical Sciences, Poland
[2] University of Milano-Bicocca, Department of Earth and Environmental Sciences, Italy
[*] Corresponding author: szatten@ukw.edu.pl

ABSTRACT

The processes of erosion, transport, and accumulation of river sediments are determined by the balance between the natural fluvial processes and the anthropic pressure. Evaluation of the degree of river channel stability is one of the ways to establish the pressure of human activity that could be directly reflected in the volume of eroded or accumulated sediments in a river. The research here proposed is focused on the last natural section of the Brda River (Poland), which represents a natural hotspot in a deeply anthropized fluvial system. To evaluate the human pressure on the natural river section, we developed a methodology that integrates hydrological and sedimentological studies as well as remotely sensed data. In particular, we applied: (i) the Indicators of Hydrologic Alteration (IHA) method, based on hydrological data; (ii) the erosion coefficient, based on suspended sediment balance; and (iii) spatial analyses of riverbed centerline migration of the Brda River in the section from Woziwoda to Płaskosz (northern Poland) to gain a comprehensive understanding of the fluvial dynamics in the area over a period of 60 years. A significant peculiarity of this research refers to the year 2001 when the operational regime of the Mylof Reservoir was changed from hydropeaking to run-of-river. The results obtained indicate a minor river regime transformation and sediment transport continuum disturbance. Finally, the link between the stability of the Brda riverbed, and the intensification of bank erosion (meandering) resulting from the balance of sediment supply, has been demonstrated. The results presented reflect the climate change trends (on the macro-scale) and human activity in the catchment (on the micro-scale) on the fluvial processes.

KEYWORDS

river stability; meandering river; sediment transport; the Indicators of Hydrologic Alteration (IHA); spatial analyses

Received: 12 August 2024
Accepted: 5 February 2025
Published online: 18 February 2025

Szatten, D., Bosino, A. (2025): River channel stability assessment under flow alteration: The Brda River case study (Poland). AUC Geographica 60(1), 134–150
https://doi.org/10.14712/23361980.2025.5

1. Introduction

Fluvial erosion is one of the most significant earth-modeling processes, shaping the earth's surface and creating landforms that can, directly or indirectly, impact human life (Brown et al. 2017). Fluvial geomorphology includes a wide set of landforms associated with erosion, transport, and accumulation of sediments. In general, erosive processes impact both the fluvial environment and the anthropic system. In particular, lateral erosion, as well as levee breach or meander cutoff, leads to the widening and the avulsion of the river channel within the valley (Leopold et al. 1992), causing problems connected to the sediment transport and deposition. The increase of sediments can lead to disruption of fish spawning in the gravel-bed rivers (Wood and Armitage 1997), habitat loss for species that depend on riverbank ecosystems (Florsheim et al. 2008), and interference with existing habitats, causing some species to be displaced (Poff and Zimmerman 2010). Fluvial erosion acts on both the river's bed (vertical incision) and the banks (lateral erosion). In the first case, bed erosion shapes the bottom of the river, as well as the fluvial landforms sited in the riverbed, e.g. point bars that can contribute to increasing the solid fluvial transport. On the contrary, bank erosion reshapes the river, sometimes causing the erosion of depositional landforms (e.g., flanks of fluvial islands) or causing fluvial avulsion processes (Ward et al. 2002). In general, the activity of a river can be derived from a multitemporal analysis of the channel path, occasionally indicating the activity of the erosive processes and their magnitude (Wohlfart et al. 2016; Monegaglia et al. 2018; Mandarino 2022; Bosino et al. 2024). The morphology of a river and its morphodynamics are guided by several factors like the hydrological conditions (Leopold et al. 1992), longitudinal channel slope (Montgomery and Buffington 1997), lithology (Słowik 2014), size of sediments present in the riverbed (Schuurman 2015), vegetation (Tal and Paola 2010) and anthropogenic factors (Graf 2006). Meandering channels are one of the most distinct river channel types that can be observed in lowland areas (Słowik 2013; Słowik et al. 2020; Oglęcki et al. 2021). Depending on the lithological nature, cohesion, and absorbency of the riverbank, water erosion mainly occurs during the floods causing sediment mobilization and erosion (Kleinhans et al. 2024) modifying the channel pathway. The water velocity acts on the intensity and nature of river erosion, depending on the slope, river channel shape and type, shear stress distribution, and water mass (Sylvester et al. 2019). It results in a simple dependence statement: the erosive power increases with the increase in water velocity (Leopold et al. 1992). In alluvial rivers, the type of water movement also affects the erosion process, where turbulent flow is considered highly energetic. Finally, the load and grain size of the transported sediment play a critical role in determining the intensity and type of the erosion process. Coarser sediments, such as gravel contribute more intense abrasion of the river channel and banks due to their kinetic energy, than finer sediments. The amount and grain size of the transported sediments depend in general on the catchment characteristics, e.g. geological structure (Konsoer et al. 2016), land use (Juez et al. 2018), vegetation cover (Larsen 1995), or degree of catchment transformation, e.g. presence of dams and reservoirs (Szatten et al. 2021). In meandering rivers, the sediments eroded from the riverbank are part of the sediment transport and can be partly accumulated on the opposite bank (point bar) due to the action of transverse thalweg (Sylvester et al. 2021). The constant increase of the radius of curvature leads to the cutoff of the meander pattern, shortening the river's course. The higher power of the water velocity above the cutoff point is conducive to bed erosion, which causes the bend to be blocked off from the main river. Over time, it is excluded from the river flow, becomes shallower, and an oxbow lake is formed (Shields and Abt 1989). On the other hand, the impact of humans on a fluvial system is well known to cause deep perturbations on river morphodynamics (e.g. Garzón and Alonso 2002; Walling 2006; Schuurman 2015).

Especially in the past century, most of the riverways that flowed in the alluvial plain were modified by humans for hydraulic purposes (dam construction), to protect villages and cities close by creating sometimes flood control polders, artificial riverbank protections, etc. (e.g. Habel 2013; Marren et al. 2014; Szatten et al. 2023). The impact of dam construction on floodplains as well as river morphodynamics is a worldwide phenomenon (e.g. Kingsford 2000; Marren et al. 2014; Liaghat et al. 2017). More in general, human interaction within rivers has meant that the natural conditions were replaced in large river portions. However, detecting and studying these sectors can be of fundamental importance to understand the original hydromorphological conditions of the river as well as to estimate the sources of sediments that can be directly correlated with the natural or anthropic erosion processes.

The main aim of the research is to assess the stability of the Brda riverbed on the section between Woziwoda and Płaskosz Villages, Kuyavian-Pomeranian Voivodeship, north-central Poland (Fig. 1), in relation to the catchment area's natural conditions as well as to human influence. The river transformation degree and the sediment transport dynamics were evaluated with hydrological, sedimentological, and spatial data. The research hypotheses assume that: (i) the Brda River water flow regime is transformed due to of human activity; (ii) the discharge alteration determines a change in suspended sediment transport dynamics having a direct response in channel meandering processes. The methodology proposed here, includes the long-term assessment of the mean annual variability of river discharge, the Suspended

Sediment Concentration (SSC) evaluation, its correlation with the hydrological alteration of the river (IHA method) in order to understand the hydrologic impact of human activities, the erosion coefficient (A) calculation in order to weight the erosion, transport and deposition processes, and finally, the multitemporal evaluation of the river sinuosity though dedicated Geographic Information System (GIS) analysis. Therefore, the study highlights that through modern GIS techniques and hydrological analysis, it is possible to derive information regarding channel stability in areas lacking long-term monitoring stations.

2. Material and methods

2.1 Study area

The Brda River is one of the largest lowland rivers in Poland, with a total length of 245 km and a total catchment area of 4,661 km^2 (Map of the Polish Hydrographic Division 2007). The river can be divided into three sections characterized by different environmental characteristics: (i) upper, mainly characterized by large lakes retention, (ii) middle, which preserves natural conditions and in which the study area is

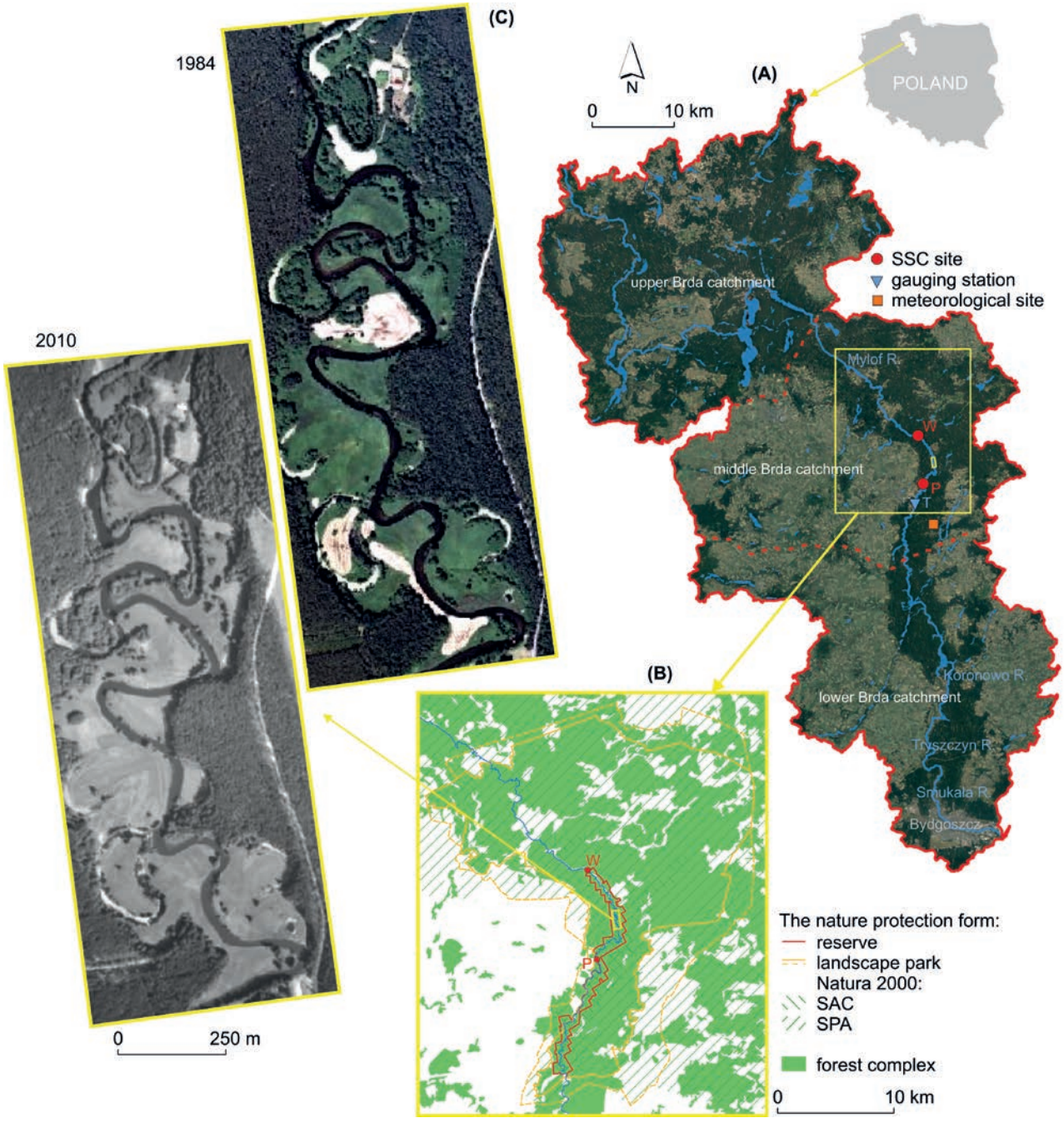

Fig. 1 Study area: (A) Land cover (Google satellite image) of the Brda catchment; (B) the nature protection form; (C) detailed study area in 1984 and 2010.

situated, and (iii) lower, which is highly modified by intense human activity (Fig. 1A).

In the upper part of the catchment, the Brda River flows through 16 natural lakes, which significantly stabilize its regime of water flow. The middle part of the Brda River catchment begins with the Great Brda Canal (104.2 km of the river course) and ends with the backwater of the Koronowo Reservoir (169.9 km of the river course). It is characterized by the dominance of forest cover quantifiable as about 60% of the entire catchment (Szatten and Habel 2020). In addition, this part of the river is characterized by the presence of the Mylof Reservoir which was created in 1848. The lower part of the catchment was already transformed in the 19th century by the construction of weirs and sluices for the mills and for timber rafting purposes (Szatten et al. 2021). Currently, the area is characterized by three artificial reservoirs: Lower Brda Cascade (Koronowo, Tryszczyn, Smukała), constructed in the 1960s (Szatten et al. 2018). In general, the Brda River is characterized by one of the lowest discharge variabilities among all Polish rivers (Choiński 1988).

The investigated study area covers a section of the Brda River enclosed between the villages of Woziwoda (140.8 km of the river course) and Płaskosz (159.0 km of the river course), where spatial analyses of channel meandering rate (section 2.3.3.) were performed for a part of the river near Gołąbek village with a length of 2.6 km (between 145.0 km and 147.6 km of the river course) (Fig. 1C). The river valley is made of fluvioglacial (outwash) sands and gravels, filled with Holocene peat sediments with a variable thickness from 1 to 2.5 m (Pikies 2009). The width of the river valley is about 400 m in the study area. In the research area, the riverbed has a uniform cross-sectional profile. It is deepest close to the concave bank, about 2.0–2.5 m at an average flow, and at the convex bank it is usually shallower – about 1 m. The average channel slope in the analyzed section is 0.23‰. This area is located on the ecotone border of two physic-geographical mesoregions, Tuchola Forest (in the north) and Brda River Valley (in the south) (Solon et al. 2018). In this sector Brda River has a meandric-shaped planimetric development and is sited in a large, densely forested complex of Bory Tucholskie. The most characteristic landforms of the area associated with the fluvial morphodynamics are the oxbow lakes, reactivated during high flow periods. The valley's edge is elevated above its bottom by about 10 m. Finally, the study area includes several nature protection forms, based on the Central Register of Nature Protection Forms provided in the web application (https://crfop.gdos.gov.pl), e.g. reserve – the Brda River Valley, Tuchola landscape park, the Special Areas of Conservation (SAC) – the Brda and Stążka Valley in Bory Tucholskie, and the Special Protection Areas (SPA) – Bory Tucholskie as part of the Natura 2000 protected area network (Fig. 1B).

The Mylof Reservoir operating regime changed in 2001. In our research, this date is considered as the threshold date for analysis because the hydropeaking operation regime (starts at the end of XIX Century, from the dam was commissioned) passed to the run-of-river operation implemented in 2001 (Fig. 2). Its introduction was related to the implementation of pro-ecological provisions of the Water Law Act (Water Law Act 2017). The first, hydropeaking operation regime resulted in a higher temporary increase in river flow downstream of the hydroelectric power plant than the second, run-of-river operational regime. This change is also observed throughout the entire Lower Brda cascade (Szatten et al. 2021).

2.2 Materials

The workflow adopted in this research is illustrated in Fig. 3.

2.2.1 Hydrological and climatological data

Hydrological data were daily values of discharge (Q, in $m^3\ s^{-1}$) for the period 1981–2017 obtained from the

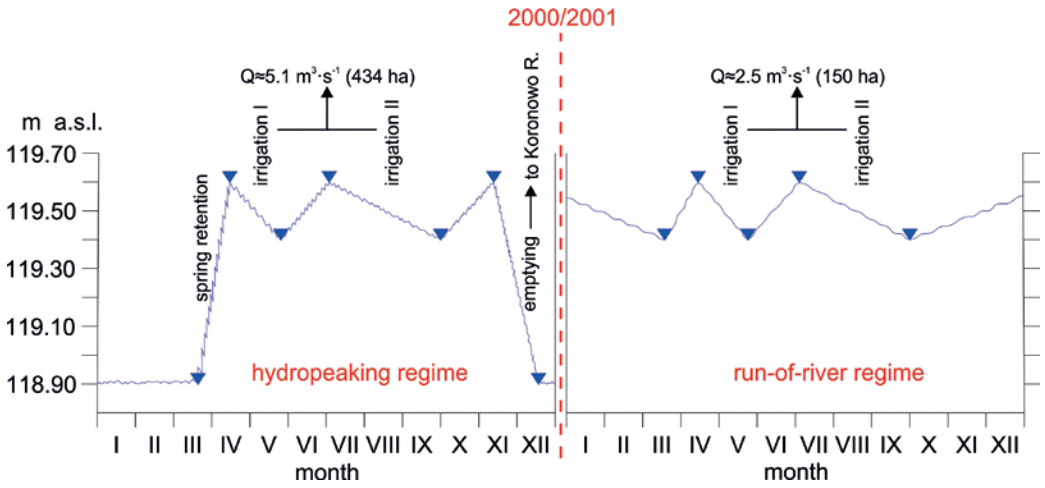

Fig. 2 The sketch of hydropeaking and run-of-river operational regime on Mylof Reservoir.

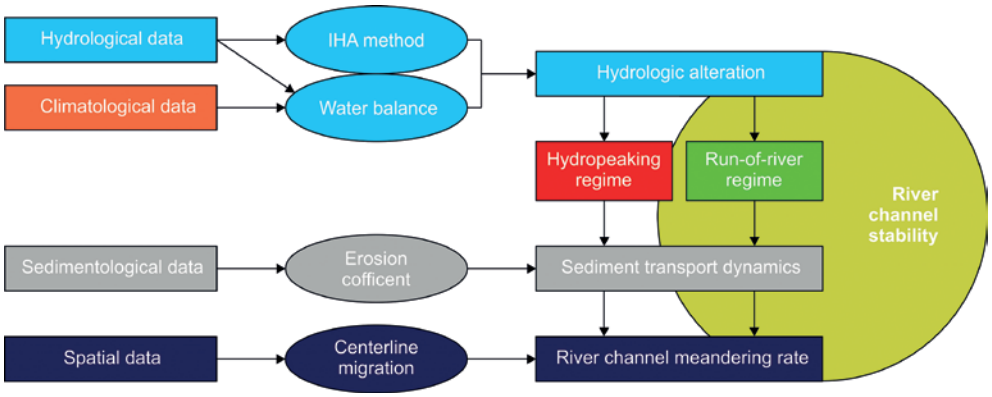

Fig. 3 General workflow of the Brda River Woziwoda-Płaskosz sub-catchment.

resources of the Institute of Meteorology and Water Management – National Research Institute (IMWM-NRI). The Tuchola water gauging station (Fig. 1A) is located 159.1 km of the Brda River course, the closest to the study area, making it a reference station in determining the hydrological conditions for this part of the sub-catchment.

The annual sums of precipitation (in mm) were used from Płazowo meteorological station belonging to the IMWM-NRI for the years 1981–2017. The statistical significance of trends was tested using Student's t-test at a significance level of 0.05. Climatic data on annual precipitation anomalies were provided by the ERA5 Explorer web application (https://cds.climate.copernicus.eu/cdsapp#!/dataset/reanalysis-era5-land?tab=overview). The precipitation anomaly is understood as the difference (in %) between the annual precipitation (in mm) over the period 1981–2018, and the long-term average (reference period 1981–2010), using a combination of forecast models and data assimilation systems to "re-analyze" previous observations (Muñoz Sabater 2019). Based on the research by Okoniewska and Szumińska (2010), the water balance was supplemented with evaporation (E), calculating the catchment retention (ΔR) using the equation:

$$P - E - Q = \Delta R, \quad (1)$$

where: P is the annual sums of precipitation (in mm), E is annual evaporation (in mm) (Okoniewska and Szumińska 2010), Q is annual river flow (in mm), and ΔR is the catchment retention (in mm).

2.2.2 Sedimentological data

Sedimentological data are characterized by average monthly values of Suspended Sediment Concentration (SSC, in mg l^{-1}) from 1984 to 2011, obtained from the resources of the National Environmental Monitoring. The observation sites were located directly: (i) above the study area (Woziwoda, 140.8 km of the Brda River course) and (ii) below (Płaskosz, 159.0 km of the Brda River course) (Fig. 1). Due to the implementation of the provisions of the Water Framework Directive (2000) directly into the Environmental Monitoring Programme, monitoring was discontinued in the sites mentioned above after 2011. Their location within the Brda River water body from Bielska Struga to Hozjanna (code id 292551) (Map of the Polish Hydrographic Division 2007) prevented further monitoring in such a dense network of sites, which is the reason for the sedimentological data lack.

2.2.3 Spatial data

Spatial data included aerial photographs and an orthophotos map from the resources of the Head Office of Geodesy and Cartography, obtained using WMS services from the access point of the Spatial Information Infrastructure (geoportal.gov.pl). The data represented the ETRF2000-PL (EPSG:2180) metric coordinate system. Their detailed characteristics are presented in Tab. 1.

Tab. 1 Characteristics of spatial data.

No.	Data (Picture no.)	Centroid coordinates		Scale	Type	Q Tuchola $m^3 s^{-1}$
		X	Y			
1.	1984-08-23 (3139)	641094.42	430591.31	12 000	B/W	21.0
2.	1996-06-07 (0855)	640525.57	431808.39	26 000	RGB	16.3
3.	2004-07-30 (4729)	640538.80	431808.39	26 000	B/W	14.2
4.	2010-07-02 (0024)	641478.07	430961.72	48 000	RGB	12.9

Explanation: picture composition B/W – black/white, RGB – red-green-blue.

2.3 Methods

2.3.1 Hydrological transformation

To determine the hydrological boundary conditions affecting the fluvial processes in the research area, long-term trends of water discharge for the Tuchola water gauging station were derived starting from the method of integral curves described by Obodovskyi and Lukianets (2017). The input data were the annual characteristics of the discharge (Q_i), i.e. minimum (Q_{min}), maximum (Q_{max}), and average (Q_{av}) values, in the period 1981–2017. The long-term mean annual variability of river discharge was calculated using the equation:

$$k_i = \frac{Q_i}{Q_{av}} \rightarrow f_{(i)} = \sum(k_i - 1), \quad (2)$$

where: k_i is the modular factor, Q_i is the value of the i-th term of the series, Q_{av} is the arithmetic mean, and $\sum(k_i - 1)$ is the sum of deviations.

The increase in the course of the curve (k_i) corresponds to the trend of increasing discharge, and conversely, when the curve decreases, a trend of decrease in discharge is observed.

Water balance (equation 1), and flow oscillation (equation 2) were verified using the distribution of annual precipitation anomaly – ERA5 model (Muñoz Sabater 2019), and together with the information about operational regime changes on Mylof Reservoir in 2001, was pointed out as boundary for further analyses.

The Indicators of Hydrologic Alteration (IHA), a method proposed by Richter et al. (1996), was utilized to assess the hydrologic impacts of human activities on the Brda River. IHA software (ver. 7.1.0) provided by The Nature Conservancy (Arlington, VA, U.S.) was employed for the calculations. The methodology included: (i) determination of input data for the periods 1984–2000, and 2001–2018, (ii) defining Non-Parametric Hydrological Statistics between time series, (iii) calculation of IHA values for 33 hydrological parameters described by Richter et al. (1996) and plotted in Fig. 4. According to Richter et al. (1996), they include 5 statistical groups: (i) the magnitude of monthly water conditions, (ii) the magnitude and duration of annual extreme water conditions, (iii) the timing of annual extreme water conditions, (iv) the frequency and duration of high and low pulses and (v) rate and frequency of water condition changes.

Classification of the discharge transformation for the 33 tested parameters was carried out based on the Range Variability Approach (RVA) criterion (Richter et al. 1997). The RVA uses the pre-development natural difference of IHA parameter values as a reference for defining the extent to which natural flow regimes have been altered and quantifies this alteration in a series of Hydrologic Alteration factors. According to the adopted method (Richter et al. 1998), the range $|RVA \leq 0.33|$ means low discharge transformation, the range $|0.34 \leq RVA \leq 0.67|$ is associated with moderate transformation, and finally, the range $|RVA \geq 0.68|$ corresponds to a large alteration.

2.3.2 Sedimentological analyses

The relation between discharge (Q) and SSC is one of the fundamental methods to determine the erosion-transport-accumulation conditions of the river catchment. This dependency is also used by Obodovskyi and Lukianets (2017) based on the erosion coefficient (A) definition, which is the antilogarithm of the value at the point of intersection with the Y-axis of the trend line from the distribution of dependencies $lg_{SSC} = f(lg_Q)$. The antilogarithm is a specific case of an exponential function, where the variable appears in the exponent (e.g., a^y). In the case of our data, a served (a) as the constant base (log10), while the exponent (y) varied (SSC or Q). Considering the availability of data described in subchapter 2.2.2, its value was determined for the Woziwoda (140.8 km of the Brda River course) and Płaskosz (159.0 km of the Brda River course) sites (Fig. 1) for the periods: 1984–2000, and 2001–2011. It is necessary to point out the weakness of our research here, because Q/SSC relationship is commonly modeled using a power function (Müller and Forstner 1968; Horowitz 2003), and lack of data made it impossible to use the best method to be expressed by hysteresis patterns (Gregory and Walling 1973) to describe this relationship. A value >7 of the A-coefficient (Obodovskyi and Lukianets 2017) is related to river channel instability, identified with intensive accumulation/sediment erosion processes. On the contrary, a low A coefficient value is characteristic of a stable riverbed. Also, based on monthly values SSC and Q was possible to calculate the Suspended Sediment Load (SSL) for the Woziwoda – Płaskosz sub-catchment from 1984 to 2010.

2.3.3 Multitemporal analysis

Spatial analyses were performed in QuantumGIS (ver. 3.22.13) and SAGA GIS (ver. 7.8.2) software (Conrad et al. 2015). The acquired aerial photographs and the orthophoto map, characterized in detail in subchapter 2.2.3, correspond to the metric spatial system ETRF2000-PL (EPSG: 2180). Using QGIS tools, the spatial extent of the Brda channel was digitized for 1984, 1996, 2004, and 2010. Then, the channel centerline was determined using the Geometric Attributes tool (Nyberg et al. 2015). The use of centerline in river planform change studies was proposed by Ikeda and Parker (1989). In the study area, 10 meanders were identified, and metric coordinates (Cx_iy_i) were assigned at characteristic points, enabling calculations of L_C – length of the river measured along the centerline, L_V – valley length, S – sinuosity index (Rust 1996) (equation 3), and MR – centerline migration rate, in m year^{-1}.

$$MR = \frac{L_C}{L_V}, (3)$$

The distances in the transects used to calculate the LC, LV, and MR indices were determined using equation 4:

$$C_{xiyi} = \sqrt{\left(x_i - x_{(i-1)}\right)^2 + \left(y_i - y_{(i-1)}\right)^2}, (4)$$

According to research by Rosgen (1994), values of sinuosity index (S) indicate straight (S < 1.1), wavy (1.1 ≤ S < 1.4), and meandering (S ≥ 1.4) channels. Additionally, the migration rate analysis included local morphometric valley conditions and erosion to the eroded (concave) bank or the point bar (convex) bank direction.

3. Results

3.1 Evaluation of hydrological alteration

The starting point for determining hydrological alteration in the Brda River was to describe the variability of water balance affecting the Brda River catchment. The analysis of annual precipitation (P), annual evaporation (E), catchment retention (ΔR) (Fig. 4A), and precipitation anomalies based on the ERA5 model

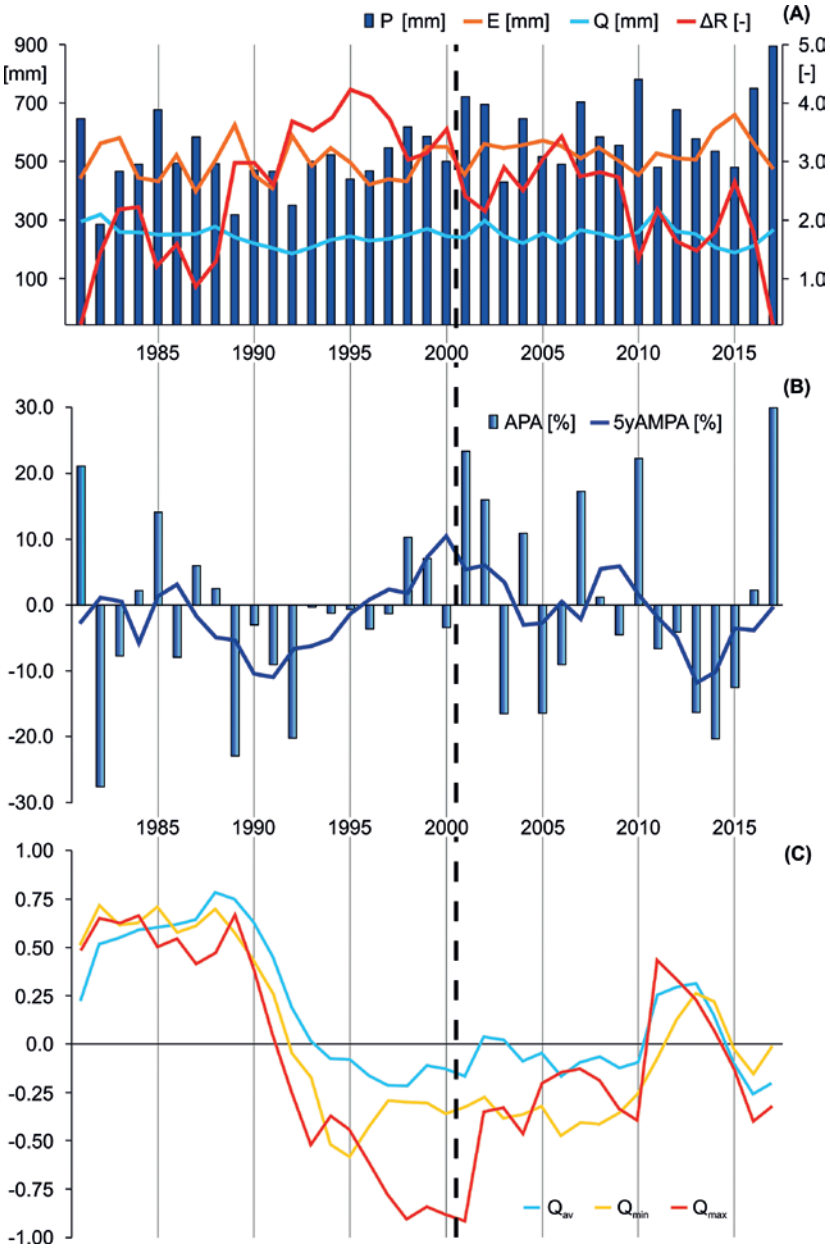

Fig. 4 The annual precipitation (P) at Płazowo site, annual sums of evaporation (E) (Okoniewska and Szumińska 2020), annual discharge (Q), and retention (ΔR) presented using the method of integral curves for the years 1981–2017 (A), the precipitation anomaly (APA) for each year in the 1981–2017 period as a percentage relative to the long-term reference period of 1981–2010 (B), and the long-term trend of water discharge for the Tuchola gauging station for $Q_{av.}$, Q_{max} and Q_{min} for the period 1981–2017 (C).

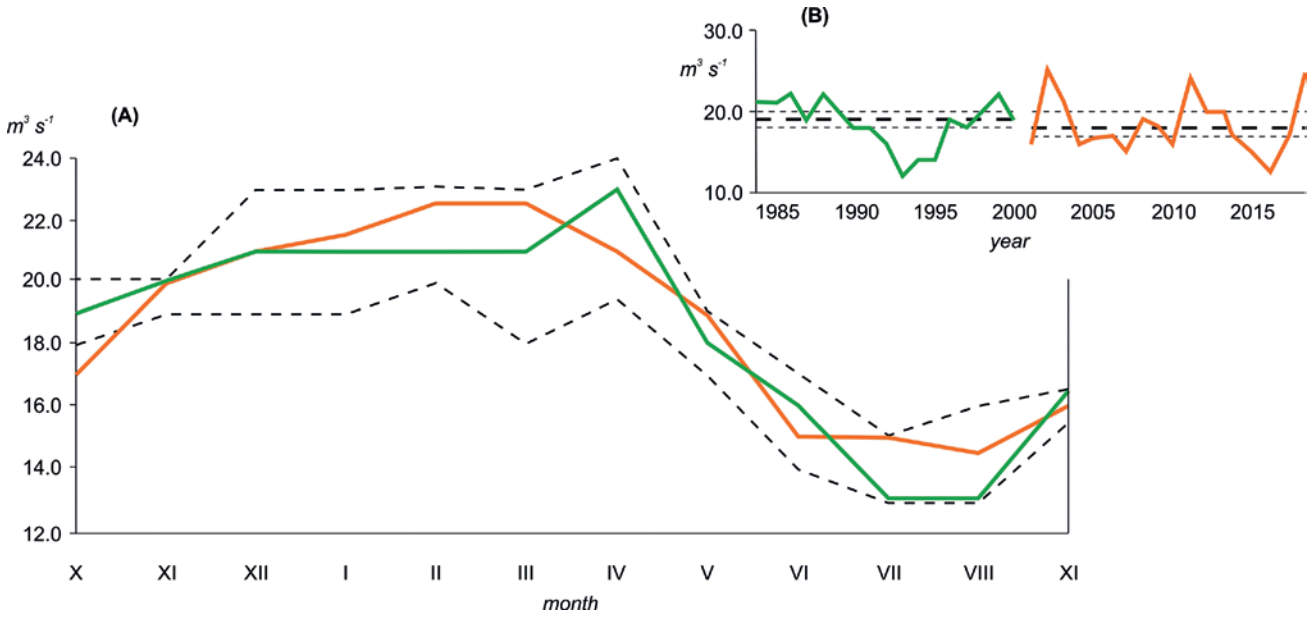

Fig. 5 Alteration of median monthly (A) and yearly (B) flows with RVA boundary (light blue area) for Tuchola gauging station in two analyzed periods (1984–2000 – green, and 2001–2018 – orange).

(Fig. 4B) in connection with the long-term trend of water discharge (Fig. 4C) enabled the determination of hydro-meteorological boundary conditions. Until the end of the 1980s, a stable trend of water discharge was observed, with a relatively stable precipitation component, and a decreasing trend of catchment retention (ΔR). The beginning of the 1990s was characterized by a reduction of atmospheric precipitation, and a strong negative precipitation anomaly, still a negative trend of retention (ΔR), which also resulted in a negative trend of water discharge. Then, a period of positive precipitation anomaly begins, which is reflected in a stabilization/slight increase in the trend of water discharge for Q_{av} and Q_{min}. However, the trend of water discharge for Q_{max} continues to decrease. Also, change in the ΔR trend is observed, indicating an increase in the retention of the catchment. The next change in the precipitation anomaly trend (Fig. 4B, from the year 2001), not clearly observed in annual precipitation (Fig. 4A) and the continued upward trend in retention (ΔR), results in an increasing direction of Q_{max} discharge trend, and a continuation of the positive trend of water discharge for Q_{av} and Q_{min}, which indicates the influence of different factors potentially including human activity, on the river regime. This indicator may be the change in the operational regime at the Mylof reservoir, allowing the indication of 2001 as the boundary year for IHA analyses. The following period (2010–2014) was characterized by positive precipitation anomalies and retetntion trend (ΔR) with negative trend of water discharge (Fig. 4). It is essential to point out that in the analysis of catchments with significant groundwater recharge and high surface retention, we observed a delay in the Q response to precipitation.

The Brda River is characterized by a typical lowland river regime, with higher discharge in the winter hydrological half-year (Fig. 5A). IHA research has shown that for October the Monthly Flow Alteration is outside of RVA boundaries, as 25th and 75th percentiles in the second period. Also, November, May, and July the Monthly Flows Alteration for the second period is very close to the RVA boundary. Moreover, for the two analyzed periods, it should be noted that the yearly flow below the RVA boundary occurred not only in the period of limited precipitation (1990s) with an average value 20.0 $m^3\ s^{-1}$, but also in the second period (2001–2017) where the annual discharge values was 18.5 $m^3\ s^{-1}$. In addition, variations significantly above and below the RVA boundaries (Fig. 5B).

In addition, considering the degree of flow transformation of the middle part of the Brda River catchment, IHA analyses indicated a significant discharge transformation in terms of individual groups of parameters. In the case of comparing the two periods (1984–2000 to 2001–2018), the greatest diversification of RVA can be noted in several parameters (Fig. 6): October Median Flows, 1-Day Minimum Flows, Date of Minimum Flows, Date of Maximum Flows, Low Pulse Count and High Pulse Count. The indicated parameters are consistent with the deviations of the water discharge trend shown in Fig. 4B.

In general, an increased dynamic in the changes of parameters is observed (Fig. 7). In the second period, the median value of 1-Day Minimum Flows outside of the RVA boundary is observed. Also, the median value of 1-Day Maximum Flows is higher in the second analyzed period. This proves the increase of extreme flow dynamics at the Tuchola gauging station. In the case

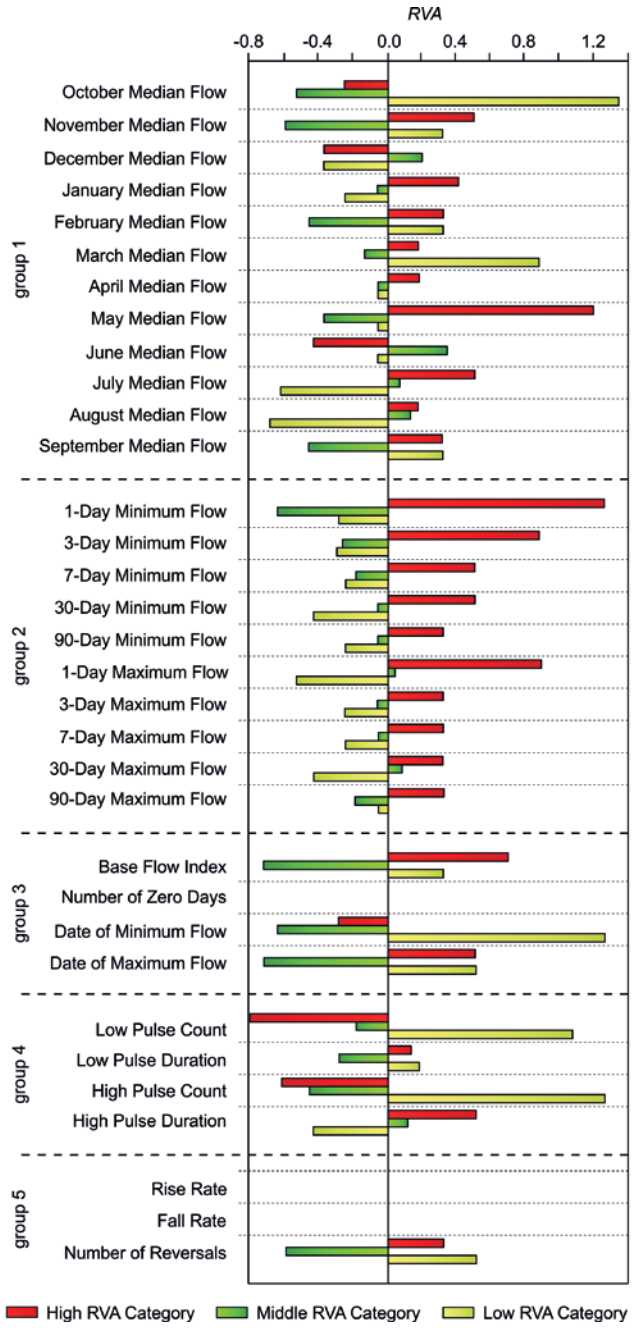

Fig. 6 Comparison of changes in the value of the greatest hydrologic alteration (HA) for 33 Indicators of Hydrologic Alteration (IHA) for the Tuchola gauging station using RVA target range between analyzed periods (1984–2000, and 2001–2018).

of the Date of Minimum Flow and Date of Maximum Flow, there was a significant acceleration (on median) from July 17 to June 30, and from February 22 to February 6, respectively. At the same time, in the second period, the median value of the above-mentioned indicators is below the lower RVA boundary. A similar situation is with the next two indicators. In the case of Low Pulse Count and High Pulse Count, there was a decrease in median values from 7 to 5 and from 8 to 6, respectively. At the same time, there is a clear tendency to decrease the dynamics of Pulse Count in the analyzed period. Changes in the dynamics of flows are also visible in the aspect of the Reversals indicator (Fig. 7).

3.2 Sedimentological response of hydrological alteration

The erosion coefficient (A) is related to the hydrological conditions and the dynamics of suspended sediment transport in the river and leads to information regarding the processes of erosion, transport, or deposition along a river. The analyzed section of the Brda River shows a high variability of sediment dynamics in time (Fig. 8). Generally, a decrease in the value of coefficient A on the Y-axis (Fig. 8) indicates a decline in SSC during the analyzed periods. However, for the period (1984–2000), a high A value for the Woziwoda site was observed, indicating the intensification of erosion processes and, thus, a decrease in the stability of the Brda riverbed. In this same period, Płaskosz site is characterized by a low A value, indicating high stability of the riverbed. The following period (2001–2018) is characterized by a decrease in the value of coefficient A, which indicates the high stability of the riverbed for all analyzed sites.

Sediment balance (SSL) confirms the assumptions of riverbed stability in the analyzed section of the Brda River. In the first period, both years with high positive and negative suspended sediment balances are observed, which confirms the thesis about the riverbed's instability. In the case of a positive balance, the erosion process predominated, and in the case of a negative balance, the accumulation of sediment predominated in the analyzed section of the Brda River. In the second period, mainly years with a relatively small positive sediment balance and years with stable conditions were observed (e.g. 2003, 2005, 2006, 2009) (Fig. 9).

3.3 Morphological response of hydrological alteration

The further step was assessing the river morphodynamics of the Brda River through the evaluation of the centerline in river planform change over time.

In the study area Brda River's meanders underwent typical spatial transformations, e.g. (i) extension (meander no. 6), or (ii) rotation (meander no. 4) (Fig. 10). Unfortunately, no case of neck erosion by chute was recorded in the analyzed period. However, on the analyzed orthophotomaps (Fig. 1) evidence of several meander cutoffs can be observed, now represented by oxbow lakes (Fig. 10).

In the analyzed period, most of the meanders are characterized by an increase in the sinuosity index (S) (Tab. 2). According to the criteria proposed by Rosgen (1994), out of the 10 analyzed meanders, 7 are characterized by an S value, which allows the classification of the channel as meandering. The highest value of the S index was recorded in meander no. 8

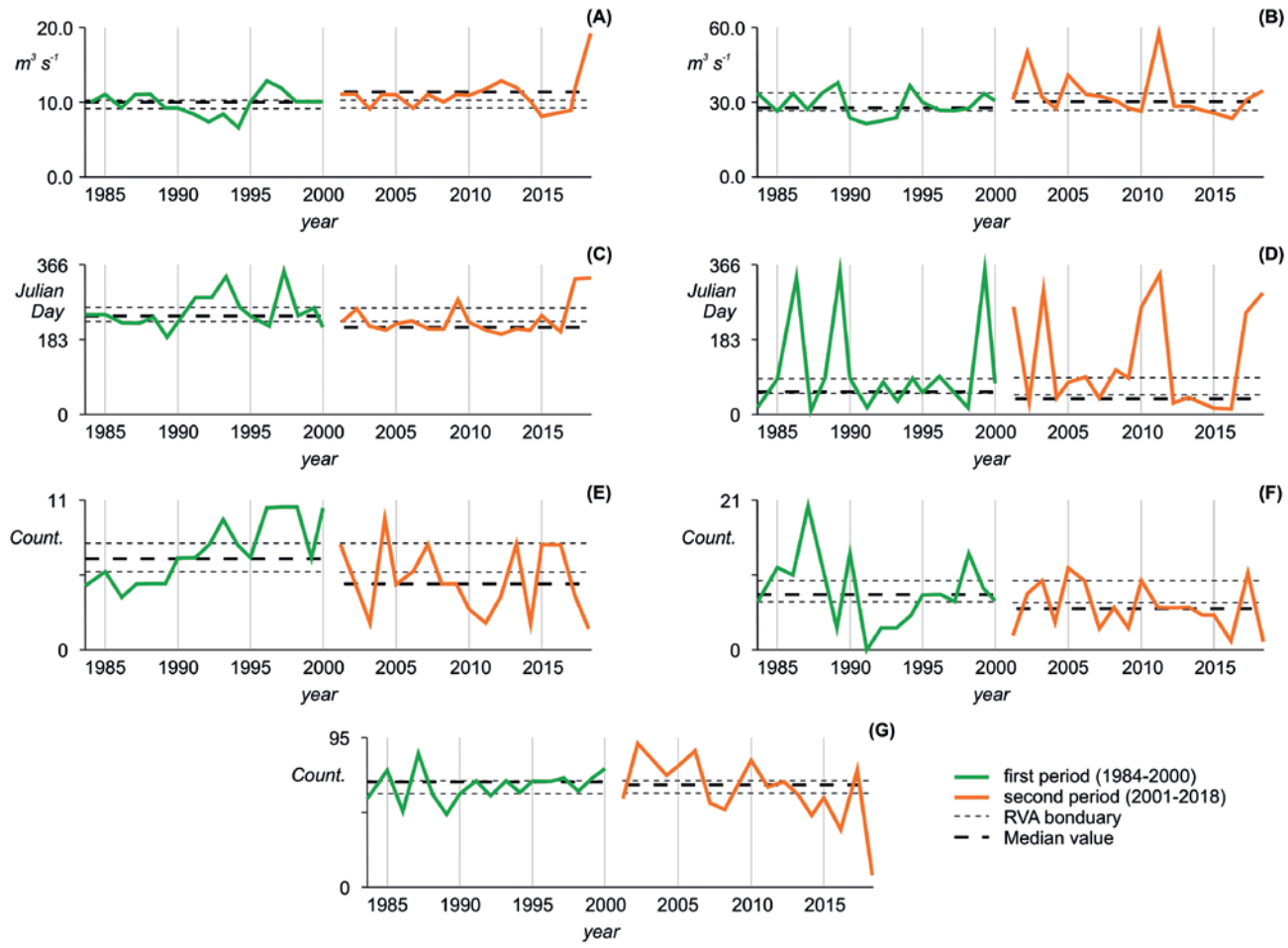

Fig. 7 Changes in medians of IHA selected indicators for the Tuchola gauging station in two analyzed periods (1984–2000, and 2001–2018): A – 1-Day Minimum Flows, B – 1-Day Maximum Flows, C – Date of Minimum Flow, D – Date of Maximum Flow, E – Low Pulse Count, F – High Pulse Count, G – Reversals (name of the indicators after Richter et al. (1996).

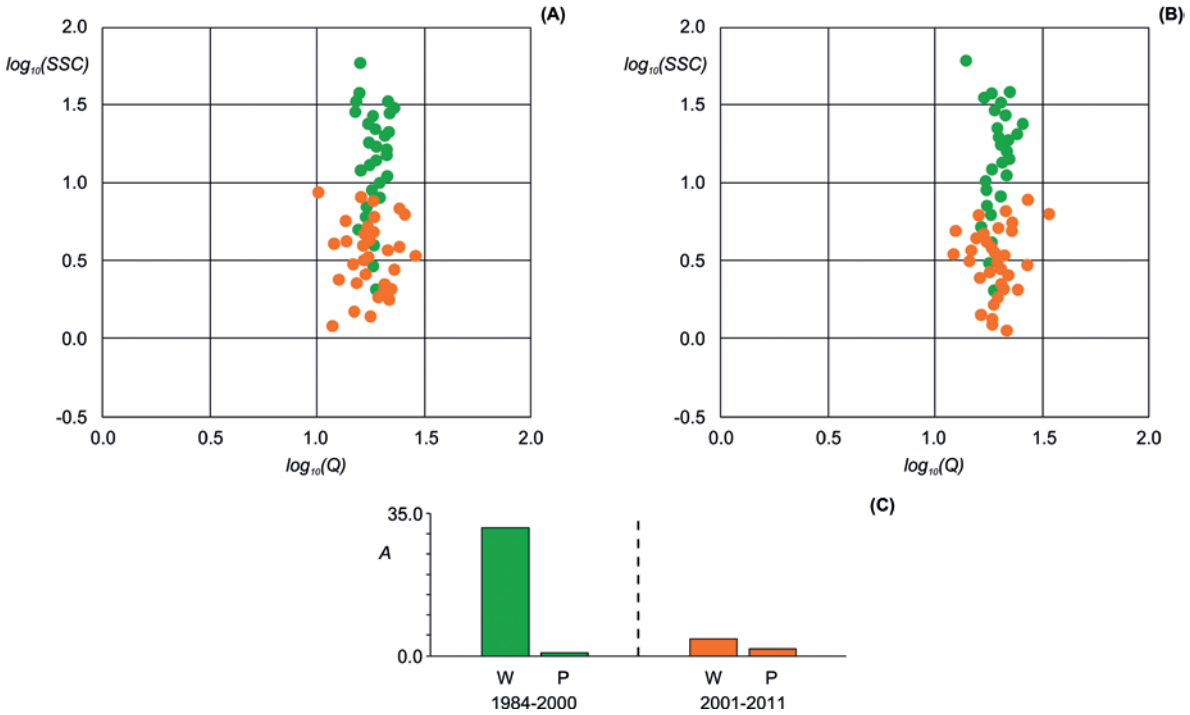

Fig. 8 The antilogarithm value of the erosion A-coefficient (C) for Woziwoda (a), and Płaskosz (b) in the analyzed periods: 1984–2000 (green), 2001–2011 (orange).

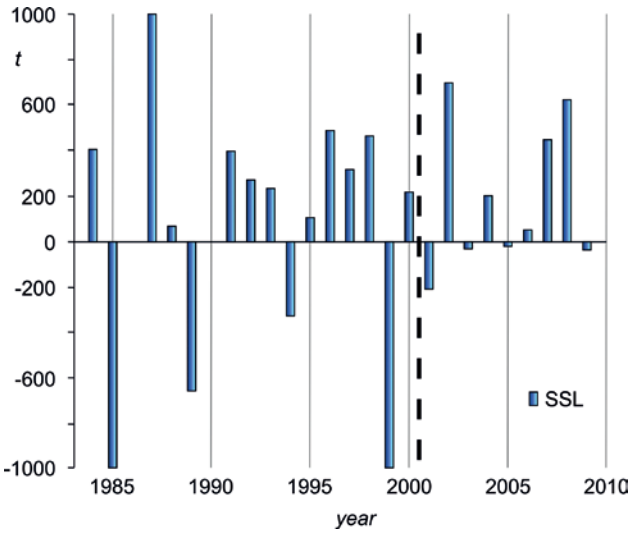

Fig. 9 Sedimentation balance (SSL) between Woziwoda and Płaskosz site (1984–2010).

Tab. 2 The sinuosity index (S) in the study area in analyzed years.

No.	1984	1996	2004	2010
1.	2.27	2.38 (+)	2.34 (–)	2.27 (–)
2.	1.26	1.31 (+)	1.36 (+)	1.37 (+)
3.	1.80	1.85 (+)	1.74 (–)	1.90 (+)
4.	1.73	1.60 (–)	1.69 (+)	1.72 (+)
5.	1.19	1.21 (+)	1.16 (–)	1.18 (+)
6.	2.25	2.38 (+)	2.38	2.41 (+)
7.	1.54	1.56 (+)	1.56	1.51 (–)
8.	7.93	8.85 (+)	9.01 (+)	9.00 (–)
9.	1.40	1.37 (–)	1.38 (+)	1.36 (–)
10.	2.06	2.25 (+)	2.11 (–)	2.20 (+)

Explanations: 1–10 meanders as Fig. 10; S index: wavy (1.1 ≤ S < 1.4) – black, and meandering (S ≥ 1.4) – red; +/– extension/cutoff year to year.

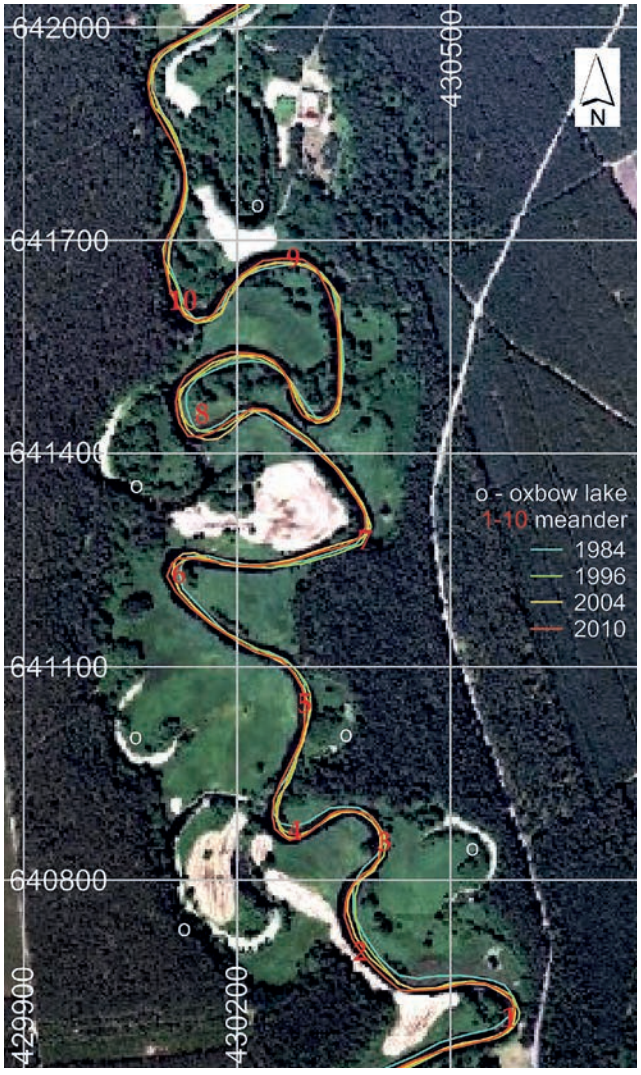

Fig. 10 Spatio-temporal changes of the Brda River centerline in the period 1984–2010 (1–10 analyzed meanders).

(S ≈ 9.00). The year-on-year change in the S index value indicates that the highest channel migration occurred in the years 1996, and 2010 (Tab. 2). This indicates substantial channel dynamics in the studied section of the Brda River. Based on the above-described criteria (Rosgen 1994), the remaining parts of the Brda riverbed (meanders no. 2, 5, 9) correspond to the wavy river channel type.

In addition, the centerline of the river channel migration rate varies, reaching a maximum of 1.0 m year^{-1} (Fig. 11). It should be noted that the migration of the channel centerline occurs due to bank erosion phenomena that shape the morphology of both the convex and concave parts of the meander. In most cases, bank erosion was observed (Fig. 11 – red color), indicating higher migration rates. It should be noted that two meanders (no. 4 and 8) covering the section of the river with the oxbow lake cutoff before 1984 (Fig. 10) were characterized by channel migration and rectification of the channel path. In the case of the other analyzed meanders, the thalweg shifted according to the fluvial processes using a change in the course of the channel. Mainly, the change in the orientation

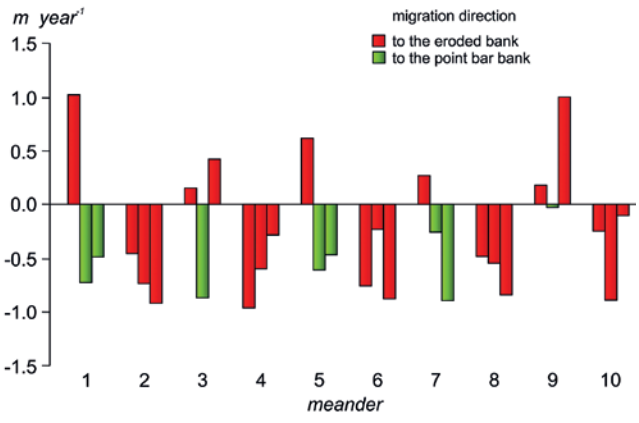

Fig. 11 The centerline of river migration rate (MR); Explanations: 1–10 meanders as Fig. 10; data bars in sequence 1984–1996, 1996–2004, and 2004–2010.

of the eroded bank in the period 1984–1996 (Fig. 11) can be observed in six (no. 1, 3, 5, 7, 9) studied meanders. It is worth noting that this concerns meanders located closer to the eastern edge of the valley. This situation may be caused by (i) the river reaching the edge of the valley, which may result in more difficult erosion, or (ii) the presence of bank vegetation. The latter has an important impact on the rate of meander migration rates (Micheli et al. 2004). Based on the qualitative analysis of trees vegetation conducted on aerial photographs and orthophotos map (Fig. 1, Tab. 1) it is noted that for meanders 1, 3, 7, and 10 it could have influenced the erosion resistance, which confirms the above thesis.

4. Discussion

Considering the significant transformation of river catchments as a result of human activity (Belletti et al. 2020), the continuity of sediment supply from source areas to coastal areas at the end of the system is disturbed (Walling 2006). The sediment continuum of the Brda River is heavily disturbed mainly due to the construction of artificial reservoirs (Szatten and Habel 2020; Szatten et al. 2021) that dramatically change the natural flow condition in the river. Today, the studied section of the river is characterized by the lowest pressure of human activity from all the Brda sub-catchments due to a lack of significant inflows (Map of the Polish Hydrographic Division 2007), point sources of pollution (Szatten and Habel 2020), presence of Bory Tucholskie forests (CLC 2018), and the presence of numerous nature protection restrictions (subchapter 2.1). In addition, it can be assumed that sediment dynamics is a derivative of natural channel processes in the studied sub-catchment, under the influence of geomorphological as well as external hydrological conditions partly connected to human activities (Marren et al. 2014).

The discharge differentiation of the Brda River is relatively small and relates to the lithological homogeneity of the bedrock that forms the catchment – outwash sands and gravels (Pikies 2009) and with the presence of a large number of lakes in the fluvial system (Choiński 1988). The above mentioned natural catchment characteristics result in a large retention capacity of the catchment and the long circulation time of water. The Brda River is characterized by a typical lowland river regime, with higher flows in spring and lower flows in summer (Fig. 5). The river flow indicators commonly established in the literature (Knighton 1998; Ward and Robinson 2000; Leopold et al. 1992; Montgomery and Buffington 1997; Słowik 2014; Schuurman 2015) are influenced by a combination of natural and anthropogenic factors: (I) climatic factors (e.g. precipitation, evapotranspiration, evaporation, seasonal variation as extreme events), (II) catchment characteristics (e.g. topography, soil type, land use, and vegetation change), (III) geological and geomorphological factors, and (IV) human activities (e.g. agricultural, urbanization, water management). The authors decided to select for the current research the parameters that were subject to the highest dynamics: factor I – precipitation, evaporation, and catchment retention, factor II – land use change, factor III – meandering dynamics related to SSC, and factor IV – change on operational system of Mylof Reservoir. The rest of the indicators were impossible to investigate due to lack of data or small variability of the indicator over time.

In the period 1981–2017, the river was significantly influenced by the precipitation component (factor I), which confirms the negative trend of water discharge in the early 1990s (Fig. 4). The observed drought was the result of fluctuations in the climatic factor. It was related to the recorded drought in Poland, e.g. in 1991, 1992, and 1994 (Somorowska, 2016). Also, it is essential to notice the time-delayed response of catchments such as the Brda River to rainfall, caused by a wide presence of forested areas (Szatten and Habel 2020) and lakes (Choiński 1988) resulting in significant water losses to evapotranspiration, especially in the summer half-year, when low water flow dominated (Fig. 5A). Furthermore, it is worth to note that in the research of Okoniewska and Szumińska (2010) a statistically significant increase in the evaporation trend in North-Western Poland was shown. Their data allowed to calculate water balance (equation 1) in the 1981–2017 period showing (i) general dominance of negative values of the retention factor (ΔR) which led to reduction of water resources in the catchment, and (ii) changes in the ΔR trend in 1995 from negative to positive, reflected in the increase of Q_{max}. However, in the long-term analyses (Fig. 4) considering the above-mentioned time-delayed response, a combination of limited precipitation supply and negative value of the water balance component – ΔR (Fig. 4A) with the occurrence of decreasing trend of water discharge (Fig. 4C) was observed, which partially links the influence of the climatic factors with the discharge.

However, the variation of the RVA category of the IHA (Fig. 6) in the second investigated period indicated pressures of human activity on the hydrological conditions. Comparing the two analyzed periods between 1984–2000 and 2001–2017, the dynamics of extreme flows on Tuchola gauging station were increasing. IHA analyses showed that particular indicators: October Median Flows, 1-Day Minimum Flows, Date of Minimum Flows, Date of Maximum Flows, Low Pulse Count, and High Pulse Count affected the largest diversity of IHA indicators (Fig. 7). The change in river regime (factor IV) is associated with the functioning of the Mylof reservoir, located above the study area, which is consistent with the results of research on other reservoirs, including Li et al. (2011), Habel (2013), Gierszewski et al. (2020), and (Szatten and Habel 2020).

Between 1990 and 2018, land use changes (factor II) in the entire Brda River catchment included a 1.8% increase in artificial surfaces and a 1.3% rise in forested and semi-natural areas, accompanied by a 2.1% decline in intensive agricultural land (Szatten and Habel 2020). These changes reflect moderate shifts primarily driven by agricultural extensification, afforestation, and urbanization processes within the catchment area.

The dynamics of hydrological conditions are directly reflected in the suspended sediment transport (factor III). In general, there was a trend of a decrease in the SSC over time (Fig. 8). It is due to the reduction in the supply from point pollution sources (Szatten and Habel 2020), which is consistent with the trend observed in Poland (Marszalewski and Piasecki 2014). We include here the reduction of point sources of water pollution related e.g. to industry, and treatment plants, and represented by the SSC indicator as per Water Framework Directive (2000) regulations. A decrease in the SSC between the studied sites was noted (Fig. 8), indicating that the section of the river between Woziwoda and Płaskosz has a generally accumulative character expressed by the surveyed suspended sediments. However, the erosion coefficient A for the Woziwoda site in the first studied period (1984–2000) assumed high values (Fig. 8) indicating that the above described hydrological transformations determined the increased channel instability. This hydrological transformation can be related to the hydropeaking operational regime at the Mylof Reservoir (factor IV). In this period, the intensive erosion/accumulation processes dominated the Brda riverbed in different parts of the river. In the second analyzed period (2001–2017), both observed sites were characterized by an increase in channel stability (Fig. 8). In general, above the study area was the sediment source supply area, which then was accumulated in the analysis section of the Brda River (Fig. 9).

The spatial analyses showed that the Brda River channel in the studied section was characterized by intensive centerline dynamics (factor III) (Fig. 10), as lowland river conditions. Studies show varying rates of increase of sinuosity index (S) in different river systems, e.g. Bolivian Amazon – increasing S from 1.4 to 3.6 between 1988 and 2010 (Monegaglia and Tubino 2019), increasing S from 0.95 to 3.25 between 1984 and 2014 (Ahmed et al. 2019). The highest dynamics were observed for the periods 1996-2010 (Tab. 2), when there was a strong migration of the river channel centerline, increasing the sinuosity index, and leading to the extension of the meanders (Fig. 10). It should be noted that the increase in the dynamics of channel migration refers to the above-described increase in the dynamics of extreme (minimum and maximum) flows, described by IHA results (Fig. 7). Abad and Garcia (2007) showed that hydrodynamics is the primary influential meandering factor. As stated by Allen (1997), during low water levels the eroded bank can be affected by water runoff, and during high water levels the riverbank can be washed by the river flow providing sediments to the fluvial system. These processes can be related to higher SSC on the Woziwoda site in the first analyzed period (Fig. 8).

The "butterfly effect" described by Meakin et al. (1996) makes the meandering river system difficult to predict in time and space. On the one hand, the meandering process is related to unstable conditions of the river catchment scale. On the other hand, the meandering process has also a stable character. The fully developed meanders of the Woziwoda-Płaskosz study area have similar characteristics of analyzed parameters, e.g. wavelength, amplitude, and meander belt width; their values are around the quasi-equilibrium

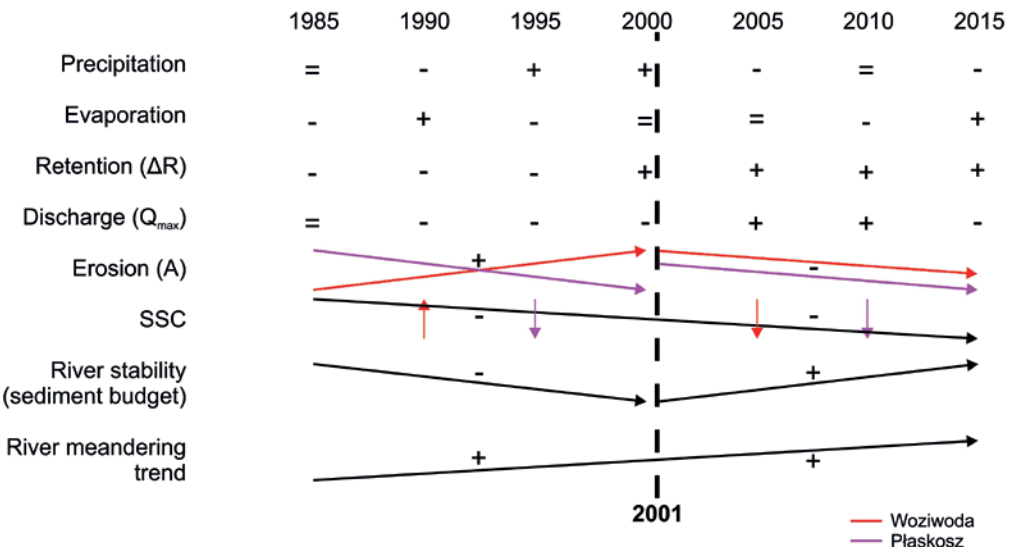

Fig. 12 Processes over time; Explanations: + ↑ increasing trend, – ↓ decreasing trend; = no trend/stability, Q_{max} – maximum discharge, A – erosion coefficient, SSC – Suspended Sediment Concentration.

state described by Xu et al. (2011), and showed stable conditions, especially in the second analyzed period. The analysis made it possible to determine the spatio-temporal source of sediment supply in the section of the river between Woziwoda and Płaskosz, which determines the sediment continuum in the middle section of the Brda catchment (Fig. 12).

5. Conclusions

This study has analyzed changes in discharge, precipitation, evaporation, catchment retention, sediment balance, and centerline migration in the Brda River caused by a combination of natural processes and human activities. Results showed that hydrological and sedimentological conditions of the sub-catchment are variable in time and space. The conducted research revealed that long-term trends of water discharge reflect the dependence between precipitation supply and evaporation components, considering the natural characteristics of the catchment (lithology, topography, etc.) constantly under the impact of negative retention capacity (ΔR). In addition, a time-delayed response of catchments is caused by a large percentage of forested areas and lakes which results in significant water losses to evaporation. In fact, our studies confirmed general rainfall-discharge trends, as exemplified by the low river flows caused by a prolonged drought observed in Poland in the 1990s. However, the greatest impact on the river flow regime on the studied section of Brda River was the change in the functioning of the Mylof Reservoir, from hydropeaking to run-of-river in 2001. Furthermore, if from one side a reduction in the sediment transport due to accumulation processes was detected, from the other side an increase of the flowing water energy, due to "hungry water" processes, was observed and related to the increase in meandering trend. The transformed river regime of the Brda River also influenced the channel meandering processes, directly related to extreme (minimum and maximum) flows. The supply of sediment to the Brda River fluvial system occurs prevalently after low water levels when material from eroded banks is washed (by runoff processes) or subjected to mass movement (down slopes under the force of gravity) into the river. As a result of water regime changes, the balance of suspended sediment of the river was disturbed in the analyzed section, decreasing the SCC values recorded in the analysis sites, with a positive SSL indicating sediment accumulation in the Płaskosz site. Worth to note, that in our research SSC does not include a detailed composition of the solids (e.g. organic part, phyto- and zooplankton). However, it will be possible to fill the gaps in our study in the future, giving a comprehensive picture of the supply sources in the catchment scale. Summarizing, our results contain valuable information that can be used to manage channel stability in areas lacking long-term monitoring stations, indicating water-sediment-land management direction at the catchment scale. The main novelty of this study is the integrated picture of fluvial processes describing long-term changes influenced by human activities from a regional perspective.

Acknowledgements

The authors are greateful to Pablo Flores for English language editing.

References

Abad, J. D., Garcia, M. H. (2008): Bed morphology in Kinoshita meandering channels: experiments and numerical simulations. In: 5th IAHR Symposium on River, Coastal and Estuarine Morphodynamics (ed. C. J. Dohmen-Janssen, S. J. Hulscher), Enschede, NL, 17–21 September 2007; 869–875; Taylor and Francis, London, UK, https://doi.org/10.1201/NOE0415453639.

Ahmed, J., Constantine, J. A., Dunne, T. (2019): The role of sediment supply in the adjustment of channel sinuosity across the Amazon Basin. Geology 47(9), 807–810, https://doi.org/10.1130/G46319.1.

Allen, P. (1997): Earth Surface Processes; Blackwell Science, https://doi.org/10.1002/9781444313574.

Belletti, B., Garcia de Leaniz, C., Jones, J., et al. (2020): More than one million barriers fragment Europe's rivers. Nature 588, 436–441, https://doi.org/10.1038/s41586-020-3005-2.

Bosino, A., Mandarino, A., De Amicis, M., Cazzini F. F., El Khair, D. A., Flores, P. (2024): Assessment of piping-sinkhole development in a fluvial-terrace scarp retreat environment: A multi-temporal analysis on the lower Ticino River (Italy). Geomorphology 450: 109082, https://doi.org/10.1016/j.geomorph.2024.109082.

Brown, A. G., Tooth, S., Bullard, J. E., Thomas, D. S. G., Chiverrell, R. C., Plater, A. J., Murton, J., Thorndycraft, V. R., Tarolli, P., Rose, J., Wainwright, J., Downs, P., Aalto, R. (2017): The geomorphology of the Anthropocene: emergence, status and implications. Earth Surface Processes and Landforms 42(1), 71–90, https://doi.org/10.1002/esp.3943.

Central Register of Nature Protection Forms. The General Directorate for Environmental Protection. Available online: https://crfop.gdos.gov.pl (accessed on 18. 12. 2024).

Conrad, O., Bechtel, B., Bock, M., Bock, M., Dietrich, H., Fischer, E., Gerlitz, L., Wehberg, J., Wichmann, V., Böhner, J. (2015): System for Automated Geoscientific Analyses (SAGA) v. 2.1.4. Geoscientific Model Development 8(7), 1991–2007, https://doi.org/10.5194/gmd-8-1991-2015.

Digital Elevation Model (2020): Head Office of Geodesy and Cartography. Available online: https://www.geoportal.gov.pl (accessed on 8. 10. 2022).

Directive 2000/60/EC of the European Parliament and of the Council of 23 October 2000 Establishing a Framework for Community Action in the Field of Water

Policy (2000): Available online: https://eur-lex.europa.eu/eli/dir/2000/60/oj (accessed on 21. 10. 2019).
European Environment Agency (2018): Corine Land Cover. Available online: https://land.copernicus.eu/pan-european/corine-land-cover/clc2018 (accessed on 10. 2. 2020).
Florsheim, J. L., Mount, J. F., Chin, A. (2008): Bank Erosion as a Desirable Attribute of Rivers. BioScience 58(6), 519–529, https://doi.org/10.1641/B580608.
Garzón, G., Alonso, A. (2002): Comparison of the flood response of a braided and a meandering river, conditioned by anthropogenic and climatic changes. Flood and Megaflood Processes and Deposits: Recent and Ancient Examples, 233–249, https://doi.org/10.1002/9781444304299.ch13.
Gierszewski, P., Habel, M., Szmańda, J., Luc, M. (2020): Evaluating effects of dam operation on flow regimes and riverbed adaptation to those changes. Science of The Total Environment 710: 136202, https://doi.org/10.1016/j.scitotenv.2019.136202.
Graf, W. L. (2006): Downstream hydrologic and geomorphic effects of large dams on American rivers. Geomorphology 79(3–4), 336–360, https://doi.org/10.1016/j.geomorph.2006.06.022.
Gregory, K. J., Walling, D. E. (1973): Drainage Basin. Form and Process: A Geomorphological Approach. Edward Arnold, London.
Habel, M. (2013): Dynamics of the Vistula River channel deformations downstream of Włocławek Reservoir; Kazimierz Wielki Univ Press, Bydgoszcz, Poland.
Horowitz, A. J. (2003): An evaluation of sediment rating curves for estimating suspended sediment concentrations for subsequent flux calculations. Hydrological Processes 17(17), 3387–3409, https://doi.org/10.1002/hyp.1299.
Ikeda, S., Parker, G. (1989): River Meandering; Water Resources Monograph AGU, Washington, United States; 485 p, https://doi.org/10.1029/WM012.
Juez, C., Hassan, M. A., Franca, M. J. (2018): The Origin of Fine Sediment Determines the Observations of Suspended Sediment Fluxes Under Unsteady Flow Conditions. Water Resources Research 54(8), 5654–5669, https://doi.org/10.1029/2018WR022982.
Kingsford, R.T. (2000): Ecological impacts of dams, water diversions and river management on floodplain wetlands in Australia. Austral Ecology 25(2), 109–127, https://doi.org/10.1046/j.1442-9993.2000.01036.x.
Kleinhans, M. G., McMahon, W. J., Davies, N. S. (2024): What even is a meandering river? A philosophy-enhanced synthesis of multilevel causes and systemic interactions contributing to river meandering. Geological Society, London, Special Publications 540(1), SP540–2022, https://doi.org/10.1144/SP540-2022-138.
Knighton, D. (1998): Fluvial Forms and Processes: A New Perspective. Don Mills, Ontario, Oxford University Press, https://doi.org/10.7202/022796ar.
Konsoer, K. M., Rhoads, B. L., Langendoen, E. J., Best, J., Ursic, M. E., Abad, J. D., Garcia, M. H. (2016): Spatial variability in bank resistance to erosion on a large meandering, mixed bedrock-alluvial river. Geomorphology 252, 80–97, https://doi.org/10.1016/j.geomorph.2015.08.002.
Larsen, E. W. (1995): Mechanics and Modeling of River Meander Migration. PhD Thesis, University of California, US. Available online: https://www.proquest.com/dissertations-theses/mechanics-modeling-river-meander-migration/docview/304181401/se-2 (accessed on 7. 11. 2023).
Leopold, L. B., Wolman, M. G., Miller, J. P. (1992): Fluvial Processes in Geomorphology. Dover Publications, Inc., New York. Available online: https://pubs.usgs.gov/publication/70185663 (accessed on 7. 11. 2023).
Li, Q., Yu, M., Lu, G., Cai, T., Bai, X., Xia, Z. (2011): Impacts of the Gezhouba and the Three Gorges reservoirs on the sediment regime in the Yangtze River, China. Journal of Hydrology 403(3–4), 224–233, https://doi.org/10.1016/j.jhydrol.2011.03.043.
Liaghat, A., Adib, A., Gafouri, H. R. (2017): Evaluating the effects of dam construction on the morphological changes of downstream meandering rivers (Case study: Karkheh River). Engineering, Technology & Applied Science Research 7(2), 1515–1522, https://doi.org/10.48084/etasr.969.
Mandarino, A. (2022): Morphological adjustments of the lower Orba River (NW Italy) since the mid-nineteenth century. Geomorphology 410: 108280, https://doi.org/10.1016/j.geomorph.2022.108280.
Map of the Polish Hydrographic Division (2007): Department of Hydrography and Morphology of River Channels Institute of Meteorology and Water Management. Available online: http://mapa.kzgw.gov.pl (accessed on 10. 12. 2016).
Marren, P. M., Grove, J. R., Webb, J. A., Stewardson, M. J. (2014): The potential for dams to impact lowland meandering river floodplain geomorphology. The Scientific World Journal 2014(1): 309673, https://doi.org/10.1155/2014/309673.
Marszalewski, W., Piasecki, A. (2014): Analysis of the development of wastewater infrastructure in Poland in ecological and economical aspects. Journals of the WULS 11(60), 127–137. Available online: http://sj.wne.sggw.pl/pdf/PEFIM_2014_n60.pdf (accessed on 15. 5. 2024).
Meakin, P., Sun, T., JøSsang, T., Schwarz, K. (1996): A simulation model for meandering rivers and their associated sedimentary environments. Physica A: Statistical Mechanics and its Applications 233(3–4), 606–618, https://doi.org/10.1016/S0378-4371(96)00197-5.
Micheli, E. R., Kirchner, J. W., Larsen, E. W. (2004): Quantifying the effect of riparian forest versus agricultural vegetation on river meander migration rates, central Sacramento River, California, USA. River Research and Applications 20(5), 537–548, https://doi.org/10.1002/rra.756.
Monegaglia, F., Zolezzi, G., Güneralp, I., Henshaw, A. J., Tubino, M. (2018): Automated extraction of meandering river morphodynamics from multitemporal remotely sensed data. Environmental Modelling & Software 105, 171–186, https://doi.org/10.1016/j.envsoft.2018.03.028.
Monegaglia, F., Tubino, M. (2019): The hydraulic geometry of evolving meandering rivers. Journal of Geophysical Research: Earth Surface 124(1), 2723–2748, https://doi.org/10.1029/2019JF005309.
Montgomery, D. R., Buffington, J. M. (1997): Channel-reach morphology in mountain drainage basins. GSA Bulletin 109(5), 596–611, https://doi.org

/10.1130/0016-7606(1997)109<0596:CRMIMD>2.3.CO;2.
Muñoz Sabater, J. (2019): ERA5-Land hourly data from 1950 to present. Copernicus Climate Change Service (C3S) Climate Data Store (CDS), https://doi.org/10.24381/cds.e2161bac (accessed on 19. 2. 2024)
Müller, G., Förstner, U. (1968): General Relationship between Suspended Sediment Concentration and Water Discharge in the Alpenrhein and some other Rivers. Nature 217, 244–245, https://doi.org/10.1038/217244a0.
Nyberg, B., Buckley, S. J., Howell, J. A., Nanson, R. A. (2015): Geometric attribute and shape characterization of modern depositional elements: A quantitative GIS method for empirical analysis. Computers & Geosciences 82, 191–204, https://doi.org/10.1016/j.cageo.2015.06.003.
Obodovskyi, O., Lukianets, O. (2017): Patterns and Forecast of Long-term Cyclical Fluctuations of the Water Runoff of Ukrainian Carpathians Rivers. Environmental Research, Engineering & Management 73(1), 33–47, https://doi.org/10.5755/j01.erem.73.1.15799.
Oglęcki, P., Ostrowski, P. S., Utratna-Żukowska, M. (2021): Natural and geomorphological response of the small lowland river valley for anthropogenic transformation. Resources 10(10): 97, https://doi.org/10.3390/resources10100097.
Okoniewska, M., Szumińska, D. (2020): Changes in Potential Evaporation in the Years 1952–2018 in North-Western Poland in Terms of the Impact of Climatic Changes on Hydrological and Hydrochemical Conditions. Water 12(3): 877, https://doi.org/10.3390/w12030877.
Pikies, R. (2009): Objaśnienia do szczegółowej mapy geologicznej Polski, arkusz Tuchola; Państwowy Instytut Geologiczny PIB, Warszawa, Poland (in Polish).
Poff, N. L., Zimmerman, J. K. H. (2010): Ecological responses to altered flow regimes: a literature review to inform the science and management of environmental flows. Freshwater Biology 55(1), 194–205, https://doi.org/10.1111/j.1365-2427.2009.02272.x.
Richter, B. D., Baumgartner, J. V., Braun, D. P., Powell, J. (1998): A spatial assessment of hydrologic alternation within a river network. Regulated Rivers: Research & Management 14(4), 329–340, https://doi.org/10.1002/(SICI)1099-1646(199807/08)14:4<329::AID-RRR505>3.0.CO;2-E.
Richter, B. D., Baumgartner, J. V., Powell, J., Braun, D. P. (1996): A Method for Assessing Hydrologic Alternation within Ecosystems. Conservation Biology 10(4), 1163–1174. https://www.jstor.org/stable/2387152.
Richter, B. D., Baumgartner, J. V., Wigington, R., Braun,D. (1997): How much water does a river need? Freshwater Biology 37(1), 231–249, https://doi.org/10.1046/j.1365-2427.1997.00153.x.
Rust, B. R. (1996): A Classification of Alluvial Channel Systems. Fluvial Sedimentology 5, 187–198.
Schuurman, F. (2015): Bar and channel evolution in meandering and braiding rivers using physics-based modeling; Dissertation, Utrecht University, Nederland. Available online: https://www.researchgate.net/publication/277020641_Bar_and_channel_evolution_in_meandering_and_braiding_rivers_using_physics-based_modeling (accessed on 4. 11. 2023).
Shields, F. D., Abt, S. R. (1989): Sediment deposition in cutoff meander bends and implications for effective management. Regulated Rivers: Research & Management 4(4), 381–396, https://doi.org/10.1002/rrr.3450040406.
Słowik, M., Dezső, J., Kovács, J., Gałka, M. (2020): The formation of low-energy meanders in loess landscapes (Transdanubia, central Europe). Global and Planetary Change 184: 103071, https://doi.org/10.1016/j.gloplacha.2019.103071.
Słowik, M. (2014): Holocene evolution of meander bends in lowland river valley formed in complex geological conditions (the Obra River, Poland). Geografiska Annaler: Series A, Physical Geography 96(1), 61–81, https://doi.org/10.1111/geoa.12029.
Słowik, M. (2013): Transformation of a lowland river from a meandering and multi-channel pattern into an artificial canal: retracing a path of river channel changes (the Middle Obra River, W Poland). Regional Environmental Change 13, 1287–1299, https://doi.org/10.1007/s10113-013-0453-3.
Somorowska, U. (2016): Changes in Drought Conditions in Poland over the Past 60 Years Evaluated by the Standardized Precipitation-Evapotranspiration Index. Acta Geophysica 64, 2530–2549, https://doi.org/10.1515/acgeo-2016-0110.
Solon, J., Borzyszkowski, J., Bidłasik, M., et al. (2018): Physico-geographical mesoregions of Poland: Verification and adjustment of boundaries on the basis of contemporary spatial data. Geographia Polonica 91(2), 143–170, https://doi.org/10.7163/GPol.0115.
Sylvester, Z., Durkin, P., Covault, J. A. (2019): High curvatures drive river meandering. Geology 47(3), 263–266, https://doi.org/10.1130/G45608.1.
Sylvester, Z., Durkin, P. R., Hubbard, S. M., Mohrig, D. (2021): Autogenic translation and counter point bar deposition in meandering rivers. GSA Bulletin 133(11–12), 2439–2456, https://doi.org/10.1130/B35829.1.
Szatten, D., Habel, M. (2020): Effects of Land Cover Changes on Sediment and Nutrient Balance in the Catchment with Cascade-Dammed Waters. Remote Sensing 12(20): 3414, https://doi.org/10.3390/rs12203414.
Szatten, D., Habel, M., Babiński, Z. (2021): Influence of Hydrologic Alternation on Sediment, Dissolved Load and Nutrient Downstream Transfer Continuity in a River: Example Lower Brda River Cascade Dams (Poland). Resources 10(7): 70, https://doi.org/10.3390/resources10070070.
Szatten, D., Habel, M., Pellegrini, L., Maerker, M. (2018): Assessment of Siltation Processes of the Koronowski Reservoir in the Northern Polish Lowland Based on Bathymetry and Empirical Formulas. Water 10(11): 1681, https://doi.org/10.3390/w10111681.
Szatten, D., Brzezińska, M., Bosino, A. (2023): New sediment continuum measurements in the Brda River (Poland): the results of the functioning of the 50-year Koronowo dam. Journal of Soils and Sediments 23, 3219–3240, https://doi.org/10.1007/s11368-023-03582-z.
Tal, M., Paola, C. (2010): Effects of vegetation on channel morphodynamics: results and insights from laboratory experiments. Earth Surface Processes and Landforms 35(9), 1014–1028, https://doi.org/10.1002/esp.1908.

Walling, D. E. (2006): Human impact on land–ocean sediment transfer by the world's rivers. Geomorphology 79(3–4), 192–216, https://doi.org/10.1016/j.geomorph.2006.06.019.

Ward, R. C., Robinson, M. (2000): Principles of Hydrology (4th ed.), McGraw-Hill.

Ward, J. V., Tockner, K., Arscott, D. B., Claret, C. (2002): Riverine landscape diversity. Freshwater Biology 47(4), 517–539, https://doi.org/10.1046/j.1365-2427.2002.00893.x.

Wohlfart, C., Liu, G., Huang, C., Kuenzer, C. (2016): A River Basin over the course of time: Multi-temporal analyses of land surface dynamics in the Yellow River Basin (China) based on medium resolution remote sensing data. Remote Sensing 8(3): 186, https://doi.org/10.3390/rs8030186.

Wood, P., Armitage, P. (1997): Biological Effects of Fine Sediment in the Lotic Environment. Environmental Management 21, 203–217, https://doi.org/10.1007/s002679900019.

Xu, D., Bai, Y., Ma, J., Tan, Y. (2011): Numerical investigation of long-term planform dynamics and stability of river meandering on fluvial floodplains. Geomorphology 132(3–4), 195–207, https://doi.org/10.1016/j.geomorph.2011.05.009.